

Carbon flows in natural plankton communities in the Anthropocene

Anna de Kluijver

*“Science is an imaginative adventure of the mind seeking truth in a world of mystery.”
Sir Cyril Herman Hinshelwood (1897-1967) English chemist. Nobel prize 1956.*

Promotoren

Prof dr. J. J. Middelburg, Utrecht University, The Netherlands

Prof. dr. K. Soetaert, Royal Netherlands Institute for Sea Research, The Netherlands, and Ghent University, Belgium

Thesis committee

Prof. dr. E. van Donk, Netherlands Institute of Ecology and Utrecht University, The Netherlands

Prof. dr. S. Schouten, Royal Netherlands Institute for Sea Research and Utrecht University, The Netherlands

Prof. dr. J.A. Downing, Iowa State University, USA

Prof. dr. Z. Liu, Nanjing Institute of Geography and Limnology, China

Prof. dr. J.-P. Gattuso, Laboratoire d'Océanographie de Villefranche, France

ISBN: 978-90-3935-846-7

The research presented in this thesis has been primarily conducted in the department of Ecosystem Studies of Royal Netherlands Institute for Sea Research in Yerseke (formerly Center for Estuarine Marine Ecology, part of NIOO-KNAW) and was partly funded by the Darwin center for Biogeosciences. Additional financial support was received from the European Project on Ocean Acidification, Schure-Beijerinck-Popping fund and MesoAqua.

Cover and thesis design: HDK architecten bna bni bnsf, the Netherlands

Cover photographs courtesy of R. Wagner, Germany (cladoceran with green algae), R. Hopcroft, USA (copepod).

Copyright © Anna de Kluijver, december 2012.

All rights reserved.

Carbon flows in natural plankton communities in the Anthropocene

**Koolstofstromen in natuurlijke plankton gemeenschappen in het
Anthropoceen**

(met een samenvatting in het Nederlands)

Proefschrift

ter verkrijging van de graad van doctor aan de Universiteit Utrecht op gezag van de rector magnificus, prof.dr. G.J. van der Zwaan, ingevolge het besluit van het college voor promoties in het openbaar te verdedigen op vrijdag 7 december 2012 des middags te 2.30 uur

door

Anna de Kluijver

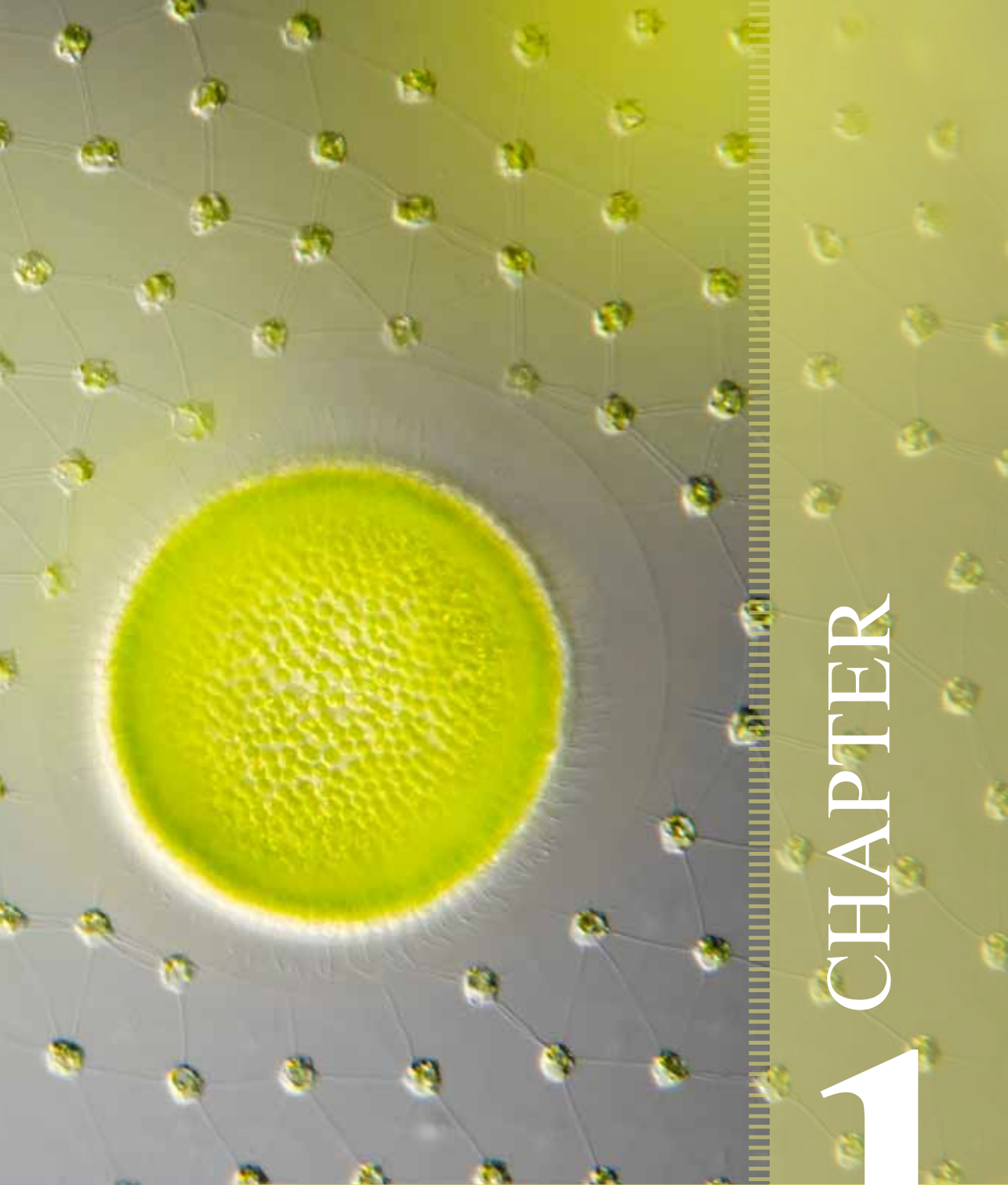
geboren op 21 juli 1982 te Spijkenisse

Promotoren: Prof.dr J.J. Middelburg
Prof. dr. K. Soetaert

Contents

Chapter 1	2
General introduction	
Chapter 2	16
Phytoplankton-bacteria coupling under elevated CO ₂ levels: a stable isotope labeling study	
Chapter 3	38
A ¹³ C labeling study of carbon fluxes in Arctic plankton communities under elevated CO ₂ levels	
Chapter 4	64
Carbon isotope constraints on lake food-web interactions along a trophic gradient	
Chapter 5	88
Cyanobacteria as a carbon source for zooplankton in eutrophic Lake Taihu, China, measured by ¹³ C labeling and fatty acid biomarkers	
Chapter 6	106
Macrophyte carbon subsidies to bacterioplankton and zooplankton in a restored part of a shallow, eutrophic lake in China	
Chapter 7	120
References	
Summary	
Nederlandse Samenvatting	
Publication list	
Dankwoord - Acknowledgements	

Photo: young volvox by Wim van Egmond



CHAPTER

1



General Introduction

1.1 The Anthropocene

Human activities have a global impact on organisms and biogeochemical processes, causing changes in ecosystem functioning, biodiversity, and biogeochemical cycles. Overexploitation of resources, loss and alterations of habitats, environmental pollution and fossil-fuel burning, are examples of human activities, which have a severe impact on ecosystems. The period and current times where humans alter the planet is called the recent age of man or the “Anthropocene”.

Carbon cycle

One of the largest impacts of humans since the industrial revolution is alteration of the global carbon (C) cycle. Carbon dioxide (CO_2) release, primarily due to burning of fossil fuels, has increased atmospheric $p\text{CO}_2$ with 30% to levels of ~ 390 ppmv compared to ~ 280 ppmv in pre-industrial times (IPCC 2007). Changes in land use, like deforestation, release CO_2 and reduce the earth's capacity for CO_2 uptake. There is strong evidence that the CO_2 rise together with an increase in other greenhouse gases caused global warming of $\sim 0.6^\circ\text{C}$ since 1861 (IPCC 2007). Temperature is such an important driver in biotic (production, metabolism) and abiotic (hydrology, ice melting) processes, that global warming became a primary focus in research and environmental policy.

The oceans act as a strong sink for CO_2 and have absorbed approximately one third of the anthropogenic CO_2 (Sabine et al. 2004). CO_2 is soluble in (sea)water ($\text{CO}_2[\text{aq}]$) and reacts with water molecules to carbonic acid (H_2CO_3), which dissociates to bicarbonate (HCO_3^-), and carbonate ions (CO_3^{2-}), while releasing protons (H^+). The sum of CO_2 species are collectively referred to as dissolved inorganic carbon (DIC) and is dominated by bicarbonate (>90 %) at normal seawater pH. The increase in ocean surface $\text{CO}_2[\text{aq}]$ increases DIC and HCO_3^- concentrations, but lowers CO_3^{2-} concentrations and sea water pH, and the latter lead to the name ocean acidification (Fig. 1.1). The average pH of the ocean has already decreased by about 0.1 units compared to pre-industrial levels from 8.2 to 8.1 and a further decrease of about 0.3-0.4 units is predicted for the year 2100, when CO_2 emissions continue at present rates (Caldeira and Wickett 2003) (Fig. 1.1).

Eutrophication

Also other elemental cycles, such as those of phosphorus (P) and nitrogen (N), are altered by human activities. Especially the intensification of agriculture, but also increases in industrial and urban wastewater production have dramatically increased the loading of N and P in aquatic systems. Atmospheric deposition of the increased nitrogen concentrations in the atmosphere, due to agriculture and fossil-fuel burning, additionally adds nutrients to aquatic systems. The anthropogenic nutrient loading led to eutrophication, one of the most severe and pertinent environmental problems, causing degradation of aquatic ecosystems and deteriorating water quality. Increased nutrients stimulate phytoplankton productivity, resulting in recurring harmful algae blooms. Due to the high primary production, the water transparency decreases and sedimentation increases. The consequent degradation of sedimented matter consumes oxygen and causes anoxia in the bottom waters, creating dead zones and massive fish kills (reviewed by Carpenter et al. 1998). Cyanobacteria are the most notorious bloom formers by their abilities to form surface scum and to produce toxic compounds (reviewed in Paerl et al. 2001). The reduced transparency induced by these organisms leads to disappearance of macrophytes (aquatic plants).

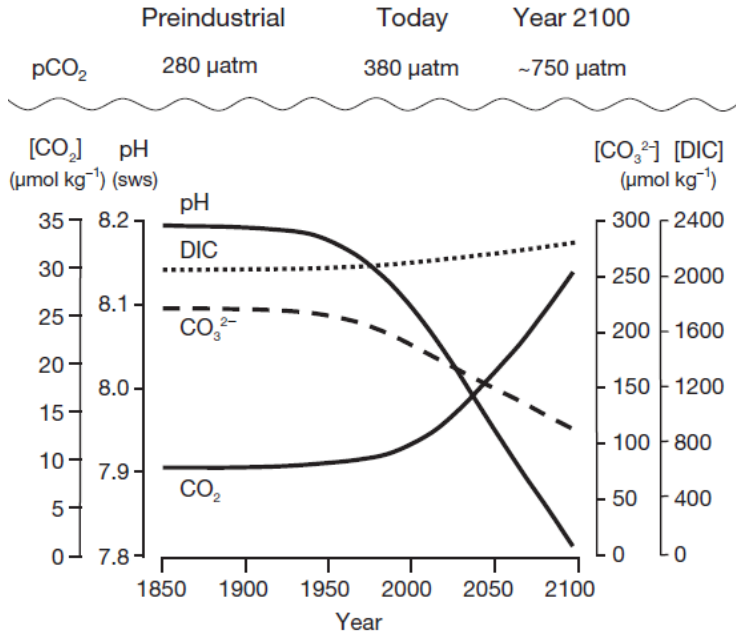


Fig. 1.1. Predicted changes in the surface seawater chemistry in response to changes in atmospheric $p\text{CO}_2$ assuming the “business as usual” scenario. Figure taken from Rost et al. 2008.

In the past decades, many shallow lakes shifted from a clear water, macrophyte dominated state to a turbid, algal dominated state, often dominated by toxic cyanobacteria (Scheffer et al. 1993).

Especially lakes are sentinels for anthropogenic disturbances, where global warming, eutrophication, and land-use changes act in conjunction (Williamson et al. 2008). Environmental problems often reinforce each other’s effect. For example, global warming is expected to reinforce eutrophication effects, including an increase in cyanobacteria blooms (Paerl and Huisman 2008) and to aggravate anoxia, due to increased water-column stratification. Increased erosion and sediment input due changes in land use, amplify terrestrial nutrient loading and enhances eutrophication effects.

1.2 Plankton community structure and the microbial food web

Environmental problems such as ocean acidification and eutrophication affect the base of aquatic food webs: the structure and functioning of plankton communities. A food web represents an ecological network of feeding interactions, where organisms can be lumped into functional groups (i.e. producers, consumers) that perform at different trophic levels (the position in the food chain). The base of aquatic food webs is formed by phytoplankton, the primary producers, which convert inorganic carbon (CO_2) and nutrients into organic matter (OM) during primary production.

Marine phytoplankton accounts for roughly half of the global primary production, despite their low biomass (Field et al. 1998). In a classical view of the aquatic food web, the phytoplankton produced particulate organic matter (POM) is grazed by zooplankton, which can be subsequently consumed by higher trophic levels, called the herbivorous food web.

Microbial food web

About 10-15 % of phytoplankton primary production is released as dissolved organic matter (DOM), a mechanism of phytoplankton to release the surplus of carbon-rich photosynthates (Fogg 1983, Baines and Pace 1991) over nutrients. The exudated DOM is a high-quality substrate for growth of heterotrophic bacteria, which are key players in the recycling of organic matter and nutrients in aquatic food webs (Azam et al. 1983). Heterotrophic bacteria (hereafter denoted by bacteria) dominate pelagic (water-column) food webs in terms of respiration and secondary production and it is estimated that 30-60% of phytoplankton primary production is finally processed by bacteria (Cole et al. 1988, Del Giorgio et al. 1997). Bacterial production forms the base of the microbial loop, which starts with the consumption of DOM by bacteria that are in turn grazed upon by small, unicellular organisms, named protozoans. Protozoans can be grazed by (metazoan, multicellular) zooplankton, which links the microbial loop with the classical food web (Fig. 1.2).

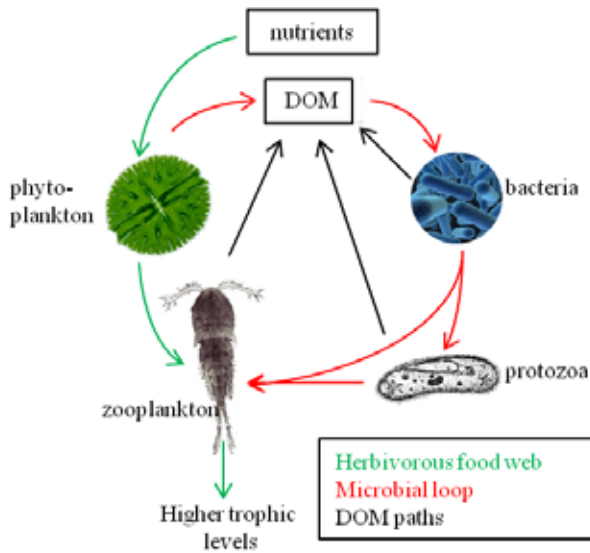


Fig. 1.2. Schematic diagram of carbon flows between different components of planktonic food webs. Modified after J.P. Torréton, IRD.

The importance of phytoplankton derived DOM as substrate for bacteria has been demonstrated amongst others, through the existence of robust, general relationships between the abundance and production of bacteria and phytoplankton (Cole et al. 1988).

Dissolved organic carbon (DOC), the largest organic carbon pool in aquatic systems, also originates from leakage of dead cells and organisms, from sloppy feeding by grazers, viral lysis, through dissolution of detritus, and by input of allochthonous organic matter, i.e. mainly terrestrial material produced outside the ecosystem. Both herbivorous and microbial food webs are present in pelagic systems and their dominance changes along a trophic continuum (Legendre and Rassoulzadegan 1995).

Plankton and the global carbon cycle

The processes in surface plankton communities largely determine the CO₂ uptake capacity of aquatic systems. In the oceans, a vertical CO₂ gradient exists from surface to deep, driven by physical and biological processes. About two third of the surface to deep inorganic carbon gradient is caused by the biological pump (Volk 1985). The biological pump is the sinking (export) of photosynthetically produced organic matter out of the euphotic zone, which is the upper 100 m of the oceans. Community respiration (dominated by bacteria) in the euphotic zone converts organic matter back into CO₂ and thus counteracts the pump. Integrated over the global oceans, export is ~15 % of primary production (Laws et al. 2000). In the deep oceans, the material can be consumed and respired, thereby producing CO₂ that is released very slowly back into the surface waters by physical mixing or upwelling. It has been estimated that, without the biological pump, atmospheric *p*CO₂ would increase to ~500 ppmv (Maier-Reimer et al 1996), thus small changes in performance of the biological pump will have large impacts on carbon cycling. The balance between production, export and in situ respiration determines the vertical flux of biogenic carbon (Rivkin and Legendre 2001).

While oceans are overall net sinks for CO₂, most lakes are net sources of CO₂ (Cole et al. 1994) because of net heterotrophy, i.e. respiration exceeds production. The net heterotrophy of most lakes is primarily caused by the high input of terrestrial carbon that constitutes the majority of the respired carbon in lakes (Cole et al. 2006) and makes lakes hotspots of organic matter remineralization. The plankton production balance in lakes is more directly affected by anthropogenic disturbances, compared to oceans. For example, the CO₂ balance of lakes is directly influenced by the relative balance between allochthonous DOC loading and nutrient input (Del Giorgio and France 1994, Hanson et al. 2003). Because of the strong feedback of planktonic food webs on atmospheric CO₂, carbon is the primary element to study food-web interactions in this thesis.

1.3 Plankton carbon flows in the anthropocene

The overall research question of this thesis is: “What are the effects of anthropogenic disturbances on carbon flows in plankton food webs?” Both marine and freshwater systems were studied, but for marine systems we focused on the effects induced by rising CO₂ levels, while in fresh water systems we focused on eutrophication effects.

CO₂ effects on marine plankton communities

CO₂ is the preferred substrate for photosynthesis by phytoplankton, despite the low relative abundance of CO₂ in seawater (<1 % of DIC). Most phytoplankton groups (taxa) have developed carbon concentrating mechanisms to increase the intracellular CO₂ concentrations (CCMs) above the ambient concentrations, but operation of these CCMs requires energy and nutrients (Beardall and Giordano 2002).

Increases in CO_2 therefore have a direct effect on photosynthesis and it can be postulated that photosynthesis will increase due to higher substrate availability, if other factors remain constant. There are indeed some indications of enhanced primary production at increasing CO_2 in laboratory experiments, as well as natural plankton community studies (reviewed in Doney et al. 2009, Riebesell and Tortell 2011). Enhanced biological CO_2 consumption relative to nutrients by natural plankton communities was observed in a pelagic CO_2 enrichment mesocosm study (Bergen 2005, Riebesell et al. 2007). The enhanced uptake was not reflected in increased organic matter production (Schulz et al., 2008) nor in increased bacterial activity (Allgaier et al., 2008) so enhanced export was the suggested sink for the extra carbon consumed at elevated $p\text{CO}_2$, although this was not measured directly (Riebesell et al., 2007, Fig. 1.3).

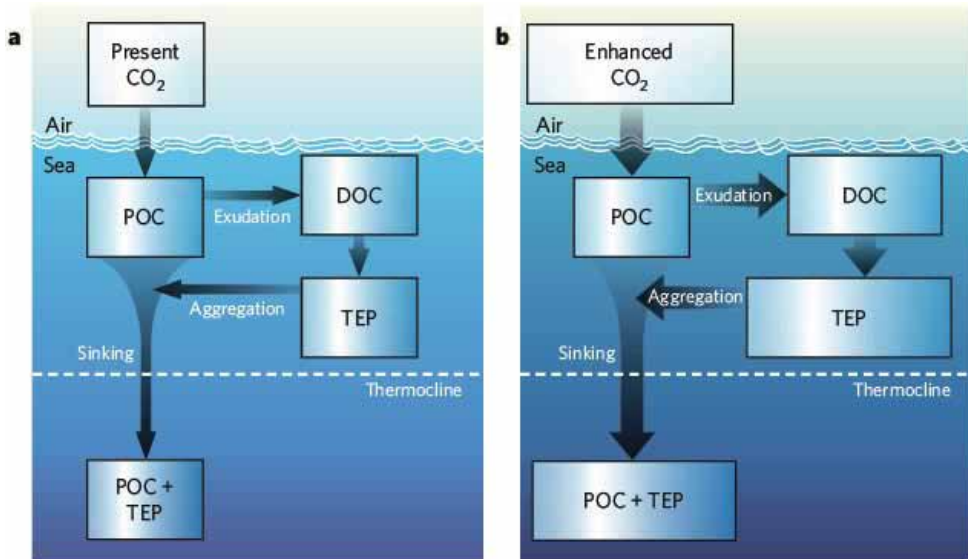


Fig. 1.3. CO_2 in the atmosphere and organic carbon in the ocean. The two panels show the relative size of different carbon pools and carbon flows in (a) the present ocean and (b) in the future ocean according to the hypothesis by Riebesell et al. 2007, where community CO_2 uptake and export is enhanced. Abbreviations are explained in the text, the thermocline presents a temperature barrier that separates the upper ocean from the deep ocean. Figure taken from Arrigo 2007.

The proposed mechanism was that the extra consumed CO_2 was exuded by phytoplankton as DOC that coalesces into transparent exopolymeric particles, named TEP. These particles can facilitate aggregation of particulate organic carbon (POC) and increase export (Engel et al., 2004a, Fig. 1.3). However, there will only be an increased export when the material is not remineralized by bacteria and other consumers in the euphotic zone. The response of bacteria to increasing DOC depends largely on the state of the microbial loop, if it is nutrient or carbon limited (Thingstad et al. 2008). Most studies have shown no direct effects of increasing CO_2 and co-occurring decreasing pH on bacteria productivity and abundance, so changes in the microbial community are likely to occur from changes in organic matter and nutrients (reviewed in Weinbauer et al. 2011).

Also zooplankton showed little direct response to increasing CO₂ (e.g. Niehoff et al 2012), so the effect of ocean acidification on zooplankton is mainly indirect, through changes in food availability.

Eutrophication effects on fresh water food webs

Eutrophication clearly influences the structure of plankton food webs. In general, eutrophication stimulates production of phytoplankton, what subsequently stimulates secondary production by consumers, like bacteria, zooplankton and higher trophic levels, due to higher food availability. However, changes in food-web structure occur along a trophic continuum from oligotrophic (low nutrients) via mesotrophic (intermediate nutrients) to eutrophic (high nutrients) systems. In oligotrophic lakes, most organic matter is in the dissolved pool and phytoplankton biomass is low, while bacteria have a relative high biomass and dominate community respiration (Fig. 1.4, Del Giorgio and Peters 1994, Biddanda et al. 2001). High bacterial biomass and production can be sustained by the subsidy of allochthonous organic matter (Tranvik 1992) and other primary producers, such as macrophytes in the littoral zone (Rooney and Kalff 2003). Furthermore, exudation of DOC by phytoplankton could be higher under low nutrient availability, when nutrients limit phytoplankton growth, but not photosynthesis (Bratbak and Thingstad 1985). When lakes move from oligotrophic to mesotrophic, phytoplankton production increases, which stimulates zooplankton grazing and production (herbivorous pathways) (Elser and Goldman 1991) such that the proportion of bacteria respiration in community production declines (Fig. 1.4, Cotner and Biddanda 2002). Although bacteria biomass increases with increasing phytoplankton biomass (Cole et al. 1988), the increase is disproportional and the relative abundance of bacteria declines with increasing trophicity (Gasol and Duarte 2000). Severe eutrophication effects develop when lakes move from mesotrophic to eutrophic and the food web structure changes again.

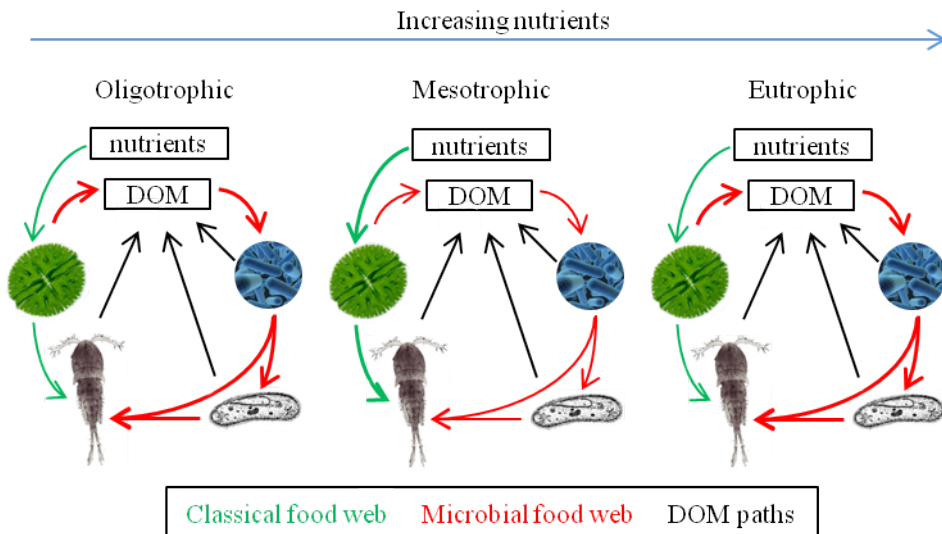


Fig. 1.4. The schematic food web of fig. 1.2 along a trophic gradient. The thickness of the arrows presents the dominance of either herbivorous or microbial food webs at each trophic state.

Because of an increasing dominance of cyanobacteria, which are considered poor food for zooplankton (Haney 1987), herbivory declines and a shift in zooplankton community from large-bodied zooplankton towards small zooplankton is often observed (Fig. 1.4, Gliwicz 1969, Haney 1987). Because of reduced herbivory, zooplankton is expected to start grazing on the microbial food web, which dominates community respiration again (Fig. 1.4, Sommaruga 1995).

Biomanipulation

The ecological concepts of aquatic food webs are used to combat eutrophication effects and improve water conditions in a tool coined as biomanipulation (Shapiro et al. 1975). The concept of biomanipulation, primarily via manipulation of the planktivorous fish community, is based on the herbivorous food web and a cascading food web. The removal of planktivorous fish reduces grazing pressure on zooplankton, supposedly followed by an increased dominance of large zooplankton that will control the production of phytoplankton. Next to manual removal of planktivorous fish, piscivorous fish can be added to control the planktivorous fish population. One of the preferred outcomes of biomanipulation is an increase in submerged macrophytes that help to maintain the restored conditions by consuming nutrients, stabilizing the sediments with their roots, and providing a refuge for zooplankton. The success of biomanipulation depends on several factors, like lake size and depth, external nutrients loading, climate, and plankton community structure (reviewed in Hansson et al. 1998). For example, biomanipulation is expected to be less successful in lakes where the microbial food web dominates aquatic energy flows.

1.4 Methodology –stable isotopes

A powerful and widely applied method to study energy and mass flows in plankton food webs and infer dietary sources for consumers is stable isotope analysis (SIA) (Fry 2006). Isotopes are forms of one element, which differ in numbers of neutrons and therefore have a different atomic weight. While radioactive isotopes are unstable and decay spontaneously, stable isotopes are not radioactive and are as their name suggests, stable. Of the elements of life, C, N, H, S, O have at least two stable isotopes, from which the light form presents >95 % of the total isotopes. Unfortunately, P has only one stable isotope and cannot be used in SIA. The isotope composition of material is usually expressed in the δ notation, which is the deviation in isotope ratio of the material from the ratio of a certified standard, and is expressed in parts per thousand (per mil, ‰). The carbon isotope delta value, $\delta^{13}\text{C} (\text{‰}) = ([r_{\text{sample}}/r_{\text{standard}}] - 1) \times 1000$ and r is the ratio $^{13}\text{C}/^{12}\text{C}$. The standard for carbon is Vienna Pee Dee Belemnite (VPDB), which contains 1.1 ‰ ^{13}C . When a sample contains relatively less of the heavy isotope it is depleted, and when it contains relatively more of the heavy isotope it is enriched.

Fractionation

Biogeochemical reactions discriminate against the heavy isotope and reaction products are therefore depleted compared to the source, a process called isotope fractionation. Isotope fractionation for carbon occurs during photosynthesis, resulting in photosynthates that are depleted in ^{13}C compared to the inorganic carbon source.

The $\delta^{13}\text{C}$ of different primary producers is variable, amongst other things due to different photosynthetic mechanisms: plants that use C_4 photosynthesis have a $\delta^{13}\text{C}$ around -14‰ and $\delta^{13}\text{C}$ associated with C_3 plants is $\sim -28\text{‰}$ (Fig. 1.5). Also, phytoplankton $\delta^{13}\text{C}$ is more enriched in marine systems (-20‰), compared to fresh water systems (-28‰). Finally, the actual $\delta^{13}\text{C}$ of phytoplankton can be very variable, because it also depends on environmental and physiological conditions (Laws et al. 1995, Popp et al. 1998).

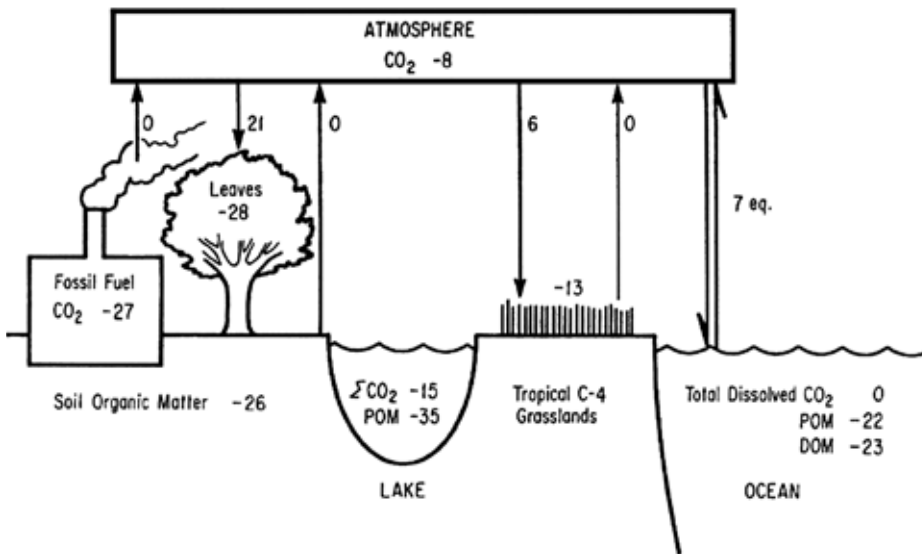


Fig. 1.5. $\delta^{13}\text{C}$ distribution in ecosystems. Numbers for pools indicate the average $\delta^{13}\text{C}$ (‰). The single arrows represent carbon flows and the double arrow presents isotopic equilibrium. The numbers on the arrows indicate the fraction in $\delta^{13}\text{C}$ during transfer. Figure taken from Fry 2006.

SIA in ecology uses the natural variety in isotope signatures ($\delta^{13}\text{C}$) at the base of the food chain to trace carbon origins. Little trophic fractionation in $\delta^{13}\text{C}$ occurs between food sources and grazers, so the $\delta^{13}\text{C}$ of consumers reflect their diet, according to the “you are what you eat” principle (deNiro and Epstein 1978). Isotope ratios of nitrogen ($\delta^{15}\text{N}$) get enriched along the food chain, on average 3.4‰ with each trophic step (deNiro and Epstein 1981, Vander Zanden and Rasmussen 2001) and are therefore more suitable to determine trophic positions.

Isotope labeling

An important condition to study food web interactions via SIA is that the sources are isotopically distinctive. However, sources might overlap in $\delta^{13}\text{C}$ and often there are multiple combinations of food sources possible that would result in a similar $\delta^{13}\text{C}$ of a consumer. A valuable alternative to study natural stable isotopic composition is to add stable isotopes (^{13}C , ^{15}N) as deliberate tracers, thereby significantly enriching the isotope signature of a potential food source.

Subsequent tracing of the enriched isotopes in consumers in time, allows quantifying up-take rates and food web interactions (Boschker and Middelburg 2002), for example addition of ^{13}C -DIC to study primary production and subsequent transfer to consumers. A drawback of isotope labeling is the requirement of semi-enclosed systems or experimental incubations. Furthermore, while isotope labeling reveals short term interaction, natural abundance isotope studies show an integrated signal over a long term.

1.5 Methodology – fatty acid biomarkers

A challenge associated with SIA in plankton food webs is to obtain pure samples of phytoplankton, bacteria and other functional groups from bulk organic matter. POM contains a mixture of phytoplankton, bacteria, detritus, terrestrial material, protozoans, and zooplankton. Zooplankton can be isolated by handpicking, but for e.g. bacteria this is an unpractical task. Size fractionation by centrifugation can be used, but most organisms have overlapping size ranges.

New perspectives for discriminating food web components opened when compound-specific isotope analyses (CSIA) allowed quantifying the isotope signatures of biomarkers (Hayes et al. 1990). Biomarkers are specific compounds that are produced by certain groups of organisms only and can thus be used to identify the presence and abundance of that group. Examples of biomarkers that are frequently used in ecology are photosynthetic pigments and certain types of lipids. Membrane lipids like phospholipid derived fatty acids (PLFA), which are also known as polar lipid derived fatty acids (PLFA), have suitable characteristics for ecological applications. They are part of the cell membrane and therefore present in a rather constant fraction of the biomass, they are quickly degraded after cell death, so they are representative for living biomass, they are present in all organisms and most important, there is taxonomic variety.

Fatty acids (FA) are notated as A:B ω C, where A is the chain length (number of C atoms), B is the number of double bonds and C is the position of the first double bond relative to the (aliphatic) end of the tail. Saturated fatty acids have no double bonds and the more double bonds, the higher the degree of unsaturation. Methyl branches are noted with iso (i) or anteiso (ai) if they are present on the second and third carbon atom from the end of the tail, respectively. Branched fatty acids (BFA) are produced by heterotrophic bacteria (Kaneda 1991). Poly-unsaturated fatty acids, fatty acids with >1 double bond (PUFA) are produced by phytoplankton in a wide variety that can also be used to distinguish different phytoplankton taxa (Dijkman and Kromkamp 2006).

A valuable application of CSIA in ecology is the combined analysis of $\delta^{13}\text{C}$ and concentrations of individual PLFA biomarkers, which provides information on abundance and isotopic composition of certain groups of organisms. Especially in stable isotope tracer studies with labeled compounds, the activity of different microbial groups can be determined by analyzing the ^{13}C incorporation in specific fatty acid biomarkers (Boschker et al. 1998). The technique has also been successfully applied to infer the biomass and $\delta^{13}\text{C}$ of bacteria and phytoplankton in aquatic food web studies (Boschker and Middelburg 2002). For example, SIA of PLFA was applied to study autochthonous (phytoplankton derived) and allochthonous (terrestrial) contributions to bacteria and zooplankton consumers in a tidal river (Van den Meersche et al. 2009) and lake (Pace et al. 2007). In a ^{13}C labeling experiment of a phytoplankton bloom, ^{13}C content of fatty acid biomarkers were used to study carbon transfer from phytoplankton to bacteria (Van den Meersche et al. 2004).

Fatty acids as trophic markers

The ω 3 and ω 6 PUFA and especially highly unsaturated fatty acids (HUFA, e.g., 20:5 ω 3 and 22:6 ω 3) are considered essential fatty acids (EFA) for metazoan consumers, such as zooplankton and fish. These organisms cannot synthesize unsaturated fatty acids themselves and therefore require them from their diet. The conservative way in which fatty acids are transferred along the food chain, makes them also suitable as qualitatively trophic markers: the fatty acid trophic marker concept (FATM) (Dalsgaard et al. 2003). Furthermore, the amount of EFA in a potential food source can be used to predict the energy transfer between the food source and metazoan consumers (Müller-Navarra et al. 2000). Eukaryotic algae are the main producers of EFA and are therefore considered high-quality food for zooplankton. Cyanobacteria however hardly produce EFA, which is considered one of the reasons for their poor food quality.

1.6 Ecological models

The next step to quantify the interactions and energy flows in (aquatic) food webs is the application of ecological modeling. Models are simple representations of a complex system or phenomenon (Soetaert and Herman 2009). For example, the food web scheme in Fig. 1.2 represents a conceptual model, in which species are lumped into functional groups that behave similarly and interactions are presented in simple arrows. The main advantages of models are that they contribute to understand and quantify complex processes. Mathematical models are useful in many ways, for example to extrapolate knowledge of small ecosystems to global biogeochemical processes, or to predict the future effect of anthropogenic disturbances (climate change models). In ecology, models are especially useful to make budgets (i.e. CO₂ sink or source) and to quantify processes that cannot be measured directly, which are often the arrows in Fig 1.2. By fitting a model to observed data, called inverse modeling, parameters can be determined. A simple example of an inverse model is the calculation of the intercept (b) and slope (a) from drawing a straight line ($y = ax + b$) through the data points. In stable isotope labeling studies, uptake and transfer rates can be quantified by fitting model equations to stable isotope data (Van den Meersche et al. 2011, Van Engeland et al. 2012).

1.7 Thesis outline

The aim of this thesis is to increase our understanding of how carbon flows in plankton communities are altered in the Anthropocene. Chapter 2 and 3 describe the effects of increasing CO₂ on carbon flows in marine plankton communities. Chapter 4 and 5 describe carbon flows in fresh water communities, with eutrophication as most important anthropogenic driver. Chapter 6 describes plankton carbon flows in a part of a lake that was biomanipulated to combat eutrophication effects. In all chapters, we used stable isotope analysis of carbon ($\delta^{13}\text{C}$), either at natural abundance or as tracer, to examine food web interactions and carbon flows. Fatty acid biomarkers were used in all chapters to determine the $\delta^{13}\text{C}$ of different groups of phytoplankton and bacteria.

Chapter 2 and 3 show the results of two mesocosm experiments where CO₂ was added to mimic future CO₂ conditions. Mesocosms are large experimental water enclosures that provide the ability to manipulate environmental factors (such as CO₂), while keeping other conditions close to natural. In both mesocosm experiments ¹³C-DIC was added as a deliberate tracer, to follow the uptake and transfer of ¹³C within the plankton community in time.

The mesocosm experiment in **chapter 2** was conducted in Bergen, Norway, where sets of mesocosms were kept under current and future CO₂ levels for 3 weeks. A phytoplankton bloom was initialized by nutrient additions. Here, we focused on the transfer from DIC into phytoplankton and subsequently bacteria and the phytoplankton-bacteria coupling for each CO₂ level was quantified with an isotope ratio model.

The mesocosm experiment in **chapter 3** was carried out in an Arctic fjord (Svalbard), a region that is especially vulnerable to ocean acidification, because CO₂ dissolves better in seawater under low temperatures. Over a period of 5 weeks, natural phytoplankton communities in nine ~50 m³ mesocosms were studied under a range of CO₂ levels and here, nutrients were added halfway through the experiment. In addition to the mesocosm experiment of chapter 2, we also studied consumption by zooplankton and export (sinking) of freshly produced organic matter. We constructed a nutrient-phytoplankton-zooplankton-detritus (NPZD) model of carbon concentrations amended with ¹³C dynamics and fitted it to the data to quantify uptake and loss rates and carbon flows under different CO₂ levels.

Chapter 4 describes plankton food web structures in lakes along a trophic gradient in a cross-system study. Twenty-two temperate lakes in Midwestern USA, which were classified as eutrophic and meso-oligotrophic, were sampled for inorganic and organic carbon concentrations and $\delta^{13}\text{C}$. Correlation analyses were used to study food-web interactions and planktonic drivers for lake metabolism. Autochthonous and allochthonous contributions to bacterial and zooplankton consumers were determined with a two-source mixing model.

In **chapter 5** the hypothesis was tested that cyanobacteria can be a carbon source for zooplankton, but that most carbon flows via bacteria-mediated pathways rather than via herbivory. The hypothesis was tested on plankton communities in lake Taihu, a shallow eutrophic lake in China, by examining natural abundance $\delta^{13}\text{C}$ in field samples and with isotope enrichment experiments.

^{13}C enriched *Microcystis* was added as live cyanobacteria, cyanobacterial detritus and cyanobacterial DOM to lake water incubations and ^{13}C was traced into bacteria and zooplankton consumers.

Chapter 6 describes the effect of lake restoration with biomanipulation, consisting of fish removal and macrophyte planting, on plankton carbon flows. Specifically, we tested the subsidy of macrophyte-derived carbon to bacterial and zooplankton consumers by comparing the restored part with unrestored parts of Huizhou West lake, a shallow eutrophic lake in China. The contributions of macrophyte and phytoplankton to zooplankton and bacteria were calculated using a two-source isotope mixing model.

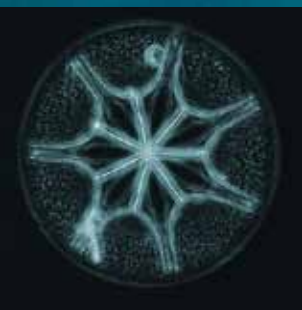
Anna de Kluijver, Karline Soetaert, Kai G. Schulz, Ulf Riebesell, Richard G. J. Bellerby,
and Jack J. Middelburg

Biogeosciences 7: 3783-3797, 2010

Photo: mesocosm by Yves Gladu



2 CHAPTER



**Phytoplankton-bacteria coupling
under elevated CO₂ levels**

Abstract

The potential impact of rising carbon dioxide (CO₂) on carbon transfer from phytoplankton to bacteria was investigated during the 2005 PeECE III mesocosm study in Bergen, Norway. Sets of mesocosms, in which a phytoplankton bloom was induced by nutrient addition, were incubated under 1x (~350 μatm), 2x (~700 μatm), and 3x present day CO₂ (~1050 μatm) initial seawater and sustained atmospheric CO₂ levels for 3 weeks. ¹³C labeled bicarbonate was added to all mesocosms to follow the transfer of carbon from dissolved inorganic carbon (DIC) into phytoplankton and subsequently heterotrophic bacteria, and settling particles. Isotope ratios of polar-lipid-derived fatty acids (PLFA) were used to infer the biomass and production of phytoplankton and bacteria. Phytoplankton PLFA were enriched within one day after label addition, whilst it took another 3 days before bacteria showed substantial enrichment. Group-specific primary production measurements revealed that coccolithophores showed higher primary production than green algae and diatoms. Elevated CO₂ had a significant positive effect on post-bloom biomass of green algae, diatoms, and bacteria. A simple model based on measured isotope ratios of phytoplankton and bacteria revealed that CO₂ had no significant effect on the carbon transfer efficiency from phytoplankton to bacteria during the bloom. There was no indication of CO₂ effects on enhanced settling based on isotope mixing models during the phytoplankton bloom, but this could not be determined in the post-bloom phase. Our results suggest that CO₂ effects are most pronounced in the post-bloom phase, under nutrient limitation.

2.1 Introduction

The ocean is one of the largest reservoirs of CO₂ on earth and one of the largest sinks for anthropogenic CO₂ emissions (Sabine et al. 2004). The biologically mediated flux of CO₂ into the oceans, called the biological pump, is the transport of organic matter (OM) produced at the oceans' surface to the ocean interior, sustaining a vertical CO₂ gradient. The strength of the biological pump is largely controlled by three processes: primary production, community respiration and the export rate of particulate organic matter (POM) into the deep ocean. Community respiration in the euphotic zone, dominated by heterotrophic bacteria, converts organic carbon back into CO₂ and thus decreases the oceans' CO₂ uptake capacity (Rivkin and Legendre 2001). The coupling between phytoplankton and heterotrophic bacteria is mainly via labile dissolved organic matter (DOM). In the upper ocean an important source for labile DOM and subsequently for heterotrophic bacteria is the release of carbon-rich substances by phytoplankton, further referred to as exudation (Larsson and Hagström 1979). Phytoplankton exudation has been defined as the release of excess photosynthates that accumulate when carbon fixation exceeds incorporation into new cell material (Fogg 1983). The rate of exudation is linked to primary production and is highest under nutrient-poor conditions, when nutrient limitation impedes phytoplankton growth, but not photosynthetic carbon fixation (Fogg 1983). Changes in primary production can potentially alter exudation and subsequently phytoplankton-bacteria coupling and the microbial food-web. Increasing CO₂ levels could stimulate primary production (Riebesell et al. 1993), which could result in an increased flow of inorganic carbon into carbon exudates. Carbon exudates tend to accrete into transparent exopolymer particles (TEP), which facilitate aggregation due to their sticky nature (Engel et al. 2004a). These aggregates can facilitate carbon export to the deep ocean if the carbon is not remineralised (Fig. 2.1).

Increased inorganic carbon consumption relative to nitrogen uptake at higher CO₂ levels was observed in natural plankton communities (Riebesell et al. 2007; Bellerby et al., 2008). The additional community uptake of CO₂, however, was not reflected in higher standing stocks of organic material in the surface layer (Fig. 2.1) (Riebesell et al. 2007; Schulz et al. 2008; Egge et al. 2009). Although carbon export could not be quantified directly, the authors proposed that the extra carbon was released as exudates that coalesced and sank to the deep (Fig. 2.1). This implies that increasing CO₂ concentrations could strengthen the biological pump and in this way act as a negative feedback on increasing atmospheric CO₂ concentrations (Arrigo 2007). However, this requires that the additional organic material escapes remineralization by heterotrophic bacteria in the upper layer, which could not be quantified. The community uptake did not account for carbon flows in and from phytoplankton to bacteria to separate primary production from remineralization (Fig. 2.1). Traditionally, the carbon coupling between phytoplankton and bacteria is derived from the relationship between production and abundance of phytoplankton and bacteria (Cole et al. 1988). The drawback of these methods is that net processes are measured and that temporal and spatial decoupling and grazing cannot be quantified. The use of carbon isotope tracers (¹³C, ¹⁴C) provides the possibility to directly quantify the flux of carbon from dissolved inorganic carbon (DIC) to phytoplankton and subsequently bacteria and this method has been successfully used in previous mesocosm experiments (Norman et al. 1995; Lyche et al. 1996) and in whole lake isotope tracer addition experiments (Kritzberg et al. 2004; Pace et al. 2007).

Since it is difficult to physically separate phytoplankton from bulk particulate organic matter (POM), the isotope signal of POM has often been used as a representative for phytoplankton, which can lead to an underestimation of phytoplankton carbon uptake. Similar methodological limitations exist to determine the bacteria isotope signature. A valuable alternative is the analysis of isotope label in biomarkers specific for bacteria and phytoplankton groups (polar-lipid-derived fatty acids, PLFA). The combined technique of isotope labeling and biomarker analysis has proven a very powerful tool to study carbon flows in natural communities, especially in perturbation experiments (Boschker and Middelburg 2002; Van Den Meersche et al. 2004; Pace et al. 2007). Furthermore, label incorporation into phytoplankton biomarkers can be used to determine group-specific growth-rates (Dijkman et al. 2009). Here, we applied the isotope labeling technique to quantify phytoplankton-bacteria coupling under different CO₂ levels. More specifically, we address potential effects of CO₂ on phytoplankton production and growth, and transfer of freshly produced organic matter to the microbial food web and into settling particles (Fig. 2.1). The results contribute to the previous published results on PeECE III by unraveling the carbon interactions between the major planktonic food-web compartments.

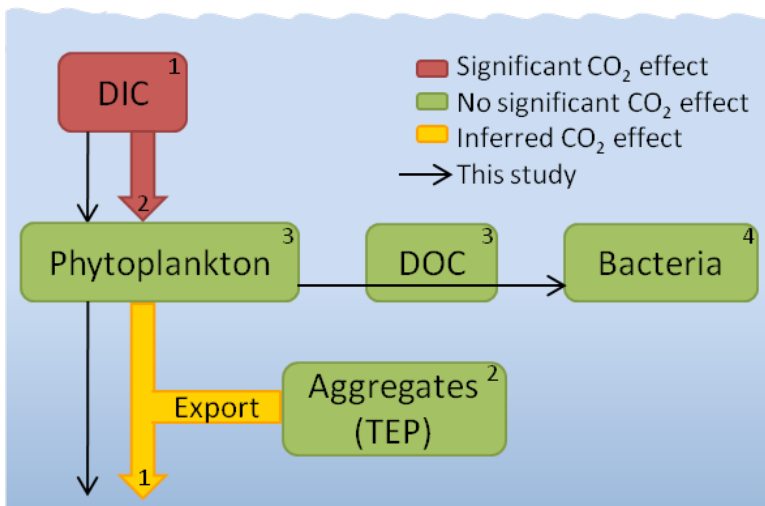


Fig. 2.1. Carbon fluxes between the major food-web compartments of this study and the previous published CO₂ effect on these compartments and fluxes in the PeECE III 2005 mesocosm study. ¹Riebesell et al. (2007) found increased cumulative DIC drawdown at increased $p\text{CO}_2$ during the bloom and inferred enhanced export at high $p\text{CO}_2$; Egge et al. (2008) demonstrated increased cumulative ¹⁴C incorporation at higher $p\text{CO}_2$ in the post-bloom phase; ³Schulz et al. (2008); ⁴Allgaier et al. (2008).

2.2 Material and methods

Set-up and sampling

The PeECE III mesocosm experiment was carried out at the Marine Biological Station, University of Bergen, Norway, between May 16 and June 10, 2005. Nine mesocosms (M1 to M9) of 9.5 m deep and with a volume of 27 m³ each were filled with unfiltered, nutrient-poor post-bloom water from the fjord, and manipulated to achieve 3 sets of different CO₂ levels in mesocosms by aeration of the water column and the overlying atmosphere with CO₂-enriched air. The partial pressures of carbon dioxide ($p\text{CO}_2$) at the start of the experiment were about 350 μatm (1x CO₂, M7-9), 700 μatm (2x CO₂, M4-6), and 1050 μatm (3x CO₂, M1-3). These concentrations are expected to happen during the first half and towards the end of this century under a business-as-usual CO₂ emission scenario. Nitrate (final concentration 15 $\mu\text{mol L}^{-1}$) and phosphate (final concentration 0.7 $\mu\text{mol L}^{-1}$) were added to the mesocosms to initiate a phytoplankton bloom. A more detailed description of the experimental set-up can be found in (Schulz et al. 2008). ¹³C-labeled bicarbonate was added to the upper 5 meter of the mesocosms between day 0 and day 1 to a final addition of ca 2.3 $\mu\text{mol kg}^{-1}$, corresponding to about 0.1 % of total DIC. Water samples for polar lipid fatty acids (PLFA) were taken from the upper layer of each mesocosm daily (day 0 - 18) or every second day (day 20, 22 and 24). The samples were filtered on pre-combusted GF/F filters and stored frozen until further analysis. Sediment traps were placed in each mesocosm at 7.5 m depth and they were collected every 3 days, on day 4, 7, 10, 13, 16, and 19.

PLFA and DIC analysis

The lipids were extracted by a modified Bligh and Dyer method (Bligh and Dyer 1959; Boschker et al. 1998). The lipids were fractionated in different polarity classes by column separation on a heat-activated-silicic acid column and subsequent elution with chloroform, acetone and methanol. The methanol fractions, containing most of the polar-lipid fatty acids, were derivatised to fatty acid methyl esters (FAME). The standards 12:0 and 19:0 were used as internal standards. PLFA concentrations were determined by gas chromatograph–flame ionization detection (GC-FID). The $\delta^{13}\text{C}$ of individual PLFA were measured using gas chromatography-combustion isotope ratio mass spectrometry (GC-C-IRMS) (Middelburg et al. 2000; Van Den Meersche et al. 2004). DIC was analyzed by coulometric titration (Bellerby et al. 2008) and its isotope ratio by a Finnigan GasBench coupled to a Mat 252 mass spectrometer.

Data analysis

Stable isotope data are expressed in the delta notation ($\delta^{13}\text{C}$) relative to VPDB standard and the ¹³C fraction ($^{13}\text{C}/(^{12}\text{C}+^{13}\text{C}) = {}^{13}r$) was derived from the delta notation. Total amount of labeled biomass (total ¹³C) is calculated as

$$\text{total } ^{13}\text{C} = ({}^{13}r_{\text{sample}} - {}^{13}r_{\text{control}}) \cdot \text{concentration} (\mu\text{g C L}^{-1}) \quad (2.1)$$

where ¹³C_{control} is the isotope fraction at day 0, see Middelburg et al. (2000) and Van Den Meersche et al. (2004) for details.

To be able to directly compare labeling of phytoplankton and bacteria biomass between the different mesocosms, the data were corrected for small differences in initial ¹³C-DIC concentrations. This correction factor was calculated for each mesocosm as total ¹³C-DIC at day 1 relative to the average total ¹³C-DIC of all mesocosms at day 1. The correction factor ranged from 0.75 to 1.09.

Out-gassing of ¹³C-DIC was calculated according to Delille et al. (2005) with chemical enhancement factors. The concentration of ¹³CO₂ (aq) was derived from ¹³C-DIC as described in Zeebe and Wolf-Gladrow (2001) with fractionation factors from Zhang et al. (1995) with CO₂ concentrations measured by Bellerby et al. (2008). An approximation of δCO₂-air of -8 ‰ was used, because no exact measures were available (Fry 2006).

The sum of PLFA ai15:0 and i15:0 was used to characterize heterotrophic (gram-positive) bacteria and in the section on methodological comparison, the PLFA 18:1ω7c (gram-negative bacteria) was included. The sum of PLFA 22:6ω3, 20:5ω3, 18:4ω3, 18:5(n-3,6,9,12,16), 18:5ω3, and 18:3ω3 were used to characterize phytoplankton dynamics (Boschker and Middelburg 2002; Dijkman and Kromkamp 2006; Dijkman et al. 2009). Phytoplankton communities were further divided into diatoms (PLFA 16:2ω4, 16:4ω1 and 20:5ω3), coccolithophores (PLFA 18:5ω3 and 18:5(n-3,6,9,12,16)), and green algae (16:4ω3 and 18:3ω3) (Dijkman and Kromkamp 2006; Dijkman et al. 2009). Phytoplankton composition based on PLFA was also estimated with the Bayesian compositional estimator (Van Den Meersche et al. 2008) with the input ratio from (Dijkman and Kromkamp 2006). The final step involved conversion from PLFA to cell biomass. Bacterial biomass was calculated using a conversion factor of 0.0059 g C (ai+i)15:0 per g C biomass, which is the product of 0.056 g C PLFA per g C biomass (Brinch Iversen and King 1990; Middelburg et al. 2000) and 0.105 g C ai15:0+i15:0 per g C PLFA (calculated from Boschker et al. (1998) and references cited therein). Calculated in the same way, the sum of ai15:0+i15:0+18:1ω7c encompassed 25 % of PLFA and the final conversion factor was 0.0137 g C (ai+i15:0, 18:1ω7c) per g C biomass. We used a carbon content of 20 fg cell⁻¹ to convert bacterial biomass to cells (Lee and Fuhrman 1987). The conversion factors for phytoplankton (groups) were derived from data on fatty acid composition in (Dijkman and Kromkamp 2006). Chlorophyll *a* (chl *a*) concentrations were converted to biomass assuming a C to chl *a* ratio of 45 based on literature values. Although conversion factors are disputable, they don't affect the general patterns nor inferred transfer dynamics from phytoplankton to bacteria. Group-specific growth rates (μ, d⁻¹) during the bloom (from day 5 to day 9) were calculated as

$$\mu = \ln \frac{{}^{13}\text{C biomass}_t + \Delta_t}{{}^{13}\text{C biomass}_t} / \Delta t \quad (2.2)$$

Data from sediment traps were only analyzed for isotope ratios of specific PLFA and not for concentrations because these were biased due to significant over trapping (Schulz et al. 2008). The material in the traps was subdivided in phytoplankton and bacteria using PLFA, similarly as for the suspended particulate matter. The fraction of material derived from the upper layer in the settled material was calculated with the mixing equation (Fry 2006). The equation used is:

$$f_{\text{upper layer}} = (\delta^{13}\text{C}_{\text{sediment}} - \delta^{13}\text{C}_{\text{control}}) / (\delta^{13}\text{C}_{\text{upper layer}} - \delta^{13}\text{C}_{\text{control}}) \quad (2.3)$$

where $\delta^{13}\text{C}_{\text{control}}$ is the isotope ratio at day 0 and $\delta^{13}\text{C}_{\text{upper layer}}$ is the isotope ratio of the pelagic PLFA, averaged over the days of settlement. This fraction provides a measure of exchange between upper and deeper layer and can therefore be used as an indication of sinking.

Within the PeECE III study, POC, inorganic nutrients, and chl *a* (Schulz et al. 2008), pigments (Riebesell et al. 2007; Schulz et al. 2008), and bacterial numbers (Allgaier et al. 2008; Paulino et al. 2008) were published earlier and used for comparative purposes in this study.

Model

A simple source-sink isotope ratio model was used to determine label transfer from phytoplankton to bacteria (Hamilton et al. 2004; Van Oevelen et al. 2006). The following equation was used

$$\frac{d\delta^{13}\text{C}_{\text{bac}}}{dt} = r_{\text{bac}} \cdot f_{\text{phyto}} \cdot \delta^{13}\text{C}_{\text{phyto}} - r_{\text{bac}} \cdot \delta^{13}\text{C}_{\text{bac}} \quad (2.4)$$

where r_{bac} = bacteria turnover (d^{-1}) and f_{phyto} = fraction of ^{13}C derived from phytoplankton.

The weighted $\Delta\delta^{13}\text{C}$ of phytoplankton was used as a forcing function and the weighted $\Delta\delta^{13}\text{C}$ of bacteria was used for model calibration. The original data were used to fit the model, instead of ^{13}C -DIC normalized data, but they would give similar results. The assumption for this model is that biomass is constant with time. The model equations were implemented in R, using the packages FME and deSolve (Soetaert and Petzoldt 2009; Soetaert et al. 2009).

The time sequence of the model was 0-24 days and initial conditions were set to 0. Parameter calibration was done with pseudo-randomization followed by Levenberg-Marquardt algorithm (Press et al. 2001). The parameters were further assessed with the Markov-Chain-Monte-Carlo technique (MCMC) (Gelman et al. 1996). During the MCMC, the model was run 5000 times for each mesocosm, resulting in approximately 1500-1750 accepted runs per mesocosm. The mean and standard deviation were calculated for each parameter.

The dependency of heterotrophic bacteria on recently fixed carbon was also calculated using mean isotope ratios over the last 10 days of the experiment ($\Delta\delta^{13}\text{C}_{\text{bac}}/\Delta\delta^{13}\text{C}_{\text{phyto}}$). This simple calculated ratio should approach f_{phyto} at steady-state (Van Oevelen et al. 2006).

Statistics

Results are reported as mean \pm standard deviation. In order to test if measured concentrations of phytoplankton and bacteria differed significantly ($p < 0.05$) over time among $p\text{CO}_2$ levels, repeated measures ANOVAs and Bonferroni post-hoc tests were applied using the software Statistica® (stat Soft, Inc., U.S., 2009). Prior to analyses, data were checked for normality, homogeneity of variance, and sphericity. Significant ($p < 0.05$) differences in phytoplankton growth rates and model parameters were assessed using one-way ANOVA.

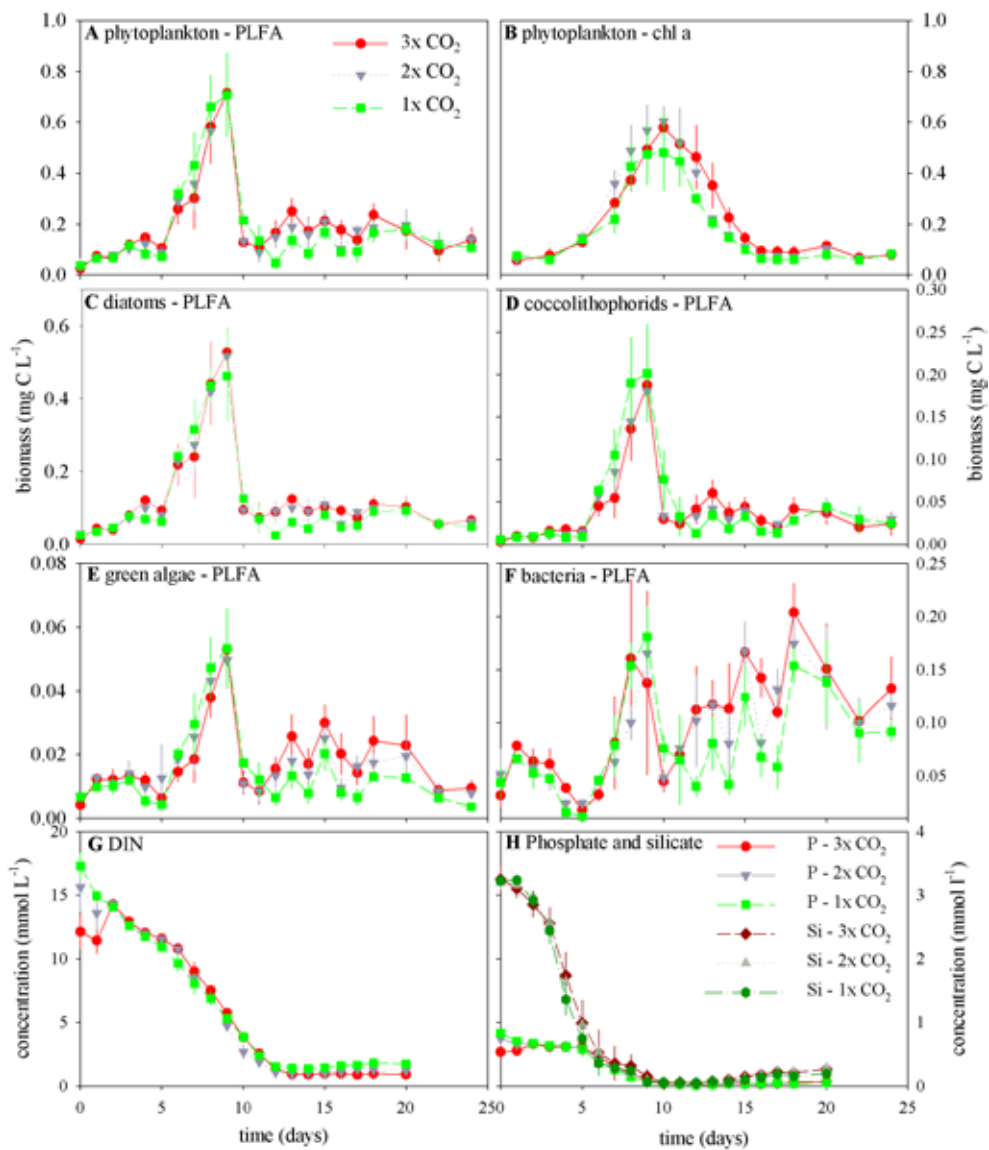


Fig. 2.2. Concentration of (A) total phytoplankton carbon based on PLFA, (B) total phytoplankton based on chlorophyll-*a* and PLFA derived carbon estimates for (C) diatoms, (D) coccolithophores, (E) green algae, (F) bacteria. Concentrations of (G) dissolved inorganic nitrogen, (H) phosphate and silicate in the different CO₂ treatments. Average and SD of the three replicates are shown.

2.3 Results

Phytoplankton dynamics

PLFA specific for phytoplankton were used to depict phytoplankton dynamics and their carbon concentrations were converted to total carbon biomass. The addition of nutrients induced a phytoplankton bloom as depicted by both PLFA (Fig. 2.2A) and chlorophyll-*a* (Fig. 2.2B). During the experiment 3 different phases in phytoplankton dynamics could be observed: before the bloom (day 0-5), the bloom (day 5-9), and the post bloom (after day 9). Based on nutrient dynamics, 4 phases were identified by Riebesell et al. (2008) and Tanaka et al. (2008). From start until day 6, there was no nutrient depletion, during day 7-9 silicate was depleted, during day 10-12 silicate and phosphate were depleted and from day 13 onwards, all nutrients were depleted.

The development of the bloom as depicted by PLFA reflects the dynamics of phosphate concentrations. When phosphate became depleted, the phytoplankton bloom collapsed (Fig. 2.2A, 2.2H). Phytoplankton biomass (based on PLFA) was low in the first five days of the experiment, with values $< 0.2 \text{ mg C L}^{-1}$. After day 5 the phytoplankton bloom started and phytoplankton biomass rapidly increased up to $0.71 \pm 0.10 \text{ mg C L}^{-1}$ at day 9, the peak of the bloom assessed using PLFA (Fig. 2.2A). The bloom collapsed after day 9 to $0.16 \pm 0.043 \text{ mg C L}^{-1}$ at day 10 and stayed around this concentration until the end of the experiment. Phytoplankton biomass (based on chl-*a*) increased from $0.064 \pm 0.0091 \text{ mg C L}^{-1}$ at day 0 to $0.55 \pm 0.11 \text{ mg C L}^{-1}$ at day 10, the peak of the bloom. From then on, the bloom continuously decreased until starting values were reached again around day 16 (Fig. 2.2B) (Schulz et al. 2008).

No CO₂ effects on phytoplankton concentrations and dynamics were observed before and during the bloom (day 0-9). During the post-bloom the phytoplankton biomass based on PLFA was significantly lower in the 1x CO₂ treatment than in the 2x and 3x CO₂ treatments (repeated measures ANOVA, $F(2,6) = 25.66, p < 0.005$) (Table 2.1). The largest differences in biomass occurred between day 12 and day 17. The development of phytoplankton biomass as determined with PLFA (Fig. 2.2A), chl-*a* (Fig. 2.2B) and particulate organic carbon (POC) are summarized in Fig. 2.3A. The range in biomass is similar for all methods, with values from 0 - 1.2 mg C L^{-1} . The timing of the bloom, however, is different for all methods. The peak of the bloom was at day 9 with PLFA, at day 10 with chl-*a*, and at day 11 for POC.

Phytoplankton was further subdivided into the major phytoplankton groups. Conversion of typical PLFA biomarkers for each group into biomass revealed that diatoms were the most abundant taxa, followed by coccolithophores and a minority of green algae (Fig. 2.2C, D, and E). The different taxa showed a similar response during the incubations, peaking at day 9. Diatom biomass rapidly increased after day 5 up to $0.50 \pm 0.081 \text{ mg C L}^{-1}$ at the peak of the bloom on day 9. The bloom declined to $0.11 \pm 0.048 \text{ mg C L}^{-1}$ at day 10 and remained low until the end of the incubations (Fig. 2.2C). A significant CO₂ effect could be detected in the post-bloom phase. The diatom biomass was significantly higher in the 2x CO₂ and 3x CO₂ treatments than in the 1x CO₂ treatment, similar as for total phytoplankton (repeated measures ANOVA, $F(2,6) = 15.51, p < 0.005$) (Table 2.1). The CO₂ effect was mainly effective from day 12 to day 17. Coccolithophore biomass rapidly increased after day 5 and reached a peak of $0.19 \pm 0.066 \text{ mg C L}^{-1}$ at day 9. Coccolithophores declined after the bloom peak to concentrations of $0.047 \pm 0.028 \text{ mg C L}^{-1}$ at day 10 and remained low during the rest of the experiment (Fig. 2.2D).

Table 2.1. Average non-labeled biomass (mg C L⁻¹) and labeled biomass (μg C L⁻¹) of major phytoplankton groups and bacteria in the post-bloom phase (day 10-day 24) with *p*-values from post-hoc Bonferroni analyses after repeated measures ANOVA.

Organism	Value	1xCO ₂	2xCO ₂	3xCO ₂	<i>p</i> 1x,2x	<i>p</i> 1x,3x	<i>p</i> 2x,3x
Total phytoplankton	Biomass	0.13	0.15	0.17	0.009	0.001	0.22
	Labeled biomass	0.12	0.14	0.15	0.061	0.010	0.49
Diatoms	Biomass	0.066	0.085	0.090	0.017	0.006	0.96
	Labeled biomass	0.054	0.067	0.070	0.017	0.004	0.62
Coccolithophores	Biomass	0.030	0.032	0.034	1.00	0.86	1.00
	Labeled biomass	0.027	0.028	0.029	1.00	1.00	1.00
Green algae	Biomass	0.011	0.014	0.017	0.072	0.003	0.080
	Labeled biomass	0.0089	0.012	0.015	0.23	0.011	0.14
Bacteria	Biomass	0.086	0.11	0.12	0.014	0.002	0.34
	Labeled biomass	0.067	0.083	0.089	0.061	0.013	0.67

Values in bold are significant (*p* < 0.05)

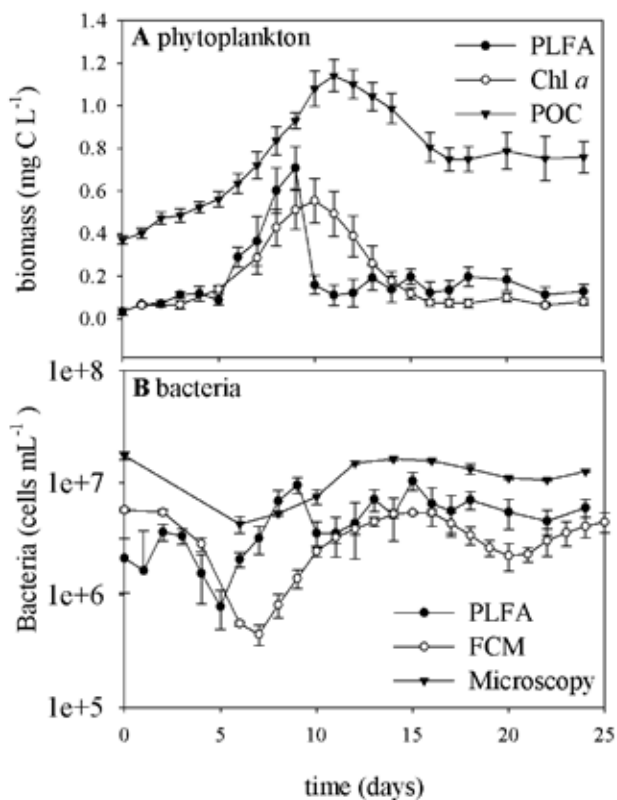


Fig. 2.3. Comparison of (A) phytoplankton biomass based on PLFA, Chl-*a*, and POC and (B) bacterial numbers based on PLFA, Flow Cytometry (FCM), and microscopy. Average and SD of all mesocosms are shown.

The development of coccolithophores in the post-bloom phase was independent of CO_2 (Table 2.1). The biomass of green algae was much lower than that of diatoms and coccolithophores with a maximum of $0.052 \pm 0.0071 \text{ mg C L}^{-1}$ at day 9 (Fig. 2.2E). The development of green algae in the post-bloom phase was dependent on CO_2 levels. Green algal biomass remained higher at elevated CO_2 levels, but only between the 1x and 3x CO_2 treatments were differences significant (repeated measures ANOVA, $F(2,6) = 17.61$, $p < 0.005$) (Table 2.1).

Bacterial dynamics

Bacterial dynamics showed more fluctuation during the experiment than phytoplankton (Fig 2.2F). Initially, the bacteria biomass declined to a minimum at day 5 of $0.018 \pm 0.0060 \text{ mg C L}^{-1}$. At the onset of the phytoplankton bloom, bacterial biomass started to increase. The bacterial biomass based on PLFA reached concentrations of $0.16 \pm 0.051 \text{ mg C L}^{-1}$ at the bloom peak on day 9 followed by a rapid decline to $0.056 \pm 0.017 \text{ mg C L}^{-1}$ at day 10 (Fig. 2.2F). After day 10, bacterial concentrations started to increase again to reach a second peak of $0.18 \pm 0.030 \text{ mg C L}^{-1}$ at day 18. In the post-bloom phase, the bacterial biomass was significantly higher at 3x CO_2 and 2x CO_2 compared to 1x CO_2 (repeated measures ANOVA, $F(2,6) = 20.30$, $p < 0.005$) (Table 2.1). The CO_2 effect was most pronounced between day 12 and day 17.

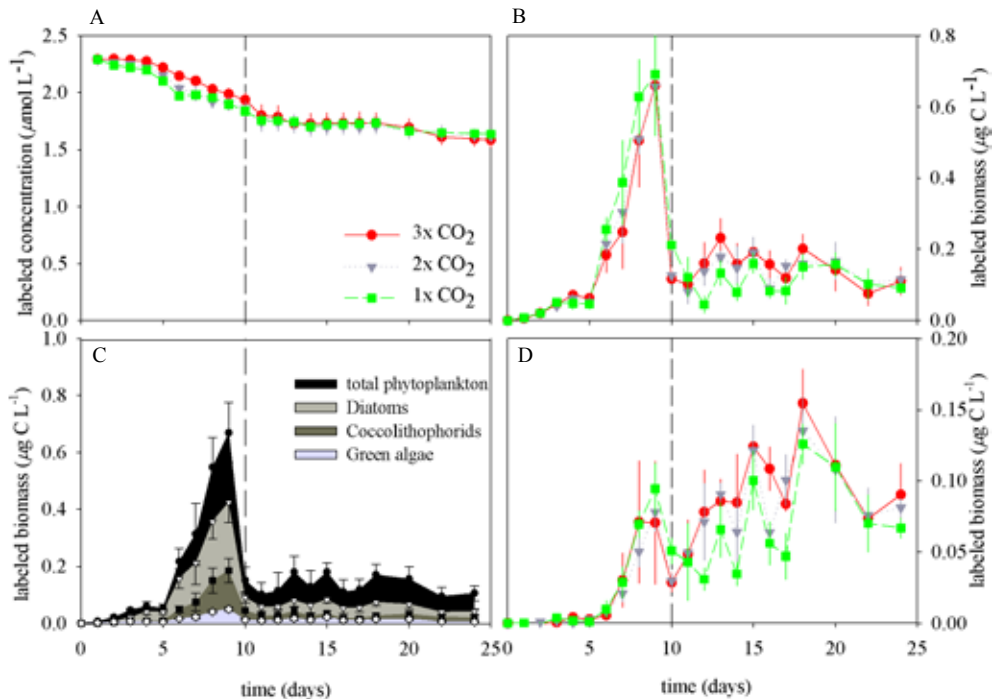


Fig. 2.4 Concentrations of ^{13}C labeled (A) DIC, (B) phytoplankton, phytoplankton groups (C), and (D) bacteria. Average and SD of the three replicates are shown for (A-C) and average and SD of all mesocosm data are shown in (D).

Bacterial cell abundances as determined by PLFA (this study, Fig. 2.2F), flow cytometry (FCM) (Paulino et al. 2008), and microscopy (Allgaier et al. 2008) are summarized in Fig. 2.3B. The range of cell numbers was similar for all methods (10^9 - 10^{10} cells L⁻¹), indicating that bacteria were quantitatively retained on the GF/F filters used. However, the development of bacteria during the experiment differed for the three methods. The most striking difference occurred around the phytoplankton peak. While flow cytometry and microscopy revealed a minimum in bacterial abundance, PLFA based numbers showed a maximum in bacterial abundance.

Labeling

¹³C-labeled DIC addition resulted in an increase of $\delta^{13}\text{C}$ -DIC with 100.5 ± 11.9 ‰, from -1.73 ± 1.01 ‰ at day 0 up to 98.8 ± 12.5 ‰ at day 1. The large variation was caused by addition of different amounts of ¹³C bicarbonate to individual mesocosms. During the experiment, the isotope ratio of DIC gradually decreased in all mesocosms to about 74 ‰ at day 25. Labeled DIC concentrations were $2.29 \mu\text{mol C L}^{-1}$ at day 1 and gradually decreased to $1.62 \pm 0.05 \mu\text{mol C L}^{-1}$ at day 25 (Fig. 2.4A). The decrease in labeled DIC was independent of CO₂ levels. The loss of label from gas exchange between water and air was calculated only for the first 5 days, when biomass was still low. Label loss due to gas exchange was negligible for all treatments (< 0.1 ‰). A large part of labeled DIC was lost due to mixing with the deeper water layers. Assuming a mixing efficiency of 12% as calculated in Schulz et al. (2008), mixing with the deeper layers could explain 63 ± 10 % of label loss.

The transfer from DIC to phytoplankton was very rapid; label enrichment in phytoplankton-specific PLFA was already detectable at day 1. The labeling of phytoplankton steadily increased from day 1 onwards and reached a maximum of 86.9 ± 10.4 ‰ at day 10, denoting that phytoplankton carbon reached steady-state with dissolved inorganic carbon. The ratios of phytoplankton isotope signature relative to DIC isotope signature, averaged over the last 10 days (day 15- 24), are presented in Table 2.2. The average value was 1.04 ± 0.033 over all mesocosms, implying complete turnover of algal biomass during the experimental period.

Table 2.2. Model parameters and steady-state ratios for each mesocosm \pm standard deviation.

Mesocosm	r_{bac} (model)	f_{phyto} (model)	$\Delta\delta_{\text{phytoplankton}}/\Delta\delta_{\text{DIC}}^*$	$\Delta\delta_{\text{bacteria}}/\Delta\delta_{\text{phytoplankton}}^*$
7 - 1x CO ₂	0.197 ± 0.0305	0.924 ± 0.0427	1.05	0.882
8 - 1x CO ₂	0.197 ± 0.0291	0.908 ± 0.0434	1.03	0.857
9 - 1x CO ₂	0.208 ± 0.0230	0.942 ± 0.0370	1.00	0.905
Average 1x CO ₂	0.201 ± 0.00667	0.925 ± 0.0170	1.03 ± 0.023	0.8810 ± 0.0241
4 - 2x CO ₂	0.208 ± 0.0267	0.208 ± 0.0267	1.01	0.885
5 - 2x CO ₂	0.191 ± 0.0243	0.925 ± 0.0375	1.02	0.879
6 - 2x CO ₂	0.230 ± 0.0516	0.888 ± 0.0513	1.10	0.851
Average 2x CO ₂	0.209 ± 0.0195	0.911 ± 0.0203	1.04 ± 0.050	0.872 ± 0.0181
1 - 3x CO ₂	0.270 ± 0.0475	0.860 ± 0.0371	1.04	0.857
2 - 3x CO ₂	0.223 ± 0.0258	0.904 ± 0.0258	1.02	0.873
3 - 3x CO ₂	0.192 ± 0.0303	0.920 ± 0.0410	1.08	0.864
Average 3x CO ₂	0.228 ± 0.0395	0.895 ± 0.0308	1.04 ± 0.031	0.865 ± 0.00769

*average ratios over the last 10 days (day 15-24)

The development of label incorporation into phytoplankton matched with total phytoplankton dynamics; the labeled biomass was low in the first 5 days and then increased to a bloom peak at day 9 of $0.67 \pm 0.10 \mu\text{g C L}^{-1}$. The labeled biomass rapidly declined to $0.15 \pm 0.046 \mu\text{g C L}^{-1}$ at day 10 and remained around this level until the end of the experiment (Fig. 2.4C). Labeled phytoplankton biomass in the post-bloom phase was significantly higher in the 3x CO₂ treatment than in the 1x CO₂ treatment, similar as for non-labeled phytoplankton biomass. The difference between the 1x CO₂ and 2x CO₂ treatments was not significant for labeled biomass in contrast to non-labeled biomass (repeated measures ANOVA, $F(2,6) = 11.51$, $p < 0.01$) (Table 2.1). The CO₂ effect was most pronounced from day 12 to day 17.

The labeling of the different phytoplankton groups was similar to labeling of total phytoplankton. Labeling of the different phytoplankton groups is presented as an average of all mesocosms in Fig. 2.4C. The CO₂ effects on the different phytoplankton groups were similar as for non-labeled biomass. Significant CO₂ effects were found in the post-bloom phase for diatoms, where biomass was higher in the 3x and 2x CO₂ treatments than in the 1x CO₂ incubations (repeated measures ANOVA, $F(2,6) = 17.02$, $p < 0.005$) and for green algae, where biomass was significantly higher in the 3x CO₂ treatment compared to the 1x CO₂ treatment (repeated measures ANOVA, $F(2,6) = 10.84$, $p = 0.01$) (Table 2.1). The specific growth rate during the bloom, as determined from label incorporation in biomass from day 5 to day 9, was highest for coccolithophores with a value of $0.76 \pm 0.11 \text{ d}^{-1}$, followed by green algae ($0.63 \pm 0.11 \text{ d}^{-1}$), and diatoms ($0.59 \pm 0.054 \text{ d}^{-1}$) (Fig. 2.5). Total phytoplankton growth rate was $0.64 \pm 0.075 \text{ d}^{-1}$. The growth rate of coccolithophores was significantly higher than the growth rates of green algae and diatoms (ANOVA, $F(2,24) = 7.40$, $p < 0.005$). Although the growth rates for each single group were not significantly affected by CO₂ treatment, it appeared that for coccolithophores, green algae and total phytoplankton, the growth rate was highest under current CO₂ levels (1x CO₂) (Fig. 2.5).

The transfer of label to bacteria was much slower than the label transfer from DIC to phytoplankton. It was only at day 3 or 4, depending on the mesocosm, that enrichment could be detected in bacterial specific PLFA (Fig. 2.4D and 2.6). Average enrichment was $3.9 \pm 3.1 \%$ on day 3 and $7.4 \pm 5.8 \%$ on day 4. The isotope ratio steadily increased until $72.3 \pm 8.8 \%$ at day 14, denoting isotope equilibrium.

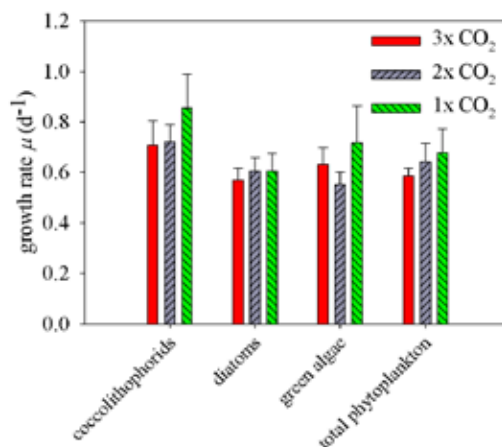


Fig. 2.5. Phytoplankton group-specific growth rates during the bloom period, day 5-9. Average and SD are shown.

The ratios of bacterial isotope signature to phytoplankton isotope signature over the last 10 days (day 15 - day 24) are presented in table 2.2 for each mesocosm. The average ratio over all mesocosms was 0.87 ± 0.017 implying that 87 % of the bacterial carbon was derived from recently fixed phytoplankton material. The other 13 % was derived from non-labeled material. The dynamics of labeled bacteria were comparable with non-labeled bacteria; biomass was low in the first 5 days and showed some fluctuation in time. The peak in biomass was reached at day 18 with concentrations of $0.14 \pm 0.022 \mu\text{g C L}^{-1}$ and declined afterwards (Fig. 2.4C). The labeled bacterial biomass was significantly higher in the post-bloom phase in the 3x CO₂ treatment compared to 1x CO₂, but not in the 2x CO₂ treatment as for non-labeled biomass. The CO₂ effect was mainly present between day 12 and 17 (repeated measures ANOVA, $F(2,6) = 10.48, p < 0.05$) (Table 2.1).

Model

The transfer from phytoplankton to bacteria was quantified using a simple source-sink model (equation 2.1). The initial parameters range was 0-1 d⁻¹ for both r_{bac} and f_{phyto} . The Bayesian approach produced a good fit to the data of all mesocosms (Fig. 2.6) and we were able to individually fit the parameters. Because of the large number of MCMC runs, reliable parameter distributions were obtained. The solid black lines are the model output, using the medians of the modeled bacterial ratios. The dark grey areas represent the 95 % posterior limits of the model uncertainties. The light grey areas present the 95 % posterior limits in predicting new observations (Malve et al. 2005; Malve et al. 2007). The turn-over rates for bacteria (r_{bac}) were $0.20 \pm 0.01 \text{ d}^{-1}$, $0.21 \pm 0.02 \text{ d}^{-1}$, and $0.23 \pm 0.04 \text{ d}^{-1}$, for 1x CO₂, 2x CO₂, 3x CO₂ treatments respectively (Table 2.2). The fractions of bacterial carbon derived from phytoplankton (f_{phyto}) were $0.92 \pm 0.02 \text{ d}^{-1}$, $0.91 \pm 0.02 \text{ d}^{-1}$, $0.89 \pm 0.03 \text{ d}^{-1}$, for 1x CO₂, 2x CO₂, 3x CO₂ treatments respectively (Table 2.2). The parameters were not significantly different for the different CO₂ treatments, but a trend with CO₂ concentrations could be observed. The value of f_{phyto} decreased with increasing CO₂ concentrations and the value of r_{bac} increased with increasing CO₂ concentrations.

Settled material

The isotope ratios of the material in the sediment traps were used to investigate whether sinking of organic matter from the upper layer to the deeper layer in the mesocosms was affected by the different treatments. The average isotope ratios of biomarker PLFA from the upper layer and the average isotope ratio of unlabeled PLFA (day 0) were used in the isotope mixing model to calculate the fraction in the traps derived from the upper layer. The fraction represents the exchange of material between upper and deeper layers. The fraction increased in time and was 0.29 ± 0.051 at day 4 and gradually increased to 0.90 ± 0.028 at day 16 for phytoplankton (Fig. 2.7A). Exchange was slightly faster in the beginning for bacterial PLFA than for phytoplankton PLFA. The fraction for bacteria was already 0.43 ± 0.12 at day 7, while it was only 0.33 ± 0.030 for phytoplankton. The exchange for bacteria gradually increased to 0.80 ± 0.077 at day 19 (Fig. 2.7B). Isotope mixing, which is an indication for sinking, was independent of CO₂ treatment.

2.4 Discussion

The combined use of stable isotopes and biomarkers provides a powerful tool to elucidate and quantify carbon fluxes in natural plankton communities (Boschker and Middelburg 2002; Van Den Meersche et al. 2004; Pace et al. 2007). Here we applied the combined technique to determine the uptake of dissolved inorganic carbon by phytoplankton and subsequent transfer within the plankton community under different CO₂ levels. To our best knowledge, this is the first time that this approach is used to directly examine the transfer from phytoplankton to bacteria under changing CO₂ levels. The broad range of measured parameters (Riebesell et al. 2008) provided the opportunity to adequately describe the community response and to validate the use of PLFA as biomarkers. The high reproducibility of data between the different mesocosms resulted in robust outcomes of this experiment.

Phytoplankton and bacterial dynamics

The addition of inorganic nutrients initiated a phytoplankton bloom. The collapse of the bloom coincided with phosphate depletion at day 10 (Fig. 2.2A, 2.2H). The phytoplankton biomass at the bloom peak based on PLFA was ~ 0.7 mg C L⁻¹, which corresponds to a moderate bloom. The peak in phytoplankton biomass as observed with PLFA occurred earlier (day 9) than the observed peak with chlorophyll-*a* (day 10) and POC (day 11) (Fig. 2.3A). The disagreement between bloom dynamics revealed with chlorophyll-*a* and PLFA is most likely due to function and structure of biomarkers and their turn-over after cell death. PLFA are structural components of the cell membrane that rapidly decay after cell death. Consistent with pigment data (Riebesell et al. 2007; Schulz et al. 2008), PLFA data revealed that the bloom was dominated by prymnesiophytes (or coccolithophores) and diatoms (Fig. 2.2C, 2.2D, 2.2E). The group-specific dynamics, however, were different between pigment and PLFA analysis. In our study, no difference in diatom and coccolithophores succession was observed with PLFA. However, Riebesell et al. (2007), showed that diatoms peaked 1-2 days before coccolithophores, based on pigment analyses. The difference in succession of diatoms and coccolithophores with HPLC can be explained by earlier depletion of silicate (day 7) compared to phosphate (day 10) (Fig. 2.2H) (Schulz et al. 2008). Phytoplankton cell numbers for different groups were determined in this study with flow cytometry, but showed much more variability in time than PLFA and pigment analyses. POC reflects the total organic carbon pool including extracellular polymeric substances and phytoplankton detritus, which explains the ongoing build-up after the bloom peak (Fig. 2.3A) (Engel et al. 2002, Van den Meersche et al. 2004). Label incorporation into PLFA has proven to be a valuable tool to determine group-specific growth rates (Dijkman et al. 2009). High net growth rates were observed during the bloom with coccolithophores growing significantly faster than green algae and diatoms (Fig. 2.4). Our findings agree with the results obtained with the dilution method combined with pigment analysis during PeECE III, where prymnesiophytes growth rates were higher than diatom growth rates during the bloom (Suffrian et al. 2008).

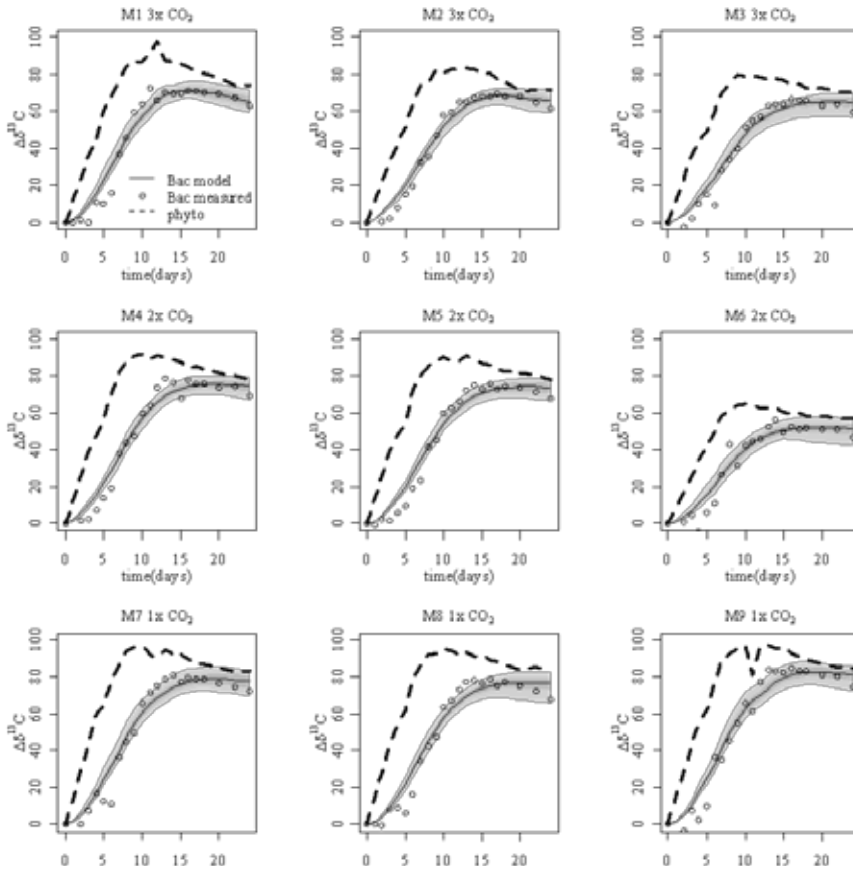


Fig. 2.6. Model simulations of ^{13}C transfer from phytoplankton to heterotrophic bacteria for individual mesocosms. Phytoplankton $\Delta\delta^{13}\text{C}$ data (dashed line) are used as forcing function for model prediction (solid line; Bacteria (Bac) model) of bacterial $\Delta\delta^{13}\text{C}$ data (open dots; Bac measured). Dark and light grey areas give 95 % limits on model uncertainty and in predicting new observations, respectively (see text).

The collapse of the phytoplankton bloom did not result in a noticeable increase in bacterial biomass and we did not observe a distinct heterotrophic phase in the second part of the experiment (Fig. 2.3). Bacterial dynamics correlated with phytoplankton dynamics during the phytoplankton bloom, with simultaneous higher concentrations of phytoplankton and bacteria. Overall, bacterial biomass increased during the experiment. In the PeECE III experiment, bacteria dynamics were also determined by microscopy (Allgaier et al. 2008) and flow cytometry (FCM) (Paulino et al. 2008). Bacterial dynamics based on PLFA biomarkers revealed a different pattern compared to dynamics based on microscopy and FCM. A striking difference between the different methods was between day 5 and 9. While microscopy and flow cytometry showed a minimum in bacterial numbers during the bloom build-up, PLFA showed a peak in bacterial abundance (Fig. 2.3B). This discrepancy can be explained by underestimation of bacterial number by FCM and microscopy due to shading by phytoplankton and a large number of phytoplankton-attached bacteria.

We chose to assess the interactions with this simple model, with a few parameters, because it was possible to directly test the effect of CO₂ on the parameters of the system. In the first 7 days the model slightly overestimates the isotope ratio of bacteria (Fig. 2.6). The explanation for this is that f_{phyto} is in fact not constant in time; it will change in response to phytoplankton abundance.

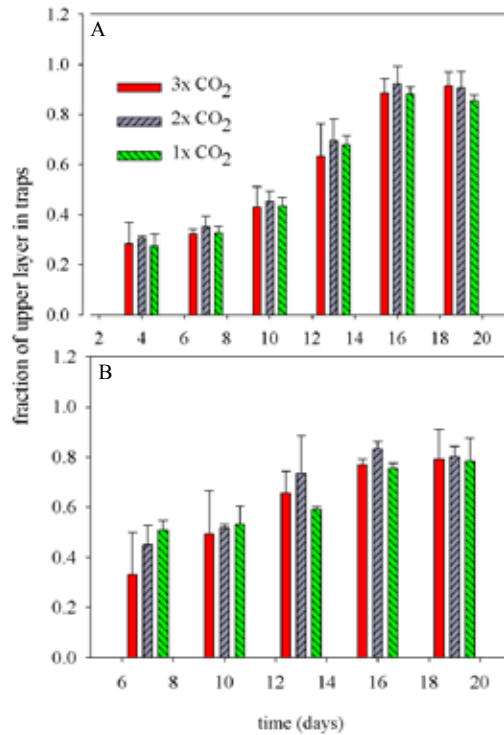


Fig. 2.7. The fractions in the sediment traps derived from the upper layer for (A) phytoplankton and (B) bacteria. Average and SD are shown for the triplicate mesocosms.

Phytoplankton –bacteria coupling

Phytoplankton derived organic matter is an important food-source for heterotrophic bacteria, resulting in a tight coupling between phytoplankton and bacterial production and abundance (Cole et al. 1988). Based on ¹³C label dynamics, we observed a transfer from freshly produced phytoplankton material to heterotrophic bacteria. The label was detected in bacteria 2-3 days after incorporation in phytoplankton. At the end of the experiment 87 % of bacterial carbon was derived from newly produced phytoplankton material (Fig. 2.4, Table 2.2). Overall the first part of the isotope curves mainly reflect uptake and turn-over dynamics, whereas the latter parts of the labeling experiment reflect food source clarification (Fry 2006). To quantify turn-over dynamics and food source clarification in relation to CO₂ levels we applied a simple source-sink model as used in (Hamilton et al. 2004; Carpenter et al. 2005; Van Oevelen et al. 2006). In this model it is assumed that loss processes do not affect the isotope ratio (Fig. 2.2F, Fig. 2.4d).

This is correct only if losses (e.g. bacterial respiration) operate on the bulk tissue. The sources however enrich the isotopic composition of the bacteria with the signature of the source compartment. We chose to assess the interactions with this simple model, with a few parameters, because it was possible to directly test the effect of CO₂ on the parameters of the system. In the first 7 days the model slightly overestimates the isotope ratio of bacteria (Fig. 2.6). The explanation for this is that f_{phyto} is in fact not constant in time; it will change in response to phytoplankton abundance.

The parameters obtained with our model are consistent with values described previously and obtained in other ways. Bacterial turn-over rates based on phytoplankton production ranged from 0.19 d⁻¹ to 0.27 d⁻¹ with an average of 0.21 d⁻¹ in this study (Table 2.2). An average bacterial production of 20 % of primary production was found in a literature survey by Cole et al. (1988). The fraction of bacterial biomass derived from phytoplankton products ranged from 0.86 to 0.94 with an average of 0.91, meaning that 91 % of carbon in bacteria was coming from freshly produced phytoplankton material. The model derived dependency factors (f_{phyto}) are slightly higher than those based on the ratio $\Delta\delta^{13}\text{C}_{\text{bac}}/\Delta\delta^{13}\text{C}_{\text{phyto}}$ (Table 2.2), because of a slight decrease in bacterial isotope ratios at the end of the experiment. Dependency factors smaller than 1 indicate that bacteria also used the unlabeled algal carbon just fixed prior to incubation or used the unlabeled, background DOC pool, or the presence of an inactive bacteria population. Measurements of ¹³C-DOC are required to test for these possibilities.

Few studies have used tracer dynamics and combined modeling to estimate carbon fluxes in natural plankton communities, making comparison limited. A similar experiment was conducted by Norrman et al. (1995) who studied ¹³C carbon transfer from phytoplankton to bacteria in an estuarine mesocosm experiment. At the end of their incubations, isotope ratios in bacteria were lower than those of POC, indicating that bacteria relied partly on not freshly produced material. A similar estimation of fluxes has been reported by Lyche et al. (1996) who traced ¹⁴C in different size fractions as probes for primary and secondary production in a mesocosm study with lake communities. Their values were slightly different from ours (Table 2.2), with bacteria assimilation rates of 0.485 d⁻¹ and a fraction of 0.704 derived from the phytoplankton. In contrast, Pace et al (2007) observed almost complete dependence of heterotrophic (gram-positive) bacteria on phytoplankton in a clear-water lake. In their study, the whole lake was enriched with ¹³C-DIC and traced into phytoplankton and bacteria, derived from ¹³C incorporation in PLFA biomarkers. Van Den Meersche et al. (2004) studied phytoplankton-bacteria interactions in a tracer experiment with estuarine water and also used PLFA biomarkers. They found a 100 % dependency of bacteria on freshly produced phytoplankton material, revealed by similar isotope ratios in bacteria and phytoplankton PLFA at the end of the experiment.

We found a delay of 2-3 days in carbon transfer from phytoplankton to bacteria in all mesocosms (Fig. 2.6). The time lag is consistent with previous studies on phytoplankton-bacteria coupling. Duarte et al. (2005) observed a time-lag of 0-4 days between phytoplankton production and bacterial production in Southern Ocean plankton incubations. Ducklow et al. (1999) also observed lag periods of several days in bacterial response to phytoplankton bloom development in Southern Ocean plankton incubations. Van Den Meersche et al. (2004) observed a ~1 day delay in labeling of bacteria compared to phytoplankton.

Studies on biomass standing stocks of phytoplankton and bacteria during phytoplankton spring blooms also revealed some uncoupling and delay in response of bacteria to phytoplankton, varying from several days to weeks (Kirchman et al. 1994; Lochte et al. 1997), while a close coupling was observed by Lancelot and Billen (1984). There are several possible explanations for these ‘lags’ or ‘uncoupling’. The most obvious explanation is the presence of unlabeled DOM at the start of the experiment, which is later replenished by labeled DOM. DOM release by phytoplankton can occur passively (leakage and viral lysis) or actively under nutrient starvation (Van Den Meersche et al. 2004). Possibly, DOM release was low in the first part of the experiment (before and during the bloom) because it occurred mainly passively and the major DOM release took place during the bloom collapse, although this was not reflected in standing-stock measurements of DOC (Schulz et al. 2008). Other explanations that concern more the physiological state of the bacteria have been summarized by Ducklow et al. (1999). They suggested that most, if not all, marine bacteria exist predominantly in a state of dormancy, under severe carbon, phosphate, and/or energy starvation. Another possibility is that the apparent lag phase reflects logistic (s-shaped) growth curves. A third scenario concerns the hypothetical existence of non-dividing subpopulations of cells which are progressively overgrown by the growing populations. The high dependency of bacteria on phytoplankton (Table 2.2) and the small increase in DOM standing stocks (Schulz et al. 2008) during the experiment indicate a strong coupling between phytoplankton and heterotrophic bacteria. Probably there was strong grazing pressure on bacteria that kept the bacterial standing stock low. Bacterivory was indeed high during the experiment as determined by measuring uptake of fluorescent labeled bacteria by protists (Tanaka and Løvdal, unpublished data, 2005).

Sinking of fresh produced material

The establishment of the halocline separated the surface layer and deep layer and the sediment traps were located in the deep layer. Unfortunately, windy conditions caused mixing of the water in the mesocosms and resuspension of already settled material, especially on day 12 when a heavy storm occurred (Schulz et al. 2008). These circumstances made it difficult to use absolute numbers of phytoplankton and bacterial biomass in the sediment traps. Consequently we limit our analysis to isotope ratios and to the first 12 days, which can still give some insight in sinking of freshly produced material. Mixing between the upper and deeper layer was not so important, since at day 10 only about half of the material in the sediment traps was derived from the upper layer (Fig. 2.7). An interesting observation is that bacteria derived material settled more rapidly than phytoplankton material. Close relationships exist between bacteria and detritus. Bacteria rapidly colonize detritus and enhance further aggregation of detritus and subsequent sinking (e.g. Biddanda and Pomeroy 1988). Because of turnover of PLFA after phytoplankton death, the detritus will contain less phytoplankton PLFA and there is thus a preferential sinking of bacteria over phytoplankton (as determined with PLFA), which could be another explanation for the low standing stock in bacteria (Fig. 2.2F and 2.3B). Because POC consists both of living biomass and detritus, the stable isotope ratio of POC would be a better source for estimating organic matter dynamics. During this study we did not measure ^{13}C content of POC, so we could only use phytoplankton PLFA.

CO₂ effects and implications for ocean acidification

In this study, we aimed to advance our understanding of the effect of elevated $p\text{CO}_2$ levels on phytoplankton and bacterial dynamics and on the interactions between them. Furthermore we aimed to gain insight on the effect of CO₂ on sinking of freshly produced material. Our results clearly show an effect of CO₂ on total and labeled standing stocks of bacteria and phytoplankton in the post-bloom phase, but not on carbon transfer from DIC to phytoplankton and subsequently bacteria. Unfortunately, during the post-bloom phase a heavy storm mixed the mesocosms, making it difficult to quantify settling processes. The phytoplankton bloom was independent of CO₂ concentrations in this study (Fig. 2.2 and 2.4). These results agree with other results obtained in PeECE III on phytoplankton bloom development. Phytoplankton bloom development based on pigments (Riebesell et al. 2007; Schulz et al. 2008), flow cytometry (Paulino et al. 2008), and particulate organic carbon (Schulz et al. 2008) was also found to be CO₂ independent during the PeECE III mesocosm experiment. Previous CO₂ enrichment mesocosm studies also showed little effect on particulate organic matter production, although the effect of CO₂ is species dependent. In PeECE I, some phytoplankton groups like coccolithophores were sensitive to changes in CO₂, where other groups like diatoms were not (Delille et al. 2005; Engel et al. 2005).

Interestingly, we did observe CO₂ related effects in the post-bloom phase of the experiment. Green algae and diatoms seemed to benefit from increased $p\text{CO}_2$ as their biomass was significantly higher under high CO₂ levels in the post-bloom phase (Fig. 2.2, Table 2.1). Current CO₂ levels are generally considered to be a non-limiting resource for diatoms and green algae, because they have efficient carbon concentrating mechanisms (CCMs) (Giordano et al. 2005). But the operation of these mechanisms requires energy, so when energy becomes limited, higher CO₂ concentrations can be beneficial. In a recent study from Feng et al. (2009), diatom abundance increased with increasing $p\text{CO}_2$ in shipboard community incubations. Moreover, Egge et al. (2009) reported higher total community primary production rates in the post-bloom phase of the PeECE III experiments in high CO₂ treatments (Fig. 2.1).

We found no indication of enhanced sinking of phytoplankton at increasing CO₂ levels based on isotope ratios in the sediment traps (Fig. 2.7). However, the results should be interpreted with caution. Sinking of freshly produced material would mainly occur during and after the bloom collapse and we don't have reliable sediment trap data for that period due to the storm event. An enhanced carbon consumption was based on DIC budgets (Riebesell et al. 2007; Bellerby et al. 2008), but was not reflected in standing stocks of biological material. The concentrations of TEP (Egge et al. 2009), POC and DOC were independent of CO₂ (Fig. 2.1) (Schulz et al. 2008). Riebesell et al. (2007) suggested that the discrepancy may have been caused by an enhanced particle sinking. Unfortunately, our sediment trap data could not be used to confirm or falsify this hypothesis.

The development of bacterial biomass showed a similar response to CO₂ as phytoplankton, with a significantly higher biomass at higher CO₂ in the post-bloom phase compared to present $p\text{CO}_2$ levels (Fig. 2.2F and 2.4D, table 2.1). In the post-bloom phase, our results concerning bacterial dynamics differ from those of other bacteria results from PeECE III studies. No differences in bacterial abundance under the different CO₂ levels were observed with flow cytometry and with microscopy (Allgaier et al. 2008; Paulino et al. 2008).

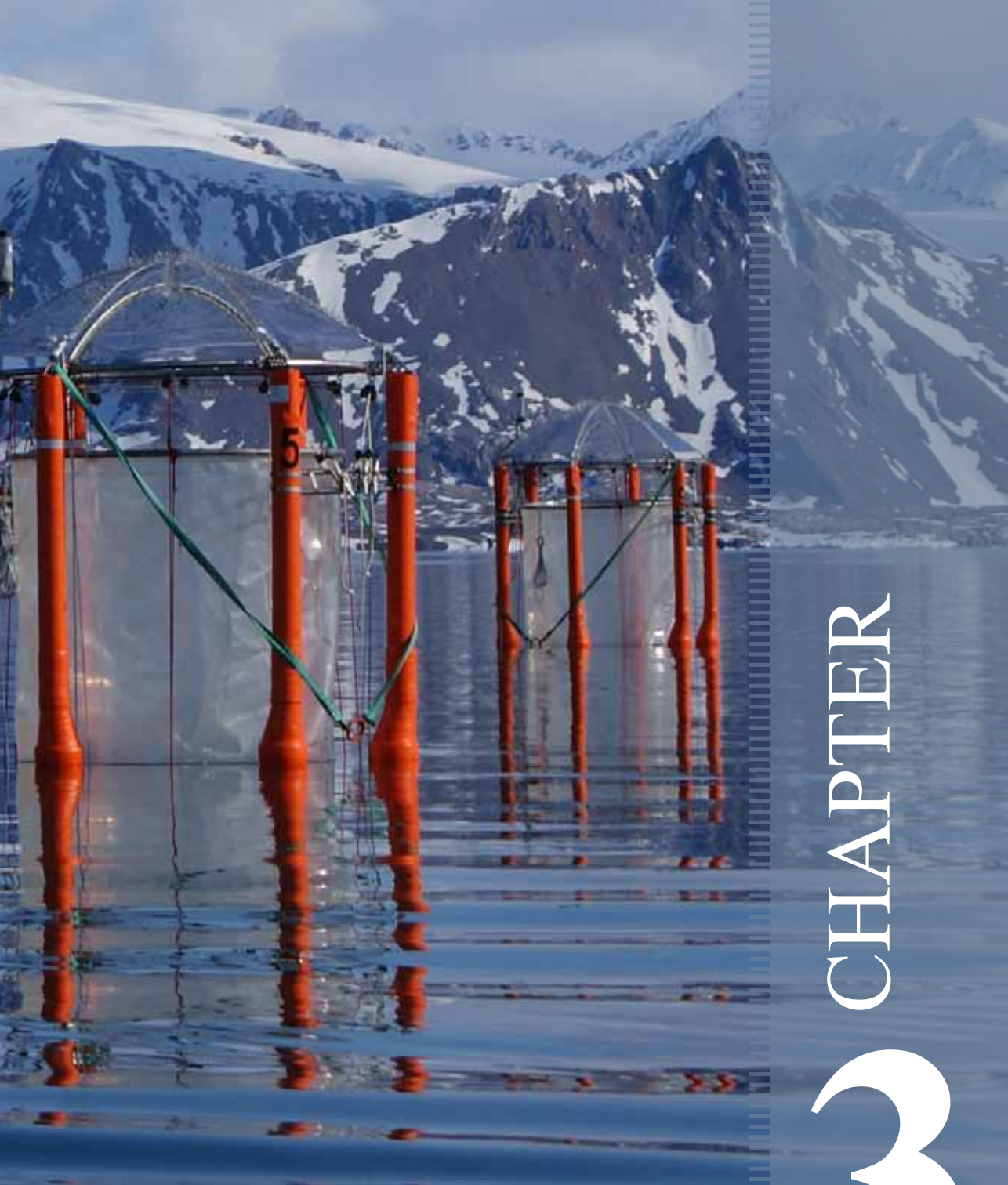
Previous studies have shown that the response of heterotrophic bacteria to changing CO₂ levels is linked to phytoplankton rather than being a direct effect of pH or CO₂ (e.g. Grossart et al. 2006). The increased biomass at higher $p\text{CO}_2$ could be a direct result of increased phytoplankton biomass at higher $p\text{CO}_2$ in the post-bloom phase. We did not observe enhanced coupling between phytoplankton and bacteria under higher $p\text{CO}_2$ with the isotope transfer model during the bloom (Fig. 2.6, Table 2.2). Due to label saturation, the coupling could only be studied before and during the bloom and not in the post-bloom phase. Phytoplankton carbon exudation generally increases at the end of a phytoplankton bloom when nutrients become limited and a CO₂ effect is thus more likely to occur in this phase (Van den Meersche et al. 2004; Engel et al. 2004b). For future CO₂ studies on phytoplankton-bacteria coupling, it can be helpful to use nutrient-limited plankton incubations or to add carbon tracer in the post-bloom phase.

Acknowledgements

The authors gratefully acknowledge the staff of the Espeyrend Marine Biological Station, University Bergen, in particular T. Sørli and A. Aadnesen, and the Bergen Marine Research infrastructure (RI) for helping organize and set up the mesocosm experiment. PeECEIII team members are thanked for the stimulating environment and for providing access to data. We thank Ulysses S. Ninnemann for technical support on DIC analyses. Marco Houtekamer and Pieter van Rijswijk are greatly acknowledged for their work on PLFA extractions and analyses. We thank Dick van Oevelen, Frederik de Laender, Eric Boschker, and Jacco Kromkamp for their help with data analyses. Thanks to Francesc Montserrat and Peter Herman for helping with statistical analyses. This study received financial support from the European Project on Ocean Acidification (EPOCA, FP7, 2211384), the Marine Ecosystem Evolution in a Changing Environment project (MEECE, FP7, 212085), the Marine Ecosystem Response to a Changing Climate (MERCLIM, NFR, 184860) and the Darwin Center for Biogeosciences supported by the Netherlands Organisation for Scientific Research.

Anna de Kluijver, Karline Soetaert, Jan Czerny, Kai G. Schulz, Tim Boxhammer,
Ulf Riebesell, and Jack J. Middelburg

Under review in Biogeosciences discussions for the special issue: Arctic ocean
acidification: pelagic ecosystem and biogeochemical responses during a mesocosm study
<http://www.biogeosciences-discuss.net/9/8571/2012/bgd-9-8571-2012.html>



3 CHAPTER



A ^{13}C labeling study on carbon fluxes in Arctic plankton communities under elevated CO_2 levels

Abstract

The effect of CO₂ on carbon fluxes in Arctic plankton communities was investigated during the 2010 EPOCA mesocosm study in Ny Ålesund, Svalbard. Nine mesocosms were set up with initial *p*CO₂ levels ranging from 185 to 1420 µatm for 5 weeks. ¹³C labeled bicarbonate was added at the start of the experiment to follow the transfer of carbon from dissolved inorganic carbon (DIC) into phytoplankton, bacteria, total particulate organic carbon (POC), zooplankton, and settling particles. Polar lipid derived fatty acids (PLFA) were used to trace carbon dynamics of phytoplankton and bacteria and allowed distinction of two groups of phytoplankton: phyto I (autotrophs) and phyto II (mixotrophs). Nutrients were added on day 13. A nutrient-phytoplankton-zooplankton-detritus model amended with ¹³C dynamics was constructed and fitted to the data to quantify uptake rates and carbon fluxes in the plankton community during the phase prior to nutrient addition (phase 1, days 0-12).

During the first 12 days, a phytoplankton bloom developed that was characterized by high growth rates (0.87 d⁻¹) for phyto I and lower growth rates (0.18 d⁻¹) for phyto II. A large part of the carbon fixed by phytoplankton (~31 %) was transferred to bacteria, while mesozooplankton grazed only ~6 % of the production. After 6 days, the bloom collapsed and part of the organic matter subsequently settled into the sediment traps. The sedimentation losses of detritus in phase 1 were low (0.008 d⁻¹) and overall export was only ~7 % of production. Zooplankton grazing and detritus sinking losses prior to nutrient addition were sensitive to CO₂: grazing decreased with increasing CO₂, while sinking increased.

Phytoplankton production increased again after nutrient addition on day 13. Although phyto II showed initially higher growth rates with increasing CO₂ (days 14-22), the overall production of POC after nutrient addition (phase 2, days 14-29) decreased with increasing CO₂. Significant sedimentation occurred towards the end of the experiment (after day 24) and much more material settled down in the sediment traps at low CO₂.

3.1 Introduction

About 30 % of anthropogenic CO₂ has accumulated in the oceans causing modification of the oceans' chemistry. The most important impacts of anthropogenic CO₂ on marine carbonate chemistry are higher concentrations of CO₂ and a concurrent drop in pH, collectively referred to as ocean acidification. The CO₂ uptake capacity of the oceans is influenced by the plankton organisms that live in the surface waters. The flux of CO₂ from atmosphere to oceans is largely controlled by three biological processes: primary production, community respiration, and export (biological pump). Primary production and subsequent sinking of organic matter (OM) to depth increases the ocean's uptake capacity for CO₂. Community respiration in the upper ocean, dominated by heterotrophic bacteria, converts organic carbon back into CO₂ and thus decreases the ocean's CO₂ uptake capacity (Rivkin and Legendre 2001). Understanding the effects of increasing CO₂ levels on these three processes is central to predict the ocean's response to rising atmospheric pCO₂. Particularly production and export showed to be potentially sensitive to changes in CO₂ (Riebesell et al. 2009).

The high-latitude oceans are especially vulnerable for anthropogenic CO₂ disturbances, because of lower temperatures. The solubility of CO₂ increases with decreasing temperatures, so that polar oceans contain naturally high CO₂ and low carbonate ion concentrations. With a lower buffer capacity, pH changes are considerably larger in the polar regions than at lower latitudes for future climate scenarios (Steinacher et al. 2009). Our knowledge about the potential effects of ocean acidification on plankton communities in polar regions is limited, but plankton community studies have been done in mid-latitude regions. In a mesocosm experiment in a Norwegian Fjord (Bergen in 2005) an increased inorganic carbon consumption relative to nutrient (N,P) uptake was observed at higher CO₂ levels in natural plankton communities (Riebesell et al. 2007; Bellerby et al. 2008). The enhanced uptake was not reflected in increased organic matter production (Schulz et al. 2008; de Kluijver et al. 2010) nor in increased bacterial activity (Allgaier et al. 2008; de Kluijver et al. 2010) so enhanced export was the suggested sink for the extra carbon consumed at elevated pCO₂ (Riebesell et al. 2007). A proposed mechanism is that CO₂ induced carbon overconsumption is exuded by phytoplankton as dissolved organic matter (DOM), which aggregates with other particles and increases export (Engel et al. 2004a). In another mesocosm experiment (Bergen 2001) no CO₂ effects on primary production (DeLille et al. 2005) were recorded, but a stimulating effect of CO₂ on bacterial activity was observed (Engel et al. 2004b; Grossart et al. 2006). In the mesocosm studies mentioned above, nutrients were added to stimulate phytoplankton production at the start of the experiments, so CO₂ effects on a eutrophic, blooming community were observed. However, throughout most of the year, plankton communities exist under low nutrient conditions dominated by regenerated production, rather than new production (Legendre and Rassoulzadegan 1995).

This mesocosm study is the first to investigate the effects of elevated CO₂ on high-latitude plankton communities and on plankton communities in a post-bloom, nutrient regenerating state. In summer 2010, nine mesocosms were set up in Kongsfjorden, Svalbard, with a range of CO₂ levels and monitored for changes in plankton community functioning. To study the uptake of carbon by phytoplankton (primary production) and subsequent transfer to bacteria and zooplankton (community respiration) and settling material (export), ¹³C-DIC was added as a tracer. The ¹³C labeling dynamics of phytoplankton and bacteria were determined by compound-specific isotope analyses of fatty acid biomarkers.

This technique has been successfully applied in the previous CO₂ enrichment mesocosm experiment (in Bergen, year 2005) to study the interactions between phytoplankton and bacteria (de Kluijver et al. 2010). In addition to the previous mesocosm experiment (Bergen 2005), ¹³C POC and zooplankton analyses as well as quantitative sediment traps samples were included in this mesocosm study. A nutrient-phytoplankton-zooplankton-detritus model was constructed to quantify uptake and loss parameters and carbon flows in the mesocosms. The obtained parameters and fluxes were tested for CO₂ sensitivity.

3.2 Materials and methods

Experimental setup and sampling

The mesocosm experiment was carried out in Kongsfjorden, Svalbard (78°56,2' N; 11°53,6' E) in June-July 2010 as part of the 2010 EPOCA (European project on Ocean Acidification) Arctic campaign. The experimental setup and mesocosm characteristics are described in detail in (Czerny et al. 2012A). Briefly, 9 mesocosms of ~50 m³ were deployed in the Kongsfjorden, about a mile off Ny Ålesund, on 28 May, 2010. During lowering to ~15 m depth, the bags filled with nutrient-poor, post-bloom fjord water. A 3 mm mesh size net was used to exclude large organisms. The bags were closed on 31 May, 2010, defined as time t-7 and time steps (t) continued per day. The CO₂ manipulation was done in steps over 5 days, from t-1 to t4 by adding calculated amounts of CO₂ enriched seawater to each mesocosm. The main additions were done from t-1 to t2 and a final adjustment was done on t4. A range of initial *p*CO₂ levels of ~185-1420 μatm was achieved (exact CO₂ levels are provided in Bellerby et al. 2012). Due to gas exchange and photoautotrophic uptake *p*CO₂ levels declined in the mesocosms, especially in the high CO₂ treatments, to a final *p*CO₂ range from ~160-855 μatm at the end of the experiment. ¹³C-bicarbonate (10 g per mesocosm), corresponding to ~0.1 % of DIC, was added to the mesocosms together with the first CO₂ addition (t-1), increasing the δ¹³C signature of DIC by ~100 ‰. At t13, inorganic nutrients were added to stimulate phytoplankton production. The total added concentrations were 5 μM nitrate, 0.32 μM phosphate, and 2.5 μM silicate. The experiment was terminated at t30. The experimental period was divided into three phases based on the applied perturbations and chl *a* dynamics. Phase 1 was before nutrient addition (t4-13). Phase 2 was after nutrient addition until the 2nd chl *a* minimum (t14-21) and phase 3 was from the 2nd chl *a* minimum until the end of the experiment (t22-29) (Schulz et al. 2012). In this manuscript we only consider two phases, phase 1 before nutrient addition (t0-12) and phase 2 after nutrient addition (t14-t29).

Depth-integrated samples (0-12 m) were taken with an integrating watersampler (IWS; Hydrobios, Kiel, Germany) on each morning (9-11 h) for core parameters (nutrients, chlorophyll, particulate organic carbon, phosphate, and nitrogen (POC, POP, PON), dissolved organic carbon, phosphate, and nitrogen (DOC, DOP, DON), dissolved inorganic carbon (DIC), ¹³C content of carbon pools (DIC, DOC, POC, biomarkers) and many other parameters (Riebesell et al. 2012). Daily samples for ¹³C-DIC and ¹³C-DOC were taken directly from the IWS and stored in dark, gas-tight glass bottles. The sediment traps were emptied every other day before daily routine sampling and processed as described in (Czerny et al. 2012A). Zooplankton samples were taken weekly in the afternoon by vertical 55 μm mesh size Apstein net hauls over the upper 12 m.

Daily ^{13}C - polar lipid fatty acid (PLFA) samples were collected on pre-combusted 47 mm GF/F filters by filtering ~3-4 L and filters were stored at -80°C . Daily ^{13}C -POC samples were collected on pre-weighted and pre-combusted 25 mm GF/F filters by filtering ~0.5 L and filters were subsequently stored at -20°C and freeze-dried afterwards. From the gas-tight water samples, headspace vials (20 mL) were filled using an overflow method and sealed with gas-tight caps for DIC isotope analyses. Mercury chloride was added for preservation and the samples were stored upside down at room temperature. Samples for dissolved organic carbon (DOC) were GF/F filtered and stored frozen (-20°) in clean (HCl and mQ rinsed) vials until further analyses. Zooplankton were transferred to filtered seawater and kept there for a minimum of 3 hours, to empty their guts. On average, 7 (range 1-30) individuals of *Calanus* sp. and 30 (range 16-35) individuals of *Cirripedia* larvae were handpicked and transferred to pre-combusted tin cups (200°C , min. 12h), which were subsequently freeze-dried. Zooplankton samples were analyzed for organic ^{13}C content. Subsamples of freeze-dried and homogenized sediment trap material were analyzed for total organic ^{13}C . Sediment trap material of the last 8 days (t22-30) was additionally analyzed for ^{13}C -PLFA to characterize the nature of settling material.

Laboratory analyses

POC, sediment trap material and zooplankton samples were analyzed for organic carbon content and isotope ratios on a Thermo Electron Flash EA 1112 analyzer (EA) coupled to a Delta V isotope ratio mass spectrometer (IRMS). For DIC isotope analyses, a helium headspace was added to the headspace vials and samples were acidified with H_3PO_4 solution. After equilibration, the CO_2 concentration and isotope ratio in the headspace was measured on EA-IRMS. PLFA were extracted using a modified Bligh and Dyer method (Bligh and Dyer 1959; Middelburg et al. 2000). The lipids were fractionated in different polarity classes by column separation on a heat activated silicic acid column and subsequent elution with chloroform, acetone and methanol. The methanol fractions, containing most of the polar lipid fatty acids were collected and derivatized to fatty acid methyl esters (FAME). The standards 12:0 and 19:0 were used as internal standards. Concentrations and $\delta^{13}\text{C}$ of individual PLFA were measured using gas chromatography-combustion isotope ratio mass spectrometry (GC-C-IRMS) (Middelburg et al. 2000; de Kluijver et al. 2010). ^{13}C -DOC samples were analysed in Hatch isotope laboratory (Ottawa, Canada), using wet chemical oxidation with high amplification isotope ratio mass spectrometry (WCO-IRMS) (Osburn and St Jean 2007). Unfortunately, the amount of ^{13}C was too low to quantitatively determine ^{13}C incorporation in DOC, but could be used to provide an upper limit to DOC production.

Data analyses

Carbon stable isotope ratios are expressed in the delta notation relative to Vienna Pee Dee Belemnite (VPDB) standard ($\delta^{13}\text{C}$). Relative (^{13}C) incorporation in carbon samples is presented as $\Delta\delta^{13}\text{C}$ (‰), calculated as $\delta^{13}\text{C}_{\text{sample}} - \delta^{13}\text{C}_{\text{background}}$. Absolute label incorporation was calculated as ^{13}C concentration = $\Delta^{13}\text{F} \times \text{concentration}$ ($\mu\text{mol C L}^{-1}$), with $\Delta^{13}\text{F}$ being $^{13}\text{F}_{\text{sample}} - ^{13}\text{F}_{\text{background}}$, and ^{13}F being the ^{13}C fraction ($^{13}\text{C}/(^{12}\text{C}+^{13}\text{C})$) derived from the delta notation. $\delta^{13}\text{C}_{\text{background}}$ and $^{13}\text{F}_{\text{background}}$ are the natural abundance isotope ratios, which were sampled before label addition. To compare ^{13}C concentrations of organic carbon pools between mesocosms, the data were corrected for small differences in initial ^{13}C -DIC concentrations using a correction factor.

The correction factor was calculated from deviations of ^{13}C -DIC from the average ^{13}C -DIC on day 3 (after main CO₂ additions) and ranged from 0.89 to 1.08. This correction is used for clarity of presentation and was not used for model calculations. ^{13}C -DIC results were corrected for gas exchange according to (Czerny et al. 2012B). The $\delta^{13}\text{C}$ of CO₂ [aq] was calculated according to (Zhang et al. 1995) and the $\delta^{13}\text{C}$ of atmospheric CO₂ was assumed -8 ‰ (Fry 2006).

$\Delta\delta^{13}\text{C}$ PLFA of phytoplankton showed 2 responses of ^{13}C incorporation: rapid label incorporation and more graduate label incorporation. Phytoplankton were therefore separated into 2 groups (phyto I and phyto II) (Fig. 3.1A). The rapidly incorporating PLFA were 18:3 ω 3, 18:4 ω 3, 18:5 ω 3(12-15), 18:5 ω 3(12-16), and 16:4 ω 3 and their weighted average (Δ) $\delta^{13}\text{C}$ was used to determine (Δ) $\delta^{13}\text{C}$ of phyto I. The PLFA with delayed incorporation were 20:5 ω 3, 22:6 ω 3 and 16:4 ω 1 and their weighted average (Δ) $\delta^{13}\text{C}$ was used to determine (Δ) $\delta^{13}\text{C}$ of phyto II. PLFA presented in phyto I are characteristic for green algae, chrysophytes, prymnesiophytes, and autotrophic dinoflagellates and PLFA of phyto II are characteristic for diatoms and (heterotrophic) dinoflagellates (Cranwell et al. 1988; Dijkman et al. 2009). It was possible to distinguish between autotrophic dinoflagellates and total dinoflagellates, because 18:5 ω 3 is considered a chloroplast fatty acid, while 22:6 ω 3 is a cell membrane lipid (Adolf et al. 2007). The branched fatty acids i15:0, ai15:0, and i17:0 were used to characterize heterotrophic bacteria. The last step involved conversion from PLFA biomass to total organic carbon (OC) concentration for each group. The conversion factor for phyto I was 0.06 (sum PLFA/OC), 0.05 (sum PLFA/OC) for phyto II, based on phytoplankton culture and literature values (Dijkman and Kromkamp 2006). The conversion factor for bacterial carbon was 0.01 (sum PLFA/OC) (van den Meersche et al. 2004).

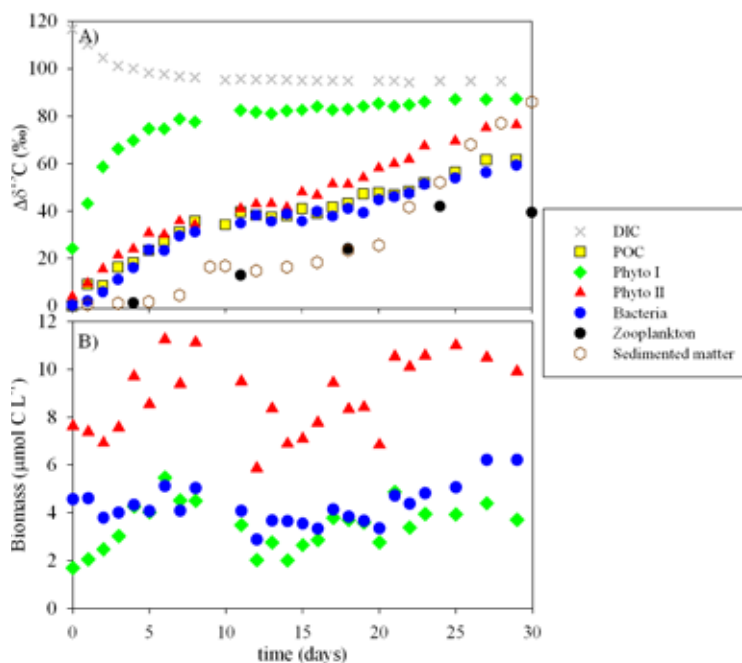


Fig. 3.1. The temporal change as averaged over all mesocosms ($n=9$) of A) isotope ratios ($\Delta\delta^{13}\text{C}$) of all measured carbon pools, and B) of biomass ($\mu\text{mol C L}^{-1}$) of phyto I, phyto II, and bacteria.

Group specific daily growth rates (μ , d^{-1}) were calculated according to Dijkman et al. (2009) as

$$\mu \text{ (d}^{-1}\text{)} = \ln \left(\frac{{}^{13}\text{C}_{\text{concentration}}_{t \rightarrow \Delta t}}{{}^{13}\text{C}_{\text{concentration}}_t} / \text{cf} \right) \quad (3.1)$$

$$\text{cf} = \text{mean} \left(1 - \frac{\Delta \delta^{13}\text{C}_{\text{phyto}}_t}{\Delta \delta^{13}\text{C}_{\text{DIC}}_t} \right)_{t \rightarrow t + \Delta t} \quad (3.2)$$

The correction factor (cf) is necessary to correct for label saturation and represents the difference between phyto and DIC labeling ($\Delta \delta^{13}\text{C}$) relative to the $\Delta \delta^{13}\text{C}$ of DIC averaged over the considered growth period for each mesocosm. Primary production rates were calculated as

$$P \text{ (}\mu\text{mol C L}^{-1} \text{ d}^{-1}\text{)} = \frac{\Delta {}^{13}\text{F}_{\text{phyto}}}{\Delta {}^{13}\text{F}_{\text{DIC}}} \times \frac{C_{\text{phyto}}}{t} \quad (3.3)$$

Model

A nutrient-phytoplankton-zooplankton-detritus (NPZD) model amended with isotope values was used to quantify carbon fluxes within the plankton food web. The model is based on those of (de Kluijver et al. 2010) and (van den Meersche et al. 2011) and a detailed description of the model and the equations can be found in (van Engeland et al. 2012). The model equations are also found in the appendix. The model code is incorporated in an R-package, which is available upon request. Briefly, the concentrations of both ^{12}C and ^{13}C were modeled separately for the following carbon pools: phyto I, phyto II, labile DOC (LDOC), bacteria, zooplankton, detritus, and sedimented OM. The nitrogen pools explicitly described in the model were DIN and DON. Nitrogen fluxes relating to the other pools were calculated from carbon fluxes with a fixed Redfield stoichiometry. POC and PON were calculated in the model as the sum of phyto I and II, bacteria, zooplankton and detritus. Light was used as forcing function for phytoplankton growth. The fractions of ^{13}C and ^{12}C in DIC were used as forcing functions for ^{13}C and ^{12}C incorporation by phytoplankton, but no growth dependency on DIC (or CO_2) was built in the model. Bacterial biomass (based on PLFA; Fig. 3.1B) and zooplankton biomass (Niehoff et al. 2012) did not show large biomass changes during the experiment and were assumed to stay constant for model simplicity. Half-saturation constants for DOC uptake by bacteria (ϵ_{DOC}) and zooplankton grazing on phytoplankton (ϵ_g) were to set low values, with the assumption that substrate limitation was of minor importance.

The model was implemented in the open source software R (R core team 2012), using the packages FME and deSolve (Soetaert and Petzoldt 2009; Soetaert et al. 2009). The output of the model was first manually fitted to the data to obtain good parameter fits. The data that were used to fit the model (observed variables) were phyto I, phyto II, bacteria, zooplankton, DIN, DON, POC, PON, and sediment POC and PON. The model was run separately before (phase 1) and after nutrient addition (phase 2). For both phases initial conditions were based on the data. The fitted parameters were calibrated using the Markov Chain Monte Carlo (MCMC) technique (Gelman 1996), as implemented in the FME package. A subset of parameters, potentially CO_2 sensitive, was calibrated with MCMC for each mesocosm.

MCMC runs were accepted when they fell into the probability distribution centred around the current value (for details see Gelman 1996). The model was run 5000 times for each mesocosm, resulting in ~2000 accepted runs. The mean and standard deviation of the MCMCs were calculated for each parameter. The calibrated parameters were used to calculate fluxes ($\mu\text{mol C L}^{-1} \text{d}^{-1}$) between the carbon pools.

Statistics

Simple Pearson correlation tests were used to test the effect of CO₂ on growth rates (equation 3.1), production rates (equation 3.3), linear increase in ¹³C concentrations, and parameters and fluxes derived from the model. The results were tested and plotted against the average *p*CO₂ level in the corresponding phase. All statistical analyses were done in the software (R development core team).

3.3 Results

¹³C-DIC dynamics

Addition of ¹³C bicarbonate together with the first CO₂ addition on t-1 caused an increase in $\delta^{13}\text{C}$ of DIC of $117 \pm 6 \text{‰}$ in all mesocosms (Fig. 3.1A). The decrease in $\Delta\delta^{13}\text{C}$ -DIC in perturbed mesocosms during the first 4 days (t0-4) can be largely explained by exchange with the dead volume, which was the space between the sediment traps and the bottom of the mesocosms and comprised ~10 % of total mesocosm volume (Schulz et al. 2012). Other processes that contributed to the initial label decrease were the subsequent (unlabeled) CO₂ additions which diluted the ¹³C-DIC pool and respiration of unlabeled organic material. The loss of ¹³C-DIC due to air-sea exchange was low (<0.15 %). From day 7 onwards, the $\Delta\delta^{13}\text{C}$ of DIC remained quite stable (Fig. 3.1A). The labeled DIC concentrations were $2.6 \pm 0.1 \mu\text{mol } ^{13}\text{C L}^{-1}$ at t0 and decreased during the first 9 days to $2.2 \pm 0.2 \mu\text{mol } ^{13}\text{C L}^{-1}$ at t10 and did not show large changes afterwards (Fig. 3.2A).

Phytoplankton dynamics

After enclosure of post-bloom water, a phytoplankton bloom developed, even though nutrient concentrations were low (0.64 and $0.05 \mu\text{mol L}^{-1}$ DIN and phosphate, respectively). Phyto I rapidly incorporated ¹³C; on t7 the whole phytoplankton community had been turned-over, as indicated by the plateau (Fig. 3.1A), although phyto I never reached the $\Delta\delta^{13}\text{C}$ of DIC. Phyto II showed clearly slower enrichment and never became saturated with ¹³C (Fig. 3.1A). Phyto I initially had low biomass ($1.2 \pm 0.05 \mu\text{mol C L}^{-1}$, ~6 % of POC) compared to phyto II ($8.3 \pm 1.2 \mu\text{mol C L}^{-1}$, ~40 % of POC) (Fig. 3.1B). Both groups contributed to the bloom during phase 1 in biomass and reached a bloom peak at t6 and declined afterwards (Fig. 3.1B). The development of ¹³C labeled biomass showed that the bloom build-up and decline were more pronounced for phyto I compared to phyto II (Fig. 3.2B, C). This was also reflected in higher growth rates ($0.85 \pm 0.06 \text{d}^{-1}$) of phyto I (μ _I) compared to phyto II (μ _{II}, $0.48 \pm 0.04 \text{d}^{-1}$) during bloom build-up (t0-6). (table 3.1). The height of the bloom peak, as well as growth rates of phyto I and phyto II were independent of CO₂.

The production rates (P) of phyto I during the build-up (t0-6) were 0.56 - $0.78 \mu\text{mol C L}^{-1} \text{d}^{-1}$ and independent of CO₂ (Fig. 3.3A). Average net production rates in total phase 1 (t0-12) were much lower, 0.09 - $0.30 \mu\text{mol C L}^{-1} \text{d}^{-1}$ and showed a positive relation with CO₂ (Fig. 3.3A, $r = 0.81$, $p < 0.01$).

The production rates of phyto II during the build-up (t0-6) were $0.45\text{--}0.62 \mu\text{mol C L}^{-1} \text{d}^{-1}$ and showed a negative correlation with CO_2 (Fig. 3.3B, $r = -0.79$, $p < 0.05$). Net production rates of phyto II were $0.21\text{--}0.37 \mu\text{mol C L}^{-1} \text{d}^{-1}$ and were independent of CO_2 (Fig. 3.3B). So both phytoplankton groups had a significant loss in (particulate) production (ΔP) during the bloom collapse, which was CO_2 dependent. The loss in (particulate) organic carbon production (ΔP) during the collapse, was $\sim 0.39 \mu\text{mol C L}^{-1} \text{d}^{-1}$ in high and $\sim 0.97 \mu\text{mol C L}^{-1} \text{d}^{-1}$ in low CO_2 treatments ($r = -0.70$, $p < 0.05$, Fig. 3.3C).

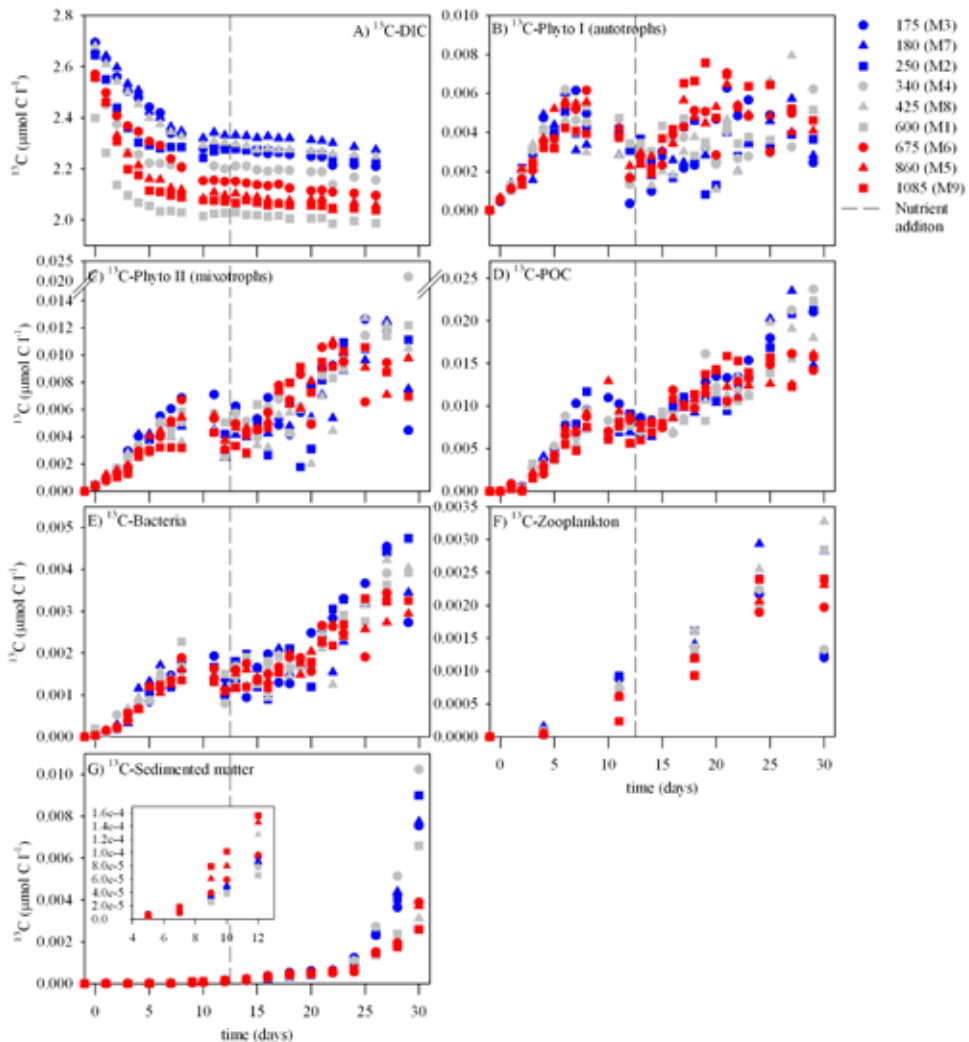


Fig. 3.2. Temporal development of ^{13}C in stocks and ^{13}C labeled biomass ($\mu\text{mol } ^{13}\text{C L}^{-1}$) of A) DIC; B) Phyto I; C) Phyto II; D) POC; E) Bacteria; F) Zooplankton (*Calanus sp.*); and G) Sedimented organic matter in each mesocosm. Red colours are used for high $p\text{CO}_2$ treatments, grey for medium, and blue for low $p\text{CO}_2$ treatments. The vertical line denotes the timing of nutrient addition. The inset of (G) zooms in on the first phase.

After nutrient addition phyto I and II increased again in biomass, but there was more variation between mesocosms. Bloom peaks of phyto I were reached on t18-29, depending on the mesocosm, but not on CO₂ (Fig. 3.2B). Bloom peaks of phyto II were reached on t22-29 and were also independent of CO₂ (Fig. 3.2C). Although ¹³C biomass of phyto II kept increasing, the total biomass of phyto II after nutrient addition remained similar to phase 1 (Fig. 3.1B). Average growth and production rates of phyto II after nutrient addition were also similar to phase 1 (table 3.1). Production rates of phyto II were initially higher in the high CO₂ treatments (t14-22, $r = 0.72$, $p < 0.05$, Fig. 3D). However, overall production rates in phase 2 (t14-t29) showed an optimum around current CO₂ levels (Fig. 3.3D). Because of label saturation (Fig. 3.1A), growth and production rates could not be determined for phyto I after nutrient addition.

Table 3.1. Growth (μ) and production (P) rates based on equation 3.1 and 3.3, respectively, for each phase. Values are presented as average of all mesocosms \pm standard deviation ($n=9$).

	Growth rate (μ , d ⁻¹)			Production rate (P, $\mu\text{mol C L}^{-1} \text{d}^{-1}$)		
	Phase 1 (t0-6)	Phase 1 (t0-12)	Phase 2 (t14-29)	Phase 1 (t0-6)	Phase 1 (t0-12)	Phase 2 (t14-29)
Phyto I	0.85 \pm 0.06	0.19 \pm 0.08	--	0.65 \pm 0.08	0.19 \pm 0.08	
Phyto II	0.48 \pm 0.04	0.23 \pm 0.02	0.22 \pm 0.06	0.55 \pm 0.06	0.30 \pm 0.06	0.40 \pm 0.13
BAC	0.68 \pm 0.11	0.33 \pm 0.02	0.13 \pm 0.04		0.47 \pm 0.03	0.20 \pm 0.15
POC					0.80 \pm 0.13	0.75 \pm 0.22

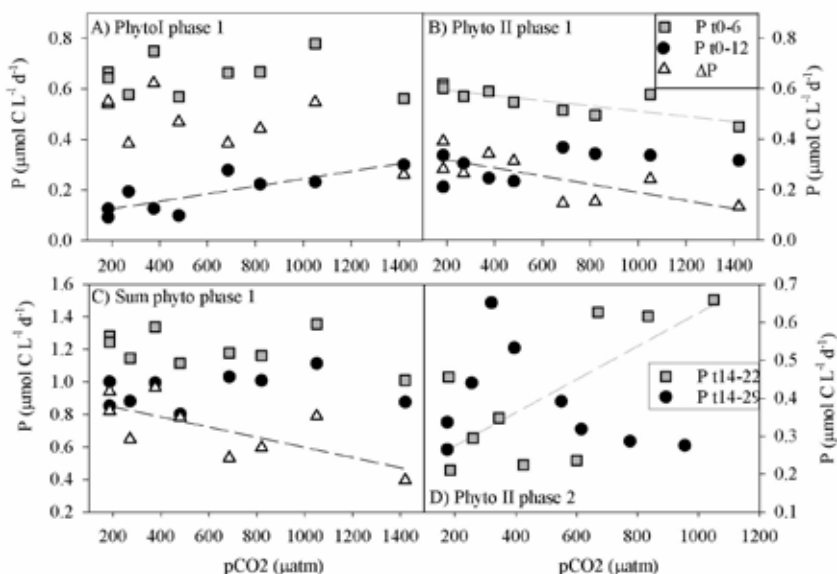


Fig. 3.3. Production rates vs. average $p\text{CO}_2$ levels of each phase based on data (equation 3.3) of A) Phyto I; B) Phyto II; and C) sum phyto I and II production rates ($\mu\text{mol C L}^{-1} \text{d}^{-1}$) in phase 1 for the build-up (t0-6), the build-up and decline (t0-12), and the production loss during decline (difference) denoted with Δ ; D) Phyto II production rates ($\mu\text{mol C L}^{-1} \text{d}^{-1}$) after nutrient addition for initial phase 2 (t14-22) and total phase 2 (t14-29).

POC and DOC production

The dynamics of phyto I and phyto II were reflected in the build-up of ^{13}C enriched POC with a peak on t8-11 and a subsequent decline (Fig. 3.2D). POC dynamics were independent of CO_2 in phase 1. Addition of nutrients again stimulated organic matter production and ^{13}C -POC kept on increasing until the end of the experiment (Fig. 3.2D). POC production rates before and after nutrient addition were quite similar: $0.65\text{--}1.06 \mu\text{mol C L}^{-1} \text{d}^{-1}$ before and $0.57\text{--}1.06 \mu\text{mol C L}^{-1} \text{d}^{-1}$ after nutrient addition (table 3.1, Fig. 3.4A). The average production rate of POC after nutrient addition (t14-29) decreased with increasing CO_2 ($r = -0.87$, $p < 0.01$, Fig. 3.4A). DO^{13}C showed a maximum increase ($\Delta\delta^{13}\text{C}$) of 3 ‰. Based on the small isotopic enrichment, the average DOC production during the whole experiment (t0-t28) was $< 0.06 \mu\text{mol C L}^{-1} \text{day}^{-1}$ and the total DOC build-up was $< 6.2 \mu\text{mol C L}^{-1}$ in phase 1 (t0-t11) and $< 11 \mu\text{mol C L}^{-1}$ in phase 2 (t14-28).

^{13}C labeling of bacteria and zooplankton consumers

Heterotrophic (gram-positive) bacterial followed the labeling pattern of POC (Fig. 3.1A). Initial bacteria biomass was $4.6 \pm 0.6 \mu\text{mol C L}^{-1}$ (~19 % of POC) and stayed constant during phase 1 (Fig. 3.1B). Due to label incorporation, the ^{13}C -enriched bacteria biomass increased in the first phase and peaked on t6-8 (Fig. 3.2E). Bacteria ^{13}C biomass increased again after nutrient addition until the end of the experiment. The average growth rate of bacteria (μ_{Bac}) was $0.33 \pm 0.02 \text{d}^{-1}$ before nutrient addition and $0.13 \pm 0.04 \text{d}^{-1}$ after nutrient addition (table 3.1). Bacteria production rates were also higher before nutrient addition (phase 1, $0.47 \pm 0.03 \mu\text{mol C L}^{-1} \text{d}^{-1}$) than after nutrient addition (phase 2, $0.20 \pm 0.15 \mu\text{mol C L}^{-1} \text{d}^{-1}$) (table 3.1). Bacteria growth and production were independent of CO_2 levels.

Zooplankton (*Calanus* sp. and *Cirripedia*) incorporated ^{13}C in a similar way and the incorporation of tracer into copepods was used as representative for the mesozooplankton community. The ^{13}C incorporation into zooplankton was low (Fig. 3.1A). With a constant biomass of $\sim 5 \mu\text{mol C L}^{-1}$ (Niehoff et al. 2012), the ^{13}C incorporation until day 18 showed a negative correlation with CO_2 ($r = -0.92$, $p < 0.001$, Fig. 3.2F, 3.4B). From day 24 onwards, the variance in ^{13}C biomass increased and the CO_2 effect disappeared (Fig. 3.2F).

^{13}C labeling of sedimented organic material

The label enrichment in sediment trap organic matter in the first 7 days was low, indicating that little freshly produced material was sinking into the traps (Fig. 3.1A). After day 7 the material became more enriched, probably because of the bloom collapse and after day 20, the $\Delta\delta^{13}\text{C}$ of sediment trap POC increased rapidly (Fig. 3.1A). After day 25, the $\Delta\delta^{13}\text{C}$ of sediment POC was higher than of water column POC, showing that there was preferential sinking of freshly produced material. The cumulative ^{13}C of sediment trap POC is shown in Fig. 3.2G. The settling of ^{13}C enriched POC in the traps was very low in the first phase ($7.13 \times 10^{-6} \mu\text{mol }^{13}\text{C L}^{-1} \text{d}^{-1}$, $\sim 7.13 \times 10^{-3} \mu\text{mol C L}^{-1} \text{d}^{-1}$) and increased with increasing CO_2 ($r = 0.75$, $p < 0.05$, Fig. 3.4C). After nutrient addition, the sinking of ^{13}C -POC was much higher ($1.14 \times 10^{-4} \mu\text{mol }^{13}\text{C L}^{-1} \text{d}^{-1}$, $\sim 0.11 \mu\text{mol C L}^{-1} \text{d}^{-1}$) and the effect of CO_2 on sedimentation was reversed compared to phase 1 (Fig. 3.2G, 3.4C); sedimentation of freshly labeled (^{13}C enriched) POC decreased with increasing CO_2 ($r = -0.78$, $p < 0.05$, Fig. 3.4C). The ^{13}C increase in POC in the water column and sediment traps showed a non-linear response to CO_2 in phase 2, which indicates a step-wise rather than a gradual CO_2 effect (Figs. 3.4A,C).

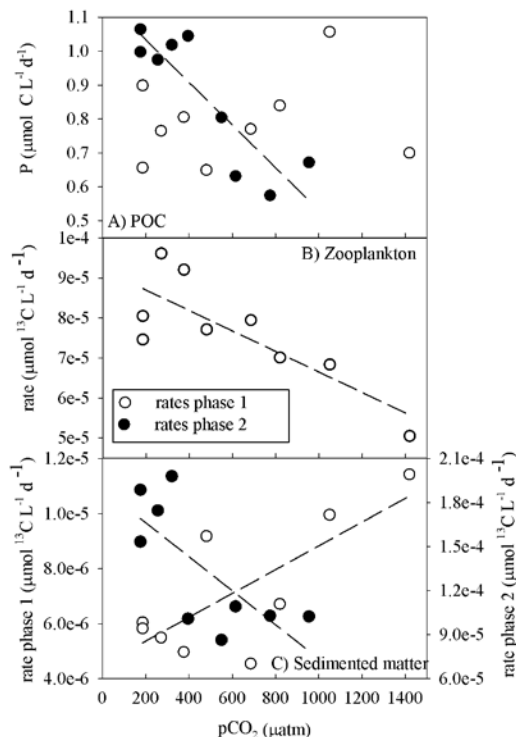


Fig. 3.4. A) POC production ($\mu\text{mol C L}^{-1} \text{d}^{-1}$) before (phase 1) and after nutrient addition (phase 2); B) ^{13}C increase in zooplankton ($\mu\text{mol } ^{13}\text{C L}^{-1} \text{d}^{-1}$) from t0-18); C) ^{13}C increase in cumulative sedimented organic matter ($\mu\text{mol } ^{13}\text{C L}^{-1} \text{d}^{-1}$) before (phase 1) and after nutrient addition (phase 2) as function of average $p\text{CO}_2$ levels of the corresponding phase.

Mesocosms with CO_2 levels below $340 \mu\text{atm}$ had high POC production and sedimentation rates, while mesocosms with CO_2 above $400 \mu\text{atm}$ had low POC production and sedimentation rates after nutrient addition (Figs. 3.4A,C). The exception was at $395 \mu\text{atm}$ (average $p\text{CO}_2$ in phase 2 in mesocosm 8) where there was high production and low sedimentation (Figs. 3.3D, F). The fatty acid composition of settling material in phase 3 revealed that all groups were present, but there were more phyto II markers than phyto I markers in the sediment traps.

Model results: parameters

The construction of a model and subsequent fitting to the data provides the possibility to study the community as a whole, instead of studying carbon production in each carbon pool separately as done above. Good model fits were obtained for the first phase of the model (t0-12). Unfortunately, no good fits could be obtained for phase 2 (t14-29), primarily because of label saturation in phyto I (Van Engeland et al. 2012) which precluded fitting the growth rate and subsequent exudation and mortality of phyto I during this phase. Fits for phase 1 of one mesocosm (M4, $375 \mu\text{atm}$) are shown in Fig. 3.5. The average parameter values of all mesocosms are given in table 3.2. The growth and build-up of plankton biomass caused a decrease in DIN and DON.

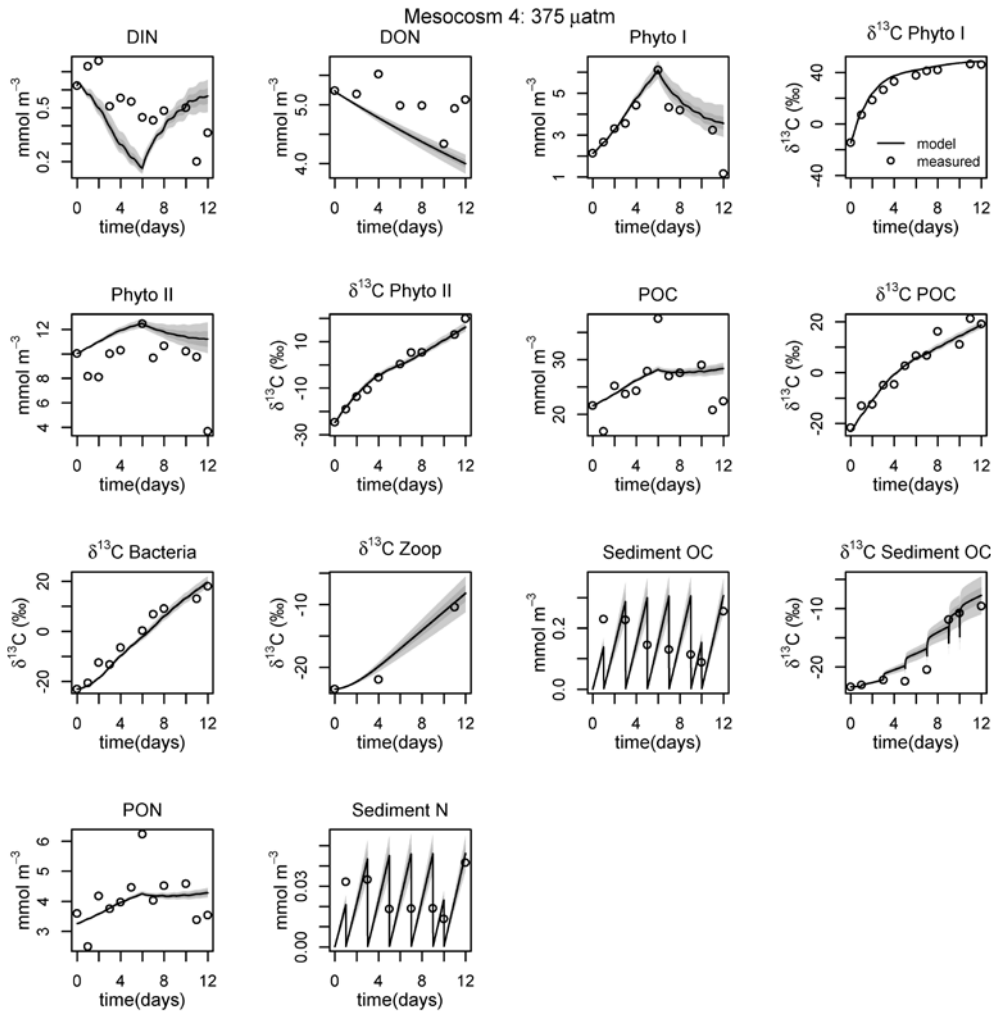


Fig. 3.5. MCMC plots showing the best fits of model output (solid line) with uncertainty (grey envelopes) fitted to the data (points) for one mesocosm (375 μatm).

To reach the high biomass of phyto I, phytoplankton mortality was set to 0 in the first six days. The growth rate of phyto I (μ_I) was $0.87 \pm 0.013 \text{ day}^{-1}$. After t6 phytoplankton mortality was included to produce the decline in biomass. The mortality rate of phyto I (ζ_I) was $0.29 \pm 0.081 \text{ d}^{-1}$. The growth rate of phyto II (μ_{II}) was $0.18 \pm 0.010 \text{ d}^{-1}$. The estimated loss rate of phyto II (ζ_{II}) was low, only $0.045 \pm 0.025 \text{ d}^{-1}$. Hence mortality mainly affected phyto I. Part of the phytoplankton loss was assumed to be respired, part to end up in DOM, and part to end as detritus. The loss part that went into detritus (f_{Det}) was 0.37 ± 0.050 and the part that ended in DOM (f_{DOM}) was 0.056 ± 0.037 , meaning that the rest (0.57) of the dead material was respired into the DIC pool (table 3.2). Both phytoplankton groups exuded DOM that was assumed to have the isotope signature of phytoplankton. The exudation rate of phytoplankton I (γ_I) was $0.31 \pm 0.023 \text{ d}^{-1}$ and the exudation rate of phyto II (γ_{II}) was $0.24 \pm 0.017 \text{ d}^{-1}$. No build-up of labile DOC (LDOC) was observed, because the freshly produced DOM was rapidly consumed by bacteria. Bacteria biomass was assumed constant (Fig. 3.1B), meaning that growth and loss (respiration/mortality/grazing) were balanced.

Table 3.2. Parameter descriptions and values of the food web model for phase I (t0-12). Values are presented as average of all mesocosms \pm standard deviation (n=9) derived from MCMC fitting procedures.

Parameters that were tested for different CO ₂ levels			
Parameter	Unit	Description	Value
μ_I	d ⁻¹	growth rate of Phyto I	0.87 ± 0.013
μ_{II}	d ⁻¹	growth rate of Phyto II	0.18 ± 0.010
ζ_I	d ⁻¹	mortality rate of Phyto I	0.29 ± 0.081
ζ_{II}	d ⁻¹	mortality rate of Phyto II	0.045 ± 0.025
μ_g	d ⁻¹	grazing rate of Zooplankton	0.022 ± 0.005
γ_I	d ⁻¹	exudation rate of Phyto I	0.31 ± 0.023
γ_{II}	d ⁻¹	exudation rate of Phyto II	0.24 ± 0.017
γ_{II}	d ⁻¹	growth rate of Bacteria	0.36 ± 0.029
r_{sink}	d ⁻¹	sinking rate of detritus	0.0082 ± 0.0048
ρ	d ⁻¹	mineralisation rate	0.020 ± 0.004
f_{DOM}	-	part of Phyto mortality to DOM	0.056 ± 0.037
f_{Det}	-	part of Phyto mortality to detritus	0.37 ± 0.05
Parameters that were kept constant for different CO ₂ levels			
Parameter	Unit	Description	Value
ϵ_N	$\mu\text{mol L}^{-1}$	half saturation constant for DIN	0.5
ϵ_l	W m^{-2}	half saturation constant for light	120
ϵ_g	$\mu\text{mol L}^{-1}$	half saturation constant for phyto I+II	1
ϵ_{DOC}	$\mu\text{mol L}^{-1}$	half saturation constant for LDOC	0.001
f_{faeces}	-	part of zooplankton grazing to faeces	0.149
ζ_{Zoo}	-	Zooplankton loss into sediment traps	0.654
NC	-	Stoichiometric ratio	16/106

Bacteria maximum growth (μ_{Bac}) was $0.36 \pm 0.029 \text{ d}^{-1}$. Mesozooplankton was assumed to graze on phytoplankton and low grazing rates for zooplankton (μ_{g}) were observed, only $0.022 \pm 0.005 \text{ d}^{-1}$ and the fraction of grazing that went into faeces (f_{faeces}) was 0.15. Zooplankton biomass in the mesocosms stayed constant, but a large number of zooplankton (cirripedia) was found in the sediment traps (Niehoff et al. 2012; Czerny et al. 2012A). The part of zooplankton losses (which balanced zooplankton gains) that ended in the traps (ζ_{Zoo}) was 65 % and the other 35 % was respired. Detritus was mainly formed of dead phytoplankton, so started to increase after day 6, when mortality of phytoplankton occurred. The mineralisation rate (ρ) of detritus into DIN and DIC was $0.020 \pm 0.004 \text{ d}^{-1}$ and sinking rate of detritus (r_{sink}) was $0.008 \pm 0.005 \text{ d}^{-1}$ (table 3.2). Two of the twelve model parameters potentially sensitive to CO_2 showed to be indeed affected by CO_2 treatments. Grazing rates (μ_{g}) decreased with increasing CO_2 (Fig. 3.6A, $r = -0.79$, $p < 0.05$). Sinking rates (r_{sink}) showed a positive correlation with pCO_2 ($r = 0.81$, $p < 0.01$, Fig. 3.6B). The sinking was 5 times higher at high CO_2 ($0.016 \pm 0.0034 \text{ d}^{-1}$) compared to lower CO_2 ($0.0020 \pm 0.0014 \text{ d}^{-1}$). For validation of the parameters, the model was also tested with ζ_{Zoo} included as CO_2 sensitive parameter. ζ_{Zoo} is the part of zooplankton carbon gain that ended in the sediment traps. ζ_{Zoo} was found to be CO_2 independent. The amount of zooplankters that ended in the traps were also independent of CO_2 levels (Niehoff et al. 2012). As including the parameter increased the model uncertainty it was therefore excluded from MCMC analysis.

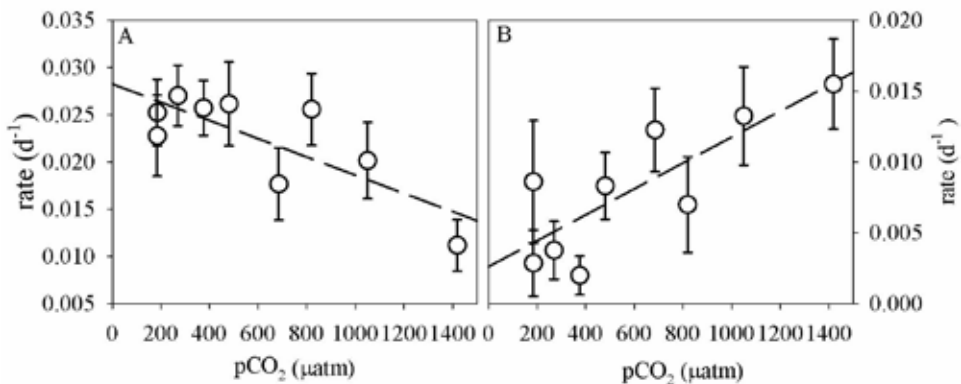


Fig. 3.6. Model parameters (d^{-1}) with uncertainties for A) zooplankton grazing rates and B) sinking rates vs. average CO_2 levels in phase 1.

Model results: carbon fluxes

The set of parameters that was selected during the MCMC analysis was used to calculate average carbon fluxes over phase 1 (t0-12). The flux from DIC to phytoplankton was $1.78 \pm 0.17 \mu\text{mol C L}^{-1} \text{ d}^{-1}$, with a flux of $1.17 \pm 0.10 \mu\text{mol C L}^{-1} \text{ d}^{-1}$ to phyto I and a flux of $0.61 \pm 0.089 \mu\text{mol C L}^{-1} \text{ d}^{-1}$ to phyto II (Fig. 3.7). Large parts from gross phytoplankton production were exudated as DOC, $0.36 \pm 0.05 \mu\text{mol C L}^{-1} \text{ d}^{-1}$ and $0.19 \pm 0.03 \mu\text{mol C L}^{-1} \text{ d}^{-1}$ from phyto I and II respectively, so $0.59 \pm 0.06 \mu\text{mol C L}^{-1} \text{ d}^{-1}$ in total, and $30.7 \pm 1.2 \%$ of total primary production. DOC was assumed to be the only carbon source for bacteria and the consumption rate of bacteria was $0.60 \pm 0.062 \mu\text{mol C L}^{-1} \text{ d}^{-1}$.

3.4 Discussion

Plankton carbon flows under low nutrients

While most of the CO₂ enrichment mesocosm experiments involved inorganic nutrient addition and focussed on production and export food chains, this study investigated ocean acidification in a nutrient regenerating food chain, at least during phase 1 of the experiment. The low nutrient concentrations, low chl *a*, and high heterotrophic biomass in Kongsfjorden waters were characteristic for a post-bloom situation (Rokkan-Iversen and Seuthe 2011). Although nutrient concentrations were low, a small phytoplankton started right after enclosure, probably fueled by efficient recycling of nutrients accompanied with remineralisation of DON. Total primary production rates in our experiment (21 mmol C m⁻² d⁻¹, integrated over the 12 m sampling depth) were similar to the median particulate primary production of 20 mmol C m⁻² d⁻¹ in Arctic regions (synthesis by Kirchman et al. 2009a). However, particulate primary production in this study was lower, ~14 mmol C m⁻² d⁻¹ (integrated over the 12 m sampling depth), suggesting nutrient limitation in our study. The primary production during the bloom was dominated by autotrophs or nanoplankton (comprised in phyto I) as indicated by their high growth and production rates (table 3.1, 3.2). Despite their low biomass, they were responsible for two thirds of the primary production in phase I. The other third of primary production was contributed by the phyto II. Although phyto II dominated in terms of biomass, they had lower growth and production rates, likely attributable to the mixotrophic character of the group. The difference in model based primary production and data based particulate primary production is the dissolved primary production: exudation of recent fixed organic matter. Two thirds of GPP was used for net particulate primary production (1.2 μmol C L⁻¹ d⁻¹, table 3.1) and the other one third was exuded as dissolved primary production to fuel bacterial production. Bacteria were an important component of the pelagic food web and a rapid consumer of primary production, as indicated by rapid transfer of label from phytoplankton to bacteria (Fig. 3.1A). Bacteria production amounted to a third of total phytoplankton production (34 %). A remarkably similar average BP:PP ratio (34 %) was observed in Arctic transect studies by Kirchman et al. (2009b), although their absolute production rates were much lower. In a data synthesis by (Cole et al. 1988), the BP:PP in the euphotic zone was typically 20-30 %. Bacterial growth rates in phase 1 (0.33-0.36 d⁻¹) were relatively high compared to average Arctic bacterial growth rates (Kirchman et al. 2009a). Despite the high growth rates, the biomass of bacteria did not increase (Fig. 3.1B), indicating a strong removal pressure (top-down control) on bacteria e.g. by viruses or microzooplankton (heterotrophic dinoflagellates) grazing. The high abundance of heterotrophic dinoflagellates indicates that microzooplankton grazing likely controlled bacterial biomass (Schulz et al. 2012). Also mesozooplankton had high biomass, but grazing rates of mesozooplankton on primary production were very low, as indicated by maximum daily grazing rates of 0.022 d⁻¹ on phytoplankton biomass. In phase 1, only 11 % of primary production was consumed by mesozooplankton. Summarized, the high BP:PP, high microzooplankton abundance, and low mesozooplankton grazing indicate that the microbial food web was more important in this study than a herbivorous food web (Legendre and Razouldagan 1995). Our results on plankton food web structure fit very well with the previously described post-bloom (May-July) situation in Kongsfjorden (Rokkan Iversen and Seuthe 2011) with high BP:PP production and a prominent role for the microbial food web.

However, they suggested a control of phytoplankton biomass by mesozooplankton grazing, because of low phytoplankton biomass, high primary production, and high zooplankton biomass, which is not supported by our findings. Viral infections likely caused the bloom to collapse after t6, since phytoplankton decline coincided with a peak in virus abundance (Brussaard et al. 2012). Mortality affected phyto I much more than phyto II, consistent with virus-host specificity. Phytoplankton mortality rates of up to 0.3 d⁻¹, as observed for phyto I, have been recorded during bloom declines as well as in oligotrophic systems (reviewed in Brussaard 2004). When phytoplankton cells die, the cells lyse and a large portion is released into DOM, which can be subsequently used by bacteria (reviewed in Brussaard 2004). In our study, phytoplankton mortality did not stimulate bacterial production *per se*, since bacterial production declined after 6 as well. Possible explanations for the decline in bacterial production are concurrent viral infections or a shift from microzooplankton grazers from phyto I to bacteria. DOC accumulation after mortality was observed in the mesocosms (Czerny et al. 2012A, Engel et al. 2012). The material released by viral lysis is sticky and viral induced mortality can enhance formation and persistence of large aggregates (Peduzzi and Weinbauer 1993). Although it was difficult to constrain, we estimated that approximately one third of dying phytoplankton ended up as detritus. Detritus formed only a small part of total POC (10 %) and was thus mainly formed of dead algae. The sedimentation losses of detritus were low (0.008 d⁻¹) and in phase 1, sinking detritus comprised only 1% of primary production. In phase 1, zooplankton contributed substantially to sedimented organic material (Niehoff et al. 2012). Together with zooplankton settling in the traps, the average export corresponded to ~about 7 % of primary production. In contrast, the calculated export in a previous mesocosm experiment with nutrient addition was ~24 times higher than the export rates in this experiment (Riebesell et al. 2007).

Plankton carbon flows after nutrient addition

The addition of nutrients did not increase phytoplankton and bacterial biomass in the mesocosms (Fig. 3.1B). However, chl *a* increased after nutrient addition (Schulz et al. 2012), indicating that phyto II shifted towards an autotrophic community. The production rate of phyto II also slightly increased after nutrient addition (table 3.1). Interestingly, bacterial production and growth decreased after nutrient addition (table 3.1), contrary to the generally observed positive relation between nutrient concentrations and growth efficiency (del Giorgio and Cole 1998). Bacteria in phase 2 could have been limited by substrate (DOC) availability, since extra cellular release decreased after nutrient addition (Engel et al. 2012). In agreement with our findings, a similar decrease in bacterial growth after nutrient addition was found with radioactive leucine incorporation during the experiment (Piontek et al. 2012). The largest change in phase 2 compared to phase 1 was an increase in sedimentation. Large sedimentation of (freshly produced) organic matter occurred after day 24, when chain-forming diatoms started to dominate the mesocosms (Czerny et al. 2012 A). The diatoms probably formed aggregates that facilitated sinking of organic matter. The higher isotopic enrichment of sedimented organic matter compared to the water column (Fig. 3.1A) showed that the aggregates were formed of freshly produced organic matter and the dominance of diatoms was confirmed by the high presence of phyto II markers in the sediment trap material.

Methodological considerations and assumptions

^{13}C labeling combined with modelling has been used successfully in previous mesocosm studies to quantify carbon flows and interactions in plankton food webs (van den Meersche et al. 2004, 2011; de Kluijver et al. 2010). However, there are some assumptions and potential errors that need attention. A main advantage of using a ^{13}C tracer is that production can be measured *in situ*, in contrast to other methods like radioactive tracers that require side incubations with perturbed environmental (e.g. light) conditions. Using PLFA biomarkers, phytoplankton and bacteria group specific primary production can be estimated in addition to total POC production (Dijkman et al. 2009). However, PLFA based production (phyto I, II, bacteria) slightly overestimated the production of total POC (table 3.2), what can be explained by potential errors in conversion factors and uncertainties arising from averaging numbers. A comparison of community production measurements performed during the experiment with different methods (DIC, oxygen, ^{14}C , ^{13}C) is presented by (Tanaka et al. 2012). There was a good correlation between ^{13}C -POC and DIC based NCP, as we expected, since they were both measured *in situ* (Tanaka et al. 2012).

Although PLFA can be used as taxonomic markers (Dijkman and Kromkamp 2006) the majority of PLFA markers do not allow distinction between heterotrophic and autotrophic phytoplankton, like mixotrophic dinoflagellates, and therefore we had to consider heterotrophic dinoflagellates as part of phyto II. Phyto II had the largest biomass (36 % of POC) and comparison with chl *a* as a proxy for autotrophic biomass, after subtraction of phyto I, indicated that >65 % of phyto II in phase I was heterotrophic (Czerney et al. 2012A). The ^{13}C incorporation method is limited when phytoplankton is saturated with tracer, i.e. it has taken the signature of the source, corrected for fractionation, in which case uptake of substrate will not cause further changes in ^{13}C . Saturation was observed in phyto I after the first six days precluding growth estimates after this period and precluding model application for phase II. For future experiments an additional ^{13}C spike with nutrient addition is recommended (van Engeland et al. 2012). The other carbon pools did not get saturated with tracer (Fig. 3.1A) and bacteria never reached the isotope labeling of phytoplankton (Fig. 3.1A). Assuming that phytoplankton is the only carbon source for bacteria, this implies a senescent or dorming pool of bacteria that did not grow during the experiment. Another explanation is that bacteria grew on total POC, which is likely, since they closely followed the labeling of POC (Fig. 3.1A). Zooplankton never reached label enrichment of any carbon pool (Fig. 3.1A). Mesozooplankton has a slow turnover in response to dietary changes, what contributes to low labeling patterns. A study on carbon turnover in Arctic crustaceans showed low turnover in stable isotopes, with a half life of 14 days (Kaufman et al. 2008). For simplicity, one grazing rate on phytoplankton was assumed in the model, but there was probably selective grazing on different phytoplankton groups. Due to the labeling differences between phyto I and II, grazing rates would decrease if zooplankton primarily grazes on phyto I and increase if zooplankton primarily grazes on phyto II.

Production processes are relatively easy to determine with ^{13}C incorporation, but it is more challenging to quantify and allocate loss processes. The partitioning of carbon from phytoplankton mortality was difficult to constrain (van Engeland et al. 2012). The partitioning in the particulate fraction was relatively easy to determine, because of direct POC measurements, but partitioning into dissolved material was more difficult, because of lack of accurate ^{13}C -DOC measurements. Measuring isotope labeling in DOC is challenging because of methodological constraints (Osburn and St Jean 2007; van den Meersche et al. 2011) and because of the high background concentrations of total DOC (4 times POC).

Moreover, it is expected that freshly produced DOC is rapidly consumed rather than accumulating in the DOC pool. DOC production derived from the model to fuel bacteria production was 10 times higher than DOC production based on ¹³C incorporation. For sufficient ¹³C enrichment in DOC, the amount of added tracer should be >10 times higher.

The data from the sediment trap samples have to be considered with care. The sediment traps were positioned only ~15 m deep, so the material in the sediment traps cannot quantitatively be considered to be exported compared to studies where traps were placed below the euphotic zone. The sediment traps were also within the daily migration zone of zooplankton and there were a large number of *Cirripedia* settling in the sediment traps. Zooplankton can contribute largely to settling material, especially in shallow traps and contributions of 14-90 % of zooplankton to POC in traps were reported by Buesseler et al. (2007). In the model a 82 % contribution of zooplankton to sediment trap material was necessary to achieve the low labeling of sediment material in phase 1. Preferential settling of old, unlabeled material in the traps could have contributed to the low labeling as well, but this was not considered in the model. Although above processes can cause potential errors in the estimated carbon fluxes, they do not explain the observed CO₂ effects, since they are expected to occur in all mesocosms.

CO₂ effects

In this study, we aimed to increase our understanding of CO₂ effects on primary production, community respiration, and export in Arctic communities by looking at individual uptake and loss rates and by quantifying the interactions between food web compartments with a food web model. Some of the CO₂ effects in phase 1 that were observed in individual fluxes (grey arrows in Fig. 3.7) were not shown in the integrated food web, so we consider them with care.

Although it was not captured by the model, the data suggest that loss in phytoplankton production due to mortality can be CO₂ sensitive. When the bloom collapsed (after t₆), the loss in particulate primary production was significantly lower at higher CO₂ levels (Fig. 3.3C). Furthermore, both simple regression (Fig. 3.4C) and model inference (Fig. 3.6B) showed that sedimentation of fresh organic matter increased with increasing CO₂. These observations suggest the presence of CO₂ effects on phytoplankton mortality in phase 1. Since mortality rates were not sensitive to CO₂ and viral numbers were not CO₂ dependent (Brussaard et al. 2012), we speculate that there were CO₂ effects on the partitioning of dead phytoplankton in particulate and dissolved organic matter fractions. The organic material released at high CO₂ could be of more sticky nature serving as precursor of transparent exopolymer particles (TEP) or less degradable (Engel et al. 2002; Czerny et al. 2012A; Engel et al. 2012). When more phytoplankton mortality ends in aggregates or particles, it could lead to enhanced sinking at high CO₂, as observed in phase 1. Future research on CO₂ effects on partitioning of phytoplankton mortality is needed to support our hypotheses.

Both simple regression (Fig. 3.4B) and model output (Fig. 3.6A), showed reduced zooplankton grazing in phase I with increasing CO₂. There was no CO₂ effect found on zooplankton numbers (Niehoff et al. 2012) and we can only speculate about the mechanisms. One potential explanation is that reduced grazing is a direct consequence of higher sedimentation at higher CO₂ during phase 1. Reduced grazing could also result from the reduced initial production of phyto II at higher CO₂ (Fig. 3.3B).

Other possible explanations for reduced grazing could be CO₂ induced changes in food quality, i.e. the production of less essential fatty acids. However, there were no CO₂ dependent shifts in fatty acid compositions observed in phase 1 (this study, Leu et al. 2012). A hampering CO₂ effect on *Cirripedia* development to the next stage was observed (Niehoff et al. 2012), but whether this was related to lower grazing, needs to be further addressed.

In this study, no CO₂ effect on bacteria growth and production were observed. There was also no CO₂ effect on carbon exudation by phytoplankton as source for bacteria, although this process is considered potentially CO₂ sensitive. It has been hypothesized that increasing CO₂ could stimulate carbon overconsumption and subsequent extracellular release, but most studies done so far showed no effects on DOC production in community-level CO₂ enrichment studies (e.g. Engel et al. 2004b). Previous mesocosm studies focussed on nutrient replete situations and it was suggested that CO₂ effects on extracellular release would be more pronounced under nutrient limitation (Thingstad et al. 2008; de Kluijver et al. 2010). The results here show that bacterial production on phytoplankton exudation is also not enhanced with CO₂ in a post bloom situation. However, when bacterial growth is limited by nutrient availability, a lack of bacterial response does not necessarily mean that there was no stimulation of extracellular release. Exudates are also important players in formation of TEP and marine snow and subsequent export (Engel et al. 2004a).

After nutrient addition phytoplankton production (phyto II) was initially stimulated by higher CO₂ (t14-22), but showed an optimum around current CO₂ levels of 340 µatm over the whole phase after nutrient addition (t14-t28; Fig. 3.3C). The response of phyto II was likely an indirect effect of CO₂ due to competition with other phytoplankton groups. The proposed mechanism (based on pigments and flow cytometry) is that increasing CO₂ stimulated production of picoplankton directly after nutrient addition and outcompeted larger phytoplankton like diatoms in the final stage of the experiment (Schulz et al. 2012). The response to CO₂ after nutrient addition was also not gradual for POC production and sedimentation. POC production after nutrient addition showed a non-linear response to CO₂ with a transition point around current CO₂ levels (Fig. 3.4A). Production was lower at CO₂ levels above 400 µatm and because of the large export in phase 3, the CO₂ effect on POC production was directly reflected in settling material (Fig 3.4C). Our findings suggest that CO₂ effects on some processes are stepwise rather than gradual, which can be of interest for future research.

3.5 Conclusions

This mesocosm study is the first to study ocean acidification effects on Arctic plankton communities, in a system dominated by regenerated production. Before nutrient addition (phase 1) the pelagic food web was characterized by high BP:PP, high microzooplankton abundance, low mesozooplankton grazing and low export. Comparable production rates, but increased export were observed after nutrient addition (phase 2). CO₂ effects were subtle and different for each phase. We observed a stimulating effect of CO₂ on export and a hampering effect on community (mesozooplankton) respiration in phase 1 and a hampering effect of CO₂ on production and export in phase 2. Generally, more research on plankton communities with different composition and nutrient states are necessary to improve our understanding of pelagic food web processes under future CO₂ conditions.

Acknowledgements

This work is a contribution to the “European Project on Ocean Acidification” (EPOCA) which received funding from the European Community’s Seventh Framework Programme (FP7/2007-2013) under grant agreement no. 211384. We gratefully acknowledge the logistical support of Greenpeace International for its assistance with the transport of the mesocosm facility from Kiel to Ny-Ålesund and back to Kiel. We also thank the captains and crews of M/V ESPERANZA of Greenpeace and R/V Viking Explorer of the University Centre in Svalbard (UNIS) for assistance during mesocosm transport and during deployment and recovery in Kongsfjorden. We thank the staff of the French-German Arctic Research Base at Ny-Ålesund, in particular Marcus Schumacher, for on-site logistical support. We thank the Dutch Station and especially Maarten van Loon for accommodation in Ny-Ålesund. We thank the mesocosm team and especially the people of GEOMAR for their support during the experiment. The excellent team spirit made the experiment enjoyable and successful. We thank Pieter van Rijswijk of NIOZ for preparation and lab support. The analytical lab at NIOZ is acknowledged for stable isotope analyses. We thank Richard Bellerby of Bjerknes Centre for Climate Research for DIC numbers. Mehdi Ghourabi is acknowledged for his help with model construction. Financial support was provided through Transnational Access funds by the EU project MESOAQUA under grant agreement no. 22822, the European Project on Ocean Acidification (EPOCA, FP7, 2211384), and the Darwin Center for Biogeosciences supported by the Netherlands Organization for Scientific Research.

Appendix: Model formulations

Table 3.1: State variables, model forcings, and derived output variables for which calibration data were available. The * indicates availability of a data counterpart for calibration. The subscript i refers to the two phytoplankton groups (i I,II) (after Van Engeland et al. 2012).

State variables			
DIN	dissolved inorganic nitrogen	$\mu\text{mol l}^{-1}$	*
DON	dissolved organic nitrogen	$\mu\text{mol l}^{-1}$	*
$^{13}\text{C}_{Phyto_i}$	^{13}C in phytoplankton group i	$\mu\text{mol l}^{-1}$	
$^{12}\text{C}_{Phyto_i}$	^{12}C in phytoplankton group i	$\mu\text{mol l}^{-1}$	
$^{13}\text{C}_{Zoo}$	^{13}C in zooplankton	$\mu\text{mol l}^{-1}$	
$^{13}\text{C}_{Det}$	^{13}C in detritus	$\mu\text{mol l}^{-1}$	
$^{12}\text{C}_{Det}$	^{12}C in detritus	$\mu\text{mol l}^{-1}$	
$^{13}\text{C}_{Bac}$	^{13}C in bacteria	$\mu\text{mol l}^{-1}$	
$^{13}\text{C}_{LDOC}$	^{13}C in labile dissolved organic carbon	$\mu\text{mol l}^{-1}$	
$^{12}\text{C}_{LDOC}$	^{12}C in labile dissolved organic carbon	$\mu\text{mol l}^{-1}$	
$^{13}\text{C}_{Sed}$	^{13}C in sediment	$\mu\text{mol l}^{-1}$	
$^{12}\text{C}_{Sed}$	^{12}C in sediment	$\mu\text{mol l}^{-1}$	
forcing functions			
$^{13}\text{C}_{DIC}$	^{13}C in dissolved inorganic carbon	$\mu\text{mol l}^{-1}$	
$^{12}\text{C}_{DIC}$	^{12}C in dissolved inorganic carbon	$\mu\text{mol l}^{-1}$	
I	irradiance	W m^{-2}	
derived output variables for calibration			
DOC_{tot}	total DOC (labile + refractory background)	$\mu\text{mol l}^{-1}$	*
POC	particulate organic carbon	$\mu\text{mol l}^{-1}$	*
PON	particulate organic nitrogen	$\mu\text{mol l}^{-1}$	*
C_{Phyto_i}	carbon in phytoplankton group i	$\mu\text{mol l}^{-1}$	*
C_{Sed}	carbon in sedimented detritus	$\mu\text{mol l}^{-1}$	*
N_{Sed}	nitrogen in sedimented detritus	$\mu\text{mol l}^{-1}$	*
$\delta^{13}\text{C}_{Phyto_i}$	$\delta^{13}\text{C}$ of phytoplankton group i	‰	*
$\delta^{13}\text{C}_{Zoo}$	$\delta^{13}\text{C}$ of zooplankton	‰	*
$\delta^{13}\text{C}_{Bac}$	$\delta^{13}\text{C}$ of bacteria	‰	*
$\delta^{13}\text{C}_{Sed}$	$\delta^{13}\text{C}$ of sedimented detritus	‰	*
$\delta^{13}\text{C}_{POC}$	$\delta^{13}\text{C}$ of POC	‰	*

Table 3.2: Rate equations, mass balance equations for the state variables, and equations for the calculation of derived output variables. The subscript i refers to the phytoplankton groups ($i \in I, II$). The superscript x refers to the carbon isotope ($x = 12, 13$) (after Van Engeland et al. 2012).

Rate equations	
$F_{DIC}^{13C} = pref \times \frac{^{13}C_{DIC}}{^{13}C_{DIC} + ^{12}C_{DIC}}$	$Loss_{Zoo}^{Det} = f_{faeces} \times \sum_i graz_{Phyto_i}$
$growth_{Phyto_i} = \mu_i \times \frac{DIN}{DIN + ks_N} \times \frac{I}{I + ks_I} \times C_{Phyto_i}$	$Loss_{Zoo}^{Sed} = \xi_{Zoo} \times \sum_i graz_{Phyto_i}$
$mort_{Phyto_i} = \xi_i \times C_{Phyto_i}$	$growth_{Bac} = \mu_{Bac} \times \frac{LDOC}{LDOC + ks_{DOC}} \times C_{Bac}$
$Loss_{Phyto_i}^{DOM} = f_{DOM} \times mort_{Phyto_i}$	$resp_{Bac} = growth_{Bac}$
$Loss_{Phyto_i}^{Det} = f_{Det} \times mort_{Phyto_i}$	$min_{DON} = \rho \times DON$
$resp_{Phyto_i} = (1 - f_{Det} - f_{DOM}) \times \sum_i mort_{Phyto_i}$	$min_{Det} = \rho \times C_{Det}$
$exud_{Phyto_i} = \gamma_i \times growth_{Phyto_i}$	$sinking = r_{sink} \times C_{Det}$
$graz_{Phyto_i} = \mu_g \times \frac{C_{Phyto}}{C_{Phyto} + ks_g} \times C_{Zoo}$	$resp_i = \sum_i resp_{Phyto_i} + resp_{Zoo} + resp_{Bac}$
$resp_{Zoo} = (1 - f_{faeces} - \xi_{Zoo}) \times \sum_i graz_{Phyto_i}$	
$\frac{dDIN}{dt} = \left(- \sum_i growth_{Phyto_i} + min_{Det} + resp \right) \times NC + min_{DON}$	
$\frac{dDON}{dt} = \left(\sum_i exu_{Phyto_i} - growth_{Bac} \right) \times NC + \sum_i Loss_{Phyto_i}^{DOM} \times NC - min_{DON}$	
$\frac{d^x C_{Phyto_i}}{dt} = F_{DIC}^x \times growth_{Phyto_i} - F_{Phyto_i}^x \times (mort_{Phyto_i} + graz_{Phyto_i} + exu_{Phyto_i})$	
$\frac{d^x C_{Det}}{dt} = \sum_i \left[F_{Phyto_i}^x \times Loss_{Phyto_i}^{Det} + F_{Zoo}^x \times Loss_{Zoo}^{Det} \right] - F_{Det}^x \times (min_{Det} + sinking)$	
$\frac{d^x C_{LDOC}}{dt} = \sum_i \left[F_{Phyto_i}^x \times Loss_{Phyto_i}^{DOM} \right] - F_{LDOC}^x \times growth_{Bac}$	
$\frac{d^x C_{Sed}}{dt} = F_{Det}^x \times sinking + F_{Zoo}^x \times Loss_{Zoo}^{Sed}$	
$\frac{d^{13}C_{Bac}}{dt} = (F_{LDOC}^{13C} - F_{Bac}^{13C}) \times growth_{Bac}$	
$\frac{d^{13}C_{Zoo}}{dt} = \sum_i \left[(F_{Phyto_i}^{13C} - F_{Zoo}^{13C}) \times (1 - f_{faeces}) \times graz_{Phyto_i} \right]$	

Additional output variables

$$C_{Phyto_i} = {}^{13}C_{Phyto_i} + {}^{12}C_{Phyto_i}$$

$$C_{Det} = {}^{13}C_{Det} + {}^{12}C_{Det}$$

$$C_{Sed} = {}^{13}C_{Sed} + {}^{12}C_{Sed}$$

$$N_{Sed} = C_{Sed} \times NC$$

$$LDOC = {}^{13}C_{LDOC} + {}^{12}C_{LDOC}$$

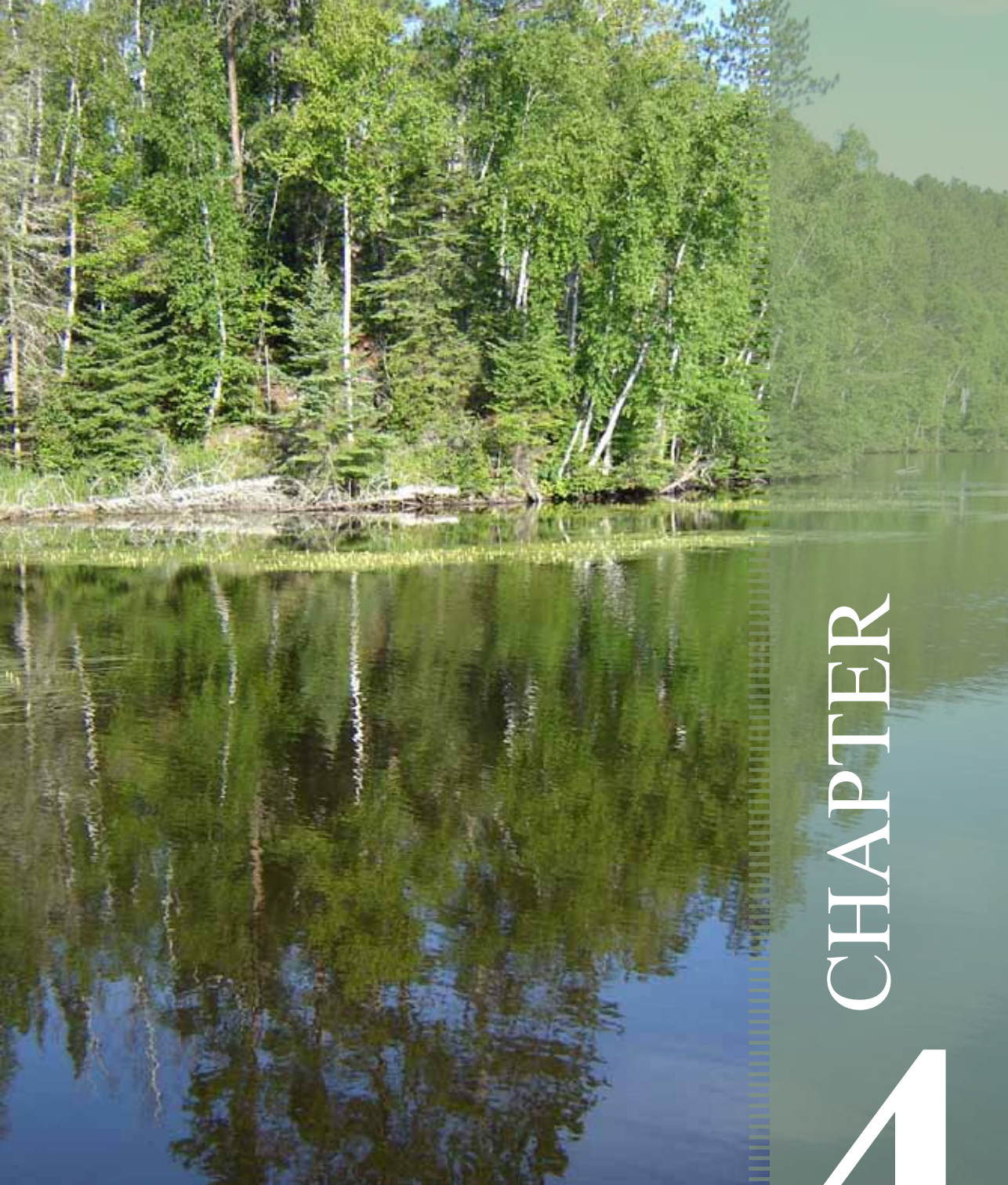
$$POC = \sum_i C_{Phyto_i} + C_{Zoo} + C_{Det} + C_{Bac}$$

$$PON = POC \times NC$$

$$DOC_{tot} = DOC + LDOC$$

Anna de Kluijver, Petra L. Schoon, John A. Downing, Stefan Schouten,
and Jack J. Middelburg

In preparation



CHAPTER

4



Carbon isotope contents on lake
food-web interactions along a
trophic gradient

Abstract

Carbon isotope variability in planktonic producers and consumers were studied in a survey of 22 North-American meso-oligotrophic to eutrophic lakes that were classified as meso-oligotrophic and eutrophic to assess food-web interactions along a trophic gradient. Carbon isotope ratios ($\delta^{13}\text{C}$) of dissolved inorganic and organic carbon (DIC and DOC), particulate organic carbon (POC), phytoplankton, allochthonous material, and bacterial and zooplankton consumers were analyzed. The $\delta^{13}\text{C}$ of phytoplankton producers and bacterial consumers were determined from $\delta^{13}\text{C}$ of fatty acid biomarkers. Lake $p\text{CO}_2$ was primarily determined by autochthonous production (phytoplankton biomass), especially in eutrophic lakes, and governed $\delta^{13}\text{C}$ of DIC. All organic-carbon pools showed larger variability in $\delta^{13}\text{C}$ in eutrophic lakes compared to meso-oligotrophic lakes caused by high variability in $\delta^{13}\text{C}$ at the base of the food web (both autochthonous and allochthonous carbon). Phytoplankton $\delta^{13}\text{C}$ was negatively related to lake $p\text{CO}_2$ over all lakes and positively related to phytoplankton biomass in eutrophic lakes, which was also reflected in a large range in photosynthetic isotope fractionation ($\epsilon_{\text{CO}_2\text{-phyto}}$, 8-25 ‰). Carbon isotope ratios of bacteria matched those of POC, but not those of DOC in all lakes. In meso-oligotrophic lakes, bacteria used a mixture of carbon from various sources, while they depended more on phytoplankton in eutrophic lakes. The $\delta^{13}\text{C}$ of zooplankton showed strong correlation with $\delta^{13}\text{C}$ of phytoplankton in all lakes, independent of trophic state, suggesting that phytoplankton were the main carbon source for zooplankton. Additionally, we calculated autochthonous and allochthonous carbon contributions to bacteria and zooplankton and found higher autochthonous contributions to zooplankton (59 %) than to bacteria (48 %), which were independent of trophic state. Overall, our results underline the importance of lake trophicity in controlling plankton food web structure.

4.1 Introduction

Recent studies suggest that lakes, in disproportion to their relative surface area, contribute significantly to the carbon budget of terrestrial ecosystems and vent a considerable amount of CO₂ to the atmosphere (Cole et al. 2007). Freshwater systems are very active in processing terrestrial carbon and a large part is respired in lakes, making many lake overall heterotrophic (Cole et al. 1994). The food-web composition of lakes largely governs carbon cycling and the balance between primary production and community respiration (lake metabolism) determines whether lakes are possibly sources or sinks of CO₂. Primary (autochthonous) production increases with increasing trophity (nutrient concentrations) and lakes with high autochthonous carbon production, i.e. eutrophic lakes, are considered to be sinks for CO₂ (Schindler et al. 1997). The loading of allochthonous (terrestrial) carbon is a key factor controlling community respiration of lakes. The metabolic balance of lakes is directly influenced by allochthonous organic carbon loading and trophic state (Del Giorgio and Peters 1994, Hanson et al. 2003).

The contribution of allochthonous vs. autochthonous carbon to plankton food webs has therefore been a primary research focus in recent years. Heterotrophic bacteria (shortly bacteria) are key players in processing organic matter from autochthonous (Cole et al. 1988) and allochthonous origin (Tranvik 1992), primarily as dissolved organic carbon (DOC). It is estimated that bacteria process 30-60 % of primary production and bacteria production often exceeds primary production, especially in unproductive systems (Del Giorgio et al. 1997). Phytoplankton is considered the primary food source for zooplankton, via herbivory, but zooplankton can also obtain energy from bacteria (Wylie and Currie 2001) and terrestrial carbon (Cole et al. 2006). Plankton food-web structure, with multiple interactions is known to change along a trophic continuum (Legendre and Rassoulzadegan 1995). Especially in oligotrophic, humic lakes with low primary production and high input of terrestrial carbon, bacteria have high biomass and dominate community respiration (Tranvik 1992, Biddanda et al. 2001). When lakes move from oligotrophic towards eutrophic, with higher primary production, the herbivorous food web becomes more important and the relative contribution of bacteria as heterotrophs declines (Cotner and Biddanda 2002). Continuing towards the other side of the spectrum from eutrophic towards hyper-eutrophication, the microbial food web starts to dominate again, what can be explained by an increasing dominance of cyanobacteria and a co-occurring shift in zooplankton community structure (Gliwicz 1969). Thus, both allochthonous input into lakes and trophic state determine plankton food-web structure, which in return has a large impact on lake metabolism.

Stable isotope analyses (SIA) of organic matter are a powerful tool to study food web interactions in lakes. The stable carbon isotope variability in sources and consumers has been used to trace carbon flows and origins in plankton food webs (Fry 2006). A major challenge in SIA is to elucidate the isotope signatures ($\delta^{13}\text{C}$) of the different carbon sources, especially $\delta^{13}\text{C}$ of microbial organisms, such as phytoplankton and bacteria. Because it is difficult to separate these potential carbon sources from bulk particulate organic carbon (POC), most studies use indirect methods to determine $\delta^{13}\text{C}$ of phytoplankton ($\delta^{13}\text{C}_{\text{phyto}}$), allochthonous material, and bacteria. Common methods to determine $\delta^{13}\text{C}_{\text{phyto}}$ are the use of $\delta^{13}\text{C}$ of particulate organic carbon (POC) with correction for non-phytoplankton carbon and estimates based on $\delta^{13}\text{C}$ of dissolved inorganic carbon (DIC) with a fractionation factor (ϵ).

Other methods are the use of zooplankton consumers as proxy for $\delta^{13}\text{C}_{\text{phyto}}$ or size fractionation of organic matter and subsequent determination of $\delta^{13}\text{C}$ of different size classes. A comparison and evaluation of the different methods can be found in Marty and Planas (2008).

Bacteria isotope signatures in field studies have been derived from re-growing bacteria in bioassays (Coffin et al. 1989) or dialysis cultures (Kritzberg et al. 2004), with measurement of ^{13}C in POC or respired CO_2 (McCallister et al. 2008) and from biomarkers like nucleic acids (Coffin et al. 1990) and lipids (Bontes et al. 2006, Pace et al. 2007). Some studies used $\delta^{13}\text{C}$ of DOC as proxy for $\delta^{13}\text{C}$ of bacteria, assuming that DOC was the primary carbon source for bacteria (Taipale et al. 2008). A commonly used proxy for allochthonous $\delta^{13}\text{C}$ is the $\delta^{13}\text{C}$ of terrestrial C_3 plants, which dominates most terrestrial vegetation and has a $\delta^{13}\text{C}$ of $\sim -28\text{‰}$ (Fry 2006). However, when vegetation is dominated by C_4 plants, which are common in tropical areas and agricultural areas with corn production and have a $\delta^{13}\text{C}$ of $\sim -14\text{‰}$ (Fry 2006), the isotope signature of allochthonous carbon can be significantly enriched. In lakes with large terrestrial input, $\delta^{13}\text{C}$ of DOC can be used as a proxy for allochthonous $\delta^{13}\text{C}$, since terrestrial carbon forms the largest fraction of DOC (Kritzberg et al. 2004).

Compound specific isotope analysis (CSIA) of polar lipid fatty acid biomarkers (PLFA) has shown to be a valuable tool to determine the isotope signature of plankton producers and consumers (Boschker and Middelburg 2002). Groups of phytoplankton and bacteria have different fatty acids (FA) compositions, so by analyzing the $\delta^{13}\text{C}$ of specific FA, the $\delta^{13}\text{C}$ of phytoplankton and bacteria can be inferred. The combined use of stable isotopes and FA biomarkers has been successfully applied to study autochthonous and allochthonous carbon contributions to zooplankton in a tidal river (Van den Meersche et al. 2009). Few studies have applied CSIA to study carbon flows in plankton food webs in lakes. Examples are a phytoplankton-zooplankton interaction study in a eutrophic lake (Pel et al. 2003), a biomanipulation effect study (Bontes et al. 2006), a ^{13}C lake enrichment study (Pace et al. 2007) and a cyanobacteria-zooplankton interaction study (de Kluijver et al. 2012). To our best knowledge, none has applied natural abundance compound-specific $\delta^{13}\text{C}$ to study carbon flows in plankton food webs along a trophic gradient.

In this study, we used compound-specific isotope analyses to examine carbon flows in plankton food webs in temperate (North-American) lakes. The lake survey encompassed a range in trophic states from meso-oligotrophic lakes, with an expected larger allochthonous input, to eutrophic lakes, with an expected lower allochthonous input. In this trophic range, we explored patterns of isotopic variability in DIC, phytoplankton, allochthonous carbon, heterotrophic bacteria and zooplankton consumers and their relationships. Further, we looked at autochthonous and allochthonous contributions to bacteria and zooplankton consumers and to food web control on lake $p\text{CO}_2$.

4.2 Material and Methods

Field sampling

A total of 22 lakes in Iowa and Minnesota (USA) were sampled in July - August 2009 as part of the ongoing lake monitoring program of the Limnological laboratory of Iowa State University. Key parameters, such as temperature, pH, secchi depth, inorganic nutrients, oxygen, and carbon concentrations were measured as part of and according to the lake monitoring program.

All samples were taken of the upper 2 m of the deepest point of each lake. More information on data collection, lake characteristics, and methods can be found on <http://limnoweb.eeob.iastate.edu/itascalakes> and <http://limnology.eeob.iastate.edu/lakereport>.

Triplicate water samples were taken for stable isotope analyses and concentrations of the major carbon pools. Headspace vials (20 ml and 2 ml) were filled on board with sampled water using the overflow method and sealed with gas-tight caps for DIC isotope analyses and concentrations, respectively. Mercury chloride was added for preservation and the samples were stored upside down at room temperature. For DOC analyses, 20 ml sampled water was filtered over GF/F (0.7 μm pore size, 25 mm diameter) and stored frozen in clean (acid and milli-Q rinsed) vials until further analyses.

Seston samples for particulate organic carbon (POC) and carbohydrates were collected by filtering 0.4 to 1 L of sampled water on pre-weighted and pre-combusted GF/F filters (0.7 μm pore size, 47 mm diameter), which were subsequently dried at 60° (POC) or freeze-dried (carbohydrates); PLFA samples were collected by filtering ~2 L sampled water on pre-combusted GF/F filters (0.7 μm , 47 mm) and filters were stored frozen. Pigment samples were taken for concentrations only and collected by filtering ~600 ml sampled water on GF/F filters (0.7 μm , 47 mm) in the dark and filters were stored frozen. Zooplankton was collected with a Wisconsin (63 μm mesh-size) net. In the laboratory, they were transferred to demineralized water to empty their guts. Total zooplankton, and if there was enough, ~20 individuals of individual groups, were handpicked and transferred to pre-weighted and pre-combusted tin cups, which were subsequently freeze-dried.

Laboratory analyses

POC and zooplankton samples were analyzed for carbon content and isotope ratios on a Thermo Electron Flash EA 1112 analyzer (EA) coupled to a Delta V isotope ratio mass spectrometer (IRMS) (Nieuwenhuize et al. 1994). For DIC isotope analyses, a helium headspace was created in the headspace vials and samples were acidified with H_3PO_4 solution. After equilibration, the CO_2 concentration and isotope ratio in the headspace was measured using EA-IRMS (Gilikin and Bouillon 2007). DIC concentrations were measured using spectrophotometry according to Stoll et al. (2001). For DOC analyses, the samples were acidified and flushed with helium to remove DIC and subsequently oxidized with sodium persulfate ($\text{Na}_2\text{S}_2\text{O}_8$); the produced isotope ratio and concentration of CO_2 was measured using high performance liquid chromatography - isotope ratio mass spectrometry (HPLC-IRMS) (Boschker et al. 2008). PLFA samples were extracted according to a modified Bligh and Dyer method (Bligh and Dyer 1959, Middelburg et al. 2000). The lipids were fractionated in different polarity classes by column separation on a heat activated silic acid column and subsequent elution with chloroform, acetone and methanol. The methanol fractions, containing most of the PLFA were collected and derivatized to fatty acid methyl esters (FAME). The 12:0 and 19:0 FAME were added as internal standards. Concentrations and $\delta^{13}\text{C}$ of individual PLFA were measured using gas chromatography-combustion isotope ratio mass spectrometry (GC-C-IRMS) (Middelburg et al. 2000). Pigment samples were extracted with 90 % acetone in purified (miliQ) water with intense shaking and concentrations of individual pigments were measured on HPLC (Wright et al. 1991). Carbohydrate samples were hydrolyzed in H_2SO_4 , neutralized with SrCO_3 and precipitated with BaSO_4 . The supernatant was collected and measured using HPLC-IRMS according to Boschker et al. (2008).

Data analyses

The lakes were divided into eutrophic and meso-oligotrophic lakes based on average summer total phosphorus (TP) concentrations. Lakes with TP values $>24 \mu\text{g L}^{-1}$ and a corresponding trophic state index >50 were classified as eutrophic, and lakes with TP values $<24 \mu\text{g L}^{-1}$ as meso-oligotrophic (Carlson 1977). All lakes in Iowa and one lake in Minnesota were classified as eutrophic, while all meso-oligotrophic lakes were located in Minnesota. The different components of the CO_2 system were calculated from temperature, laboratory pH, and DIC concentrations using a salinity of 0 using R package AquaEnv (Hofmann et al. 2010). Stable isotope ratios are expressed in the delta notation ($\delta^{13}\text{C}$), which is the $^{13}\text{C}/^{12}\text{C}$ ratio relative to VPDB standard, in permille (‰). The isotope ratio of CO_2 (aq) ($\delta^{13}\text{C}_{\text{CO}_2}$) was calculated from $\delta^{13}\text{C}_{\text{DIC}}$ according to Zhang et al. (1995). The used formula was

$$\delta^{13}\text{C}_{\text{CO}_2} = \delta^{13}\text{C}_{\text{DIC}} - 0.0144 \times T(^{\circ}\text{C}) \times f\text{CO}_3^{2-} + 0.107 \times T(^{\circ}\text{C}) - 10.53 \quad (4.1)$$

$f\text{CO}_3^{2-}$ is the fraction of CO_3^{2-} in total DIC, calculated from pH and DIC concentrations.

Poly-unsaturated fatty acids (PUFA) are abundant in and can be used as chemotaxonomic markers for phytoplankton (Dijkman and Kromkamp 2006). The most abundant PUFA in all lakes were 18:3 ω 3, 18:4 ω 3, 20:5 ω 3, 22:6 ω 3 and 20:4 ω 6 and their concentration-weighted $\delta^{13}\text{C}$ were used to determine phytoplankton isotope ratios ($\delta^{13}\text{C}_{\text{phyto}}$). Phytoplankton is considered a mixture of eukaryotic algae and cyanobacteria. Branched fatty acids (BFA) are abundant in heterotrophic bacteria (Kaneda 1991). The most abundant BFA were i15:0, ai15:0 and i17:0 and their weighted $\delta^{13}\text{C}$ were used to determine heterotrophic bacteria isotope ratios ($\delta^{13}\text{C}_{\text{bac}}$), which we further consider bacteria. Isotope fractionation (ϵ) between CO_2 and phytoplankton was calculated as

$$\epsilon_{\text{CO}_2\text{-phyto}} (\text{‰}) = \frac{\delta^{13}\text{C}_{\text{CO}_2} - \delta^{13}\text{C}_{\text{phyto_cor}}}{1 + \delta^{13}\text{C}_{\text{phyto_cor}}/1000} \quad (4.2)$$

$\delta^{13}\text{C}_{\text{phyto_cor}}$ was derived from $\delta^{13}\text{C}_{\text{phyto}}$ with a correction of +3 ‰ for the isotopic offset between FA and total cells ($\Delta\delta^{13}\text{C}_{\text{FA-cell}}$) (Hayes 2001), although isotopic offset can be variable (Schouten et al. 1998). Two proxies for allochthonous carbon ($\delta^{13}\text{C}_{\text{allo}}$) were used, the isotope signatures of DOC ($\delta^{13}\text{C}_{\text{DOC}}$) and detritus ($\delta^{13}\text{C}_{\text{det}}$). $\delta^{13}\text{C}_{\text{det}}$ was calculated from a mass balance and mixing model, similar to Marty and Planas (2008) amended with zooplankton and bacteria. We assumed that POC consists of phytoplankton, detritus, bacteria and zooplankton and that the $\delta^{13}\text{C}$ of POC represents a mixture of the weighted $\delta^{13}\text{C}$ of the individual groups. Subsequently, $\delta^{13}\text{C}_{\text{det}}$ was derived from $\delta^{13}\text{C}_{\text{POC}}$:

$$\delta^{13}\text{C}_{\text{det}} (\text{‰}) = (\text{POC} \times \delta^{13}\text{C}_{\text{POC}} - C_{\text{phyto}} \times \delta^{13}\text{C}_{\text{phyto_cor}} - C_{\text{bac}} \times \delta^{13}\text{C}_{\text{bac}} - C_{\text{zoo}} \times \delta^{13}\text{C}_{\text{zoo}}) / C_{\text{det}} \quad (4.3)$$

$$C_{\text{det}} (\text{mg C L}^{-1}) = \text{POC} - C_{\text{phyto}} - C_{\text{bac}} - C_{\text{zoo}} \quad (4.4)$$

Phytoplankton carbon (C_{phyto}) (mg C L^{-1}) was calculated as the average of chl *a* derived biomass ($C:\text{chl } a = 50$) and phytoplankton FA derived biomass, to minimize the error associated with each method. Phytoplankton FA biomass was calculated from the sum of phytoplankton PLFA ($\sum 18:3\omega3, 18:4\omega3, 20:5\omega3, 22:6\omega3, \text{ and } 20:4\omega6$) and a C: specific FA ratio of 60 based on culture studies, summarized in (Dijkman and Kromkamp 2006). The two approaches yielded similar results. Bacterial carbon (C_{bac}) (mg C L^{-1}) was calculated from the summed concentrations of bacteria specific FA (i15:0, ai15:0, and i17:0) and a $C_{\text{bac}}:\text{FA}$ ratio of 50 (Middelburg et al. 2000). Zooplankton carbon (C_{zoo}) used in equation 3 was estimated to be $\sim 10\%$ of C_{phyto} (Del Giorgio and Gasol 1995). Uncertainty in $\delta^{13}\text{C}$ and biomass of phytoplankton and bacteria were not included in calculating $\delta^{13}\text{C}_{\text{det}}$. The contributions of autochthonous carbon (f_{auto}) and allochthonous carbon (f_{allo}) to zooplankton and bacteria consumers were calculated as

$$f_{\text{auto}} (\%) = \frac{\delta^{13}\text{C}_{\text{allo}} - \delta^{13}\text{C}_{\text{consumer}}}{\delta^{13}\text{C}_{\text{allo}} - \delta^{13}\text{C}_{\text{phyto_cor}}} \times 100 ; f_{\text{allo}} (\%) = 100 - f_{\text{auto}} \quad (4.5)$$

The uncertainty in $\delta^{13}\text{C}$ in carbon sources and consumers were considered in the calculations by creating normal distributions with average and standard deviation (sd) for each value and taking random samples ($n=1000$) from the normal distributions. Only values with outcome between 0 and 100 % were accepted. Standard deviations for $\delta^{13}\text{C}_{\text{phyto_cor}}$ and $\delta^{13}\text{C}_{\text{bac}}$ were based on uncertainty in $\Delta\delta^{13}\text{C}_{\text{FA-cell}}$, which was 1 ‰, around a correction factor of 3 ‰ and 1 ‰, respectively. For allochthonous carbon, average values of $\delta^{13}\text{C}_{\text{allo}} \pm \text{sd}$ of lakes located in Iowa ($n=10$) and in Minnesota ($n=12$) were used, because we expected that $\delta^{13}\text{C}_{\text{allo}}$ should be rather uniform in each state and standard deviations based on individual measurements should cover the variation. For zooplankton consumers, the mean $\pm \text{sd}$ based on individual samples in each lake was used.

Data that were part of the lake monitoring program and $p\text{CO}_2$ values represent single samples of each lake. Data on carbon concentrations and isotope signatures in each lake convey averages of triplicate samples. Average values for eutrophic lakes ($n=11$) and oligotrophic lakes ($n=11$) are presented $\pm \text{sd}$. Statistical analyses were done with software package “R”. Prior to correlation analyses, data were checked for normal distribution (Shapiro test) and log-transformed when necessary to achieve normal distribution. Correlation coefficients were calculated using Pearson product-moment correlation coefficient (normal distribution) or Spearman’s rank correlation coefficient (non-normal distribution). The correlations were tested for total lakes ($n=22$) and for eutrophic lakes ($n=11$) and meso-oligotrophic lakes ($n=11$). Differences between eutrophic and meso-oligotrophic lakes were statistically tested using student t-tests.

4.3 Results

Lake chemistry

The sampled lakes covered a large range of nutrients and CO_2 system characteristics (Table 4.1). TP concentrations ranged from 1.9 to 209 $\mu\text{g L}^{-1}$ and total nitrogen (TN) concentrations ranged from 5.0 to 9320 $\mu\text{g L}^{-1}$ (Table 4.1). DIC values ranged from 0.052 to 4.6 mmol L^{-1} , alkalinity values ranged from 0.07 to 2.4 mmol L^{-1} and pH ranged from 6.1 to 9.8 (Table 4.1). The calculated $p\text{CO}_2$ values were in the range from 10–4500 μatm , covering a broad range from under- to supersaturation.

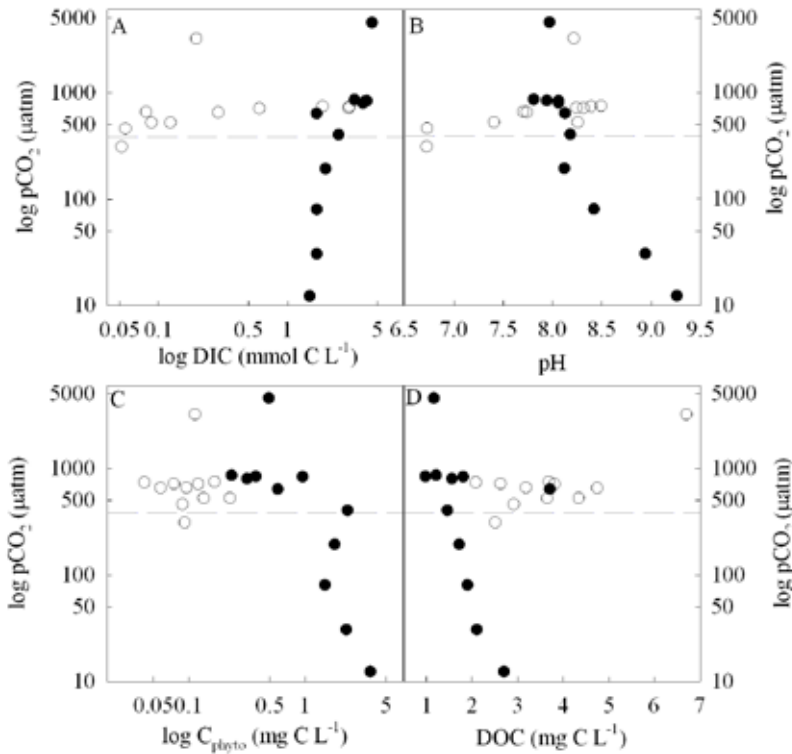


Fig. 4.1. The relation of $p\text{CO}_2$ in eutrophic lakes (filled circles, $n=11$) and meso-oligotrophic lakes (open circles, $n=11$) to A) DIC; B) pH; C) C_{phyto} ; D) DOC. The dashed line indicates atmospheric $p\text{CO}_2$ ($385 \mu\text{atm}$)

The CO_2 system in eutrophic and meso-oligotrophic lakes showed a very different character. The eutrophic lakes had on average higher DIC, alkalinity, and pH than the meso-oligotrophic lakes (Fig. 4.1). In the eutrophic lakes, there were positive correlations between alkalinity and DIC and $p\text{CO}_2$ values ($r = 0.79$ and $r = 0.82$ respectively; $p < 0.01$ for both) (Fig. 4.1A, Table 4.2) and a negative correlation between pH and $p\text{CO}_2$ (Fig. 4.1B; $r = -0.98$, $p < 0.001$). The $p\text{CO}_2$ values were not related to pH, alkalinity, or DIC in the meso-oligotrophic lakes. Both lake systems showed supersaturation (average $p\text{CO}_2$ $838 \mu\text{atm}$ in both), but the $p\text{CO}_2$ range was much larger in eutrophic lakes (10 - $4500 \mu\text{atm}$) compared to meso-oligotrophic lakes (310 - $3200 \mu\text{atm}$) (Fig. 4.1).

Organic Carbon and fatty acid concentrations

POC, C_{phyto} and C_{bac} concentrations were higher and DOC concentrations were lower in the eutrophic lakes compared to the meso-oligotrophic lakes (Table 4.1). C_{phyto} was on average $1.3 \pm 1.1 \text{ mg C L}^{-1}$ and $0.11 \pm 0.03 \text{ mg C L}^{-1}$, corresponding to $44 \% \pm 17 \%$ and $10 \% \pm 5 \%$ of POC in eutrophic and oligotrophic lakes, respectively. C_{phyto} and C_{bac} were significantly related to phosphorus ($r = 0.89$ and $r = 0.82$ respectively, $p < 0.001$ for both), but not to nitrogen concentrations and there was a good correlation between C_{phyto} and C_{bac} in both systems ($r = 0.89$, $p < 0.0001$, Fig. 4.2).

Table 4.1. Limnological characteristics of the sampled lakes. $p\text{CO}_2$ was determined from temperature, DIC and pH. C_{phyto} presents the average of chl a and fatty acid based phytoplankton biomass. C_{bac} presents fatty acid derived bacteria carbon biomass.

Name	U.S. State	Trophic State	Temperature (°)	pH	Alkalinity (mmol L ⁻¹)	DIC (mol L ⁻¹)	$p\text{CO}_2$ (µatm)	TN (mg L ⁻¹)	TP (µg L ⁻¹)	Chl a (µg L ⁻¹)	DOC (mg L ⁻¹)	POC (mg L ⁻¹)	C_{phyto} (mg L ⁻¹)	C_{bac} (mg L ⁻¹)
Beaver	I	Eu	24.1	9.5	1.03	1.70	30	1.69	152.8	72.6	2.10	5.07	2.26	0.251
Beeds	I	Eu	23.8	8.5	2.28	4.15	835	9.32	36.1	9.1	0.97	0.93	0.38	0.023
Big Creek	I	Eu	25.0	8.5	1.97	3.89	795	6.12	21.3	8.0	1.56	1.30	0.32	0.047
Coralville	I	Eu	24.2	7.8	2.37	4.55	4545	6.50	207.1	10.9	1.16	1.91	0.49	0.074
Little Splithand	M	Eu	19.2	8.2	1.04	1.69	635	0.01	29.5	19.5	3.70	2.07	0.58	0.026
Lower Pine	I	Eu	24.1	8.6	1.44	2.51	400	4.15	128.3	60.2	1.46	4.00	2.32	0.213
McBride	I	Eu	22.0	8.8	1.18	1.98	195	1.27	67.9	42.6	1.71	2.84	1.80	0.103
Meyers	I	Eu	27.1	9.8	1.08	1.49	10	2.14	208.7	86.2	2.70	9.91	3.65	0.190
Rodgers park	I	Eu	24.3	8.4	1.82	3.34	855	6.81	50.6	5.4	1.20	0.68	0.23	0.038
Saylorville	I	Eu	25.3	8.5	2.05	4.03	830	4.90	116.3	23.0	1.80	1.30	0.96	0.165
Three Mile	I	Eu	21.3	9.1	0.98	1.69	80	1.00	44.9	37.8	1.90	2.66	1.48	0.122
Beaver	M	M-O	19.7	6.9	0.09	0.09	520	0.12	16.2	3.6	4.34	1.50	0.13	0.017
Brush Shanty	M	M-O	20.3	7.4	0.28	0.29	655	0.34	10	1.4	4.75	0.56	0.06	0.014
Hatch	M	M-O	20.3	8.4	1.81	3.04	735	0.55	1.9	0.8	2.08	0.30	0.04	0.008
Horsehead	M	M-O	19.9	6.7	0.07	0.06	460	0.09	6.9	1.8	2.91	2.11	0.09	0.033
Kelly	M	M-O	20.2	6.9	0.08	0.05	310	0.01	8.9	2.6	2.50	1.22	0.09	0.017
Leighton	M	M-O	19.4	8.4	1.84	2.99	715	0.49	8.1	2.4	2.62	0.67	0.07	0.007
Little Sand	M	M-O	22.8	8.2	0.75	1.88	745	0.19	11.9	4.9	3.68	1.24	0.17	0.023
O'Leary	M	M-O	19.2	6.7	0.09	0.08	655	0.44	13.8	2.6	3.18	2.28	0.10	0.029
Sand Lake	M	M-O	19.9	7.7	1.18	0.61	710	0.66	20.4	3.1	3.81	0.85	0.12	0.016
South Sturgeon	M	M-O	18.6	6.1	0.22	0.20	3200	0.03	14.4	3.6	6.71	0.55	0.11	0.005
Thirty	M	M-O	22.0	7.1	0.13	0.12	525	0.10	15.7	6.3	3.65	3.02	0.23	0.066

This relation between phytoplankton and bacteria carbon can be described by a power law: $C_{\text{bac}}=0.09 \times C_{\text{phyto}}^{0.76}$, showing a non-linear increase of bacteria with increasing phytoplankton. However, the amount of bacteria carbon relative to POC was significantly lower in the meso-oligotrophic lakes than in the eutrophic lakes (t-test, $p < 0.05$). Average C_{bac} was $0.11 \pm 0.08 \text{ mg C L}^{-1}$ and $0.021 \pm 0.017 \text{ mg C L}^{-1}$ in eutrophic and meso-oligotrophic lakes, respectively.

Overall, lake $p\text{CO}_2$ decreased with increasing C_{phyto} ($r = -0.59, p < 0.01$), but the effect was strongest in eutrophic lakes ($r = -0.80; p < 0.01$) (Fig. 4.1C). In the meso-oligotrophic lakes, lake $p\text{CO}_2$ increased with increasing DOC ($r = 0.75, p < 0.01$), but this effect was caused by one point: the high $p\text{CO}_2$ at high DOC in lake Sturgeon. The negative trend between $p\text{CO}_2$ and DOC in eutrophic lakes (Fig. 4.1D) can be explained by an observed common increase of DOC and phytoplankton concentrations.

Table 4.2. Significant correlation coefficients (r) between tested variables in all lakes and in eutrophic and meso-oligotrophic lakes separately. Significance levels: * $p < 0.05$, ** $p < 0.01$, *** $p < 0.001$.

Variables	Eutrophic lakes (n=11) r	Meso-oligotrophic lakes (n=11) r	overall (n=22) r
log alkalinity and log $p\text{CO}_2$	0.79**		
DIC and log $p\text{CO}_2$	0.82**		
pH and log $p\text{CO}_2$	-0.98***		
log C_{phyto} and log $p\text{CO}_2$	-0.80**		-0.59***
DOC and log $p\text{CO}_2$		0.75**	
log TP and log C_{phyto}	0.61*	0.77**	0.89***
log TP and log C_{bac}	0.74**		0.82***
log C_{phyto} and log C_{bac}	0.85***	0.61*	0.89***
log $p\text{CO}_2$ and $\delta^{13}\text{C}_{\text{DIC}}$	-0.63*	-0.81**	-0.48*
POC and $\delta^{13}\text{C}_{\text{DIC}}$	0.61*		
DOC and $\delta^{13}\text{C}_{\text{DIC}}$		-0.62*	
log TP and $\Delta(\delta_{\text{gluc}} - \delta_{\text{FA}})$			0.52*
log C_{phyto} and $\delta^{13}\text{C}_{\text{phyto}}$	0.90***		
log $p\text{CO}_2$ and $\delta^{13}\text{C}_{\text{phyto}}$	-0.79**	-0.90***	-0.73***
$\delta^{13}\text{C}_{\text{CO}_2}$ and $\delta^{13}\text{C}_{\text{phyto}}$		0.82**	0.54**
log C_{phyto} and ϵ	-0.70*		
$\delta^{13}\text{C}_{\text{POC}}$ and $\delta^{13}\text{C}_{\text{phyto}}$	0.86***	0.78**	0.78***
$\delta^{13}\text{C}_{\text{POC}}$ and $\delta^{13}\text{C}_{\text{DOC}}$		0.76**	0.43*
$\delta^{13}\text{C}_{\text{POC}}$ and $\delta^{13}\text{C}_{\text{bac}}$	0.93***	0.63*	0.86***
$\delta^{13}\text{C}_{\text{phyto}}$ and $\delta^{13}\text{C}_{\text{bac}}$	0.85***		0.69***
$\delta^{13}\text{C}_{\text{gluc}}$ and $\delta^{13}\text{C}_{\text{bac}}$	0.78**		0.76***
$\delta^{13}\text{C}_{\text{POC}}$ and $\delta^{13}\text{C}_{\text{zoo}}$	0.80**	0.85**	0.82***
$\delta^{13}\text{C}_{\text{phyton}}$ and $\delta^{13}\text{C}_{\text{zoo}}$	0.95***	0.93***	0.86***
$\delta^{13}\text{C}_{\text{bac}}$ and $\delta^{13}\text{C}_{\text{zoo}}$	0.78**		0.73***
$\delta^{13}\text{C}_{\text{DOC}}$ and $\delta^{13}\text{C}_{\text{detritus}}$		0.79**	0.54*
$\delta^{13}\text{C}_{\text{detritus}}$ and $\delta^{13}\text{C}_{\text{bac}}$	0.72*	0.60*	0.72***
$\delta^{13}\text{C}_{\text{detritus}}$ and $\delta^{13}\text{C}_{\text{zoo}}$		0.71*	0.49*
log C_{bac} and $f_{\text{auto bac}}$	0.61*		
DOC and $f_{\text{auto bac}}$		-0.62*	
$f_{\text{auto bac}}$ and log $p\text{CO}_2$		-0.68*	-0.49*

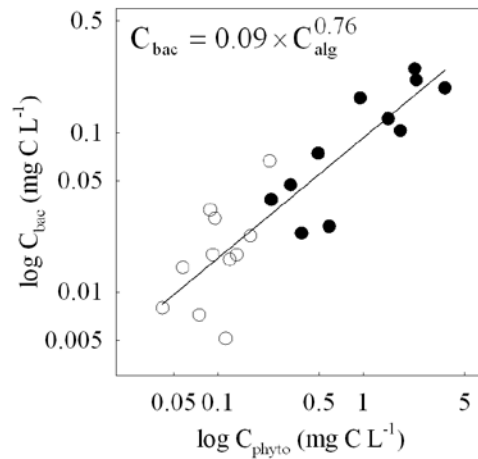


Figure 4.2. Phytoplankton and bacteria carbon biomass in eutrophic lakes (filled circles, $n=11$) and meso-oligotrophic lakes (open circles, $n=11$). The line represents best fit ($r^2 = 0.80$, $p < 0.001$).

$\delta^{13}\text{C}$ of DIC and CO_2

$\delta^{13}\text{C}_{\text{DIC}}$ ranged from -9.3 to $+1.5$ ‰ and $\delta^{13}\text{C}_{\text{CO}_2}$ (derived from $\delta^{13}\text{C}_{\text{DIC}}$) was on average 10.9 ± 0.3 ‰ depleted relative to DIC, with a range of -20.8 to -8.9 ‰. $\delta^{13}\text{C}_{\text{DIC}}$ and $\delta^{13}\text{C}_{\text{CO}_2}$ showed no correlation with alkalinity, DIC, pH, temperature and lake area. A weak negative relation between $p\text{CO}_2$ and $\delta^{13}\text{C}_{\text{DIC}}$ was observed ($r = -0.48$, $p < 0.05$), which was stronger in meso-oligotrophic lakes ($r = -0.82$, $p < 0.01$) than in eutrophic lakes ($r = -0.63$, $p < 0.05$) (Fig. 4.4A). The highest $p\text{CO}_2$ lakes had the most depleted $\delta^{13}\text{C}_{\text{DIC}}$, what suggest that respiration of organic matter influenced $\delta^{13}\text{C}_{\text{DIC}}$. Low CO_2 lakes had enriched $\delta^{13}\text{C}_{\text{DIC}}$, indicating influence of primary production. Weak, but significant relations were observed for POC and DOC with $\delta^{13}\text{C}_{\text{DIC}}$. In eutrophic lakes, $\delta^{13}\text{C}_{\text{DIC}}$ increased with increasing POC (Fig. 4.4B; $r = 0.61$, $p < 0.05$), while in meso-oligotrophic lakes, $\delta^{13}\text{C}_{\text{DIC}}$ decreased with increasing DOC (Fig. 4.4C; $r = -0.62$, $p < 0.05$).

$\delta^{13}\text{C}$ of organic carbon pools

The isotope ratios of the major carbon pools in each lake are presented in Table 4.3 and in boxplots (median and percentiles) in Figure 4.3. The isotope signature of DOC ($\delta^{13}\text{C}_{\text{DOC}}$) had the narrowest range of all carbon pools, only -28.8 to -27.0 ‰ (mean -28.0 ‰) in the meso-oligotrophic lakes (Fig. 4.3B) and a slightly larger range of -27.6 to -23.7 ‰ (mean -25.4 ‰) in the eutrophic lakes (Fig. 4.3A). The $\delta^{13}\text{C}$ isotopic range of POC ($\delta^{13}\text{C}_{\text{POC}}$) was larger than of DOC in both lake types and on average 2.0 ‰ depleted compared to $\delta^{13}\text{C}_{\text{DOC}}$, with mean values of -27.8 ± 3.6 ‰ in eutrophic and -29.7 ± 2.8 ‰ in meso-oligotrophic lakes. $\delta^{13}\text{C}$ of particulate carbohydrates are represented by $\delta^{13}\text{C}$ of glucose ($\delta^{13}\text{C}_{\text{gluc}}$), the most abundant carbohydrate. $\delta^{13}\text{C}_{\text{gluc}}$ was always enriched compared to $\delta^{13}\text{C}_{\text{POC}}$ and the enrichment was similar in eutrophic (3.1 ± 1.7 ‰) and meso-oligotrophic lakes (2.8 ± 1.5 ‰). In contrary, the concentration-weighted average $\delta^{13}\text{C}$ of all fatty acids $\delta^{13}\text{C}_{\text{FA}_{\text{tot}}}$ was always depleted compared to $\delta^{13}\text{C}_{\text{POC}}$ (Fig. 4.3). The depletion of $\delta^{13}\text{C}_{\text{FA}_{\text{tot}}}$ relative to POC was higher in eutrophic lakes (5.2 ± 1.8 ‰) than in meso-oligotrophic lakes (3.1 ± 1.1 ‰).

Table 4.3. Isotope values of sampled lakes. Isotope data are presented as average ± sd (n=3). $\delta^{13}\text{C}_{\text{CO}_2}$ was calculated from $\delta^{13}\text{C}_{\text{DIC}}$ (equation 1). $\delta^{13}\text{C}_{\text{phyto}}$ and $\delta^{13}\text{C}_{\text{bac}}$ are not corrected for the offset between fatty acids and total cells, but $\epsilon_{\text{CO}_2\text{-phyto}}$ (equation 2) used the corrected $\delta^{13}\text{C}$ of phytoplankton. Autochthonous contributions present average ± sd from a normal sampling distribution (n=1000).

Lake name	Trophic State	$\delta^{13}\text{C}_{\text{DIC}}$ (‰)	$\delta^{13}\text{C}_{\text{CO}_2}$ (‰)	$\delta^{13}\text{C}_{\text{POC}}$ (‰)	$\delta^{13}\text{C}_{\text{DOC}}$ (‰)	$\delta^{13}\text{C}_{\text{phyto}}$ (‰)	$\epsilon_{\text{CO}_2\text{-algae}}$	$\delta^{13}\text{C}_{\text{bac}}$ (‰)	$\delta^{13}\text{C}_{\text{gluc}}$ (‰)	$\delta^{13}\text{C}_{\text{zoo}}$ (‰)	$f_{\text{auto_bac}}$ (‰)	$f_{\text{auto_zoo}}$ (‰)
Beaver (I)	Eu	-4.2 ± 0.6	-15.2	-21.9 ± 0.2	-24.2 ± 0.0	-25.9 ± 1.9	7.8	-22.4 ± 0.3	-19.2		77 ± 21	
Beeds (I)	Eu	-2.4 ± 0.1	-13.1	-32.2	-23.7 ± 0.1	-38.0 ± 2.5	22.7	-29.1 ± 0.0	-31.1	-30.1 ± 1.1	33 ± 15	50 ± 17
Big Creek (I)	Eu	-3.2 ± 0.1	-14.1	-32.2 ± 0.1	-26.4 ± 0.9	-40.8 ± 2.2	24.7	-31.5 ± 0.7	-30.4	-32.8 ± 1.1	42 ± 14	60 ± 15
Coralville (I)	Eu	-6.4 ± 0.0	-17.6	-27.9 ± 0.5	-24.6 ± 0.3	-37.4 ± 1.5	17.4	-29.4 ± 0.9	-21.4	-29.1 ± 2.2	37 ± 16	47 ± 23
Little Splithand (M)	Eu	-3.8 ± 0.1	-14.7	-32.3 ± 0.4	-27.6 ± 0.4	-37.0 ± 0.5	20.0	-31.7 ± 0.7	-27.3	-29.7 ± 0.8	46 ± 21	33 ± 18
Lower Pine (I)	Eu	-2.4 ± 0.1	-13.2	-26.2 ± 0.2	-25.3 ± 0.5	-30.6 ± 1.1	14.8	-27.2 ± 0.8	-24.0	-28.0 ± 4.0	59 ± 26	55 ± 29
McBride (I)	Eu	-2.8 ± 0.1	-13.6	-25.6 ± 0.4	-25.6 ± 0.3	-27.3 ± 0.6	11.0	-27.2 ± 1.0	-21.5	-23.9 ± 0.2	43 ± 24	70 ± 22
Meyers (I)	Eu	1.0 ± 0.3	-9.5	-22.1 ± 0.1	-26.2 ± 0.6	-29.3 ± 1.7	17.3	-24.5 ± 0.6	-19.7	-25.2 ± 2.2	43 ± 27	59 ± 28
Rodgers Park (I)	Eu	-6.1 ± 0.0	-17.3	-29.0	-24.8 ± 0.3	-38.6	19.0	-30.3	-26.3	-29.7 ± 2.2	42 ± 15	49 ± 25
Saylorville (I)	Eu	-4.1 ± 0.0	-15.1	-29.2 ± 0.1	-25.8 ± 1.2	-37.3 ± 1.4	19.8	-29.5 ± 0.4	-28.1	-30.5 ± 0.2	40 ± 17	59 ± 14
Three Mile (I)	Eu	-4.3 ± 0.3	-15.3	-27.8 ± 0.4	-25.5 ± 1.0	-29.8 ± 2.3	11.9	-28.5 ± 0.6	-23.7	-25.3 ± 1.4	64 ± 25	56 ± 27
Beaver (M)	M-O	-4.1 ± 0.5	-15.1	-30.5 ± 0.2	-28.7 ± 0.2	-32.4 ± 0.2	14.8	-30.4 ± 2.0	-28.3	-29.9 ± 0.2	58 ± 27	69 ± 20
Brush Shanty (M)	M-O	-2.5 ± 0.2	-13.3	-29.6 ± 0.2	-28.1 ± 0.4	-33.6 ± 2.1	17.9	-30.0 ± 3.0	-25.0		52 ± 28	
Hatch (M)	M-O	-3.7 ± 0.1	-14.6	-31.4 ± 0.4	-28.8 ± 0.2	-34.5 ± 1.3	17.4	-30.6 ± 2.4	-28.6	-32.3 ± 0.5	51 ± 26	73 ± 20
Horsehead (M)	M-O	-3.7 ± 0.9	-14.7	-25.0 ± 0.1	-27.0 ± 0.1	-29.1 ± 0.7	11.7	-27.8 ± 2.0		-26.5 ± 0.2	56 ± 24	64 ± 19
Kelly (M)	M-O	1.5 ± 0.5	-8.9	-27.8 ± 0.7	-27.9 ± 0.4	-30.1 ± 1.0	18.7	-26.6 ± 2.6	-22.1	-26.3 ± 0.1	73 ± 21	77 ± 17
Leighton (M)	M-O	-3.3 ± 0.0	-14.2	-32.3 ± 0.3	-28.2 ± 0.7	-34.4 ± 1.3	17.7	-30.9 ± 1.3	-31.8	-30.7 ± 0.3	55 ± 25	71 ± 20
Little Sand (M)	M-O	-2.2 ± 0.1	-12.9	-30.4 ± 0.2	-28.1 ± 0.0	-33.7 ± 1.7	18.4	-29.4 ± 1.8		-30.7 ± 0.5	42 ± 26	66 ± 22
O'Leary (M)	M-O	-1.3 ± 0.7	-12.0	-28.1 ± 0.3	-27.4 ± 0.7	-31.3 ± 0.4	16.7	-26.8 ± 0.8	-26.3	-27.2 ± 1.7	63 ± 29	57 ± 27
Sand Lake (M)	M-O	-4.7 ± 0.1	-15.7	-31.5 ± 0.4	-28.0 ± 0.1	-36.4 ± 0.1	18.3	-29.6 ± 1.8	-28.7		27 ± 18	
South Sturgeon (M)	M-O	-9.3 ± 0.1	-20.8	-31.8 ± 0.9	-28.0 ± 0.0	-41.4 ± 1.4	18.2	-30.5 ± 1.2	-29.4	-34.4 ± 1.8	18 ± 19	59 ± 20
Thirty (M)	M-O	1.5 ± 0.6	-8.9	-28.7 ± 0.1	-27.8 ± 0.1	-30.2 ± 1.4	18.8	-32.0 ± 1.2	-26.4	-28.4 ± 0.1	26 ± 18	39 ± 23

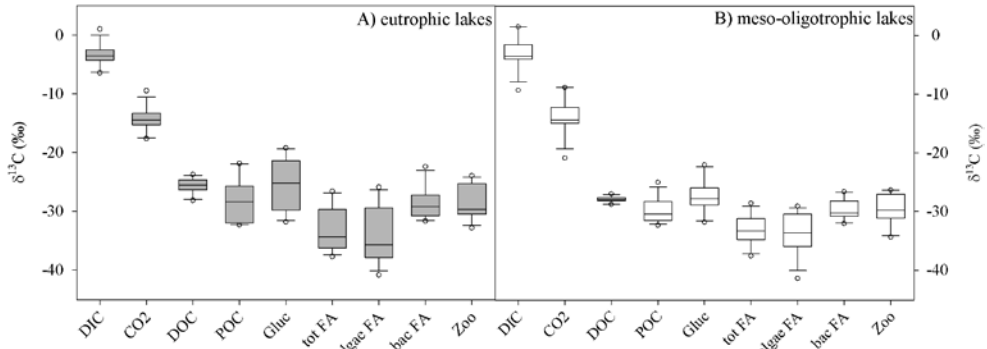


Fig. 4.3. Box and whisker plot of the $\delta^{13}\text{C}$ of inorganic and organic carbon pools in A) eutrophic lakes ($n=11$) and B) and meso-oligotrophic lakes ($n=11$).

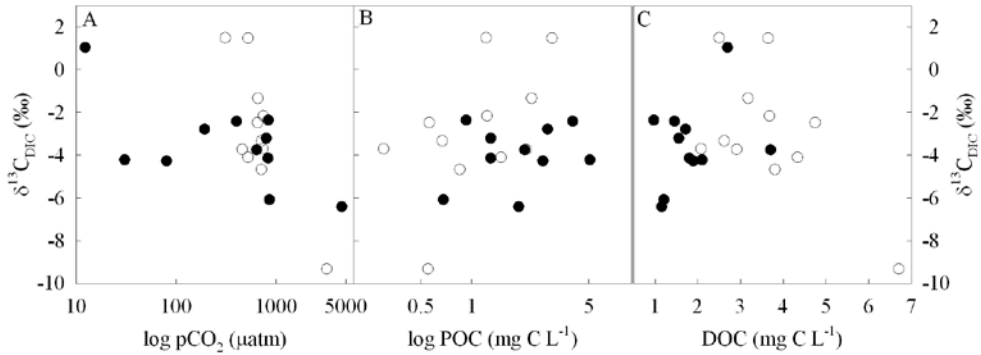


Fig. 4.4. The relation of $\delta^{13}\text{C}_{\text{DIC}}$ in eutrophic lakes (filled circles, $n=11$) and meso-oligotrophic lakes (open circles, $n=11$) to A) $p\text{CO}_2$; B) C_{phyto} ; C) DOC.

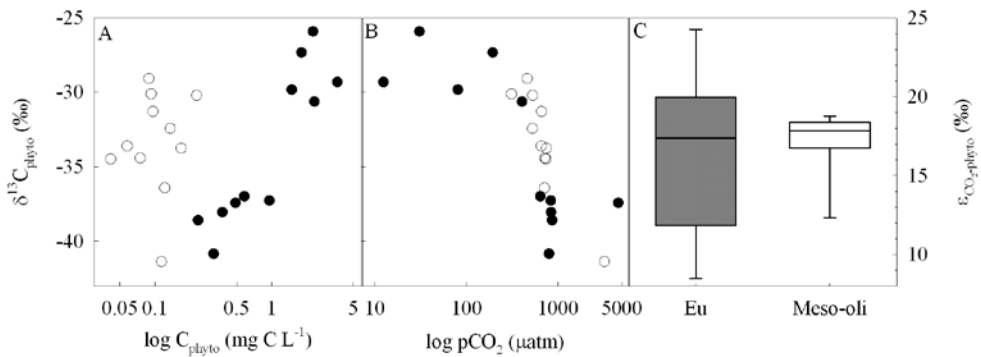


Fig. 4.5. The relation of $\delta^{13}\text{C}_{\text{phyto}}$ in eutrophic lakes (filled circles, $n=11$) and meso-oligotrophic lakes (open circles, $n=11$) to A) C_{phyto} and B) $p\text{CO}_2$. Panel C presents a box whisker plot of calculated $\epsilon_{\text{CO}_2\text{-algae}}$ in eutrophic (Eu) and meso-oligotrophic (Meso-oli) lakes.

The isotopic difference between glucose and $\delta^{13}\text{C}_{\text{FA}_{\text{tot}}}$: $\Delta\delta^{13}\text{C}_{\text{gluc-FA}_{\text{tot}}}$ was highly variable with a range of 1.6 to 14.6 ‰. The isotopic differences between glucose and $\delta^{13}\text{C}_{\text{FA}_{\text{tot}}}$ did not correlated with CO_2 , but with nutrient levels, i.e. $\Delta\delta^{13}\text{C}_{\text{gluc-FA}_{\text{tot}}}$ increased with increasing TP ($r = 0.53, p < 0.05$).

There was a large variability among $\delta^{13}\text{C}$ of different FA with some consistent differences over all lakes. Compared to the $\delta^{13}\text{C}$ of 16:0 (the most abundant FA), the bacterial FA markers were always enriched by 1.4 - 5.0 ‰, therefore the overall $\delta^{13}\text{C}$ of bacterial FA ($\delta^{13}\text{C}_{\text{bac}}$) was more enriched than $\delta^{13}\text{C}_{\text{FA}_{\text{10}}}$ in both lake systems (Fig. 4.3). The poly-unsaturated fatty acids (PUFA) used as markers for phytoplankton showed consistent differences throughout the lakes. The 22:6 ω 3, common in dinoflagellates (Dalsgaard et al. 2003), was found to be enriched with 4.6 ‰ compared to 16:0 while PLFA 18:3 ω 3, common in cyanobacteria (de Kluijver et al. 2012), was 4.7 ‰ depleted compared to 16:0. The other phytoplankton markers were not statistically different from 16:0. The weighted $\delta^{13}\text{C}$ of phytoplankton FA ($\delta^{13}\text{C}_{\text{phyto}}$) was the most depleted of all carbon pools (Fig. 4.3) with an average of -33.8 ± 5.3 ‰ in eutrophic lakes and -33.4 ± 3.5 ‰ in meso-oligotrophic lakes. $\delta^{13}\text{C}_{\text{bac}}$ were on average 4.7 ‰ enriched compared to $\delta^{13}\text{C}_{\text{phyto}}$.

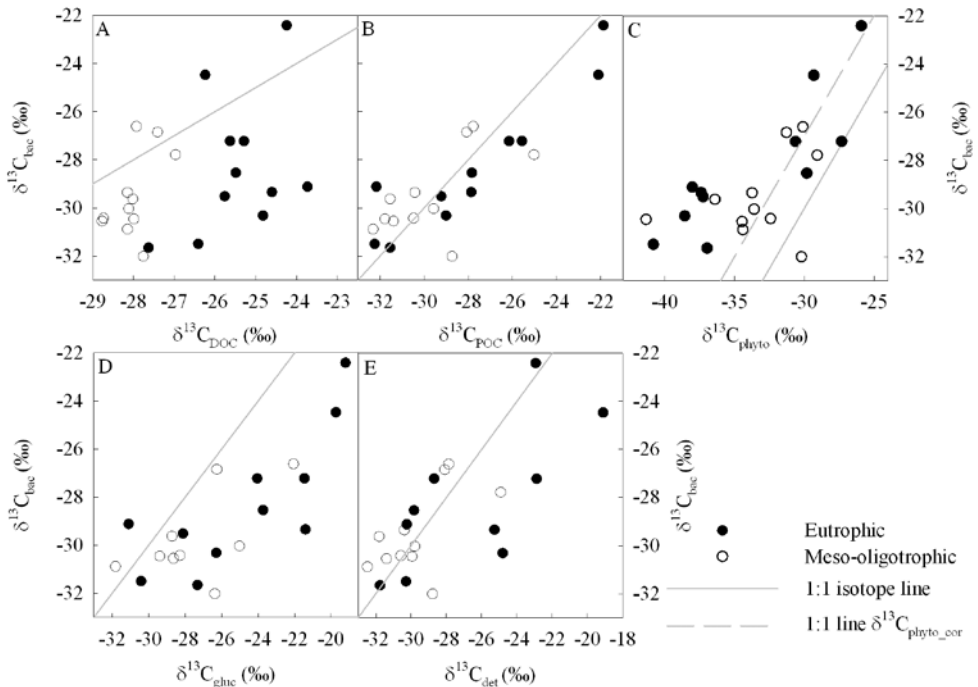


Fig. 4.6. Relation of $\delta^{13}\text{C}_{\text{bac}}$ in eutrophic (filled circles, $n=11$) and meso-oligotrophic lakes (open circles, $n=11$) to A) $\delta^{13}\text{C}_{\text{DOC}}$; B) $\delta^{13}\text{C}_{\text{POC}}$; C) $\delta^{13}\text{C}_{\text{phyto}}$; D) $\delta^{13}\text{C}_{\text{gluc}}$; E) $\delta^{13}\text{C}_{\text{det}}$. The solid line presents isotopic similarity (1:1 line) and the dashed line presents the 1:1 line with $\delta^{13}\text{C}_{\text{phyto_cor}}$.

Carbon isotopic composition of phytoplankton

$\delta^{13}\text{C}_{\text{phyto}}$ depends on the $\delta^{13}\text{C}_{\text{CO}_2}$ and the isotope fractionation $\varepsilon_{\text{CO}_2\text{-phyto}}$ associated with primary production. $\delta^{13}\text{C}_{\text{phyto}}$ in the eutrophic lakes became more enriched with increasing C_{phyto} ($r = 0.90$; $p < 0.001$; Fig. 4.5A) and decreasing $p\text{CO}_2$ ($r = -0.79$; $p < 0.01$; Fig. 4.5B). No relation between $\delta^{13}\text{C}_{\text{phyto}}$ and C_{phyto} was observed in the meso-oligotrophic lakes (Fig. 4.5A), but there was a strong negative relation with $p\text{CO}_2$ ($r = -0.90$, $p < 0.001$; Fig. 4.5B). The influence of C_{phyto} on $\delta^{13}\text{C}_{\text{phyto}}$ in the eutrophic lakes was also reflected in fractionation; $\varepsilon_{\text{CO}_2\text{-phyto}}$ was highly variable in eutrophic lakes, while it was less variable in oligotrophic lakes (Fig. 4.5C). The range of $\varepsilon_{\text{CO}_2\text{-phyto}}$ was 7.8 to 24.7 ‰ (mean 16.9 ‰) in eutrophic and 11.7 to 18.8 ‰ (mean 17.1 ‰) in meso-oligotrophic lakes, when $\delta^{13}\text{C}_{\text{phyto_cor}}$ was used (Table 4.3). The less variable ε in meso-oligotrophic lakes resulted in a good correlation between $\delta^{13}\text{C}_{\text{CO}_2}$ and $\delta^{13}\text{C}_{\text{phyto}}$ ($r = 0.82$, $p < 0.005$), which was absent in the eutrophic lakes. However, $\varepsilon_{\text{CO}_2\text{-phyto}}$ correlated negatively with C_{phyto} ($r = -0.70$, $p < 0.05$) in eutrophic lakes. The variability in $\delta^{13}\text{C}_{\text{phyto}}$ in eutrophic lakes can be mainly attributed to the presence of two clusters: a ^{13}C -enriched cluster at the highest C_{phyto} and a depleted cluster at lower C_{phyto} (Fig. 4.5A). The eutrophic lakes within the enriched cluster also had relative high concentrations of zeaxanthin, a marker pigment for cyanobacteria (data not shown here).

Carbon isotopic composition of bacteria

Although DOC is the proximate carbon substrate for bacteria, $\delta^{13}\text{C}_{\text{bac}}$ was unrelated to the $\delta^{13}\text{C}_{\text{DOC}}$ in both lake systems (Fig. 4.6A). An overall strong relation between $\delta^{13}\text{C}_{\text{bac}}$ and $\delta^{13}\text{C}_{\text{POC}}$ was observed ($r = 0.86$, $p < 0.001$; Fig. 4.6B). $\delta^{13}\text{C}_{\text{bac}}$ showed an overall good correlation with $\delta^{13}\text{C}_{\text{phyto}}$ in all lakes ($r = 0.69$, $p < 0.001$), indicating that phytoplankton were an important carbon source for bacteria (Fig. 4.6C). Particulate glucose is a potential important carbon source for bacteria and a good correlation of $\delta^{13}\text{C}_{\text{gluc}}$ with $\delta^{13}\text{C}_{\text{bac}}$ was observed ($r = 0.76$, $p < 0.001$; Fig. 4.6D). However, when the lakes were analyzed separately for trophic state (eutrophic and meso-oligotrophic), the correlations of $\delta^{13}\text{C}_{\text{bac}}$ in meso-oligotrophic lakes were lower ($\delta^{13}\text{C}_{\text{POC}}$) or not significant anymore ($\delta^{13}\text{C}_{\text{phyto}}$ and $\delta^{13}\text{C}_{\text{gluc}}$), compared to eutrophic lakes (Table 4.2). Likely, all pools were largely influenced by phytoplankton carbon in eutrophic lakes, while bacteria in meso-oligotrophic lakes were feeding on a mixture of organic carbon sources.

Carbon isotopic composition of zooplankton

Because the $\delta^{13}\text{C}$ of cladocerans and copepods did not differ significantly from each other in most of the lakes, total zooplankton was considered. Exceptions were Meyers lake and South Sturgeon, which were the most productive lake (highest chl *a* and P) and the lake with the highest DOC, respectively, but in the correlation analyses total zooplankton was considered for consistency. The average isotope signatures of total zooplankton ($\delta^{13}\text{C}_{\text{zoo}}$) in the different lakes displayed quite a large range from -34.4 to -23.9 ‰ (Fig. 4.3). $\delta^{13}\text{C}_{\text{zoo}}$ showed a strong correlation with $\delta^{13}\text{C}_{\text{POC}}$ ($r = 0.82$, $p < 0.001$) (Fig. 4.7A) and an even stronger relation with $\delta^{13}\text{C}_{\text{phyto}}$ ($r = 0.86$, $p < 0.001$) hinting that phytoplankton or phytoplankton derived material was their most important carbon source (Fig. 4.7B). In the eutrophic lakes, $\delta^{13}\text{C}_{\text{zoo}}$ did not show a significant correlation with individual PUFA, indicating selective grazing on phytoplankton. $\delta^{13}\text{C}_{\text{zoo}}$ was most related to $\delta^{13}\text{C}$ of 20:5 ω 3 (abundant in diatoms, Volkman et al. 1989) ($r = 0.90$, $p < 0.001$), while no relation with $\delta^{13}\text{C}$ of 18:3 ω 3 (abundant in cyanobacteria) was observed.

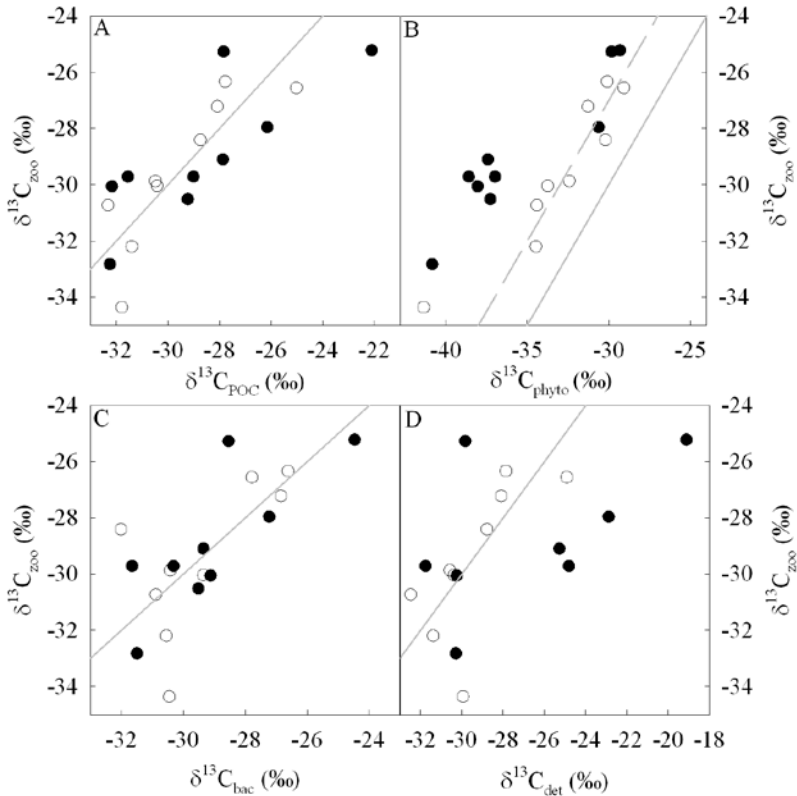


Fig. 4.7. Relation of $\delta^{13}C_{zoo}$ in eutrophic (filled circles, $n=10$) and meso-oligotrophic lakes (open circles, $n=9$) to A) $\delta^{13}C_{POC}$; B) $\delta^{13}C_{phyto}$; C) $\delta^{13}C_{bac}$; D) $\delta^{13}C_{det}$. The solid line presents isotopic similarity (1:1 line) and the dashed line presents the 1:1 line with $\delta^{13}C_{phyto_cor}$.

Good correlations of zooplankton with all PUFA were found in the meso-oligotrophic lakes. A relation between $\delta^{13}C_{bac}$ and $\delta^{13}C_{zoo}$ could be seen in the eutrophic lakes ($r = 0.73$, $p < 0.001$), but not in the meso-oligotrophic lakes (Fig. 4.7C). This correlation could indicate grazing of zooplankton on bacteria, but might as well be the result of their common dependence on phytoplankton.

Carbon isotopic composition of allochthonous carbon

$\delta^{13}C_{DOC}$ and $\delta^{13}C_{det}$ (equation 4.3) were both used and compared as a proxy for $\delta^{13}C_{allo}$. Detritus, calculated from POC, formed a large part of POC, $47\% \pm 20\%$ and $87\% \pm 5\%$ in eutrophic and meso-oligotrophic lakes, respectively. In the meso-oligotrophic lakes, $\delta^{13}C_{DOC}$ was $-28.0 \pm 0.5\%$, corresponding to a C_3 vegetation signal and average $\delta^{13}C_{det}$ was slightly more negative ($-29.6 \pm 2.1\%$). There was a good correlation between $\delta^{13}C_{DOC}$ and $\delta^{13}C_{det}$ ($r = 0.79$, $p < 0.01$). Allochthonous carbon proxies in eutrophic lakes, $\delta^{13}C_{DOC}$ and $\delta^{13}C_{det}$, were more enriched with $-25.4 \pm 1.1\%$ and $-26.6 \pm 4.2\%$ respectively. The enrichment in eutrophic lakes can be partly explained by land use in the water shed; almost all eutrophic lakes were located in Iowa state, where corn (C_4 plants, -14%) is cultivated.

$\delta^{13}\text{C}_{\text{DOC}}$ and $\delta^{13}\text{C}_{\text{det}}$ did not relate to each other in eutrophic lakes. While bacteria did not correlate with $\delta^{13}\text{C}_{\text{DOC}}$ (Fig. 4.6A), they did with $\delta^{13}\text{C}_{\text{det}}$ (Fig. 4.6E; $r = 0.72$, $p < 0.001$), probably due to higher amounts of labile material in POC compared to DOC. Zooplankton did not show a significant relation to detritus in eutrophic lakes, but did in meso-oligotrophic lakes (Fig. 4.7D; $r = 0.71$, $p < 0.05$).

Autochthonous carbon contributions

The estimated contribution of autochthonous carbon to zooplankton ($f_{\text{auto_zp}}$) and bacteria ($f_{\text{auto_bac}}$) are presented per lake in Table 4.3. Autochthonous and allochthonous carbon contributed roughly half to bacteria and zooplankton consumers in all lakes. The two different estimates of allochthonous carbon (DOC and detritus) were rather similar $f_{\text{auto_zp}}$: $59\% \pm 11\%$ and $58\% \pm 16\%$, respectively and $f_{\text{auto_bac}}$: $50\% \pm 16\%$ and $45\% \pm 15\%$, respectively, so their average was used. Overall, there was a higher autochthonous contribution to zooplankton ($59\% \pm 12\%$) compared to bacteria ($48\% \pm 15\%$) (t-test, $p < 0.05$). Despite higher concentrations of autochthonous carbon in eutrophic lakes compared to meso-oligotrophic lakes (Fig. 4.2) and differences in correlations (Table 4.3), $f_{\text{auto_zp}}$ and $f_{\text{auto_bac}}$ were not significantly different between the trophic states. There were no relations between $f_{\text{auto_zp}}$ and any carbon pool, but there were for $f_{\text{auto_bac}}$. In the eutrophic lakes, $f_{\text{auto_bac}}$ increased with increasing bacteria biomass ($r = 0.69$, $p < 0.05$). In the meso-oligotrophic lakes, $f_{\text{auto_bac}}$ decreased with increasing DOC ($r = -0.62$, $p < 0.05$). An overall weakly negative correlation was found between $p\text{CO}_2$ and $f_{\text{auto_bac}}$ ($r = -0.49$, $p < 0.05$), which was only significant for meso-oligotrophic lakes ($r = -0.68$, $p < 0.05$), when lakes were considered separately for trophic state (Fig. 4.8). There were also interesting observations when looking into the lakes individually. The lowest $f_{\text{auto_bac}}$ was observed in the highest DOC lake (South Sturgeon, Table 4.3), while the highest $f_{\text{auto_bac}}$ was observed in the 2nd highest chl *a* lake (Beaver, Table 4.3). The three highest $f_{\text{auto_zp}}$ ($> 70\%$) were found in oligotrophic lakes, characterized by low chl *a*.

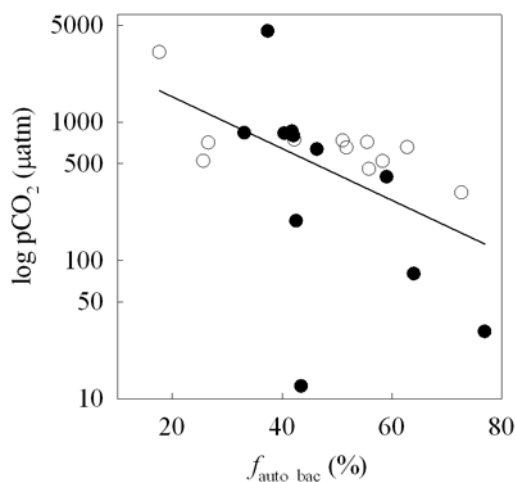


Fig. 4.8. Relation between $f_{\text{auto_bac}}$ and $p\text{CO}_2$ in eutrophic lakes (filled circles, $n=11$) and meso-oligotrophic lakes (open circles, $n=11$). The line presents the best fit ($r^2 = 0.24$, $p < 0.05$).

The highest DOC lake (South Sturgeon) was one of the two lakes with an isotopic difference between cladocerans and copepods, what was reflected in different $f_{\text{auto_zp}}$. Copepods had significantly higher autochthonous contributions ($74\% \pm 14\%$) compared to cladocerans ($36\% \pm 14\%$). The other lake was Meyers, the most eutrophic lake; here copepods had lower autochthonous contributions ($41\% \pm 26\%$) than cladocerans ($59\% \pm 26\%$).

4.4 Discussion

CO₂ dynamics

In our study 3/4 of the lakes were supersaturated with $p\text{CO}_2$, consistent with literature (Cole et al. 1994). Despite the supersaturation, what should be caused by community respiration, lake productivity (phytoplankton biomass) was found the most important factor in determining lake $p\text{CO}_2$ (Fig. 4.1C,D). Phytoplankton biomass decreased the $p\text{CO}_2$, as expected because of CO₂ consumption during algal growth. Bacteria often dominate community respiration and bacterial to phytoplankton production has been proposed as a good predictor for $p\text{CO}_2$ dynamics (Del Giorgio et al. 1997). In our study, absolute or relative bacterial carbon did not relate with $p\text{CO}_2$, but the relative bacterial consumption of autochthonous and allochthonous carbon did influence lake $p\text{CO}_2$ (Fig. 4.8). The $p\text{CO}_2$ increased when allochthonous contributions to bacteria became more important and this was most evident in the meso-oligotrophic lakes.

Inorganic carbon $\delta^{13}\text{C}$

Lake metabolic activity also impacted $\delta^{13}\text{C}_{\text{DIC}}$ dynamics. Previous studies showed that $\delta^{13}\text{C}$ composition of DIC in lakes is driven by carbonate chemistry, hydrology (i.e. groundwater inflow), and metabolic activity. Primary production enriches $\delta^{13}\text{C}_{\text{DIC}}$ because of the preferential uptake of ^{12}C (isotope fractionation), while organic matter respiration depletes $\delta^{13}\text{C}_{\text{DIC}}$. Similar to the $p\text{CO}_2$ control in our lakes, $\delta^{13}\text{C}_{\text{DIC}}$ was most depleted at the highest DOC in meso-oligotrophic lakes (Fig. 4.4C). The depletion of $\delta^{13}\text{C}_{\text{DIC}}$ with increasing DOC, as an indication of the importance of respiration, in meso-oligotrophic lakes has been shown by a number of studies (Lennon et al. 2006). Beside community respiration, methanotrophic bacteria in high DOC lakes could decrease $\delta^{13}\text{C}_{\text{DIC}}$ (Jones et al. 1999). However, based on the fatty acid patterns, we did not find support for any influence of methanotrophs, i.e. $\delta^{13}\text{C}$ of fatty acids, abundant in or specific to methanotrophs, were not more depleted than other fatty acids and their $\delta^{13}\text{C}$ was independent of DOC. The relation between $p\text{CO}_2$ and $\delta^{13}\text{C}_{\text{DIC}}$ can likely be attributed to lake metabolism.

Phytoplankton $\delta^{13}\text{C}$

The determination of $\delta^{13}\text{C}_{\text{phyto}}$ is one of the major challenges in aquatic ecology. Fatty acid biomarkers as proxy for $\delta^{13}\text{C}_{\text{phyto}}$ have the advantage that there is a large certainty that measured $\delta^{13}\text{C}$ values represent parts of phytoplankton carbon. The main uncertainty using $\delta^{13}\text{C}_{\text{FA}}$ as marker for $\delta^{13}\text{C}_{\text{phyto}}$ comes from the isotopic offset between lipids and total cells ($\Delta\delta^{13}\text{C}_{\text{FA-cell}}$) which depends on species composition (summarized in e.g. Hayes 2001) and growth conditions (e.g. Riebesell et al. 2000). The $\delta^{13}\text{C}$ of zooplankton, POC and phytoplankton FA correlated very well, with only a slight depletion of $\delta^{13}\text{C}_{\text{phyto_cor}}$ (2 ‰) relative to $\delta^{13}\text{C}_{\text{POC}}$ and $\delta^{13}\text{C}_{\text{zoo}}$. Isotope fractionation between CO₂ and phytoplankton was variable (8-25 ‰) in our study, so reverse wise, determination of $\delta^{13}\text{C}_{\text{phyto}}$ using $\delta^{13}\text{C}_{\text{CO}_2}$ and a constant fractionation factor, produces values that strongly deviate from the other methods.

A similar deviation of $\delta^{13}\text{C}_{\text{phyto}}$ based on $\delta^{13}\text{C}_{\text{CO}_2}$ and a single fixed fractionation factor from the other methods was observed in a methodological comparison by Marty and Planas (2008) and McCallister et al. (2008). The historically used value for photosynthetic fractionation in phytoplankton is $\sim 20\text{‰}$, based on C_3 photosynthesis (Fry 2006), but several studies that determined ϵ in lakes showed that actual fractionation is usually lower than this value (Cole et al. 2002; Bade et al. 2006). Also in our study, fractionation was lower (17‰) in most of the lakes, and very variable, especially in eutrophic lakes. There are several explanations to explain this variability. 1) Actual fractionation has shown to be dependent on several variables, including growth rate (Bidigare et al., 1997), and CO_2 availability (Laws et al. 1995). Fractionation is highest under high CO_2 availability and low growth rates. In the less productive meso-oligotrophic lakes, the conditions favor optimal fractionation and therefore, fractionation was rather constant (Fig. 4.5C). In the productive, eutrophic lakes, actual fractionation was influenced by $p\text{CO}_2$ and C_{phyto} , with lowest fractionation in the most productive (low CO_2 and high C_{phyto}) lakes (Fig. 4.5). Two clusters in $\delta^{13}\text{C}_{\text{phyto}}$ were present (Fig. 4.5) and the shift occurred when lakes were below $20\ \mu\text{mol L}^{-1}\ \text{CO}_2$ in the eutrophic lakes. When CO_2 becomes limiting, phytoplankton can also shift to bicarbonate, which is isotopically enriched by $\sim 8\text{‰}$ compared to CO_2 . 2) Variability may come from diversity in phytoplankton community, because different taxa have different isotope signatures (Bontes et al. 2006, Vuorio et al. 2006, Van den Meersche et al. 2009). The lakes with enriched phytoplankton had high zeaxanthin to chl *a* ratios. Cyanobacteria are known to be able to fix atmospheric CO_2 and bicarbonate, which are isotopically enriched. Consequently, scum forming cyanobacteria can be enriched by 10‰ compared to water column cyanobacteria (Bontes et al. 2006, de Kluijver et al. 2012). However, the enrichment in $\delta^{13}\text{C}_{\text{phyto}}$ in high zeaxanthin lakes was not a direct consequence of enrichment in cyanobacteria. FA that are abundant in cyanobacteria were not more enriched than FA that are absent in cyanobacteria; in fact, they were the most depleted of all FA. The most enriched phytoplankton FA was 22:6 ω 3, which is abundant in dinoflagellates (Dalsgaard et al. 2003). Dinoflagellates were also more enriched compared to other phytoplankton in a subtropical lake (Zohary et al. 1994). One reason for enriched dinoflagellates can be their mixotrophic character, so that part of their isotope signature reflects consumer $\delta^{13}\text{C}$. 3) Finally, variability in $\Delta\delta^{13}\text{C}_{\text{FA-cell}}$ can contribute to the observed variability. In laboratory studies, the offset between lipids and bulk material has shown to be variable (van Dongen et al. 2002, Fiorini et al. 2011). However, one can expect that in field studies, with several species, these cellular variations would disappear in overall, larger trends. If we assume an overall mean $\Delta\delta^{13}\text{C}_{\text{FA-cell}}$, then the uncertainty on the actual value does affect the fractionation values, but not the observed variability in fractionation.

Allochthonous $\delta^{13}\text{C}$

While variability of $\delta^{13}\text{C}_{\text{phyto}}$ has been a focus of many studies, variability in $\delta^{13}\text{C}_{\text{allo}}$, has received less attention. The isotope signature of allochthonous carbon depends on land use and vegetation in lake catchments and ground-water input. The results of this study argue against a fixed value for allochthonous carbon, especially in areas with abundant C_4 vegetation. In those areas, $\delta^{13}\text{C}_{\text{DOC}}$ or $\delta^{13}\text{C}_{\text{det}}$ might be better proxies. The meso-oligotrophic lakes were surrounded by forest (C_3 vegetation) and both $\delta^{13}\text{C}_{\text{DOC}}$ and $\delta^{13}\text{C}_{\text{det}}$ correlated well and reflected a terrestrial C_3 signal. There was more uncertainty in $\delta^{13}\text{C}_{\text{allo}}$ in the eutrophic lakes for two main reasons. First, we expect a substantial autochthonous contribution to DOC and detritus in productive lakes, what contributes to the larger range in $\delta^{13}\text{C}_{\text{DOC}}$ and $\delta^{13}\text{C}_{\text{det}}$ (Fig. 4.3).

Second, the presence of C_3 and C_4 vegetation with their distinct isotope signatures can create a variable $\delta^{13}C_{\text{allo}}$. $\delta^{13}C_{\text{det}}$ was slightly more enriched than $\delta^{13}C_{\text{POC}}$ (+0.6 ‰). In lakes, detritus is often found to be enriched in ^{13}C , due to preferential mineralization of ^{12}C leaving enriched detritus or to subsidies from littoral vegetation or to the presence of enriched allochthonous material, e.g. from corn.

Carbohydrates and bacteria $\delta^{13}C$

The enrichment of carbohydrates and depletion of lipids relative to total cells (mainly amino acids) has been shown in culture studies of phytoplankton (Van Dongen et al. 2002) and in culture studies of several primary producers and consumers (Teece and Fogel 2007). Results of this study show that the enrichment in carbohydrates as well as the depletion in fatty acids relative to bulk material can also be detected in field samples (Fig. 4.3). We observed that $\delta^{13}C_{\text{FA-cell}}$ increased with TP, but whether this represents a general trend or a coincidence needs further exploration.

Bacterial FA were more enriched than phytoplankton FA in all lakes (Fig. 4.3). This observation can be explained by 1) differences in carbon source or 2) differences in $\Delta\delta^{13}C_{\text{FA-cell}}$ between phytoplankton and bacteria. Carbohydrates, present in high concentrations in DOC, form an important carbon source for bacteria. Since carbohydrates were the most enriched carbon source, a preferential use of carbohydrates, would result in ^{13}C enriched bacteria (Figs. 4.3 and 4.6C). Another explanation is that isotope fractionation during FA synthesis was smaller in bacteria compared to phytoplankton. There are no field studies on $\Delta\delta^{13}C_{\text{FA-cell}}$ in fresh-water bacteria, but field studies on sediment and marine bacteria report a range of 0-5 ‰ in $\Delta\delta^{13}C_{\text{FA-cell}}$ (Burke et al. 2003, Bouillon and Boschker 2006). Burke et al. (2003) suggested that in field samples, with complex communities and substrates, $\Delta\delta^{13}C_{\text{FA-cell}}$ would be ~ 0 ‰. The results of our study support this idea, since bacterial FA had a similar $\delta^{13}C$ as POC (Fig. 4.6B). If a similar $\Delta\delta^{13}C_{\text{FA-cell}}$ for phytoplankton and bacteria would be used, bacteria would be more enriched than its potential carbon sources in half of the studied lakes, which is rather unlikely. Our study argues against using DOC as proxy for $\delta^{13}C$ of bacteria, since there was no correlation between $\delta^{13}C_{\text{DOC}}$ and $\delta^{13}C_{\text{bac}}$ (Fig. 4.6A). The measured DOC reflects the refractory pool, which is not the labile organic carbon pool used by bacteria.

Food-web structure

In agreement with the traditional view of an herbivorous food web, phytoplankton was the most important carbon source for zooplankton, independent of trophic state. However, there were indications of allochthonous contributions, in agreement with literature (Carpenter et al. 2005, Cole et al. 2011). The mean allochthonous contribution to zooplankton in our study (41 %, range 23-67 %) was in the upper end of the range of 20-40 % that was calculated from natural abundance hydrogen, carbon, and nitrogen isotopes in a cross-system survey (Cole et al. 2011), but slightly lower than the contributions (47 %) recently shown for a humic lake (Karlsson et al. 2012). Large ranges in terrestrial contributions to zooplankton have been reported. For example, allochthonous contributions to zooplankton were <10 % in a clear water lake (Pace et al. 2007), while allochthonous subsidies were >50 % in a small, humic lake (Taipale et al. 2008). In both studies, $^{13}C_{\text{DIC}}$ was added to enrich autochthonous production (Pace et al. 2007, Taipale et al. 2008). In a recent study of Karlsson et al. (2012), allochthonous carbon supported half of zooplankton biomass in a humic lake.

The transfer of allochthonous carbon to zooplankton can be directly, by zooplankton grazing on detrital particles or via bacteria utilizing external DOC. Our results indicate that zooplankton in meso-oligotrophic lakes grazed on allochthonous carbon directly rather than on bacteria (Fig. 4.7C, Table 4.1). Allochthonous POC was also found to be more important than allochthonous DOC as carbon source for zooplankton in a model study on four ^{13}C enriched lakes (Cole et al. 2006). Van den Meersche et al. (2009) reported that zooplankton relied primarily on direct consumption of allochthonous POC rather than DOC via bacteria in a tidal river. There was a relation between bacteria and zooplankton in eutrophic lakes, what can be explained by their common dependence by phytoplankton or that zooplankton feeds on bacteria (Fig. 4.7C). In cyanobacteria dominated lakes, the transfer of phytoplankton carbon to zooplankton via bacteria can be a significant pathway (de Kluijver et al. 2012). The dominance of cyanobacteria (having low nutritional value) in the eutrophic lakes can also explain the rather low autochthonous contributions, even with high phytoplankton biomass. There was no indication of zooplankton grazing on cyanobacteria directly in our study. The zooplankton isotope values did not correlate with the isotope signatures of cyanobacteria FA, while they did agree with long chain PUFA present in other phytoplankton. The long chain PUFA (e.g. 20:5 ω 3, 22:6 ω 3) are considered essential fatty acids (EFA) and the lack of EFA is one of the main reasons why cyanobacteria and allochthonous carbon are poor quality food sources for zooplankton. Even if zooplankton was fed with large fraction of allochthonous POC, it selectively incorporated EFA (Brett et al. 2009). This can also explain the high correlations between $\delta^{13}\text{C}_{\text{phyto}}$ (which is based on these fatty acids) and zooplankton in this study, even if zooplankton would be feeding on a mixture of organic carbon sources. The higher autochthonous contribution to copepods compared to cladocerans in the high DOC lake fits well to the common observation that copepods are selective feeders that preferentially feed on living phytoplankton and larger particles, while cladocerans are more general filter-feeders, who feed on phytoplankton, detritus and bacteria (DeMott 1988, de Kluijver et al. 2012).

Bacteria depend less on phytoplankton than zooplankton as seen by isotopic similarities and food-source contribution calculations. Although the food-source calculations did not show significant difference between the different trophic states, isotope correlations did. In eutrophic lakes, bacteria isotope signatures matched best with POC, subsequently followed by phytoplankton, particulate glucose, and detritus, but were not related to DOC (Fig. 4.6, Table 4.2). Bacteria in the meso-oligotrophic lakes, matched less with all carbon pools compared to eutrophic lakes. The best relation was with POC and detritus, but not with phytoplankton, particulate glucose, and DOC (Fig. 4.6, Table 4.2). The correlations in our study showed that bacteria were mainly fuelled by phytoplankton in eutrophic lakes, while they consumed a mixture of organic carbon pools in meso-oligotrophic lakes. These findings can explain the relative higher $C_{\text{bac}}:C_{\text{phyto}}$ in meso-oligotrophic lakes compared to eutrophic lakes, which is represented in the non-linear increase of C_{bac} with C_{phyto} (Fig. 4.2). Decreasing bacterial production relative to primary production with increasing trophity is commonly observed (Cotner and Biddanda 2002). Our calculated $f_{\text{auto_bac}}$ (mean 48 %) was rather similar to autochthonous subsidies of 30-65 % in small forested lakes where ^{13}C -DIC was added (Kritzberg et al. 2004, Cole et al. 2006). In these lakes, terrestrial DOC was observed to be more important for bacteria than terrestrial POC (Cole et al. 2006). The high correlation between POC and bacteria and the lack of correlation between DOC and bacteria, suggest that particulate material was more important for bacteria in our study.

4.5 Conclusions

To conclude, our results show that trophic state has a large influence on lake metabolism and carbon cycling in plankton food webs. Overall, eutrophic lakes had larger variability in $\delta^{13}\text{C}$ in all organic carbon pools than meso-oligotrophic lakes, caused by larger isotopic variability in the base of the food web in eutrophic lakes (both allochthonous and autochthonous carbon). In eutrophic lakes, $\delta^{13}\text{C}_{\text{phyto}}$ showed that two clusters of phytoplankton were present, with the most enriched phytoplankton at high CO_2 and phytoplankton biomass. Dominance of cyanobacteria played a role, but enrichment was present in all phytoplankton, as seen in specific PLFA. Generally, bacteria showed more response to changes in trophic state in carbon uptake pathways than zooplankton. In meso-oligotrophic lakes bacteria used a mixture of carbon from various sources, while they depended more on phytoplankton in eutrophic lakes. Zooplankton was primarily feeding on phytoplankton, but probably not on cyanobacteria in eutrophic lakes.

Acknowledgements

We gratefully acknowledge Kelly Poole, Amber Erickson, Dan Kendall, and Josh McGinnis from the limnological laboratory, Iowa State University, for their assistance during sampling preparation, lake sampling, and processing. We thank colleagues from the NIOZ Royal Netherlands Institute for Sea Research in Yerseke: Pieter van Rijswijk, Marco Houtekamer, Peter van Breugel, and Jurian Brasser for laboratory support and Karline Soetaert for analyses support. We thank Jan van Ooijen and Karel Bakker from NIOZ Texel for laboratory support. This work received financial support from Schure-Beijerinck-Popping (SBP) Fonds and from the Darwin Center for Biogeosciences supported by the Netherlands Organization of Scientific Research (NWO).

Anna de Kluijver, Jinlei Yu, Marco Houtekamer, Jack J. Middelburg, and Zhengwen Liu

Limnology and Oceanography 57: 1245–1254, 2012



CHAPTER

5



Cyanobacteria as a carbon source for zooplankton in eutrophic Lake Taihu, China, measured by ^{13}C labeling and fatty acid biomarkers

Abstract

Using a combined stable isotope and fatty acid approach we examined carbon transfer routes from the cyanobacterium *Microcystis* to zooplankton in eutrophic Lake Taihu, China. *Microcystis* is generally considered poor food for zooplankton and we hypothesized that most *Microcystis* carbon flows to zooplankton via dissolved organic matter (DOM)-bacteria and detritus-bacteria pathways rather than via direct grazing. The hypothesis was tested by analyzing ^{13}C isotopes at natural abundance in field samples and in tracer experiments with ^{13}C enriched *Microcystis*. ^{13}C enriched *Microcystis* was added as live *Microcystis*, *Microcystis* detritus, or *Microcystis* DOM to lake water incubations with *Bosmina* sp. and *Daphnia similis* as the dominant species. The ^{13}C isotope signatures of *Microcystis*, heterotrophic bacteria, and eukaryotic algae in seston were determined from isotope analyses of specific fatty acids, and the presence and labeling of these fatty acids were also analyzed in zooplankton consumers. *Bosmina* and *Daphnia* consumed carbon via all pathways, but the amount of carbon transfer from the *Microcystis* DOM was the highest, followed by the *Microcystis* detritus. *Bosmina* consumed relative more live *Microcystis* than *Daphnia*. The presence and high ^{13}C enrichment of bacteria-specific fatty acids in the zooplankton consumers showed that heterotrophic bacteria were an important link between *Microcystis* and zooplankton. Microbial pathways dominate the energy flow from cyanobacteria to zooplankton in eutrophic lakes with heavy cyanobacteria blooms such as Lake Taihu.

5.1 Introduction

Eutrophication is one of the most widespread and pertinent environmental problems in aquatic environments; it often results in degradation of aquatic ecosystems, causing shifts in primary producers, bacterial, and zooplankton communities (Carpenter et al. 1998). Severe eutrophication in freshwater ecosystems causes extensive and recurrent cyanobacteria blooms, which are expected to occur more frequently in a future warmer climate. Studies on zooplankton-cyanobacteria interactions have generally shown that cyanobacteria cause rapid decrease of large crustaceans in favor of smaller crustaceans and rotifers (Fulton and Paerl 1988). Such studies have primarily examined herbivory and proposed poor nutritional value, filtering rate interference and toxicity as important adverse factors (Haney 1987; Lampert 1987). Grazing on cyanobacteria, or herbivory, is however, only one of the energy pathways from primary producers to consumers. Zooplankton can also acquire carbon via the microbial food web by grazing on heterotrophic bacteria directly or on protists (ciliates and heterotrophic flagellates) as intermediate trophic link. Some earlier laboratory studies indicated that cladocerans are efficient grazers on bacteria (Peterson et al. 1978; Porter et al. 1983). Field studies confirmed that zooplankton can meet a large part of their carbon requirement via the microbial food web (Hessen et al. 1990; Wylie and Currie 1991; Koshikawa et al. 1996). The importance of the microbial food web as a food source for zooplankton depends largely on lake productivity and on plankton community structure (Pace et al. 1983). Generally, the microbial food web becomes more important when lakes move towards eutrophic systems and this phenomenon can be explained by an increasing dominance of cyanobacteria and a co-occurring shift in zooplankton community structure (Gliwicz 1969). Based on this knowledge, we hypothesize that in eutrophic systems, cyanobacteria are an important carbon source for zooplankton, but that much more carbon flows via the microbial food web rather than via the herbivory pathway. The importance of the microbial food web as carbon source for zooplankton during and after a cyanobacteria bloom was previously demonstrated by Christoffersen et al. (1990). Their results were based on carbon budgets combined with modeling. Here we present an integrated stable-isotope, biomarker approach to trace the importance of *Microcystis* carbon for zooplankton nutrition.

Stable isotope analysis (SIA) of carbon at natural abundance is a powerful tool that enables us to trace organic carbon flows and examine food web interactions in ecosystems. Zooplankton consumers generally reflect the carbon isotope signature ($\delta^{13}\text{C}$) of their diet, so portions of resources in the diet of zooplankton can be determined when carbon sources are sufficient isotopically distinctive. A major challenge in aquatic ecology is to separate the $\delta^{13}\text{C}$ of potential carbon sources at the base of the food web from bulk particulate organic carbon (POC). Compound specific isotope analysis (CSIA) of fatty acid biomarkers is a valuable method to determine the isotope signature of certain groups of organisms (Boscher and Middelburg 2002) and was used in this study to determine $\delta^{13}\text{C}$ of eukaryotic algae, cyanobacteria, and heterotrophic bacteria. Although, SIA of carbon at natural abundance can be used to identify carbon origins, it is limited in resolving pathways from basal resources to consumers. It is for example difficult to distinguish direct grazing by zooplankton on phytoplankton from indirect grazing on phytoplankton-derived detritus or bacteria that grew on phytoplankton carbon. Furthermore, the isotope signatures of *Microcystis* and eukaryotic algae are likely to overlap, although large isotopic differences have been reported for different phytoplankton groups (Bontes et al. 2006; Vuorio et al. 2006).

A valuable alternative to avoid the problem of overlapping resources is to manipulate the isotope signature of a potential carbon source by ^{13}C enrichment and subsequently trace the incorporation into consumers (Middelburg et al. 2000; Pel et al. 2003). In this study, we combine a natural abundance and tracer ^{13}C study with fatty acid measurements to assess the importance of carbon from *Microcystis* in zooplankton nutrition. We first analyzed natural abundance isotope composition of carbon sources and zooplankton consumers in field samples. Then, we examined the assimilation of ^{13}C enriched carbon sources derived from *Microcystis* within the plankton food web in lake water incubations, with the cladocerans *Bosmina* sp. and *Daphnia similis* as end-consumers. These species are representatives for small and large cladocerans respectively, and we expected higher consumption of *Microcystis* carbon by *Bosmina* than by *Daphnia*. The different labeled substrates were 1) live *Microcystis* to test for herbivory, 2) *Microcystis* derived (particulate) detritus and, 3) *Microcystis* derived dissolved organic matter (DOM) to test for carbon flow via the microbial food web. Fatty acids were used to quantify biomass and isotope composition of *Microcystis*, algae, and bacteria in the seston. We also examined the presence of labeled fatty acids in zooplankton, to retrieve additional information on zooplankton grazing on labeled *Microcystis* and bacteria. Finally, fatty acid profiles were used to retrieve dietary information. This fatty acid trophic marker approach (FATM) is based on the conservative incorporation of fatty acids from the food source into primary consumers like zooplankton (Dalsgaard et al. 2003; Brett et al. 2006). FATM has been successfully applied to show feeding of zooplankton on phytoplankton and bacteria in previous studies (Taipale et al. 2009).

5.2 Methods

Site description

The study was conducted in Lake Taihu, the third biggest fresh water lake of China with a total area of 2338 km². The lake is located in the Yangtze Delta in eastern China (30°55′-31°32′N, 119°52′-126°36′E) and has economic and social important values in the region. The lake is shallow, with an average depth of ~2 m. Increased nutrient inputs into the lake during the last decades caused eutrophication of Lake Taihu, leading to massive, toxic and recurring blooms of *Microcystis* (cyanobacteria) in summers. Meiliang Bay, located in the northern part of the lake, is perhaps the most eutrophic part of the lake: it is characterized by high densities of *Microcystis* sp., of up to 98 % of total phytoplankton biovolume in summer (Chen et al. 2003).

The study was conducted in May 2009 in Meiliang Bay; at the time of sampling, the phytoplankton community in Meiliang Bay was dominated by the cryptophyte *Cryptomonas erosa* ($3.94 \pm 2.24 \text{ mm}^3 \text{ L}^{-1}$), and *Microcystis* sp. ($1.63 \pm 2.24 \text{ mm}^3 \text{ L}^{-1}$). Cyanobacteria bloom or surface scum was absent during our sampling. The zooplankton community was dominated by *Bosmina* sp. ($152 \pm 10 \text{ individuals (ind.) L}^{-1}$). Other zooplankton genera included *Ceriodaphnia* ($34 \pm 10 \text{ ind. L}^{-1}$), rotifers ($24 \pm 4 \text{ ind. L}^{-1}$), and *Cyclopoid* copepods ($22 \pm 9 \text{ ind. L}^{-1}$).

^{13}C labeled substrate production

Floating *Microcystis* was collected using a 200 μm net from the surface of Lake Taihu and concentrated by subsequent collection of the upper layer. The concentrate was transferred to GF/C filtered lake water. *Microcystis* was labeled in two different cultures;

the first culture was used to produce the detritus and DOM substrates and the second culture was labeled closely before the experiment and used to produce live *Microcystis* substrate. The final *Microcystis* concentration was 21.3 g fresh weight L⁻¹ and 10.6 g fresh weight L⁻¹ in the first and second culture respectively. The cultures were incubated outside in air-tight and magnetically stirred bottles for 24 h with 20 % ¹³C-bicarbonate (> 98 % pure ¹³C) and 30 % ¹³C-bicarbonate in the first and second culture, respectively. To check for physical label uptake and non-photosynthetic or dark uptake, a small part of the culture was filtered immediately after label addition and the other part was incubated in the dark. There was no physical or dark uptake of label. After incubation, *Microcystis* was rinsed at least three times using a 30µm sieve to remove the label adhering to the surface of the cells. Size-distribution analysis of *Microcystis* collected with the same method revealed that *Microcystis* consisted for 55 % of colonies smaller than 25 µm and for 39 % of colonies in the range of 25-60 µm (Wang 2008).

Labeled *Microcystis* for DOM and detritus production (first culture) was concentrated by centrifugation (10 min, 4500 g) and freeze-dried. The freeze-dried culture was resuspended in demi water to induce osmosis-induced lysis of the cells (Kim et al. 2009). The particulate and dissolved fractions were separated by centrifugation (15 min, 4500 g). The pellet was again resuspended in demi water, split into dissolved and particulate fractions and this was repeated a couple of times. The pooled dissolved fraction was GF/F filtered and the particulate fraction was additionally rinsed and both fractions were freeze-dried again and stored frozen until used in the experiments. Live *Microcystis* (second culture) was rinsed and concentrated and could be used directly in the experiments. A subsample of each substrate was kept for carbon content and isotope labeling analyses and a subsample from live *Microcystis* was kept for composition and isotope labeling of fatty acids.

Incubation experiments

The incubation experiments were carried out at the Taihu research station, Wuxi, China between 28 and 31 May 2009. *Daphnia similis* was added to natural lake water of Meiliang Bay to a final concentration of 30 individuals L⁻¹. The water was divided over 12 twelve buckets with 6 liters each. The buckets were floating in a pond to avoid large temperature changes, tight with ropes, and covered with nets. Triplicate buckets were used for the three treatments and control. Live *Microcystis* (treatment 1) was added to a final concentration of 2 g L⁻¹ fresh weight, i.e., 86 mg L⁻¹ dry weight, corresponding to a bloom situation (Qin et al. 2010). *Microcystis* detritus (treatment 2) and *Microcystis* DOM (treatment 3) were both added to a final concentration of 8.6 mg L⁻¹ dry weight. This corresponds to a DOM concentration increase of ~25 %. In the control treatment (treatment 4), no substrate was added. The incubations were run for 3 days and water in the buckets was mixed ~4 times a day. As a result of differences in substrate additions, the final POC concentrations were 8.6 times higher in treatment 1 (30.6 ± 3.6 mg C L⁻¹) compared to treatments 2 (3.8 ± 0.8 mg C L⁻¹) and 3 (3.3 ± 0.5 mg C L⁻¹).

Sampling

Field sampling was done in the center of Meiliang Bay, where triplicate water samples were taken with a 5 liter Plexiglas water-sampler from the upper 0.5 m of the water column and triplicate zooplankton samples were taken with a 64 µm mesh-size net from the upper 1 m of the water column. Triplicate water samples for t₀ or control measurements of the experiment were taken before the water was divided over the different buckets.

Water samples of the incubations were only taken at the end of the experiment (t_{end}). Start and end samples of the incubations for zooplankton were collected using a 64 μm mesh-size net. Both field and experiment water samples were subdivided for particulate organic carbon (POC), dissolved organic carbon (DOC), polar lipid fatty acids in seston (PLFA), and dissolved inorganic carbon (DIC) analyses. Start and end samples from the experiment were also taken for counting algae, bacteria and zooplankton numbers (data not shown) and for temperature, pH, alkalinity, chlorophyll a , and inorganic nutrients (data not shown).

Analyses

For POC analyses, ~ 400 mL water was filtered over pre-combusted and pre-weighed GF/F filters, which were dried at 60°C . The carbon concentration and isotopic composition of POC were analyzed on a Thermo Electron Flash EA 1112 elemental analyzer (EA) coupled to a Delta V isotope ratio mass spectrometer (IRMS). Headspace vials (10 mL) were filled with GF/F filtered water, preserved with mercury chloride and stored at room temperature for DIC analyses. In the lab, a helium headspace was created and samples were acidified with H_3PO_4 solution. The CO_2 concentration and isotope ratio in the headspace were measured on the same EA-IRMS. GF/F filtered water was stored frozen in clean vials for DOC analysis. In the laboratory, the samples were acidified and flushed with helium to remove DIC and subsequently the DOC was measured with liquid chromatography-isolink-IRMS (Boschker et al. 2008). Individual zooplankters were sampled for measurements of carbon content and isotope ratios, and fatty acid concentrations and isotope ratios. For the incubation experiments, the zooplankters were collected on a 112 μm sieve and transferred to clean, demi water and made to stay for a minimum of 4 hours to remove label adhering onto the animals and to clear their gut contents. About 15 *Daphnia* and 50 *Bosmina* were handpicked for each analysis. About 15 cyclopoids and 50 *Bosmina* were handpicked from the field samples. The zooplankton samples were dried at 60°C for total carbon analyses and those for fatty acids (FA) analyses were stored frozen. The carbon content and isotopic composition of zooplankton was measured in the same way as for POC. Zooplankton and seston lipids were extracted by a modified Bligh and Dyer method (Middelburg et al. 2000). For seston, the lipids were fractionated in different polarity classes by column separation on a heat activated silic acid column and subsequent elution with chloroform, acetone and methanol. The methanol fractions, containing the polar lipid fatty acids, were collected and derivatized to fatty acid methyl esters (FAME). For zooplankton, total fatty acids were analyzed. 12:0 and 19:0 fatty acids were used as internal standards. (PL)FA were separated on the non-polar HP5 column (60 m \times 0.32 mm \times 0.25 μm) and the $\delta^{13}\text{C}$ of individual (PL)FA were measured using gas chromatography-combustion isotope ratio mass spectrometry (GC-C-IRMS) (Middelburg et al. 2000). As *Bosmina* FA concentrations were low, the extracts were analyzed using large volume (20 μL) injection with a Cis4 PTV injector (Gerstel, Germany). The GC settings used were: start temperature 35°C for 0.5 minutes, warm up by 16°C s^{-1} to 150°C for 0 minutes and finally warm up by 12°C s^{-1} to 300°C for 3 minutes. The injection speed was 2.5 $\mu\text{L s}^{-1}$ with the solven vent mode of injection. In this way, sample injections could be increased to 100 μL .

Data analyses

Stable isotope ratios are expressed in the delta notation ($\delta^{13}\text{C}$), which is the isotope ratio of $^{13}\text{C} : ^{12}\text{C}$ relative to Vienna- PeeDee Belemnite standard (VPDB) standard. The weighted isotope ratio of specific fatty acids was used to determine the isotope signature of the carbon source. *Microcystis* in this study, contained high amounts of 16:0, followed by relatively high concentrations of C18 mono-unsaturated fatty acids (e.g., 18:1 ω 7c, 18:1 ω 9c) and C18 poly-unsaturated fatty acids (PUFA) (e.g., 18:4 ω 3, 18:3 ω 3), in agreement with other studies on fatty acid composition of *Microcystis* (Ahlgren et al. 1992; Gugger et al. 2002). Some of the abundant *Microcystis* fatty acids are also present in bacteria (e.g., 18:1 ω 7c) or cryptophytes (e.g., 18:4 ω 3), the most important algae in our samples, and these FA were not used as markers. The weighted $\delta^{13}\text{C}$ of fatty acids 18:3 ω 3, 18:3 ω 6, 18:2 ω 6c, and 18:1 ω 9c were used to determine *Microcystis* isotope ratios. Long Chain (C20, C22) PUFA are generally absent in cyanobacteria (Ahlgren et al. 1992), so the weighted ratio of PUFA 20:5 ω 3, 20:4 ω 6, and 20:3 ω 6 were used to determine (eukaryotic) algae. Branched fatty acids are characteristic for heterotrophic (gram-positive) bacteria, so the weighted $\delta^{13}\text{C}$ of the branched FA i14:0, ai15:0, and i15:0 were used to determine bacteria isotope ratios. Because fatty acids are generally depleted relative to other structural components, a fractionation factor of 3 ‰ was applied to obtain $\delta^{13}\text{C}$ values for whole cells in the natural abundance analyses (Hayes 2001).

Table 5.1. Average natural-abundance $\delta^{13}\text{C}$ values (\pm SD; $n = 3$) of carbon pools in Lake Taihu during spring 2009.

Carbon pool	Isotope ratio $\delta^{13}\text{C}$ (‰)
POC	-26.5 \pm 0.5 ‰
Bacteria in seston	-26.1 \pm 0.5 ‰
Algae in seston	-29.2 \pm 0.6 ‰
<i>Microcystis</i> in seston	-30.6 \pm 0.5 ‰
<i>Microcystis</i> of surface bloom	-20.9 \pm 0.4 ‰
Bosmina	-26.9 \pm 0.2 ‰
Copepods	-29.0 \pm 3.4 ‰
Bacteria in Bosmina	-24.6 \pm 0.1 ‰
Algae in Bosmina	-28.9 \pm 0.6 ‰
<i>Microcystis</i> in Bosmina	-29.5 \pm 0.6 ‰

Label uptake is reflected in enrichment in $\delta^{13}\text{C}$ and is calculated as $\Delta\delta^{13}\text{C}$ (‰) = $\delta^{13}\text{C}_{\text{sample}} - \delta^{13}\text{C}_{\text{background}}$. Label uptake in consumers reflects relative consumption: uptake of the enriched carbon source relative to consumer carbon biomass. To compare labeling in the different treatments, the data were normalized for the amount of ^{13}C that was added to each of the incubations.

All results are presented as average \pm SD ($n=3$). The contribution of potential carbon sources to zooplankton was examined using natural-abundance isotope ratios with the Isosource computer program, with 1 % increment and 0.01 % tolerance (Phillips and Gregg 2003). Bacteria, algae, and *Microcystis* were used as potential carbon sources for both cyclopoid copepods and *Bosmina* sp. To test for statistically significant ($p < 0.05$) differences between zooplankton species and treatments in the labeling experiment, (factorial) analyses of variance (ANOVAs) and Bonferroni post-hoc tests were applied to the data.

5.3 Results

Natural abundance isotope ratios

The average $\delta^{13}\text{C}$ of the different carbon pools in Meiliang bay are summarized in Table 5.1. POC and bacteria had similar $\delta^{13}\text{C}$ values of -26.5 ± 0.48 ‰ and -26.1 ± 0.53 ‰. Both algae and *Microcystis* were more depleted with isotope values of -29.2 ± 0.64 ‰ and -30.6 ± 0.48 ‰ respectively. This implies the presence of ^{13}C enriched detritus in POC. The carbon sources of ^{13}C enriched detritus were unknown, but scum-forming *Microcystis* could be a possible source. The floating, scum forming *Microcystis* we collected for substrate production, had much more enriched ^{13}C values than *Microcystis* in the field samples. The isotope signature of scum *Microcystis* was -20.9 ± 0.36 ‰ when analyzed in total or -22.6 ‰ based on fatty acids. The isotope value of *Bosmina* (-26.9 ± 0.20 ‰) was similar to those of POC and bacteria, while $\delta^{13}\text{C}$ of cyclopoid copepods (-29.0 ± 3.4 ‰) reflects a more mixed diet. Overall, the isotope range of carbon sources was quite narrow, from -26.1 ‰ to -30.6 ‰, what makes it difficult to precisely allocate the contribution of each source to zooplankton consumers. Isotope mixing models using isosource indicate that *Bosmina* received 77 ± 2.5 % of their carbon via bacteria, 14 ± 8.3 % from algae and 9.2 ± 5.7 % from *Microcystis*. Copepods received 21 ± 8 % of their carbon from bacteria, 31 ± 19 % from *Microcystis* and 48 ± 27 % from algae. *Bosmina* contained bacteria, *Microcystis*, and algae specific fatty acids and they had similar $\delta^{13}\text{C}$ values as the corresponding fatty acids in the seston (Table 5.1). The similarity of $\delta^{13}\text{C}$ in seston and zooplankton fatty acids indicates a coupling between zooplankton consumers and the measured carbon sources.

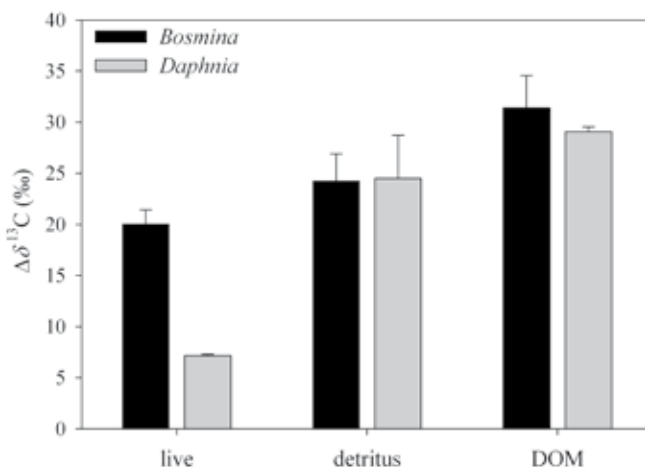


Fig. 5.1. ^{13}C enrichment ($\Delta\delta^{13}\text{C}$) of *Bosmina* and *Daphnia* for the three different labeled *Microcystis* substrates added. Data are presented as average with SD error bars ($n=3$). Note that *Bosmina* has significantly higher labeling than *Daphnia* when fed live *Microcystis* (first treatment).

Tracer assimilation

After three days of lake water incubation with ^{13}C enriched *Microcystis* substrates, ^{13}C enrichment ($\Delta\delta^{13}\text{C}$) could be detected in all major organic carbon pools. Both *Bosmina* and *Daphnia* incorporated ^{13}C of the *Microcystis* substrates, but the uptake differed per substrate (Fig. 5.1). Zooplankton showed the highest incorporation of *Microcystis* when it was added in the form of DOM, with $\Delta\delta^{13}\text{C}$ values of $31.4 \pm 3.2\text{‰}$ for *Bosmina* and $29.1 \pm 0.5\text{‰}$ for *Daphnia*, followed by *Microcystis* added as detritus with $24.2 \pm 2.7\text{‰}$ and $24.5 \pm 4.2\text{‰}$ for *Bosmina* and *Daphnia* respectively (Fig. 5.1). Tracer assimilation was lowest for both species in the live *Microcystis* incubations, and *Daphnia* consumed significantly less live *Microcystis* ($7.17 \pm 0.11\text{‰}$) than *Bosmina* ($20.0 \pm 1.4\text{‰}$) (ANOVA, $F_{3,4} = 243$, $p < 0.0005$) relative to their carbon biomass.

^{13}C incorporation into fatty acids (FA) in the seston was used to determine bacteria, *Microcystis* and algae tracer assimilation. Heterotrophic bacterial FA showed high ^{13}C labeling in all treatments, showing that *Microcystis* is an important carbon source for bacteria (Fig. 5.2). Part of the observed labeling can be explained by the presence of labeled bacterial markers in *Microcystis* substrates (Table 5.2). However, the concentrations of substrate bacteria FA were too low to cause the observed enrichment in bacterial FA in the incubations. *Microcystis* FA showed expected high ^{13}C labeling in the live *Microcystis* incubations followed by the detritus incubations (Fig. 5.2), because of their presence in the *Microcystis* substrates. Small ^{13}C enrichment was detected in algae in the live *Microcystis* and DOM treatments (Fig. 5.2). Part of their labeling can be explained by presence of algae biomarkers in the substrate (Table 5.2) and by growth on respired ^{13}C -DIC; DIC was enriched in all treatments, ranging from 5.7‰ (live treatments) to 15.2‰ (DOM treatments). DOC also showed ^{13}C enrichment in all treatments and the enrichment was highest in the additions where labeled *Microcystis* DOM was added, with 33.7‰ , as expected. POC was also enriched in all treatments, with highest enrichment in the detritus additions (19.4‰).

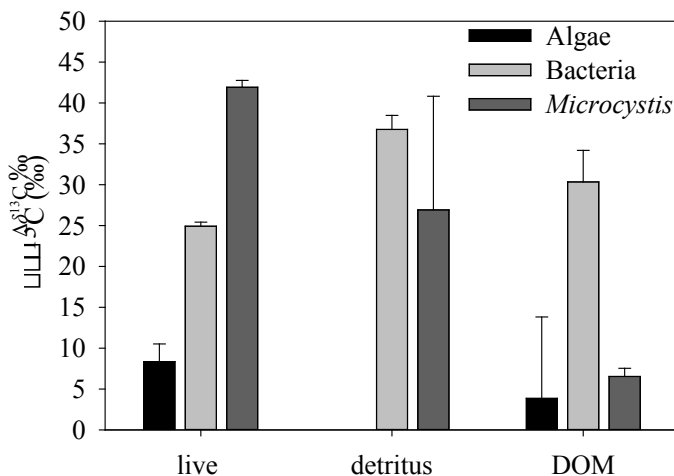


Fig. 5.2. ^{13}C enrichment ($\Delta\delta^{13}\text{C}$) of algae, bacteria, and *Microcystis* in the seston for the three different labeled *Microcystis* substrates added. Data are presented as average with SD error bars ($n=3$).

Fatty acid labeling in zooplankton

The presence and isotope enrichment of the bacteria, algae, and *Microcystis* fatty acids in zooplankton enabled us to combine *Microcystis* carbon incorporation with fatty acids as trophic markers. Both *Bosmina* (Fig. 5.3A) and *Daphnia* (Fig. 5.3B) contained fatty acids representative for each resource. The bacterial fatty acids in zooplankton showed the highest labeling in the *Microcystis* DOM additions, clearly showing that *Bosmina* and *Daphnia* grazed on the bacteria that grew on *Microcystis* DOM (Fig. 5.3). Zooplankters in the detritus treatments also contained relatively high labeled bacterial fatty acids, showing that zooplankton grazed on bacteria living on *Microcystis* detritus (Fig. 5.3). Even *Bosmina* in the live treatments contained labeled bacterial fatty acids, demonstrating that part of the live *Microcystis* that *Bosmina* consumed was shuttled via bacteria (Fig. 5.3A). The bacteria might have been attached to *Microcystis*, since there were no labeled bacterial markers found in *Daphnia* in the live *Microcystis* treatments (Fig. 5.3B). Consumption of live *Microcystis* by *Bosmina* was confirmed by the presence of labeled *Microcystis* markers in the zooplankters (Fig. 5.3A).

Table 5.2. Average percentages of marker fatty acids to total fatty acids (\pm SD, $n=3$) in zooplankton (1,2) and seston (3) in control incubations (without substrate) and in *Microcystis* used to produce the substrates (4).

Carbon pool	% Algae (PUFA)	% Bacteria FA	% <i>Microcystis</i> FA
1) <i>Bosmina</i>	5.9 \pm 1.1	0.7 \pm 0.3	8.9 \pm 1.8
2) <i>Daphnia</i>	9.9 \pm 0.4	4.2 \pm 0.4	21.4 \pm 1.1
3) Seston	4.6 \pm 1.6	2.8 \pm 0.2	27.8 \pm 2.0
4) <i>Microcystis</i>	0.8	0.6	28.5

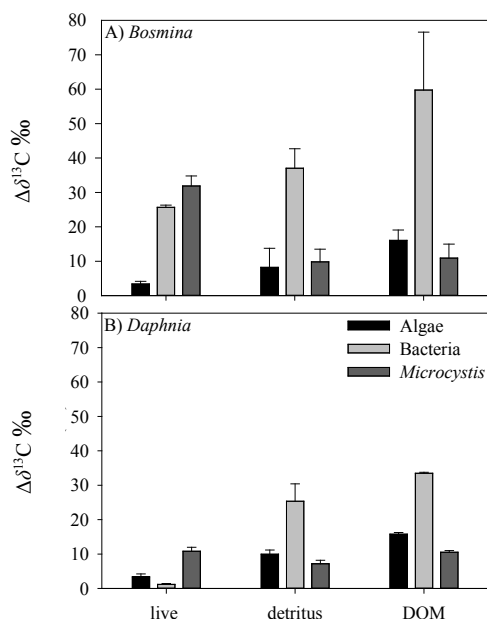


Fig. 5.3. ^{13}C enrichment ($\Delta\delta^{13}\text{C}$) of algae, bacteria, and *Microcystis* specific fatty acids within zooplankton for the three different labeled *Microcystis* substrates added; (A) *Bosmina* and (B) *Daphnia*. Data are presented as average with SD error bars ($n=3$).

Fatty acid concentrations

The results on fatty acid composition are only presented for control incubations, where substrate addition did not influence fatty acid composition of the seston. Although the fatty acids found in zooplankton matched the fatty acids in seston, the relative abundance of fatty acids differed (Table 5.2). The percentage of long-chain PUFA or algae markers was higher in zooplankton than in seston (ANOVA, $F_{2,6} = 19$, $p < 0.05$), indicating a preferential uptake or incorporation of those markers (Table 5.2). *Microcystis* markers however were more abundant in seston than in zooplankton (ANOVA, $F_{2,6} = 99$, $p < 0.05$) (Table 5.2). *Daphnia* contained relatively more algae and *Microcystis* markers than *Bosmina*. Bacterial markers were most abundant in *Daphnia*, followed by seston and they were least abundant in *Bosmina* (ANOVA, $F_{2,6} = 103$, $p < 0.05$) (Table 5.2). Overall, *Bosmina* had lower percentages of marker FA than *Daphnia*, because *Bosmina* contained relative more unsaturated fatty acids like C18:0 than *Daphnia* and had an overall higher diversity of fatty acids. The percentages of bacteria and algae markers in *Bosmina* and *Daphnia* were similar between the different treatments, but the percentage of *Microcystis* FA differed between treatments. *Microcystis* FA were lower in *Daphnia* in the DOM treatment compared to the other treatments (ANOVA, $F_{3,8} = 13$, $p < 0.05$) and higher in *Bosmina* in the *Microcystis* additions compared to the other treatments (ANOVA, $F_{3,8} = 8.3$, $p < 0.01$).

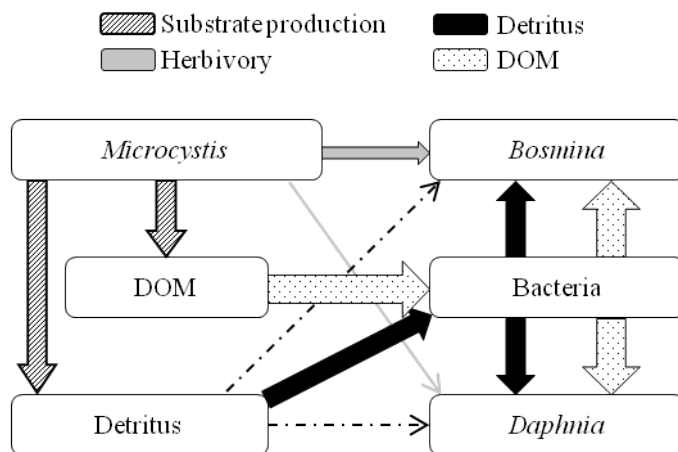


Fig. 5.4. A scheme of carbon flows from *Microcystis* and *Microcystis* derived substrates to zooplankton based on our study in Meilang Bay, Lake Taihu, China during spring 2009. Thickness of the arrow indicates the relative importance, the dashed arrows could not be confirmed.

5.4 Discussion

Carbon can flow from *Microcystis* to zooplankton via various pathways (Fig. 5.4) and it is not simple to identify and disentangle these routes under natural field conditions. Here we combined stable carbon isotope at natural abundance, fatty acids as trophic transfer markers and ^{13}C as a deliberately added tracer as complementary tools. Each approach has its strengths and weaknesses, but together they provide clear evidence for multiple pathways from *Microcystis* to zooplankton, and specifically for the dominance of microbial pathways.

Natural abundance stable isotope analyses

Carbon stable isotope analysis is a powerful tool to study food web interactions and has been successfully applied to allocate carbon sources of zooplankton. The natural values of carbon isotope ratios have been used to calculate the contribution of *Microcystis* carbon to zooplankton diets with bacteria and eukaryotic algae as the other potential carbon sources. While stable isotope signatures of metazoan consumers can be easily determined by handpicking the organisms, determination of the isotope signatures of the potential food sources remains challenging. By using compound specific isotope analyses, we could resolve the isotope signatures of bacteria, *Microcystis* and eukaryotic algae. Another pitfall is the natural variability of carbon isotope signatures within sources and the overlap between sources. Phytoplankton cells are known to have variable isotope signatures, which are partly taxa dependent, but are also influenced by physiology (e.g., growth) and environmental characteristics like temperature and CO₂ availability (Laws et al 1995; Vuorio et al. 2006). Cyanobacteria display especially large variability in isotope signatures, which can be partly explained by colony cell density and subsequently CO₂ availability. Furthermore, cyanobacteria are known to be able to fix aqueous CO₂, atmospheric CO₂, and bicarbonate, which have distinct isotope signatures and thus contribute to variability. In this study, the isotopic difference within *Microcystis* was larger (8 ‰) than that between *Microcystis* and other algae (<1 ‰) (Table 5.1), complicating resolution of eukaryotic algae vs. cyanobacteria contributions to zooplankton diets. A very large range in isotope signatures of cyanobacteria, from -32 ‰ to -5.9 ‰, was also found in Finnish lakes (Vuorio et al. 2006). Similar to our study, Bontes et al. (2006) observed higher $\delta^{13}\text{C}$ in scum-forming *Microcystis* than in water-column *Microcystis* in a shallow Dutch eutrophic lake. Enrichment in the scum-forming *Microcystis* can be partly explained by CO₂ limitation due to higher density and fixation of atmospheric CO₂ or bicarbonate.

The carbon isotope signature of bacteria resembled more that of POM than that of phytoplankton, indicating that carbon of the total POM pool was utilized by bacteria rather than phytoplankton only (Table 5.1). The enrichment of POM relative to phytoplankton can be explained by the presence of detritus. In lakes, detritus is often found to be enriched in ¹³C, due to preferential mineralization of ¹²C or presence of enriched allochthonous material (Del Giorgio and France 1996). In Taihu, enriched-scum forming *Microcystis* probably contributed to enriched detritus.

In spite of overlapping resources it was still possible to differentiate between bacteria-POM vs. phytoplankton (algae and *Microcystis*) contributions to zooplankton diets. In our study, *Bosmina* received a high (average 77 %) carbon contribution from POM-bacteria, while copepods were feeding more on algae (average 48 %). This is in agreement with the general consensus that cladocerans can graze effectively on bacteria, while copepods generally feed selectively on larger particles (Wylie and Currie 1991). Due to overlap in isotope signatures, feeding of the cladoceran *Bosmina* on bacteria could not be distinguished from consumption of bulk POM. However, the presence of bacterial fatty acids in *Bosmina* indicated that they were grazing on bacteria. The $\delta^{13}\text{C}$ of fatty acids in *Bosmina* matched the $\delta^{13}\text{C}$ of seston fatty acids, providing additional evidence that the zooplankter feeds on bacteria.

Fatty acid biomarkers

The presence of fatty acids in zooplankton consumers can be used to infer dietary information, specifically feeding on different types of algae and bacteria. Fatty acids present in the food are often directly incorporated into consumers and the zooplankton fatty acid profile therefore mimics the diet (Dalsgaard 2003; Taipale et al. 2009). However, zooplankton can selectively assimilate certain fatty acids, making it difficult to apply them in a quantitative way. The poly-unsaturated fatty acids (PUFA) are physiological essential and cannot be synthesized by zooplankton; therefore they are considered essential fatty acids (EFA). The long chain PUFAs 20:5 ω 3, 20:4 ω 6, and 22:6 ω 3 are high-quality fatty acids for zooplankton and their absence in the diet can limit growth and reproduction of cladocerans (Von Elert 2002). These fatty acids will be preferentially assimilated by zooplankton and stored. However, when these fatty acids are short in supply, zooplankton can convert 18 ω 3 PUFA, present in *Microcystis*, into the necessary long-chain PUFAs, although this would be at higher energetic costs. In agreement with previous studies on PUFA concentrations in zooplankton (Brett et al. 2006), zooplankton PUFA content was higher than seston PUFA concentrations in this study, indicating a preferential assimilation of PUFA (Table 5.2). Less attention has been paid to the trophic transfer of bacterial fatty acids within the plankton food web (Taipale et al. 2009; Kürten et al. 2011). Bacterial fatty acids are not essential for zooplankton and whether they semi-quantitatively reflect the bacterial contribution to zooplankton diets remains to be tested, because these fatty acids are likely metabolized rather than stored or assimilated.

Fatty acid labeling

In addition to higher concentrations in zooplankton, the algae markers in zooplankton also showed higher labeling than algae markers in the seston. There are at least three possible explanations for accumulation of labeled algae markers in zooplankton. 1) Zooplankton could selectively assimilate fatty acids of newly produced and thus labeled algae. During the experiment, ^{13}C present in the substrates got respired, resulting in ^{13}C increase in DIC, which was subsequently assimilated by primary producers. This can also explain the labeling of algae in the seston (Fig. 5.2). 2) The algae markers could have been produced by the zooplankton itself, by transformation of 18C-PUFA (18:3 ω 3, 18:4 ω 3, 18:2 ω 6, and 18:3 ω 6), which were present in *Microcystis* and *Microcystis* derived substrates. 3) They could have been produced by protists (ciliates and heterotrophic nanoflagellates) as part of the microbial food web, which were subsequently consumed by zooplankton. Protists feeding on bacteria are known to produce PUFA and other essential molecules, causing trophic upgrading of food quality along the food chain (Zhukova and Kharlamenko 1999). In this study we cannot distinguish transfer of carbon via protists from direct uptake of bacteria by zooplankton and we considered them all to be part of the microbial food web. The high labeling of bacterial markers in the seston showed that *Microcystis* and *Microcystis* derived substrates were an important carbon source for bacteria (Fig. 5.2). The high labeling of bacterial FA in zooplankton suggests consumption of bacteria or bacterivorous protists by zooplankton (Fig. 5.3). Comparison of fatty acid labeling between the zooplankton species is difficult, because of their different fatty acid profiles (Table 5.2). For example, higher labeling of bacterial markers in *Bosmina* compared to *Daphnia* could result from higher bacterial consumption, but also because of lower concentrations in *Bosmina* compared to *Daphnia*.

It should also be noted that the produced substrates were not from axenic *Microcystis* cultures, but from field concentrates, where other organisms were present as well. Trace amounts of labeled algae PUFA were present in our labeled *Microcystis* cultures and can potentially explain the relative high labeling of algae in the seston in the live treatments (Fig. 5.2). *Microcystis* has been shown to be a hot-spot for bacterial activity (Worm and Søndergaard 1998) and bacterial markers were labeled in the same way as *Microcystis* markers during substrate production. A small part of the measured bacterial labeling can thus be due to substrate labeling.

Bacteria as carbon source

The importance of bacteria as a food source for zooplankton has been long known, from laboratory studies with bacteria as single food source (Peterson et al. 1978; Porter et al. 1983) or labeled bacteria in mixed assemblages (Gophen et al. 1974) and studies under more natural conditions (Pace et al. 1983). The general consensus is that cladocerans are bacterivores, while copepods are not, so the importance of the microbial loop as a carbon source for zooplankton depends on zooplankton composition (Karlsson et al. 2007; Sanders et al. 1989; Wylie and Currie 1991) i.e., the presence of cladocerans that feed on bacteria, in addition to algae. Our findings of ~77 % of carbon coming from bacteria in cladocerans and ~23 % in copepods, based on an isotope mixing model with natural abundance data, supports these earlier works. Although copepods are not grazing directly on bacteria, cyclopoid and calanoid copepods can be effective grazers on larger bacterivores like ciliates (Sanders and Wickham 1993). The importance of the microbial loop as food source for zooplankton also depends on the amount of bacterial production relative to primary production (Pace et al. 1983; Sanders et al. 1989). Wylie and Currie (1991) calculated that bacterial carbon contributed 16-21 % of carbon ingested by cladocerans in an oligotrophic lake based on isotope labeling combined with modeling. In a marine mesocosm experiment with labeled carbon compounds, an equal contribution of bacterial and algae carbon to zooplankton (copepods and doliolida) was found (Koshikawa et al. 1996). In humic lakes, which are largely fueled by allochthonous carbon, detritus and bacteria can have a high carbon contribution to zooplankton (Hessen et al. 1990). In an isotope labeling experiment in a humic lake, Hessen et al. (1990), found bacteria growing on labeled DOM to contribute 11-42 % to zooplankton carbon, with an even higher contribution of (unlabeled) detritus (46-82 %) that could have passed through bacteria as well. The significance of bacteria and the microbial food web as a food source for zooplankton increases with increasing eutrophication (Gliwicz 1969). This phenomenon can be largely explained by the observed phytoplankton community shifts with lake eutrophication towards cyanobacteria. Still, there are few studies that showed a direct link from cyanobacteria carbon to zooplankton via bacteria and the microbial food web. Christoffersen et al. (1990) studied carbon fluxes in a plankton community during a cyanobacteria bloom, based on carbon budgets and causal relationships. They showed that macrozooplankton (mainly *Daphnia*) were assimilating carbon when cyanobacteria dominated the phytoplankton community and that this carbon apparently originated from phytoplankton and thus cyanobacteria. Christoffersen et al. (1990) also calculated that cyanobacteria were an important carbon source for bacteria and that macrozooplankton were more important bacterivores than microzooplankton. Work and Havens (2003) showed that macrozooplankton were grazing extensively on cyanobacteria and on bacteria in a eutrophic lake, but the authors did not show a link between cyanobacteria and bacteria as is shown here with the help of isotope labeling.

Decomposed *Microcystis* and other cyanobacteria were found to be a more important carbon source for zooplankton than living ones in a laboratory study by Hanazato and Yasuno (1987) and a labeling study by Gulati et al. (2001). In our study, the pathway from *Microcystis* DOM to bacteria and subsequently to zooplankton was more important than the *Microcystis* detritus-bacteria-zooplankton pathway (Figs. 5.1,3). It is generally not known what fraction of *Microcystis* ends up in particulate or dissolved form, but both fractions are expected to be significant. Hansen et al. (1986) showed that cyanobacteria dominated phytoplankton communities lost up to 43 % of the cellular carbon content as dissolved carbon within 24 hours after cell death and that a large part of the fresh DOM (71 %) was used by bacteria in 24 hours.

Zooplankton competition

The effect of cyanobacteria on different types of zooplankton and their competitive relations have been extensively studied over the past decades. Traditionally, most studies have focused on food quality of bloom-forming cyanobacteria for grazing zooplankton, thus on the herbivory pathway. Our results support that zooplankton community changes are mainly caused by differences in grazing behavior, since only treatments with live *Microcystis* showed a significant difference in carbon assimilation between *Bosmina* and *Daphnia*, with 48 % for *Bosmina* vs. 17 % for *Daphnia* (Fig. 5.1). *Microcystis* is generally considered 'poor' food for herbivorous zooplankton; it produces toxic substances, lacks essential nutrients and can form inedible colonies and filaments (reviewed in DeBernardi and Giussani 1990). In laboratory feeding experiments, cladocerans showed reduced survivorship, growth, and reproduction when they were fed solely with cyanobacteria (reviewed in Lampert 1987). Consistent with our results, Fulton and Pearl (1987) showed higher use efficiency of *Microcystis* carbon by *Bosmina* than by *Daphnia*. The morphology of *Microcystis* colonies has shown to be the most important intrinsic property in grazing inhibition of *Daphnia*, because it interferes with the filtering system (Fulton and Pearl 1987). In the treatment with live *Microcystis* feeding inhibition in both *Bosmina* and *Daphnia* likely contributed partially to their low consumption due to high densities of *Microcystis* colonies, which are common in Lake Taihu (Qin et al. 2010). Field studies also showed that larger cladocerans are more susceptible to the inhibiting effects than smaller ones (DeMott et al. 2001; Ghadouani et al. 2006), consistent with the observed lower carbon use in *Daphnia* than *Bosmina* in the experiments with live *Microcystis*. The body size of cladocerans is not a good predictor of ability to graze on bacteria, especially on free living bacteria. DeMott (1982) studied consumption of bacteria and green algae by *Bosmina* and *Daphnia* and observed that *Bosmina* consumed fewer bacteria than *Daphnia* relative to green algae. This could be explained by differences in feeding strategies: *Bosmina* is a more selective feeder than *Daphnia* (DeMott and Kerfoot 1982). The results of our study on the other hand indicate that *Daphnia* and *Bosmina* are both efficient grazers on total (solitary and attached) bacteria (Figs. 5.1,3).

A shift in zooplankton community from large cladocerans towards small-bodied cladocerans is generally observed in eutrophic systems with cyanobacteria blooms (Gliwicz 1969). One important cause is feeding on large zooplankters by planktivorous fish, especially in lakes that are shallow and/or lack a hypolimnetic or macrophyte- bed refuge. As described above, the cyanobacteria bloom itself can contribute to the shift in zooplankton species due to feeding inhibition of larger cladocerans (DeMott et al. 2001; Ghadouani et al. 2006).

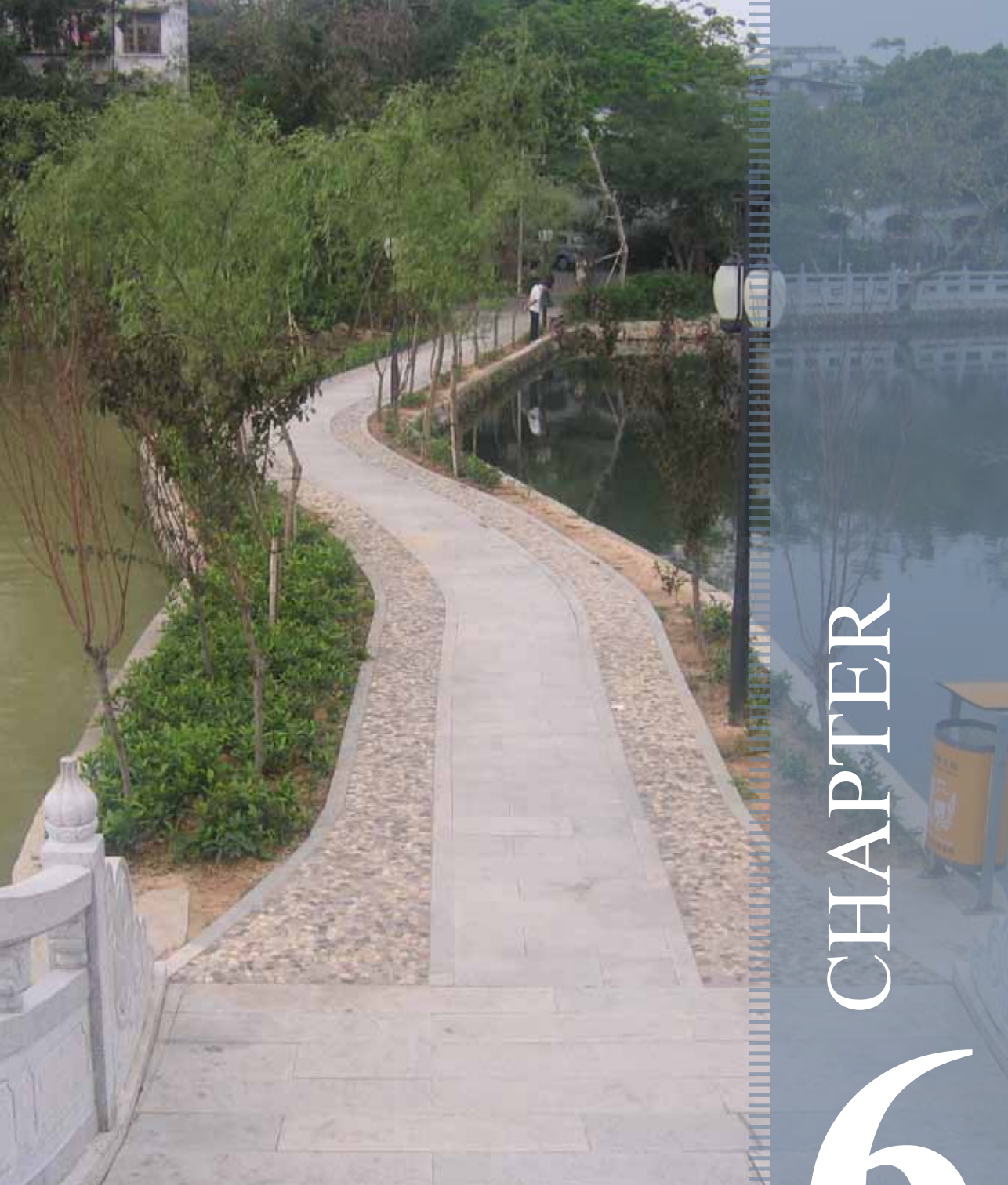
The conceptual diagram in Fig. 5.4 shows the major findings of this study; 1) the cyanobacterium *Microcystis* is an important carbon source for zooplankton growth in Taihu, 2) *Microcystis* carbon flows to zooplankton mainly via DOM and detritus, and 3) heterotrophic bacteria play a key role in the carbon flow from *Microcystis* DOM and detritus to zooplankton. Moreover, *Bosmina* assimilated relatively more *Microcystis* carbon than *Daphnia*, mainly because *Bosmina* grazed more on live *Microcystis* than *Daphnia*.

Acknowledgements

We thank all those from Taihu field station and Nanjing Institute of Geography and Limnology who helped in the field and with carrying out the experiment and analyses, but especially: Weiwei Jiang, Deyong Zhou, Hu He, Xiaolan Song, Leiyan Zhang, and Xing Peng. We thank colleagues from the Royal Netherlands Institute for Sea Research in Yerseke: Pieter van Rijswijk and Peter van Breugel for laboratory support, Dick van Oevelen for analyses support. We thank Ramesh D. Gulati for manuscript recommendations and William DeMott for the constructive review. This study received financial support from the Darwin Center for Biogeosciences supported by the Netherlands Organization of Scientific Research (NWO) and Chinese projects (2008CB418100, U1033602, and 41073057).

Anna de Kluijver, Jiajia Ning, Zhengwen Liu, and Jack J. Middelburg

In preparation



CHAPTER

6



Macrophyte carbon subsidies to bacterioplankton and zooplankton in a restored part of a shallow, eutrophic lake in China

Abstract

The subsidy of macrophyte-derived carbon to bacterial and zooplankton consumers was assessed using stable isotope analyses in a biomanipulation project. Part of a shallow, eutrophic lake in China was restored with submerged macrophytes after fish removal and compared to the unrestored part for plankton carbon flows. Macrophyte presence alters pelagic energy flows, yet their subsidy to pelagic food webs is not fully understood. Macrophytes, seston, and zooplankton were bimonthly sampled for natural abundance isotope ratios of carbon ($\delta^{13}\text{C}$) and nitrogen ($\delta^{15}\text{N}$) over a whole year period (2010). The $\delta^{13}\text{C}$ of phytoplankton and heterotrophic bacteria in seston (bacterioplankton) were determined from $\delta^{13}\text{C}$ of fatty acid biomarkers. Macrophyte and attached periphyton were the most $\delta^{13}\text{C}$ enriched of all organic carbon pools and were considered together as macrophytes. Macrophyte carbon signal was detected in particulate organic carbon (POC), bacterioplankton, and zooplankton in the restored part (M+), which were significantly enriched in $\delta^{13}\text{C}$ compared to the unrestored part (M-), while phytoplankton and dissolved organic carbon had similar $\delta^{13}\text{C}$ in both parts. The zooplankton community in both M+ and M- was dominated by copepods with only few cladocerans, which had similar $\delta^{13}\text{C}$, but different $\delta^{15}\text{N}$. Copepods were more enriched in $\delta^{15}\text{N}$ than cladocerans, indicating that they were feeding on the same carbon source, but at a higher trophic position. A two-source (macrophytes and phytoplankton) mixing model showed that macrophytes contributed 14-86 % to bacterioplankton (average 55 %) in M+ depending on the season. Macrophyte contribution to zooplankton in M+ was 26-87 % (average 47 %) depending on the season. Our study demonstrates that lake restoration with submerged macrophytes clearly influences energy flows in the lowest parts of planktonic food webs.

6.1 Introduction

Many shallow lakes have shifted from a clear, macrophyte rich state to a turbid, phytoplankton dominated state during the last century, due to ongoing eutrophication. Both states are maintained by stabilizing feedback mechanisms; in the turbid state, low light prevents macrophytes from growing and resuspension of unprotected sediments by fish and waves further decreases water transparency. Since macrophytes are natural refuges for zooplankton, the absence of macrophytes causes high grazing of zooplankton by planktivorous fish to abundances that are too low to control phytoplankton development (Scheffer et al. 1993). The reversion of turbid lakes back into clear-water lakes is a difficult task. Biomanipulation, including fish removal or macrophyte planting, became a popular tool in lake restoration. Biomanipulation focuses primarily on cascading trophic interactions and the classical food web: the consumption of nutrients by phytoplankton, which are grazed by zooplankton, which are then preyed upon by planktivorous fish (Shapiro et al. 1975).

Because biomanipulation measures are based on the classical food chain and cascading food webs, less attention has been paid to the role and importance of bacterioplankton and the microbial food web in biomanipulation studies. However, bacterioplankton dominate pelagic food webs in terms of respiration and secondary production (Cole 1999). Phytoplankton derived dissolved organic carbon (DOC), produced either directly via exudation or indirectly via grazing and cell lysis, is considered a primary carbon source for bacterioplankton, but other sources of DOC, like terrestrial carbon (Tranvik 1992) and macrophyte carbon (Rooney and Kalff 2003) can fuel bacterial metabolism as well. Bacterioplankton are primarily grazed upon by protists, like heterotrophic flagellates and ciliates, which are part of the microbial food web and considered trophic intermediates between small particles and large zooplankton. Large zooplankton can graze directly on bacterioplankton, which can be a substantial part of zooplankton diet (Wylie and Currie 1991). Especially cladocerans, like *Daphnia* showed to be effective bacterivores in multiple studies (Pace et al. 1983, Wylie and Currie 1991, Karlsson et al. 2007, de Kluijver et al. 2012). Copepods are selective feeders that feed on larger particles and generally don't graze on bacterioplankton directly, but do graze on bacterivores, such as protists (Sanders and Wickham 1993). Protists can synthesize essential molecules, like poly-unsaturated fatty acids (PUFA), thereby upgrading food quality within the microbial food web and providing compensation for nutritional shortcomings of herbivory (Klein-Breteler et al. 1999, Zhukova and Kharlamenko 1999).

Whether macrophyte carbon subsidizes bacterioplankton and subsequent zooplankton in macrophyte restored, eutrophic lakes is not fully understood, but we hypothesized that contributions might be substantial. Macrophytes are known to release part of their organic carbon as DOC (Penhale and Smith 1979, Søndergaard 1981) that can be subsequently consumed by bacteria (Findlay et al. 1986). Theil-Nielsen and Søndergaard (1999) compared twin lakes with and without macrophytes and observed high production of epiphytic bacteria (bacteria attached to macrophytes) and higher production rates per unit of bacterioplankton in the macrophyte lake compared to lakes without macrophytes. An increase in bacterioplankton production relative to phytoplankton biomass with increasing macrophyte coverage was observed by Rooney and Kalff (2003). However, it is challenging to unravel if bacterioplankton is supported by macrophytes directly or if changes in bacterioplankton are due to indirect changes in nutrients and pelagic food web structure.

Stable isotope analysis (SIA) revealed that carbon stable isotope ratios ($\delta^{13}\text{C}$) in zooplankton were more enriched during periods with high macrophyte coverage (Boll et al. 2012). Although the enrichment was suggested to be due to changes in $\delta^{13}\text{C}$ of phytoplankton (Boll et al. 2012), it could also indicate carbon subsidy of macrophytes, since macrophytes are usually enriched in $\delta^{13}\text{C}$ compared to phytoplankton (Fry 2006). Little trophic fractionation in $\delta^{13}\text{C}$ occurs between consumers and their diet, so $\delta^{13}\text{C}$ of sources and consumers can be used to reveal dietary pathways and calculate food source contributions (DeNiro and Epstein 1978). Additional SIA of nitrogen ($\delta^{15}\text{N}$) can help establishing trophic positions of consumers, since $\delta^{15}\text{N}$ gets enriched along the food chain due trophic fractionation (Minagawa and Wada 1984). A major challenge in aquatic ecology is to separate the $\delta^{13}\text{C}$ of plankton sources and consumers from bulk particulate organic carbon (POC). Compound specific isotope analysis (CSIA) of fatty acid biomarkers is a valuable method to determine the isotope signature of certain groups of organisms and has been frequently used to determine the $\delta^{13}\text{C}$ of phytoplankton and bacterioplankton (Boschker and Middelburg 2002).

Here we applied SIA to assess the subsidy of macrophyte derived carbon to bacterioplankton and zooplankton in a restored part compared to unrestored parts of a shallow, eutrophic lake. Using two-source mixing model we could determine macrophyte and phytoplankton carbon contributions to bacterioplankton and zooplankton consumers. The $\delta^{15}\text{N}$ of particulate organic nitrogen (PON) and zooplankton was additionally analysed to retrieve information on trophic positions. The results revealed a clear macrophyte subsidy to bacterioplankton and zooplankton.

6.2 Methods

Site description

Huizhou West Lake is a tropical urban lake in southern China (23° 06' N, 114° 23' E). The total surface area of the lake is about 1.6 km² and the mean depth is about 1.6 m. The lake consists of several basins which are connected through waterways. Due to the increased waste water input, the lake became eutrophic and submerged macrophytes have been absent since 1980s (Li et al. 2007). In order to improve water quality, a large-scale biomanipulation was carried out in a 12 ha basin in Huizhou West Lake in May of 2007 (Fig. 6.1). The biomanipulation measures included fish removal, followed by submerged macrophyte planting. The coverage of submerged macrophytes reached about 80% in 2009 in the restored part (M+). The concentrations of phosphorus, nitrogen and chl *a* were reduced to much lower levels in M+ compared to the unrestored part (M-). The phytoplankton community in Huizhou West lake was dominated by cyanobacteria, which were significantly reduced in M+ compared to M- (Chen et al. 2010).

Copepods were the main crustacean both in M+ and M- while cladocerans were present in extremely low proportion. For the composition of copepods, the unrestored lake was dominated by cyclops such as *Thermocyclops taihokuensis* while the restored lake was dominated by calanoids *Neodiantomus schmackeri*. Dominant cladocerans included *Diaphanosoma brachyurum*, *Moina micrura* and *Bosmina* spp. The species richness, abundance, biomass and biodiversity of crustacean plankton were all higher in restored lake than in the unrestored lake.

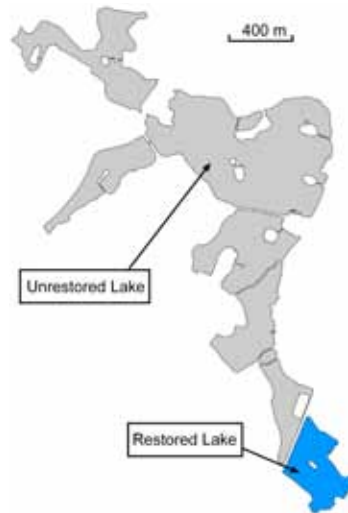


Fig. 6.1. Map of Huizhou West Lake, with the restored lake (blue) and unrestored lakes (grey). The arrows point the sampling locations.

Sampling

The restored lake (M+) and unrestored lake (M-) were bimonthly sampled from February 2010 to February 2011 at the locations shown in Fig. 6.1. All samples were taken 0.5 m below surface from each lake. Chl *a* concentrations were determined spectrophotometrically after filtration of sampled water on cellulose acetate filters and extraction into 90 % acetone. Triplicate samples were taken for stable isotope analyses and concentrations of the major carbon pools. Headspace vials (20 ml and 2 ml) were filled on board with sample water using the overflow method and sealed with gas-tight caps for DIC isotope analyses. Mercury chloride was added for preservation and the samples were stored upside down at room temperature. Samples for DOC were GF/F filtered and stored frozen in clean vials until further analyses. Seston samples for particulate organic matter (POM) were taken on pre-weighed and pre-combusted GF/F filters and dried at 60°; Polar lipid fatty acids (PLFA) samples were collected on pre-combusted GF/F filters and freeze-dried. Zooplankton was collected with a 63 µm mesh-size net. Back in the laboratory, they were transferred to demineralized water to empty their guts. ~98 individual copepods (range 15-370), and 20-50 individual cladocerans were handpicked and transferred to pre-weighed and pre-combusted tin cups, which were subsequently freeze-dried.

Samples of macrophytes were collected for each species. Periphyton was collected from macrophytes with a wire or nylon brush in a plastic container filled with clean water. All visible non-periphyton particles were removed manually and samples were then filtered through a 100 µm mesh, followed by filtration onto pre-combusted GF/F filters. Macrophyte leaves were subsequently chopped. Sediment samples were collected with a Peterson grab sampler, and the top cm of sediment was scraped off with a metal spoon. Finally, leaves and soil were sampled nearby the lake. Samples of leave material from some common types of vegetation were collected and subsequently chopped. All samples were rinsed with distilled water and dried at 60°C. Then, samples were ground with a mortar and pestle and stored in desiccators until further analyses.

Stable isotope analyses

Stable isotope ratios are expressed in the delta (δ) notation, defined as parts per thousand (per mil, ‰) deviation from a certified standard; $\delta^{13}\text{C}$ or $\delta^{15}\text{N} = ([R_{\text{sample}}/R_{\text{standard}}]-1) \times 1000$ and R is the ratio $^{13}\text{C}/^{12}\text{C}$ and $^{15}\text{N}/^{14}\text{N}$. The standards for $\delta^{13}\text{C}$ and $\delta^{15}\text{N}$ were VPDB (Vienna Pee Dee Belemnite) and atmospheric nitrogen, respectively. Isotopic enrichment means that the sample contains relatively more of the heavy isotope, resulting in a more positive (less negative for carbon) isotope ratio and isotopic depletion means the opposite. POM, macrophytes, periphyton, soil, sediment, leaves, and zooplankton samples were analyzed for carbon and nitrogen content and $\delta^{13}\text{C}$ and $\delta^{15}\text{N}$ on a Thermo Electron Flash EA 1112 analyzer (EA) coupled to a Delta V isotope ratio mass spectrometer (IRMS). For DIC $\delta^{13}\text{C}$ analyses, a helium headspace was created in the headspace vials and samples were acidified with H_3PO_4 solution. After equilibration, the CO_2 concentration and isotope ratio in the headspace was measured using EA-IRMS. For DOC $\delta^{13}\text{C}$ analyses, the samples were acidified and flushed with helium to remove DIC and subsequently oxidized with sodium persulfate ($\text{Na}_2\text{S}_2\text{O}_8$); the produced isotopes were measured using high performance liquid chromatography - isotope ratio mass spectrometry (HPLC-IRMS) (Boschker et al. 2008). PLFA samples were extracted according using a modified Bligh and Dyer method (Middelburg et al. 2000). The lipids were fractionated in different polarity classes by column separation on a heat activated silic acid column and subsequent elution with chloroform, acetone and methanol. The methanol fractions, containing most of the polar lipid fatty acids were collected and derivatized to fatty acid methyl esters (FAME). The standards 12:0 and 19:0 were used as internal standards. Concentrations and $\delta^{13}\text{C}$ of individual PLFA were measured using gas chromatography-combustion isotope ratio mass spectrometry (GC-C-IRMS) (Middelburg et al. 2000).

Data analyses

PLFA were used as chemotaxonomic markers for phytoplankton and heterotrophic bacteria (hereafter bacterioplankton). The most abundant branched fatty acids in both M+ and M- were i14:0, i15:0, and ai15:0, which are characteristic for heterotrophic, gram-positive bacteria (Kaneda 1991). Their concentration-weighted $\delta^{13}\text{C}$ was used as marker for $\delta^{13}\text{C}$ of heterotrophic bacteria ($\delta^{13}\text{C}_{\text{bac}}$) and their sum of concentrations was used as marker for bacterioplankton abundance. The most abundant PUFA in both M+ and M- were 18:3 ω 3, 18:4 ω 3, 20:5 ω 3, and 22:6 ω 3, which are markers for phytoplankton (both cyanobacteria and eukaryotic algae). Their concentration-weighted $\delta^{13}\text{C}$ was used as marker for $\delta^{13}\text{C}$ of phytoplankton ($\delta^{13}\text{C}_{\text{phyto}}$). The biomass of phytoplankton was calculated from chl a concentrations and a C:chl a ratio of 40, a commonly used value (Middelburg et al. 2000).

Data of each month are shown as mean \pm standard deviation (sd) of triplicate samples. Total annual averages (ta) are presented as mean \pm sd of the means of each sampling event ($n=7$). Differences between M+ and M- were statistically tested using the mean values of each sampling event ($n=7$) with student t-tests.

For food source calculations, the $\delta^{13}\text{C}_{\text{phyto}}$ was corrected for the depletion in fatty acids (FA) compared to total cells ($\Delta\delta^{13}\text{C}_{\text{FA-cell}}$). $\Delta\delta^{13}\text{C}_{\text{FA-cell}}$ is variable, but a value of 3 ‰ is often used and was adopted in this study (Hayes 2001), so $\delta^{13}\text{C}_{\text{phyto_cor}} = \delta^{13}\text{C}_{\text{phyto}} + 3$ ‰. For bacterioplankton, it is suggested that in field samples $\Delta\delta^{13}\text{C}_{\text{FA-cell}}$ would be ~ 0 ‰ (Burke et al. 2003), a value we adopted.

The contributions of macrophyte carbon and phytoplankton carbon as carbon source for zooplankton ($f_{\text{macro_zoo}}$ and $f_{\text{phyto_zoo}}$, respectively) and bacterioplankton ($f_{\text{macro_bac}}$ and $f_{\text{phyto_bac}}$, respectively) in the restored lake were calculated using an isotope mixing model:

$$f_{\text{macro}} (\%) = \frac{\delta^{13}\text{C}_{\text{phyto}} - \delta^{13}\text{C}_{\text{consumer}}}{\delta^{13}\text{C}_{\text{phyto}} - \delta^{13}\text{C}_{\text{macro}}} \times 100 ; f_{\text{phyto}} (\%) = 100 - f_{\text{macro}} \quad (6.1)$$

The uncertainties in $\delta^{13}\text{C}$ of carbon sources and consumers were considered in the calculations using random sampling ($n=1000$) from a normal distribution. The normal distribution was created from the mean value \pm sd of sources and consumers. For macrophytes and zooplankton, the mean $\delta^{13}\text{C} \pm$ sd of all genera were used. Only outcomes between 0 and 100 % was accepted and contributions are presented as average \pm sd of the accepted outcomes. Correlation coefficients of normally distributed data were calculated using Pearson product-moment correlation. Random sampling and statistical analyses were done in R software (R development core team 2011).

6.3 Results and discussion

Organic carbon concentrations

POC concentrations were ~ 2 mg C L⁻¹ lower in M+ compared to M- (Fig. 6.2A), what is largely caused by the difference in phytoplankton (chl *a* based) biomass, which was ~ 1.2 mg C L⁻¹ lower in M+ compared to M- (Fig. 6.2B). Phytoplankton made up 13 ± 14 % (M+) and 23 ± 12 % (M-) of POC. The decrease in phytoplankton in macrophyte-restored lakes can have several causes, including nutrient and light competition and release of inhibitory substances by macrophytes (reviewed in Van Donk and Van De Bund 2002). The decrease in phytoplankton in M+ shows the desired effect of biomanipulation (Shapiro 1975). The concentrations of bacterial FA were ~ 5 times higher in the M- compared M+ (Fig. 6.2C). The decrease in bacterial abundance in M+ lakes can be explained by several mechanisms. 1) Because of the importance of phytoplankton DOC as carbon source for bacteria, the observed decrease in phytoplankton in M+ resulted in a decrease of bacterioplankton. 2) The observed decrease of nutrients in M+ could induce nutrient limitation in bacterioplankton. A decrease in bacterial abundance in macrophyte dominated lakes due to nutrient limitation and nutrient competition with macrophytes was demonstrated by Huss and Wehr (2004).

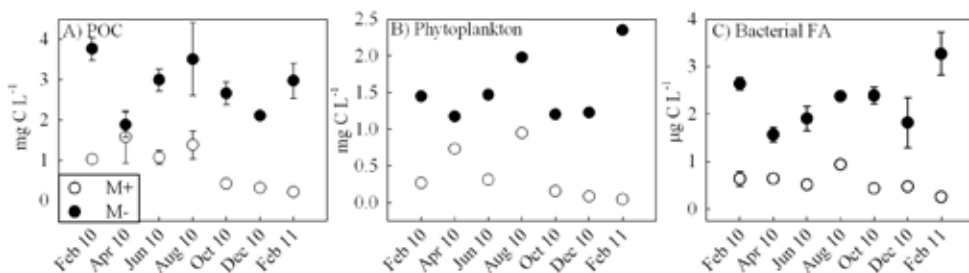


Fig. 6.2. Temporal development of concentrations of A) POC, B) Phytoplankton (from chl *a*), C) Bacteria FA in the restored (M+, open circles) and unrestored (M-, closed circles) lake. Points present the average \pm sd ($n=3$).

3) The decrease could be due to higher number of zooplankton in M+, so stronger grazing pressure (top-down control). In biomanipulation studies on temperate lakes, the decrease in bacterioplankton was ascribed to increased *Daphnia* abundance that controlled bacterial abundance (Jürgens and Jeppesen 1998, Søndergaard et al. 1998). Large cladocerans, such as *Daphnia* were nearly absent in our study. Cascading effects of zooplankton extending to bacterioplankton seems to occur only when *Daphnia* is present, and not with abundant copepods (Wickham 1995), so top-down control seems unlikely. Despite the decrease in bacterial abundance, the ratio of bacteria to phytoplankton abundance was higher in M+ compared to M-, what could indicate macrophyte carbon support.

Nitrogen stable isotopes ($\delta^{15}\text{N}$)

Lake restoration had a clear influence on nitrogen stable isotope signatures of PON and zooplankton consumers (Fig. 6.3). $\delta^{15}\text{N}$ of PON and zooplankton had significantly lower in M+ than in M- (Table 6.1).

There are several drivers for variability in $\delta^{15}\text{N}$ of PON, such as external loading, nitrogen cycling processes, and fractionation processes (reviewed in Gu 2009). External loading is expected to be similar in M+ and M-, because they are located in the same watershed, so variability is probably due to within lake processes. Beside differences in nitrogen cycling processes (such as nitrogen fixation and denitrification) which were not determined in this study, $\delta^{15}\text{N}$ of PON increases with increasing phytoplankton productivity, because of reduced isotopic fractionation at higher production and nitrogen uptake rates (Gu 2009). Periphyton and macrophytes were slightly more enriched than PON (Table 6.1). Zooplankton (dominated by copepods) was generally more enriched in $\delta^{15}\text{N}$ than PON, as expected due to trophic fractionation.

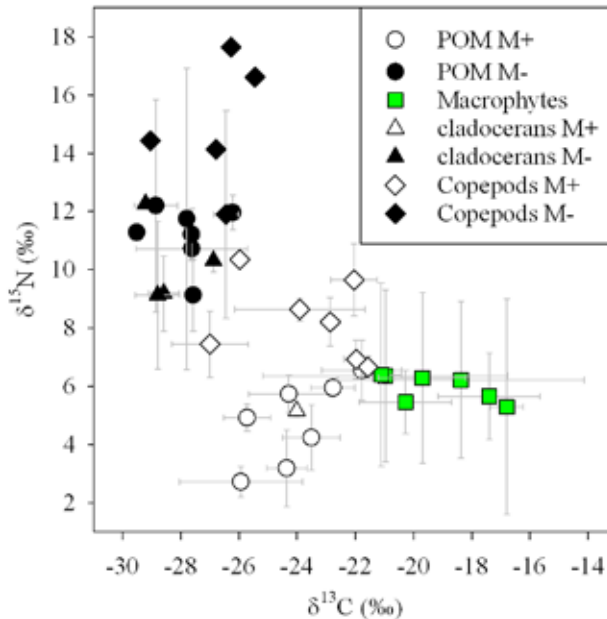


Fig. 6.3. $\delta^{15}\text{N}$ and $\delta^{13}\text{C}$ of POC and zooplankton in restored (M+, open symbols) and unrestored (M-, closed symbols) and average of all macrophytes in M+. Single data points present the mean of each sampling event \pm sd (n=3).

The average difference in $\delta^{15}\text{N}$ between copepods and PON was 3.5 ± 1.6 ‰ ($n=7$) in M+ and 3.6 ± 1.8 ‰ ($n=5$) in M- (Fig. 6.3), which are trophic fractionation values expected for carnivorous zooplankton (Vander Zanden and Rasmussen 2001). Cladocerans were rarely observed and showed less or no trophic fractionation: 2.4 ‰ in M+ in April ($n=1$) and -0.7 ± 2.3 ‰ in M- ($n=4$) (Fig. 6.3). The fractionation in M+ is indicative for herbivory (Vander Zanden and Rasmussen 2001) and the low fractionation in M- suggests that cladocerans feed selectively on parts of the PON, what were suggested to be bacteria by Karlsson et al. (2004). Enrichment in $\delta^{15}\text{N}$ of copepods compared to cladocerans has been observed in several studies (Karlsson et al. 2004, Sommer and Sommer 2006), showing that copepods are grazing at a higher trophic level. Because copepods are selective and omnivorous feeders, they can selectively feed on the trophic intermediates of the microbial food web, like ciliates, and on other zooplankton, like rotifers, small copepods, and cladocerans (Wickham 1995). The low fractionation in cladocerans in M- supports the idea of bacteria mediated carbon flow from cyanobacteria to cladocerans, which is a major pathway in cyanobacteria dominated systems (De Kluijver et al. 2012).

Table 6.1. Average (ta) isotope ratios \pm sd of nitrogen ($\delta^{15}\text{N}$) and carbon ($\delta^{13}\text{C}$) of analysed organic and inorganic carbon and nitrogen pools in restored (M+) and unrestored (M-) parts of Huizhou West lake. N gives the number of samples over the year and p gives the significance level of differences between M+ and M- from t-tests (* $p < 0.05$, ** $p < 0.01$, *** $p < 0.001$).

	$\delta^{15}\text{N}$ (‰)				$\delta^{13}\text{C}$ (‰)			
	ta M+	ta M-	N	p	ta M+	ta M-	N	p
POM	4.8 ± 1.4	11.2 ± 1.0	7,7	***	-24.1 ± 1.5	-27.9 ± 1.1	7,7	***
Macrophytes	5.5 ± 1.2		7,-	-	-17.8 ± 1.8		7,-	-
Periphyton	6.3 ± 2.2		7,-	-	-19.2 ± 1.7		7,-	-
Copepods	8.3 ± 1.4	14.9 ± 2.3	7,5	***	-24.1 ± 2.0	-26.6 ± 1.3	7,5	*
Cladocerans	5.2	10.2 ± 1.5	1,4	-	-24	-28.4 ± 1.0	1,4	-
Total zooplankton	8.2 ± 1.5	13.7 ± 2.5	7,7	***	-23.7 ± 2.0	-27.1 ± 1.3	7,7	**
DOC					-26.2 ± 2.8	-27.9 ± 2.4	7,7	NS
Bacterial FA					-22.6 ± 1.1	-29.0 ± 1.3	7,7	***
Phytoplankton FA					-31.8 ± 5.3	-33.6 ± 5.4	7,7	NS
DIC					-4.7 ± 1.2	1.5 ± 1.3	7,7	***

Carbon stable isotopes ($\delta^{13}\text{C}$)

Macrophytes and attached periphyton were the most ^{13}C enriched of all organic carbon pools and were considered together as macrophytes (Fig. 6.3). The presence of macrophytes resulted in a significant enrichment in $\delta^{13}\text{C}$ of POC in M+ compared to M and in total zooplankton (Table 6.1). In M+, cladocerans ($n=1$) and copepods ($n=7$) had similar $\delta^{13}\text{C}$, indicating that the carbon was ultimately derived from the same carbon source (Table 6.1, Fig. 6.3). Therefore, total zooplankton ($\delta^{13}\text{C}_{\text{Zoo}}$) was used in the food source calculations. In M-, copepods were slightly more enriched than cladocerans, but the difference was not significant (Table 6.1). Zooplankton was more enriched in M+ than in M- in most sampling periods, except October and December, where $\delta^{13}\text{C}$ were similar or even more depleted (Fig 6.4A).

Carbon isotope analyses of FA showed that bacterioplankton were significantly enriched in $\delta^{13}\text{C}$ in M+ compared to M- throughout the year (Fig. 6.4B, Table 6.1), indicating that macrophytes were subsidizing bacterioplankton. After macrophytes (with periphyton), bacterioplankton were the most enriched organic carbon pool in M+ (Table 6.1). The $\delta^{13}\text{C}_{\text{phyto}}$ values were not statistically different between M+ and M- (Fig. 6.4C, Table 6.1), showing that $\delta^{13}\text{C}_{\text{phyto}}$ was not directly related to phytoplankton biomass (chl *a*) as shown in other studies (Laws et al. 1995), or to the presence of macrophytes.

There was one carbon pool, DIC, which showed an opposite result with significant depletion in $\delta^{13}\text{C}$ in M+ compared to M- (Fig. 6.4D, Table 6.1). This can probably be attributed to a biomanipulation effect on the respiration-production balance. Respiration of organic matter (OM) causes depletion of $\delta^{13}\text{C}_{\text{DIC}}$ due to addition of depleted OM-derived C, while production causes enrichment in $\delta^{13}\text{C}_{\text{DIC}}$ due to preferential uptake of ^{12}C by phytoplankton. The higher phytoplankton biomass (as indication of higher productivity) in M- can thus explain the enriched $\delta^{13}\text{C}$ of DIC. The enrichment in $\delta^{13}\text{C}$ in macrophytes compared to phytoplankton can be attributed to 1) substrate availability and 2) different photosynthetic pathways. All macrophyte genera in M+ were submerged plants and therefore used aquatic CO_2 . 1) In lakes with low turbulence, stagnant boundary layers of water may form around macrophytes, restricting DIC diffusion and trapping enriched $\delta^{13}\text{C}_{\text{DIC}}$ around the macrophytes (Smith and Walker 1980). This also explains the enrichment in the periphyton, since it grows attached to macrophytes and uses the same DIC pool. 2) Most macrophyte species, including the ones present in this study, have plastic photosynthetic mechanisms that allow them to survive under low CO_2 conditions.

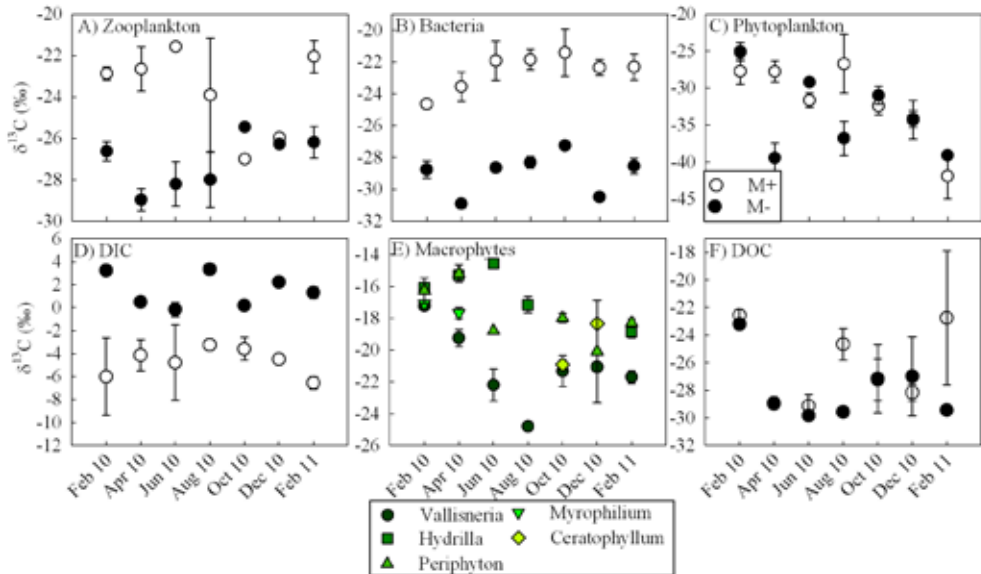


Fig. 6.4. Temporal development of $\delta^{13}\text{C}$ (‰) in A) Zooplankton, B) Bacteria FA, C) Phytoplankton FA, D) DIC, F) DOC in restored (M+, open circles) and unrestored (M-, closed circles) lakes. The temporal development of different macrophyte genera and periphyton in M+ are showed in E. Each data point presents the average \pm sd of three measurements.

They possess mechanisms characteristic of C_3 , C_4 metabolism, including bicarbonate uptake, root CO_2 uptake, and C_4 enzymes (reviewed in Bowes and Salvucci 1989). Variability in substrate availability and application of different photosynthetic mechanisms can also explain the variability in $\delta^{13}C$ between macrophyte genera (Fig. 6.4E). *Hydrilla verticillata* was the most enriched macrophyte (-16.4 ± 1.7 ‰) and *Vallisneria* sp. the most depleted (-21.1 ± 2.4 ‰) and *Ceratophyllum demersum* and *Myriophyllum spicatum* had values in between.

Macrophytes as a carbon source for bacterioplankton

The carbon contributions of phytoplankton ($f_{\text{phyto_bac}}$) and macrophytes ($f_{\text{macro_bac}}$) to bacterioplankton in M+ were calculated for each sampling period (equation 6.1). Values of $f_{\text{macro_bac}}$ were on average 55 ± 29 % and showed seasonal variability (Fig. 6.5). The highest $f_{\text{macro_bac}}$ (84 and 86 %) were observed in October and February (2011) and the lowest (14 %) was found in February (2010). The differences in February among years can be attributed to the start of the phytoplankton bloom. In February 2010, phytoplankton concentrations and temperature were higher than in February 2011, indicating an earlier start of the bloom (Fig. 6.1B). Overall, $f_{\text{macro_bac}}$ showed a significant negative correlation with POC concentrations ($r = -0.82$, $p < 0.05$), what suggests that macrophyte carbon was mainly released and consumed as DOC. Interestingly, the $\delta^{13}C$ of DOC in M+ was only more enriched than $\delta^{13}C$ of DOC in M- in August and in February 2011, but not in the other months (Fig 6.4F) and there was no overall enrichment in $\delta^{13}C$ of DOC (Table 6.1). The macrophyte carbon signal could be masked by a large refractory DOC pool and macrophyte carbon could be more labile and thus preferentially consumed. The macrophyte contribution was more visible in POC, what can be due to physical aggregation of macrophyte DOC into POC, the conversion of DOC into POC by bacterioplankton, and release of macrophyte particles (detritus) (Mann 1988). Throughout most of the year macrophytes contributed more to bacterioplankton than phytoplankton. Our estimates were rather conservative, because of the assumption that $\delta^{13}C$ of bacterial FA were representative for bacterial cells. When a correction of +3 ‰ for $\Delta\delta^{13}C_{\text{FA-cell}}$ would be applied ($\delta^{13}C_{\text{hbc_cor}}$, $\delta^{13}C_{\text{bac}}$ becomes more enriched (-19.6 ‰) and $f_{\text{macro_bac}}$ would be 74 ± 18 % on average, ranging from 45 to 94 %.

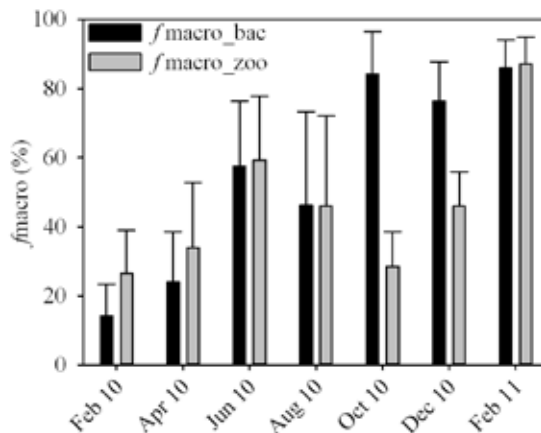


Fig. 6.5. The contribution of macrophyte carbon (%) in each sampled month to bacteria (black fills) and zooplankton (grey fills) in the restored lake (M+). The other carbon source is phytoplankton and together they sum to 100 %. The error bars present the uncertainty on the calculations.

Macrophytes as a carbon source for zooplankton

The average contribution of macrophytes to zooplankton ($f_{\text{macro_zoo}}$) was $47 \pm 21\%$, and varied per month. The lowest $f_{\text{macro_zoo}}$ was observed in February (2010) with only 26% and the highest in February (2011), 87% (Fig. 6.5), similar as $f_{\text{macro_bac}}$. As discussed above, the differences among years can be attributed to the start of the bloom. Even though phytoplankton are considered the primary food source for zooplankton, almost half of the zooplankton carbon was derived from macrophytes. In most months, $f_{\text{macro_bac}}$ and $f_{\text{macro_zoo}}$ were rather similar; supporting the idea of bacterioplankton mediated carbon flow from macrophytes to zooplankton (Fig. 6.5). The zooplankton community was dominated by copepods, so direct consumption of bacterioplankton is not expected. However, by selective grazing on protists, bacterioplankton mediated carbon flow to copepods can still be important (Sanders and Wickham 1993). In marine systems, ciliates were found to support $\sim 30\%$ of daily carbon consumption of copepods (Calbet and Saiz 2005). In addition, zooplankton could have grazed directly on macrophyte derived particles, aggregates and detritus, present in seston. The second pathway is expected to be less important, because copepods are expected to select for high food quality like phytoplankton and protists that have high PUFA rather than for macrophyte detritus of low nutritional quality. In autumn (October, December) there was a strong decoupling between $f_{\text{macro_bac}}$ and $f_{\text{macro_zoo}}$ (Fig. 6.5). In those months, $f_{\text{macro_zoo}}$ was low and $\delta^{13}\text{C}$ of zooplankton in M+ and M- were rather similar (Fig. 6.3), suggesting that zooplankton grazing on phytoplankton was more important than grazing on bacterioplankton. Based on $\delta^{13}\text{C}$ signatures, we cannot distinguish consumption of detritus, bacterioplankton, or bacterivores, but we can conclude that macrophytes constituted a substantial part to the base of the food web.

The contribution of allochthonous or terrestrial carbon to bacterioplankton and zooplankton were not considered in the calculations, although a large part of POC can be derived from terrestrial carbon. Studies that looked into autochthonous vs. allochthonous contributions found substantial terrestrial support (20-40%) to zooplankton (Cole et al. 2011). In our study, the average $\delta^{13}\text{C}$ of surrounding vegetation and soil was $-28.9 \pm 2.4\%$. This is rather close to the corrected $\delta^{13}\text{C}_{\text{phyto}}$ in M+ ($-29.8 \pm 5.2\%$) and can therefore not explain the observed enrichment in bacterioplankton and zooplankton in M+.

6.4 Conclusions

Lake restoration with macrophyte planting resulted in a significant decrease of phytoplankton (mainly cyanobacteria) and bacterioplankton. The presence of macrophytes resulted in a significant enrichment in $\delta^{13}\text{C}$ of POC, zooplankton, and bacterioplankton, but not of phytoplankton. Macrophytes contributed substantially to the carbon diet of bacterioplankton and zooplankton, $\sim 50\%$ over all seasons and the other half was provided by phytoplankton. Similar macrophyte subsidies to bacterioplankton and zooplankton in most months indicated bacteria mediated carbon flows, from macrophytes via DOC and bacterioplankton to zooplankton. The trophic ($\delta^{15}\text{N}$) enrichment of copepods suggests that they were likely feeding on bacterivorous protists, rather than on bacterioplankton directly. Our results underline the importance of microbial food web mediated carbon flows seen in shallow eutrophic lakes.

Acknowledgements

We thank our colleagues from Jinan University who helped collecting field samples, and especially: Long Han, Jie Mao, Fengwen Wang, Tingting Ming and Yuanyu Bao. We thank our colleagues from the Royal Netherlands Institute for Sea Research in Yerseke: Pieter van Rijswijk, Marco Houtekamer, and Peter van Breugel for laboratory support. This study received financial support from the Darwin Center for Biogeosciences supported by the Netherlands Organization of Scientific Research (NWO) and Chinese projects (2012CB956100, U1033602, and 31000219).





CHAPTER 7



References, Summary,
Nederlandse samenvatting,
Publication list,
Dankwoord - Acknowledgements

REFERENCES

- Adolf, J. E., A. R. Place, D. K. Stoecker, and L. W. Harding. 2007. Modulation of polyunsaturated fatty acids in mixotrophic *Karodinium veneticum* (Dinophyceae) and its prey, *Storeatula major* (Cryptophyceae). *J. Phycol.* **43**: 1259-1270.
- Ahlgren, G., I. B. Gustafsson, and M. Boberg. 1992. Fatty-acid content and chemical-composition of fresh-water microalgae. *J. Phycol.* **28**: 37-50.
- Allgaier, M., U. Riebesell, M. Vogt, R. Thyrhaug, and H. P. Grossart. 2008. Coupling of heterotrophic bacteria to phytoplankton bloom development at different $p\text{CO}_2$ levels: a mesocosm study. *Biogeosciences* **5**: 1007-1022.
- Arrigo, K. R. 2007. Carbon cycle - Marine manipulations. *Nature* **450**: 491-492.
- Azam, F., T. Fenchel, J. G. Field, J. S. Gray, L. A. Meyerreil, and F. Thingstad. 1983. The ecological role of water-column microbes in the sea. *Mar. Ecol.-Prog. Ser.* **10**: 257-263.
- Bade, D. L., M. L. Pace, J. J. Cole, and S. R. Carpenter. 2006. Can algal photosynthetic inorganic carbon isotope fractionation be predicted in lakes using existing models? *Aquat. Sci.* **68**: 142-153.
- Baines, S. B., and M. L. Pace. 1991. The production of dissolved organic-matter by phytoplankton and its importance to bacteria-patterns across marine and fresh-water systems. *Limnol. Oceanogr.* **36**: 1078-1090.
- Beardall, J., and M. Giordano. 2002. Ecological implications of microalgal and cyanobacterial CO_2 concentrating mechanisms, and their regulation. *Functional Plant Biology* **29**: 335-347.
- Bellerby, R. G. J. and others 2008. Marine ecosystem community carbon and nutrient uptake stoichiometry under varying ocean acidification during the PeECE III experiment. *Biogeosciences* **5**: 1517-1527.
- Bellerby, R. G. J., and others 2012. Marine carbonate system evolution during the EPOCA Arctic pelagic ecosystem experiment in the context of simulated future Arctic ocean acidification. submitted to the special issue in BGD.
- Biddanda, B. A., and L. R. Pomeroy. 1988. Microbial aggregation and degradation of phytoplankton-derived detritus in seawater. 1. Microbial succession. *Mar. Ecol.-Prog. Ser.* **42**: 79-88.
- Biddanda, B., M. Ogdahl, and J. Cotner. 2001. Dominance of bacterial metabolism in oligotrophic relative to eutrophic waters. *Limnol. Oceanogr.* **46**: 730-739.
- Bidigare, R. R. and others 1997. Consistent fractionation of ^{13}C in nature and in the laboratory: Growth-rate effects in some haptophyte algae. *Glob. Biogeochem. Cycle* **11**: 279-292.
- Bligh, E. G., and W. J. Dyer. 1959. A rapid method of total lipid extraction and purification. *Can. J. Biochem. Physiol.* **37**: 911-917.
- Boll, T. and others 2012. Changes in benthic macroinvertebrate abundance and lake isotope (C, N) signals following biomanipulation: an 18-year study in shallow Lake Vaeng, Denmark. *Hydrobiologia*: 1-11.
- Bontes, B. M., R. Pel, B. W. Ibelings, H. T. S. Boschker, J. J. Middelburg, and E. Van Donk. 2006. The effects of biomanipulation on the biogeochemistry, carbon isotopic composition and pelagic food web relations of a shallow lake. *Biogeosciences* **3**: 69-83.
- Boschker, H. T. S. and others 1998. Direct linking of microbial populations to specific biogeochemical processes by ^{13}C -labeling of biomarkers. *Nature* **392**: 801-805.

- Boschker, H. T. S., and J. J. Middelburg. 2002. Stable isotopes and biomarkers in microbial ecology. *FEMS Microbiol. Ecol.* **40**: 85-95.
- Boschker, H. T. S., T. C. W. Moerdijk-Poortvliet, P. Van Breugel, M. Houtekamer, and J.J. Middelburg. 2008. A versatile method for stable carbon isotope analysis of carbohydrates by high-performance liquid chromatography/isotope ratio mass spectrometry. *Rapid Commun. Mass Spectrom.* **22**: 3902-3908.
- Bouillon, S., and H. T. S. Boschker. 2006. Bacterial carbon sources in coastal sediments: a cross-system analysis based on stable isotope data of biomarkers. *Biogeosciences* **3**: 175-185.
- Bowes, G., and M. E. Salvucci. 1989. Plasticity in the photosynthetic carbon metabolism of submersed aquatic macrophytes. *Aquatic Botany* **34**: 233-266.
- Bratbak, G., and T. F. Thingstad. 1985. Phytoplankton-bacteria interactions – an apparent paradox – analysis of a model system with both competition and commensalism. *Mar. Ecol.-Prog. Ser.* **25**: 23-30.
- Brett, M. T., D. C. Muller-Navarra, A. P. Ballantyne, J. L. Ravet, and C. R. Goldman. 2006. *Daphnia* fatty acid composition reflects that of their diet. *Limnol. and Oceanogr.* **51**: 2428-2437.
- Brett, M. T., M. J. Kainz, S. J. Taipale, and H. Seshan. 2009. Phytoplankton, not allochthonous carbon, sustains herbivorous zooplankton production. *Proc. Natl. Acad. Sci. U. S. A.* **106**: 21197-21201.
- Brinchiversen, J., and G. M. King. 1990. Effects of substrate concentration, growth-state, and oxygen availability on relationships among bacterial carbon, nitrogen and phospholipid phosphorus-content. *FEMS Microbiol. Ecol.* **74**: 345-355.
- Brussaard, C. P. D. 2004. Viral Control of Phytoplankton Populations—a Review. *J. Euk. Microbiol.* **51**: 125-138.
- Brussaard, C. P. D. and others 2012. Ocean acidification impact on Arctic microbial dynamics, submitted to the special issue in BGD.
- Buesseler, K. O. and others 2007. An assessment of the use of sediment traps for estimating upper ocean particle fluxes. *J. Mar. Res.* **65**: 345-416.
- Burke, R. A., M. Molina, J. E. Cox, L. J. Osher, and M. C. Piccolo. 2003. Stable Carbon Isotope Ratio and Composition of Microbial Fatty Acids in Tropical Soils. *J. Environ. Qual.* **32**: 198-206.
- Calbet, A., and E. Saiz. 2005. The ciliate-copepod link in marine ecosystems. *Aquat. Microb. Ecol.* **38**: 157-167.
- Caldeira, K., and M. E. Wickett. 2003. Anthropogenic carbon and ocean pH. *Nature* **425**: 365-365.
- Carlson, R. E. 1977. A Trophic State Index for Lakes. *Limnol. and Oceanogr.* **22**: 361-369.
- Carpenter, S. R., N. F. Caraco, D. L. Correll, R. W. Howarth, A. N. Sharpley, and V. H. Smith. 1998. Nonpoint pollution of surface waters with phosphorus and nitrogen. *Ecological Applications* **8**: 559-568.
- Carpenter, S. R. and others 2005. Ecosystem subsidies: Terrestrial support of aquatic food webs from ¹³C addition to contrasting lakes. *Ecology* **86**: 2737-2750.
- Chen, Y. W., B. Q. Qin, K. Teubner, and M. T. Dokulil. 2003. Long-term dynamics of phytoplankton assemblages: Microcystis-domination in Lake Taihu, a large shallow lake in China. *J. Plankton Res.* **25**: 445-453.
- Chen, L., X.-F. Zhang, and Z.-W. Liu. 2010. The Response of a Phytoplankton Community to Ecosystem Restoration in Huizhou West Lake. *Journal of Wuhan Botanical Research* **28**:453–459 (in Chinese with an English abstract).

- Christoffersen, K., B. Riemann, L. Hansen, A. Klysner, and H. Sørensen. 1990. Qualitative importance of the microbial loop and plankton community structure in a eutrophic lake during a bloom of cyanobacteria. *Microb. Ecol.* **20**: 253-272.
- Coffin, R. B., B. Fry, B. J. Peterson, and R. T. Wright. 1989. Carbon Isotopic Compositions of Estuarine Bacteria. *Limnol. and Oceanogr.* **34**: 1305-1310.
- Coffin, R. B., D. Velinsky, R. Devereux, W. Price, and L. Cifuentes. 1990. Stable carbon isotope analysis of nucleic acids to trace sources of dissolved substrates used by estuarine bacteria. *Appl. Environ. Microbiol.* **56**: 2012-2020.
- Cole, J. J., S. Findlay, and M. L. Pace. 1988. Bacterial production in fresh and saltwater ecosystems – a cross-system overview. *Mar. Ecol.-Prog. Ser.* **43**: 1-10.
- Cole, J. J., N. F. Caraco, G. W. Kling, and T. K. Kratz. 1994. Carbon Dioxide Super-saturation in the Surface Waters of Lakes. *Science* **265**: 1568-1570.
- Cole, J. J. 1999. Aquatic microbiology for ecosystem scientists: New and recycled paradigms in ecological microbiology. *Ecosystems* **2**: 215-225.
- Cole, J. J., S. R. Carpenter, J. F. Kitchell, and M. L. Pace. 2002. Pathways of organic carbon utilization in small lakes: Results from a whole-lake ¹³C addition and coupled model. *Limnol. and Oceanogr.* **47**: 1664-1675.
- Cole, J. J., S. R. Carpenter, M. L. Pace, M. C. Van De Bogert, J. L. Kitchell, and J. R. Hodgson. 2006. Differential support of lake food webs by three types of terrestrial organic carbon. *Ecol. Lett.* **9**: 558-568.
- Cole, J. J. and others 2007. Plumbing the global carbon cycle: Integrating inland waters into the terrestrial carbon budget. *Ecosystems* **10**: 171-184.
- Cole, J. J., S. R. Carpenter, J. Kitchell, M. L. Pace, C. T. Solomon, and B. Weidel. 2011. Strong evidence for terrestrial support of zooplankton in small lakes based on stable isotopes of carbon, nitrogen, and hydrogen. *Proc. Natl. Acad. Sci. U. S. A.* **108**: 1975-1980.
- Cotner, J. B., and B. A. Biddanda. 2002. Small players, large role: Microbial influence on biogeochemical processes in pelagic aquatic ecosystems. *Ecosystems* **5**: 105-121.
- Czerny, J. and others 2012A: Element budgets in an Arctic mesocosm CO₂ perturbation study, submitted to the special issue in BGD.
- Czerny, J., K. G. Schulz, A. Ludwig, U. Riebesell. 2012B. A simple method for gas exchange measurements in mesocosms and its application in mesocosm carbon budget calculations, submitted to the special issue in BGD.
- Cranwell, P. A., M. E. Creighton, and G. H. M. Jaworski. 1988. Lipids of four species of freshwater chrysophytes. *Phytochemistry* **27**: 1053-1059.
- Dalsgaard, J., M. St John, G. Kattner, D. Muller-Navarra, and W. Hagen. 2003. Fatty acid trophic markers in the pelagic marine environment, p. 225-340. *Advances in Marine Biology*, Vol 46. *Advances in Marine Biology*. Academic Press Ltd.
- De Kluijver, A., K. Soetaert, K. G. Schulz, U. Riebesell, R. G. J. Bellerby, and J. J. Middelburg. 2010. Phytoplankton-bacteria coupling under elevated CO₂ levels: a stable isotope labeling study. *Biogeosciences* **7**: 3783-3797.
- De Kluijver, A., J. Yu, M. Houtekamer, J. J. Middelburg, and Z. Liu. 2012. Cyanobacteria as a carbon source for zooplankton in eutrophic Lake Taihu, China, measured by ¹³C labeling and fatty acid biomarkers. *Limnol. Oceanogr.* **57**: 1245-1254.
- Debernardi, R., and Giussanig. 1990. Are blue-green algae a suitable food for zooplankton – an overview. *Hydrobiologia* **200**: 29-41.
- Del Giorgio, P. A., and R. H. Peters. 1994. Patterns in Planktonic P:R Ratios in Lakes:

- Influence of Lake Trophy and Dissolved Organic Carbon. *Limnol. and Oceanogr.* **39**: 772-787.
- Del Giorgio, P. A., and J. M. Gasol. 1995. Biomass Distribution in Freshwater Plankton Communities. *The Am. Nat.* **146**: 135-152.
- Del Giorgio, P. A., and R. L. France. 1996. Ecosystem-specific patterns in the relationship between zooplankton and POM or microplankton $\delta^{13}\text{C}$. *Limnol. Oceanogr.* **41**: 359-365.
- Del Giorgio, P. A., J. J. Cole, and A. Cimleris. 1997. Respiration rates in bacteria exceed phytoplankton production in unproductive aquatic systems. *Nature* **385**: 148-151.
- Del Giorgio, P. A., and J. J. Cole. 1998. Bacterial growth efficiency in natural aquatic systems. *Annu. Rev. Ecol. Syst.* **29**: 503-541.
- Delille, B. and others 2005. Response of primary production and calcification to changes of $p\text{CO}_2$ during experimental blooms of the coccolithophorid *Emiliania huxleyi*. *Glob. Biogeochem. Cycle* **19**.
- Demott, W. R. 1982. Feeding selectivities and relative ingestion rates of *Daphnia* and *Bosmina*. *Limnol. Oceanogr.* **27**: 518-527.
- Demott, W. R. 1988. Discrimination between algae and detritus by freshwater and marine zooplankton. *Bull. Mar. Sci.* **43**: 486-499.
- Demott, W. R., R. D. Gulati, and E. V. Donk. 2001. *Daphnia* food limitation in three hypereutrophic Dutch lakes: Evidence for exclusion of large-bodied species by interfering filaments of cyanobacteria. *Limnol. Oceanogr.* **46**: 2054-2060.
- Demott, W. R., and W. C. Kerfoot. 1982. Competition among cladocerans: Nature of the interaction between *Bosmina* and *Daphnia*. *Ecology* **63**: 1949-1966.
- DeNiro, M. J., and S. Epstein. 1978. Influence of diet on the distribution of carbon isotopes in animals. *Geochim. Cosmochim. Acta* **42**: 495-506.
- DeNiro, M. J., and S. Epstein. 1981. Influence of diet on the distribution of nitrogen isotopes in animals. *Geochim. Cosmochim. Acta* **45**: 341-351.
- Dijkman, N., H. Boschker, J. Middelburg, and J. Kromkamp. 2009. Group-specific primary production based on stable-isotope labeling of phospholipid-derived fatty acids. *Limnol. Oceanogr. Meth.* **7**: 612-625.
- Dijkman, N. A., and J. C. Kromkamp. 2006. Phospholipid-derived fatty acids as chemotaxonomic markers for phytoplankton: application for inferring phytoplankton composition. *Mar. Ecol.-Prog. Ser.* **324**: 113-125.
- Duarte, C. M. and others 2005. Experimental test of bacteria-phytoplankton coupling in the Southern Ocean. *Limnol. Oceanogr.* **50**: 1844-1854.
- Ducklow, H., C. Carlson, and W. Smith. 1999. Bacterial growth in experimental plankton assemblages and seawater cultures from the *Phaeocystis antarctica* bloom in the Ross Sea, Antarctica. *Aquat. Microb. Ecol.* **19**: 215-227.
- Egge, J. K. and others 2009. Primary production during nutrient-induced blooms at elevated CO_2 concentrations. *Biogeosciences* **6**: 877-885.
- Elser, J. J. and C. R. Goldman. 1991. Zooplankton effects on phytoplankton in lakes of contrasting trophic status. *Limnol. Oceanogr.* **36**(1): 64-90.
- Engel, A. 2002. Direct relationship between CO_2 uptake and transparent exopolymer particles production in natural phytoplankton. *J. Plankton Res.* **24**: 49-53.
- Engel, A., S. Thoms, U. Riebesell, E. Rochelle-Newall, and I. Zondervan. 2004A. Polysaccharide aggregation as a potential sink of marine dissolved organic carbon. *Nature* **428**: 929-932.

REFERENCES

- Engel, A. and others 2004B. Transparent exopolymer particles and dissolved organic carbon production by *Emiliana huxleyi* exposed to different CO₂ concentrations: a mesocosm experiment. *Aquat. Microb. Ecol.* **34**: 93-104.
- Engel, A. and others 2005. Testing the direct effect of CO₂ concentration on a bloom of the coccolithophorid *Emiliana huxleyi* in mesocosm experiments. *Limnol. Oceanogr.* **50**: 493-507.
- Engel, A., C. Borchard, J. Piontek, K. G. Schulz, R. G. J. Bellerby. 2012. CO₂ increases ¹⁴C-primary production in an Arctic plankton community, *Biogeosciences Discuss.* **9**: 10285-10330, doi:10.5194/bgd-9-10285-2012.
- Feng, Y. Y. and others 2009. Effects of increased pCO₂ and temperature on the North Atlantic spring bloom. I. The phytoplankton community and biogeochemical response. *Mar. Ecol.-Prog. Ser.* **388**: 13-25.
- Field, C. B., M. J. Behrenfeld, J. T. Randerson, and P. Falkowski. 1998. Primary production of the biosphere: Integrating terrestrial and oceanic Components. *Science* **281**: 237-240.
- Findlay, S., L. Carlough, M. T. Crocker, H. K. Gill, J. L. Meyer, and P. J. Smith. 1986. Bacterial growth on macrophyte leachate and fate of bacterial production. *Limnol. Oceanogr.* **31**: 1335-1341.
- Fiorini, S., J.-P. Gattuso, P. Van Rijswijk, and J. Middelburg. 2010. Coccolithophores lipid and carbon isotope composition and their variability related to changes in seawater carbonate chemistry. *J. Exp. Mar. Biol. Ecol.* **394**: 74-85.
- Fogg, G. E. 1983. The ecological significance of extracellular products of photosynthesis. *Bot. Marina* **26**: 3-14.
- Fry, B. 2006. *Stable isotope ecology*. Springer.
- Fulton, R. S., and H. W. Paerl. 1987. Effects of colonial morphology on zooplankton utilization of algal resources during blue-green algal (*Microcystis aeruginosa*) blooms. *Limnol. Oceanogr.* **32**: 634-644.
- Fulton, R. S., and H. W. Paerl. 1988. Effects of the blue-green alga *Microcystis aeruginosa* on zooplankton competitive relations. *Oecologia* **76**: 383-389.
- Gasol, J. M., and C. M. Duarte. 2000. Comparative analyses in aquatic microbial ecology: how far do they go? *FEMS Microbiol. Ecol.* **31**: 99-106.
- Gelman, A. 1996. Inference and monitoring convergence. Markov chain Monte Carlo in practice: 131-143.
- Ghadouani, A., B. Pinel-Alloul, and E. E. Prepas. 2006. Could increased cyanobacterial biomass following forest harvesting cause a reduction in zooplankton body size structure? *Can. J. Fish. Aquat. Sci.* **63**: 2308-2317.
- Gillikin, D. P., and S. Bouillon. 2007. Determination of δ¹⁸O of water and δ¹³C of dissolved inorganic carbon using a simple modification of an elemental analyser - isotope ratio mass spectrometer: an evaluation. *Rapid Commun. Mass Spectrom.* **21**: 1475-1478.
- Giordano, M., J. Beardall, and J. A. Raven. 2005. CO₂ concentrating mechanisms in algae: Mechanisms, environmental modulation, and evolution. *Annu. Rev. Plant Biol.* **56**: 99-131.
- Gliwicz, Z. 1969. Studies on the feeding of pelagic zooplankton in lakes with varying trophy. *Ekol. pol* **17**: 663-708.
- Gophen, M., B. Z. Cavari, and T. Berman. 1974. Zooplankton feeding on differentially labeled algae and bacteria. *Nature* **247**: 393-394.

- Grossart, H. P., M. Allgaier, U. Passow, and U. Riebesell. 2006. Testing the effect of CO₂ concentration on the dynamics of marine heterotrophic bacterioplankton. *Limnol. Oceanogr.* **51**: 1-11.
- Gu, B. 2009. Variations and controls of nitrogen stable isotopes in particulate organic matter of lakes. *Oecologia* **160**: 421-431.
- Gugger, M. and others 2002. Cellular fatty acids as chemotaxonomic markers of the general *Anabaena*, *Aphanizomenon*, *Microcystis*, *Nostoc* and *Planktothrix* (cyanobacteria). *Int. J. Syst. Evol. Microbiol.* **52**: 1007-1015.
- Gulati, R. D., M. Bronkhorst, and E. Van Donk. 2001. Feeding in *Daphnia galeata* on *Oscillatoria limnetica* and on detritus derived from it. *J. Plankton Res.* **23**: 705-718.
- Hamilton, S. K., J. L. Tank, D. F. Raikow, E. R. Siler, N. J. Dorn, and N. E. Leonard. 2004. The role of instream vs allochthonous N in stream food webs: modeling the results of an isotope addition experiment. *J. N. Am. Benthol. Soc.* **23**: 429-448.
- Hanazato, T., and M. Yasuno. 1987. Evaluation of *Microcystis* as food for zooplankton in a eutrophic lake. *Hydrobiologia* **144**: 251-259.
- Haney, J. F. 1987. Field studies on zooplankton-cyanobacteria interactions. *N. Z. J. Mar. Freshw. Res.* **21**: 467-475.
- Hansen, L., G. F. Krog, and M. Søndergaard. 1986. Decomposition of lake phytoplankton. 1. Dynamics of short-term decomposition. *Oikos* **46**: 37-44.
- Hanson, P. C., D. L. Bade, S. R. Carpenter, and T. K. Kratz. 2003. Lake metabolism: Relationships with dissolved organic carbon and phosphorus. *Limnol. Oceanogr.* **48**: 1112-1119.
- Hansson, L. A. and others 1998. Biomanipulation as an application of food-chain theory: Constraints, synthesis, and recommendations for temperate lakes. *Ecosystems* **1**: 558-574.
- Hayes, J. M. 2001. Fractionation of carbon and hydrogen isotopes in biosynthetic processes, p. 225-277. *Stable Isotope Geochemistry. Reviews in Mineralogy & Geochemistry. Mineralogical Soc America.*
- Hayes, J. M., K. H. Freeman, B. N. Popp, and C. H. Hoham. 1990. Compound-specific isotopic analyses – a novel tool for reconstruction of ancient biogeochemical processes. *Org. Geochem.* **16**: 1115-1128.
- Hessen, D. O., T. Andersen, and A. Lyche. 1990. Carbon metabolism in a humic lake: Pool sizes and cycling through zooplankton. *Limnol. Oceanogr.* **35**: 84-99.
- Hofmann, A. F., K. Soetaert, J. J. Middelburg, F. J. R. Meysman. 2010. AquaEnv - an Aquatic acid-base modeling Environment in R. R-package version 1.
- Huss, A. A., and J. D. Wehr. 2004. Strong indirect effects of a submersed aquatic macrophyte, *Vallisneria americana*, on bacterioplankton densities in a mesotrophic lake. *Microb. Ecol.* **47**: 305-315.
- Intergovernmental Panel on Climate Change (IPCC). 2007. *Climate Change 2007: The physical science basis. Contribution of working group I to the fourth assessment report of the Intergovernmental Panel on Climate Change.* edited by S. Solomon et al., Cambridge Univ. Press, Cambridge, New York.
- Jones, R. I., J. Grey, D. Sleep, and L. Arvola. 1999. Stable isotope analysis of zooplankton carbon nutrition in humic lakes. *Oikos*: 97-104.

- Jurgens, K., and E. Jeppesen. 1998. Cascading effects on microbial food web structure in a dense macrophyte bed, p. 262-273. *In* E. S. M. S. M. C. K. Jeppesen [ed.], Structuring role of submerged macrophytes in lakes. Ecological Studies : Analysis and Synthesis.
- Kaneda, T. 1991. Iso-fatty and anteiso-fatty acids in bacteria – biosynthesis, function, and taxonomic significance. *Microbiol. Rev.* **55**: 288-302.
- Karlsson, J., A. Jonsson, M. Meili, and M. Jansson. 2004. $\delta^{15}\text{N}$ of zooplankton species in subarctic lakes in northern Sweden: effects of diet and trophic fractionation. *Freshw. Biol.* **49**: 526-534.
- Karlsson, J., D. Lymer, K. Vrede, and M. Jansson. 2007. Differences in efficiency of carbon transfer from dissolved organic carbon to two zooplankton groups: an enclosure experiment in an oligotrophic lake. *Aquat. Sci.* **69**: 108-114.
- Karlsson, J. and others 2012. Terrestrial organic matter support of lake food webs: Evidence from lake metabolism and stable hydrogen isotopes of consumers. *Limnol. oceanogr.* **57**: 1042-1048.
- Kaufman, M., R. Gradinger, B. Bluhm, and D. O'brien. 2008. Using stable isotopes to assess carbon and nitrogen turnover in the Arctic sympagic amphipod *Onisimus litoralis*. *Oecologia* **158**: 11-22.
- Kim, I. S., S. Y. Kim, and H. W. Yu. 2009. Evaluation of methods for cyanobacterial cell lysis and toxin (Microcystin-LR) extraction using chromatographic and mass spectrometric analyses. *Environ. Eng. Res.* **14**: 250-254.
- Kirchman, D. L., H. W. Ducklow, J. J. McCarthy, and C. Garside. 1994. Biomass and nitrogen uptake by heterotrophic bacteria during the spring phytoplankton bloom in the North-Atlantic ocean. *Deep-Sea Res. Part I-Oceanogr. Res. Pap.* **41**: 879-895.
- Kirchman, D. L., X. a. G. Moran, and H. Ducklow. 2009A. Microbial growth in the polar oceans - role of temperature and potential impact of climate change. *Nat Rev Micro* **7**: 451-459.
- Kirchman, D. L., V. Hill, M. T. Cottrell, R. Gradinger, R. R. Malmstrom, and A. Parker. 2009B. Standing stocks, production, and respiration of phytoplankton and heterotrophic bacteria in the western Arctic Ocean. *Deep Sea Research Part II: Topical Studies in Oceanography* **56**: 1237-1248.
- Klein Breteler, W. C. M., N. Schogt, M. Baas, S. Schouten, and G. W. Kraay. 1999. Trophic upgrading of food quality by protozoans enhancing copepod growth: role of essential lipids. *Mar. Biol.* **135**: 191-198.
- Koshikawa, H., S. Harada, M. Watanabe, K. Sato, and K. Akehata. 1996. Relative contribution of bacterial and photosynthetic production to metazooplankton as carbon sources. *J. Plankton Res.* **18**: 2269-2281.
- Kritzberg, E. S., J. J. Cole, M. L. Pace, W. Granéli, and D. L. Bade. 2004. Autochthonous versus allochthonous carbon sources of bacteria: Results from whole-lake ^{13}C addition experiments. *Limnol. Oceanogr.* **49**: 588-596.
- Kürten, B., S. J. Painting, U. Struck, N. V. C. Polunin, and J. J. Middelburg. 2011. Tracking seasonal changes in North Sea zooplankton trophic dynamics using stable isotopes. *Biogeochem.*, doi:10.1007/s10533-011-9630-y
- Lampert, W. 1987. Laboratory studies on zooplankton-cyanobacteria interactions. *N. Z. J. Mar. Freshw. Res.* **21**: 483-490.

- Lancelot, C., and G. Billen. 1984. Activity of heterotrophic bacteria and its coupling to primary production during the spring phytoplankton bloom in the southern bight of the North-Sea. *Limnol. Oceanogr.* **29**: 721-730.
- Larsson, U., and A. Hagstrom. 1979. Phytoplankton exudate release as an energy-source for the growth of pelagic bacteria. *Mar. Biol.* **52**: 199-206.
- Laws, E. A., P. G. Falkowski, W. O. Smith, H. Ducklow, and J. J. Mccarthy. 2000. Temperature effects on export production in the open ocean. *Glob. Biogeochem. Cycle* **14**: 1231-1246.
- Laws, E. A., B. N. Popp, R. R. Bidigare, M. C. Kennicutt, and S. A. Macko. 1995. Dependence of phytoplankton carbon isotopic composition on growth-rate and $[\text{CO}_2]$ (aq) – theoretical considerations and experimental results. *Geochim. Cosmochim. Acta* **59**: 1131-1138.
- Lee, S., and J. A. Fuhrman. 1987. Relationships between biovolume and biomass of naturally derived marine bacterioplankton. *Appl. Environ. Microbiol.* **53**: 1298-1303.
- Legendre, L., and F. Rassoulzadegan. 1995. Plankton and nutrient dynamics in marine waters. *Ophelia* **41**: 153-172.
- Lennon, J. T., A. M. Faiia, X. H. Feng, and K. L. Cottingham. 2006. Relative importance of CO_2 recycling and CH_4 pathways in lake food webs along a dissolved organic carbon gradient. *Limnol. Oceanogr.* **51**: 1602-1613.
- Leu, E., M. Daase, K. G. Schulz, A. Stuhr, and U. Riebesell. 2012. Effect of ocean acidification on the fatty acid composition of a natural plankton community, *Biogeosciences Discuss.* **9**: 8173-8197, doi:10.5194/bgd-9-8173-2012
- Li, C. H., Z. Tan, W. Z. Zhu & J. J. Peng, 2007. Eutrophication and restoration of Huizhou Xihu Lake (in Chinese). Guangdong Science & Technology Publishing Corp. pp.65-69.
- Lochte, K., P. K. Bjornsen, H. Giesenhagen, and A. Weber. 1997. Bacterial standing stock and production and their relation to phytoplankton in the Southern Ocean. *Deep-Sea Res. Part II-Top. Stud. Oceanogr.* **44**: 321-340.
- Lyche, A., T. Andersen, K. Christoffersen, D. O. Hessen, P. H. B. Hansen, and A. Klynsner. 1996. Mesocosm tracer studies .2. The fate of primary production and the role of consumers in the pelagic carbon cycle of a mesotrophic lake. *Limnol. Oceanogr.* **41**: 475-487.
- Maier-Reimer, E., U. Mikolajewicz, and A. Winguth. 1996. Future ocean uptake of CO_2 : interaction between ocean circulation and biology. *Climate Dynamics* **12**: 711-722.
- Malve, O., M. Laine, and H. Haario. 2005. Estimation of winter respiration rates and prediction of oxygen regime in a lake using Bayesian inference. *Ecol. Model.* **182**: 183-197.
- Malve, O., M. Laine, H. Haario, T. Kirkkala, and J. Sarvala. 2007. Bayesian modeling of algal mass occurrences - using adaptive MCMC methods with a lake water quality model. *Environ. Modell. Softw.* **22**: 966-977.
- Mann, K. H. 1988. Production and use of detritus in various fresh-water, estuarine, and coastal marine ecosystems. *Limnol. Oceanogr.* **33**: 910-930.
- Marty, J., and D. Planas. 2008. Comparison of methods to determine algal $\delta^{13}\text{C}$ in freshwater. *Limnol. Oceanogr. Meth.* **6**: 51-63.

REFERENCES

- Mccallister, S. L., and P. A. Del Giorgio. 2008. Direct measurement of the $\delta^{13}\text{C}$ signature of carbon respired by bacteria in lakes: Linkages to potential carbon sources, ecosystem baseline metabolism, and CO_2 fluxes. *Limnol. Oceanogr.* **53**: 1204-1216.
- Middelburg, J. J., C. Barranguet, H. T. S. Boschker, P. M. J. Herman, T. Moens, and C. H. R. Heip. 2000. The fate of intertidal microphytobenthos carbon: An in situ ^{13}C -labeling study. *Limnol. Oceanogr.* **45**: 1224-1234.
- Minagawa, M., and E. Wada. 1984. Stepwise enrichment of ^{15}N along food chains: Further evidence and the relation between $\delta^{15}\text{N}$ and animal age. *Geochim. Cosmochim. Acta* **48**: 1135-1140.
- Müller-Navarra, D. C., M. T. Brett, A. M. Liston, and C. R. Goldman. 2000. A highly unsaturated fatty acid predicts carbon transfer between primary producers and consumers. *Nature* **403**: 74-77.
- Niehoff, B., N. Knüppel, M. Daase, J. Czerny, and T. Boxhammer. 2012. Mesozooplankton community development at elevated CO_2 concentrations: Results from a mesocosm experiment in a high Arctic fjord. *Biogeosciences Discuss.* **9**: 11479-11515, doi:10.5194/bgd-9-11479-2012
- Nieuwenhuize, J., Y. E. M. Maas, and J. J. Middelburg. 1994. Rapid analysis of organic carbon and nitrogen in particulate materials. *Mar. Chem.* **45**: 217-224.
- Norrman, B., U. L. Zweifel, C. S. Hopkinson, and B. Fry. 1995. Production and utilization of dissolved organic carbon during an experimental diatom bloom. *Limnol. Oceanogr.* **40**: 898-907.
- Osburn, C. L., and G. St-Jean. 2007. The use of wet chemical oxidation with high-amplification isotope ratio mass spectrometry (WCO-IRMS) to measure stable isotope values of dissolved organic carbon in seawater. *Limnol. Oceanogr. Meth.* **5**: 296-308.
- Pace, M. L. and others 2007. Does terrestrial organic carbon subsidize the planktonic food web in a clear-water lake? *Limnol. Oceanogr.* **52**: 2177-2189.
- Pace, M. L., K. G. Porter, and Y. S. Feig. 1983. Species- and age-specific differences in bacterial resource utilization by two co-occurring cladocerans. *Ecology* **64**: 1145-1156.
- Paerl, H., R. Fulton 3rd, P. Moisaner, and J. Dyble. 2001. Harmful freshwater algal blooms, with an emphasis on cyanobacteria. *TheScientificWorldJournal* **1**: 76.
- Paerl, H. W., and J. Huisman. 2008. Blooms like it hot. *Science* **320**: 57-58.
- Paulino, A. I., J. K. Egge, and A. Larsen. 2008. Effects of increased atmospheric CO_2 on small and intermediate sized osmotrophs during a nutrient induced phytoplankton bloom. *Biogeosciences* **5**: 739-748.
- Peduzzi, P., and M. G. Weinbauer. 1993. Effect of concentrating the virus-rich 2-200-nm size fraction of seawater on the formation of algal flocs (marine snow). *Limnol. Oceanogr.* **38**: 1562-1565.
- Pel, R., H. Hoogveld, and V. Floris. 2003. Using the hidden isotopic heterogeneity in phyto- and zooplankton to unmask disparity in trophic carbon transfer. *Limnology and Oceanography* **48**: 2200-2207.
- Penhale, P. A., and W. O. Smith, Jr. 1977. Excretion of dissolved organic carbon by eelgrass (*Zostera marina*) and its epiphytes. *Limnol. Oceanogr.* **22**: 400-407.
- Peterson, B. J., J. E. Hobbie, and J. F. Haney. 1978. *Daphnia* grazing on natural bacteria. *Limnol. Oceanogr.* **23**: 1039-1044.

- Phillips, D. L., and J. W. Gregg. 2003. Source partitioning using stable isotopes: coping with too many sources. *Oecologia* **136**: 261-269.
- Piontek, J., C. Borchard, M. Sperling, K. G. Schulz, U. Riebesell, and A. Engel. 2012. Response of bacterioplankton activity in an Arctic fjord system to elevated $p\text{CO}_2$: results from a mesocosm perturbation study. *Biogeosciences Discuss.* **9**: 10467-10511, doi:10.5194/bgd-9-10467-2012.
- Popp, B. N., E. A. Laws, R. R. Bidigare, J. E. Dore, K. L. Hanson, and S. G. Wakeham. 1998. Effect of phytoplankton cell geometry on carbon isotopic fractionation. *Geochim. Cosmochim. Acta* **62**: 69-77.
- Porter, K. G., Y. S. Feig, and E. F. Vetter. 1983. Morphology, flow regimes, and filtering rates of *Daphnia*, *Ceriodaphnia*, and *Bosmina* fed natural bacteria. *Oecologia* **58**: 156-163.
- Press, W., S. Teukolsky, W. Vetterling, and B. Flannery. 2007. Numerical recipes: the art of scientific computing. Cambridge Univ Pr.
- Qin, B., G. Zhu, G. Gao, Y. Zhang, W. Li, H. W. Paerl and W. W. Carmichael. 2010. A drinking water crisis in Lake Taihu, China: linkage to climatic variability and lake management. *Environ Manage.* **45**:105-112.
- R Development Core Team (2011). R: A language and environment for statistical computing. R Foundation for Statistical Computing, Vienna, Austria. ISBN 3-900051-07-0, URL <http://www.R-project.org/>.
- Riebesell, U., D. A. Wolfgladow, and V. Smetacek. 1993. Carbon-dioxide limitation of marine-phytoplankton growth-rates. *Nature* **361**: 249-251.
- Riebesell, U., A. T. Revill, D. G. Holdsworth, and J. K. Volkman. 2000. The effects of varying CO_2 concentration on lipid composition and carbon isotope fractionation in *Emiliania huxleyi*. *Geochim. Cosmochim. Acta* **64**: 4179-4192.
- Riebesell, U. and others 2007. Enhanced biological carbon consumption in a high CO_2 ocean. *Nature* **450**: 545-549.
- Riebesell, U., R. G. J. Bellerby, H. P. Grossart, and F. Thingstad. 2008. Mesocosm CO_2 perturbation studies: from organism to community level. *Biogeosciences* **5**: 1157-1164.
- Riebesell, U., A. Kortzinger, and A. Oschlies. 2009. Sensitivities of marine carbon fluxes to ocean change. *Proc. Natl. Acad. Sci. U. S. A.* **106**: 20602-20609.
- Riebesell, U. and P. D. Tortel. 2011. Effects of Ocean Acidification on Pelagic Organisms and Ecosystems, p 99-121. *In* J. Gattuso and L. Hansson [eds.] *Ocean Acidification*, Oxford University Press.
- Rivkin, R. B., and L. Legendre. 2001. Biogenic carbon cycling in the upper ocean: Effects of microbial respiration. *Science* **291**: 2398-2400.
- Rokkan Iversen, K., and L. Seuthe. 2010. Seasonal microbial processes in a high-latitude fjord (Kongsfjorden, Svalbard): I. Heterotrophic bacteria, picoplankton and nanoflagellates. *Polar Biol.*: 1-19.
- Rooney, N., and J. Kalff. 2003. Interactions among epilimnetic phosphorus, phytoplankton biomass and bacterioplankton metabolism in lakes of varying submerged macrophyte cover. *Hydrobiologia* **501**: 75-81.
- Rost, B., I. Zondervan, and D. Wolf-Gladrow. 2008. Sensitivity of phytoplankton to future changes in ocean carbonate chemistry: current knowledge, contradictions and research directions. *Marine Ecology Progress Series* **373**: 227-237.
- Sabine, C. L. and others 2004. The oceanic sink for anthropogenic CO_2 . *Science* **305**: 367-371.

- Sanders, R. W., K. G. Porter, S. J. Bennett, and A. E. Debiase. 1989. Seasonal patterns of bacterivory by flagellates, ciliates, rotifers, and cladocerans in a freshwater planktonic community. *Limnol. Oceanogr.* **34**: 673-687.
- Sanders, R. W., and S. A. Wickham. 1993. Planktonic protozoa and metazoa: predation, food quality and population control. *Aquat. Microb. Ecol.* **7**: 197-223.
- Scheffer, M., S. H. Hosper, M. L. Meijer, B. Moss, and E. Jeppesen. 1993. Alternative equilibria in shallow lakes. *TREE* **8**: 275-279.
- Schindler, D. E., S. R. Carpenter, J. J. Cole, J. F. Kitchell, and M. L. Pace. 1997. Influence of food web structure on carbon exchange between lakes and the atmosphere. *Science* **277**: 248-251.
- Schouten, S. and others 1998. Biosynthetic effects on the stable carbon isotopic compositions of algal lipids: Implications for deciphering the carbon isotopic biomarker record. *Geochim. Cosmochim. Acta* **62**: 1397-1406.
- Schulz, K. G. and others 2008. Build-up and decline of organic matter during PeECE III. *Biogeosciences* **5**: 707-718.
- Schulz, K. G. and others 2012. Temporal biomass dynamics of an Arctic plankton bloom in response to increasing levels of atmospheric carbon dioxide, submitted to the special issue in BGD.
- Shapiro, J., V. A. Lamarra, and M. Lynch. 1975. Biomanipulation: an ecosystem approach to lake restoration.
- Smith, F. A., and N. A. Walker. 1980. Photosynthesis by aquatic plants: Effects of unstirred layers in relation to assimilation of CO₂ and HCO₃⁻ and to carbon isotopic discrimination. *New Phytologist* **86**: 245-259.
- Soetaert, K., and P. M. J. Herman. 2009. A practical guide to ecological modeling: using R as a simulation platform. Springer Verlag.
- Soetaert, K., and T. Petzoldt. 2009. FME: A Flexible Modeling Environment for inverse modeling, sensitivity, identifiability, monte carlo analysis. R package version 1.
- Soetaert, K., T. Petzoldt, and R. W. Setzer. 2009. deSolve: General solvers for initial value problems of ordinary differential equations (ODE), partial differential equations (PDE) and differential algebraic equations (DAE). R package version 1.
- Sommaruga, R. 1995. Microbial and classical food webs: A visit to a hypertrophic lake. *FEMS Microbiol. Ecol.* **17**: 257-270.
- Sommer, U., and F. Sommer. 2006. Cladocerans versus copepods: the cause of contrasting top-down controls on freshwater and marine phytoplankton. *Oecologia* **147**: 183-194.
- Søndergaard, M. 1981. Loss of inorganic and organic carbon by ¹⁴C-labeled aquatic plants. *Aquatic Botany* **10**: 33-43.
- Søndergaard, M., J. Theil-Nielsen, K. Christoffersen, L. Schlüter, and E. Jeppesen. 1998. Bacterioplankton and carbon turnover in a dense macrophyte canopy, p. 250-261. *In* E. Jeppesen, M. Søndergaard and K. Christoffersen [eds.], *Structuring Role of Submerged Macrophytes in Lakes. Ecological Studies : Analysis and Synthesis*. Springer.
- Steinacher, M., F. Joos, T. L. Frölicher, G. K. Plattner, and S. C. Doney. 2009. Imminent ocean acidification in the Arctic projected with the NCAR global coupled carbon cycle-climate model. *Biogeosciences* **6**: 515-533.
- Stoll, M., K. Bakker, G. Nobbe, and R. Haese. 2001. Continuous-flow analysis of dissolved inorganic carbon content in seawater. *Anal. Chem* **73**: 4111-4116.

- Suffrian, K., P. Simonelli, J. C. Nejstgaard, S. Putzeys, Y. Carotenuto, and A. N. Antia. 2008. Microzooplankton grazing and phytoplankton growth in marine mesocosms with increased CO₂ levels. *Biogeosciences* **5**: 1145-1156.
- Taipale, S., P. Kankaala, H. Hamalainen, and R. I. Jones. 2009. Seasonal shifts in the diet of lake zooplankton revealed by phospholipid fatty acid analysis. *Freshw. Biol.* **54**: 90-104.
- Taipale, S., P. Kankaala, M. Tirola, and R. I. Jones. 2008. Whole-lake dissolved inorganic C-13 additions reveal seasonal shifts in zooplankton diet. *Ecology* **89**: 463-474.
- Tanaka, T. and others 2008. Availability of phosphate for phytoplankton and bacteria and of glucose for bacteria at different pCO₂ levels in a mesocosm study. *Biogeosciences* **5**: 669-678.
- Tanaka, T., and others. 2012. Metabolic balance of a plankton community in Arctic coastal waters in response to increased pCO₂, *Biogeosciences Discuss.* **9**: 11013-11039, doi:10.5194/bgd-9-11013-2012.
- Teece, M. A., and M. L. Fogel. 2007. Stable carbon isotope biogeochemistry of monosaccharides in aquatic organisms and terrestrial plants. *Org. Geochem.* **38**: 458-473.
- Theil-Nielsen, J., and M. Søndergaard. 1999. Production of epiphytic bacteria and bacterioplankton in three shallow lakes. *Oikos*: 283-292.
- Thingstad, T. F. and others 2008. Counterintuitive carbon-to-nutrient coupling in an Arctic pelagic ecosystem. *Nature* **455**: 387-390.
- Torréon, J. P. <http://www.com.univ-mrs.fr/IRD/atollpol/commatoll/images/ukbactp1.gif>
- Tranvik, L. J. 1992. Allochthonous dissolved organic matter as an energy source for pelagic bacteria and the concept of the microbial loop. *Hydrobiologia* **229**: 107-114.
- Van Den Meersche, K., J. J. Middelburg, K. Soetaert, P. Van Rijswijk, H. T. S. Boschker, and C. H. R. Heip. 2004. Carbon-nitrogen coupling and algal-bacterial interactions during an experimental bloom: Modeling a ¹³C tracer experiment. *Limnol. Oceanogr.* **49**: 862-878.
- Van Den Meersche, K., K. Soetaert, and J. J. Middelburg. 2008. A Bayesian compositional estimator for microbial taxonomy based on biomarkers. *Limnol. Oceanogr. Meth.* **6**: 190-199.
- Van Den Meersche, K., K. Soetaert, and J. J. Middelburg. 2011. Plankton dynamics in an estuarine plume: a mesocosm ¹³C and ¹⁵N tracer study. *Mar. Ecol.-Prog. Ser.* **429**: 29-43.
- Van Den Meersche, K., P. Van Rijswijk, K. Soetaert, and J. J. Middelburg. 2009. Autochthonous and allochthonous contributions to mesozooplankton diet in a tidal river and estuary: Integrating carbon isotope and fatty acid constraints. *Limnol. Oceanogr.* **54**: 62-74.
- Van Dongen, B. E., S. Schouten, and J. S. S. Damste. 2002. Carbon isotope variability in monosaccharides and lipids of aquatic algae and terrestrial plants. *Mar. Ecol.-Prog. Ser.* **232**: 83-92.
- Van Donk, E., and W. J. Van De Bund. 2002. Impact of submerged macrophytes including charophytes on phyto- and zooplankton communities: allelopathy versus other mechanisms. *Aquatic Botany* **72**: 261-274.
- Van Engeland, T., A. De Kluijver, K. Soetaert, F. J. R. Meysman and J. J. Middelburg. 2012. Isotope data improve the predictive capabilities of a marine biogeochemical model, *Biogeosciences Discuss.* **9**: 9453-9486, doi:10.5194/bgd-9-9453-2012.

- Van Oevelen, D., L. Moodley, K. Soetaert, and J. J. Middelburg. 2006. The trophic significance of bacterial carbon in a marine intertidal sediment: Results of an in situ stable isotope labeling study. *Limnol. Oceanogr.* **51**: 2349-2359.
- Vander Zanden, J. M., and J. B. Rasmussen. 2001. Variation in $\delta^{15}\text{N}$ and $\delta^{13}\text{C}$ trophic fractionation: Implications for aquatic food web studies. *Limnol. Oceanogr.* **46**: 2061-2066.
- Volk, T., and M. I. Hoffert. 1985. Ocean carbon pumps: Analysis of relative strengths and efficiencies in ocean-driven atmospheric CO_2 changes. The carbon cycle and atmospheric CO_2 : Natural variations archaic to present, *Geophys. Monogr. Ser.* **32**: 99-110.
- Volkman, J. K., S. W. Jeffrey, P. D. Nichols, G. I. Rogers, and C. D. Garland. 1989. Fatty acid and lipid composition of 10 species of microalgae used in mariculture. *J. Exp. Mar. Biol. Ecol.* **128**: 219-240.
- Von Elert, E. 2002. Determination of limiting polyunsaturated fatty acids in *Daphnia galeata* using a new method to enrich food algae with single fatty acids. *Limnol. Oceanogr.* **47**: 1764-1773.
- Vuorio, K., M. Meili, and J. Sarvala. 2006. Taxon-specific variation in the stable isotopic signatures ($\delta^{13}\text{C}$ and $\delta^{15}\text{N}$) of lake phytoplankton. *Freshw. Biol.* **51**: 807-822.
- Wang, Y. 2008. Influence of *Microcystis* on the nutrient content of the sediments in Lake Taihu (China). Master Thesis, Nanjing University of Information Science & Technology.
- Weinbauer, M. G., X. Mari and J. Gattuso. 2011. Effect of ocean acidification on the diversity and activity of heterotrophic marine microorganisms, p 83-98. *In* J. Gattuso and L. Hansson [eds.] *Ocean Acidification*, Oxford University Press
- Wickham, S. A. 1995. Trophic relations between cyclopoid copepods and ciliated protists: Complex interactions link the microbial and classic food webs. *Limnol. Oceanogr.* **40**: 1173-1181.
- Williamson, C. E., W. Dodds, T. K. Kratz, and M. A. Palmer. 2008. Lakes and streams as sentinels of environmental change in terrestrial and atmospheric processes. *Front. Ecol. Environ.* **6**: 247-254.
- Work, K. A., and K. E. Havens. 2003. Zooplankton grazing on bacteria and cyanobacteria in a eutrophic lake. *J. Plankton Res.* **25**: 1301-1306.
- Worm, J., and M. Søndergaard. 1998. Dynamics of heterotrophic bacteria attached to *Microcystis* spp. (cyanobacteria). *Aquat. Microb. Ecol.* **14**: 19-28.
- Wright, S. W. 1991. Improved HPLC method for the analysis of chlorophylls and carotenoids from marine phytoplankton. *Mar. Ecol.-Prog. Ser.* **77**: 183-196.
- Wylie, J. L., and D. J. Currie. 1991. The relative importance of bacteria and algae as food sources for crustacean zooplankton. *Limnol. Oceanogr.* **36**: 708-728.
- Zeebe, R. E., and D. A. Wolf-Gladrow. 2001. CO_2 in seawater: Equilibrium, kinetics, isotopes. Elsevier Science.
- Zhang, J., P. D. Quay, and D. O. Wilbur. 1995. Carbon-isotope fractionation during gas-water exchange and dissolution of CO_2 . *Geochim. Cosmochim. Acta* **59**: 107-114.
- Zhukova, N. V., and V. I. Kharlamenko. 1999. Sources of essential fatty acids in the marine microbial loop. *Aquat. Microb. Ecol.* **17**: 153-157.
- Zohary, T., J. Erez, M. Gophen, I. Bermanfrank, and M. Stiller. 1994. Seasonality of stable carbon isotopes within the pelagic food-web of lake Kinneret. *Limnol. Oceanogr.* **39**: 1030-1043.

Introduction

Human activities have a major impact on global biodiversity, ecosystem functioning and biogeochemical processes and the current times were coined the age of man or the Anthropocene. One of the largest impacts since the industrial revolution is alteration of the global carbon (C) cycle, what lead to a rapid increase of CO₂ in the atmosphere. Around one third of human released CO₂ has been absorbed by the oceans, causing changes in seawater chemistry. When CO₂ dissolves in seawater, hydrogen ions are released and seawater pH decreases, which is called “ocean acidification”. Ocean acidification has a brief research history (~10 years), but has shown to affect marine organisms and ecosystems. Another pertinent environmental problem is eutrophication due to ongoing nutrient loading of aquatic systems, causing degradation of ecosystems and deteriorating water quality. Especially lakes are affected by eutrophication and many lakes turned from a clear, macrophyte-dominated state into turbid, phytoplankton-dominated state, often with reoccurring cyanobacterial blooms.

These environmental problems affect the base of the food web, formed by plankton communities. Phytoplankton are the main primary producers in aquatic systems, converting CO₂ and nutrients into organic matter. In a classical food-web view, phytoplankton are eaten by zooplankton, which can be grazed upon by higher trophic levels, such as fish. Heterotrophic bacteria play a key role in the recycling of organic matter and nutrients in aquatic systems, processing roughly half of the primary production. Bacteria can be grazed by zooplankton, coupling the bacterial pathways (called microbial loop) with the classical food chain. The balance between phytoplankton production and community respiration (often dominated by bacteria) largely determines if aquatic systems are net sinks or sources for CO₂. Therefore changes in plankton food web structure can have large feedback on the global carbon cycle and human impact on carbon flows in plankton communities was the main research theme of this thesis. Both marine and freshwater systems were studied, but for marine systems we focused on the effects induced by rising atmospheric and oceanic CO₂ levels (chapter 2 and 3), while in freshwater systems we focused on eutrophication effects (chapter 4,5 and 6).

Methodology

The tool used to study carbon flows was carbon stable isotope analysis (SIA), both in natural abundance studies (chapter 4 and 6) and in deliberate tracer experiments (chapter 2, 3 and 5). Natural abundance SIA uses the natural variation in isotope ratios ($\delta^{13}\text{C}$, ratio $^{13}\text{C}/^{12}\text{C}$ relative to a standard) of sources to infer dietary information of consumers. For example, in chapter 6 the natural variety in carbon isotopic composition of phytoplankton and macrophytes was used to quantify their contributions to the diet of bacteria and zooplankton. In tracer or labeling experiments, ^{13}C is added as a deliberate tracer and the uptake and transfer of label in different food web compartments can be monitored in time. Isotope labeling experiments allow quantification of carbon flows among compartments, especially when combined with ecological modeling. In chapters 2 and 3, the CO₂ pool was enriched with ^{13}C and uptake by phytoplankton and subsequent transfer to bacteria and zooplankton was monitored in time and the carbon flows were quantified with a food web model.

The carbon isotope ratios of phytoplankton and bacteria were derived from $\delta^{13}\text{C}$ measurements of fatty-acid biomarkers. Polar-lipid derived fatty acids (PLFA) are part of the membranes of most organisms and show taxonomic variety, meaning that phytoplankton and bacteria possess distinct PLFA. Thus, by analyzing $\delta^{13}\text{C}$ of group-specific PLFA, $\delta^{13}\text{C}$ of bacteria and phytoplankton could be estimated.

Ocean acidification

The effects of increasing CO_2 levels on natural plankton communities were studied in mesocosm experiments, which are large experimental units, where CO_2 was added to mimic future CO_2 conditions. ^{13}C was added to the dissolved inorganic carbon (DIC) pool and transfers among the plankton communities were followed in time.

The mesocosm experiment of chapter 2, carried out in Bergen (Norway) with North-Atlantic seawater, was focused on CO_2 effects during a phytoplankton bloom that was initiated by nutrient additions. We found a high dependence of bacteria on phytoplankton, bacteria ^{13}C uptake and biomass closely followed those of phytoplankton and after 2 weeks, bacteria had obtained ~90 % of their carbon from phytoplankton. We found no CO_2 effect on the carbon transfer from DIC to phytoplankton and subsequently bacteria. When nutrients became exhausted, the phytoplankton bloom collapsed and CO_2 effects appeared. In the post-bloom phase, phytoplankton biomass was higher at high CO_2 , what could be due to enhanced production with elevated CO_2 under low nutrients. The operation of carbon-concentrating mechanisms requires energy and nutrients, so when nutrients become limited, higher CO_2 concentrations can be beneficial. Also bacteria biomass was higher at high CO_2 in the post-bloom phase, probably due to increased phytoplankton.

The mesocosm experiment of chapter 3 was carried out in Svalbard, the Arctic, chosen because of the vulnerability of high-latitude seawater to ocean acidification. Here we used a food- web model that comprised both concentrations and isotope ratios of phytoplankton, bacteria, zooplankton and detritus or export material. The plankton community structure was characteristic of a post-bloom situation, with efficient recycling of low nutrients and a dominance of a microbial food web. This was confirmed by high bacterial production (one third of primary production), low zooplankton grazing and export of organic matter (both less than 10% of primary production). However, in the post-bloom situation a small phytoplankton bloom developed and CO_2 effects were visible on the bloom decline. Even though export was low, it was about 10 times higher at high CO_2 levels compared to low CO_2 levels. We speculated that material released under high CO_2 was of more sticky nature and facilitated aggregation. Zooplankton grazing however was negatively affected by increased CO_2 levels, but we could not unravel the mechanisms behind it. There was neither effect on phytoplankton and bacterial production nor on their coupling. Interestingly, nutrient addition, halfway through the experiment, did not result in a large increase in organic carbon production, but export increased greatly. We found a hampering effect of CO_2 on both particulate organic carbon production and export after nutrient addition what was explained by changes in phytoplankton community composition.

Both mesocosm experiments showed that CO_2 effects on plankton communities are very subtle and often on the edge of significance. Furthermore, the response on CO_2 strongly depends on the structure of the food web, including community composition and nutrient state. Although these experiments help to understand plankton community responses to CO_2 , it will be difficult to predict a future, global response to future CO_2 conditions.

In addition, temperature is expected to increase together with CO₂ (global warming), which can amplify or reduce ocean acidification. Future research should also focus on the combined effects that are expected to occur in a high CO₂ world and that have been documented in small-scale laboratory experiments.

Eutrophication

Food-web interactions in lakes along a trophic gradient, ranging from oligotrophic to hyper-eutrophic, were studied in a cross-system analysis of 22 temperate lakes in USA. Confirmative of general knowledge, we found that both phytoplankton and bacterial biomass increased with increasing trophicity, but the ratio of bacteria to phytoplankton decreased with increasing trophicity. Lake metabolism was mainly determined by productivity, indicated by phytoplankton biomass, rather than DOC concentrations. The isotope ratios ($\delta^{13}\text{C}$) of organic carbon pools were more variable in eutrophic compared to meso-oligotrophic lakes, due to larger variability in isotope composition of phytoplankton and allochthonous carbon. Phytoplankton $\delta^{13}\text{C}$ was governed by lake CO₂ concentrations in all lakes and by phytoplankton biomass in eutrophic lakes. Phytoplankton isotope fractionation factors were low (average of 17 ‰) and showed a large range (8-25 ‰). The most enriched phytoplankton were found in the hyper-eutrophic lakes that were dominated by cyanobacteria. Carbon isotope ratios of bacteria matched best with those of POC but not with DOC, although DOC is the approximate primary carbon source for bacteria. In meso-oligotrophic lakes, bacteria used a mixture of carbon from various sources, but they depended more on phytoplankton in eutrophic lakes. Zooplankton $\delta^{13}\text{C}$ showed a strong relation to $\delta^{13}\text{C}$ of phytoplankton, indicating that phytoplankton were the primary carbon source for zooplankton, independent of trophic state. Generally, bacteria showed more response to changes in trophic state in carbon uptake pathways than zooplankton. Additionally, we calculated autochthonous (phytoplankton) and allochthonous (terrestrial) carbon contributions to bacteria and zooplankton and found higher autochthonous contributions to zooplankton than to bacteria, which were independent of trophic state. Interestingly, zooplankton $\delta^{13}\text{C}$ did not match with $\delta^{13}\text{C}$ of fatty acids that are abundant in cyanobacteria in the eutrophic lakes, what suggests that zooplankton was avoiding cyanobacteria.

Cyanobacteria are considered poor food for zooplankton, because of filtering interference, low nutritional quality and toxicity. Still zooplankton are present in lakes that are almost entirely dominated by cyanobacteria (98 % of phytoplankton), such as eutrophic lake Taihu in China. In chapter 5 the hypothesis was tested that cyanobacteria can be a carbon source for zooplankton, but that most carbon flows via bacteria-mediated pathways rather than via herbivory. Cyanobacteria were enriched with ¹³C and added to natural lake water as living cyanobacteria, cyanobacteria detritus or cyanobacteria DOM. After three days ¹³C label was found in zooplankton in all treatments, but label transfer was highest in DOM additions, followed by detritus and lowest live forms. High labeling of bacteria fatty acids in the incubations and in the zooplankton showed that bacteria were an important link between cyanobacteria and zooplankton.

Eutrophication effects can be combated by biomanipulation, a commonly used tool in lake restoration. A eutrophic lake in China was partially restored by fish removal and macrophyte planting and plankton communities in the restored and unrestored parts were monitored over a year. Nutrients, phytoplankton (mainly cyanobacteria) and bacteria were significantly reduced in the restored part, a desired effect on lake restoration. Natural abundance $\delta^{13}\text{C}$ of macrophytes were higher than those of phytoplankton.

Macrophyte presence resulted in a significant enrichment in zooplankton and bacteria, indicating macrophyte carbon subsidies to pelagic food webs. Macrophytes carbon subsidies were on average 55 % to bacteria and 47 % to zooplankton, derived from a mixing model where we assumed that phytoplankton was the other carbon source. Similar macrophyte subsidies to bacteria and zooplankton in each month, suggested bacteria mediated carbon flows.

Summarized, we found that phytoplankton (including cyanobacteria), terrestrial organic material, and macrophytes were all carbon sources for bacterial consumers and can thus (partially) sustain the microbial food web. Also zooplankton was sustained by the different carbon sources, although eukaryotic algae were always preferred. This is confirmative, since eukaryotic algae, representing the non-cyanobacteria part of phytoplankton, are considered high quality or even crucial food for zooplankton. However, in all study systems, zooplankton received a substantial part of their carbon from other, non-algae sources, with bacteria as important trophic link. In this thesis we only focused on two or three carbon sources at the same time. There is still a need to integrate the contributions of multiple carbon sources to plankton communities to understand plankton food web functioning in the Anthropocene. Since natural abundance carbon isotope signatures of basal sources may overlap, isotope labeling and additional isotope analyses should be included in research. Another missing link is the role of protozoans in food web studies, since they are too small to be handpicked and generally lack specific biomarkers. New methods like molecular techniques or NanoSims (a sophisticated machine that combines sub-micrometer microscopy with multiple stable isotope analyses) can be used to study their role in food-web carbon cycling.

Introductie

Menselijke activiteiten hebben grote invloed op wereldwijde biodiversiteit, ecosystemen en biogeochemische processen en het huidige tijdperk wordt daarom aangeduid als de Anthropocene, de tijd van de mens. Een van de grootste menselijke invloeden sinds de industriële revolutie is de verandering van de mondiale koolstof (C) cyclus, waardoor de hoeveelheid koolstofdioxide (CO₂) in de atmosfeer sterk is toegenomen. Ongeveer een derde van de door mensen uitgestoten CO₂ is opgenomen door de oceanen, wat leidt tot veranderingen in de zeewaterchemie. Als CO₂ in water oplost reageert het met water tot koolzuur en komen er waterstof ionen vrij. Hierdoor wordt de zuurgraad (pH) van het zeewater verlaagd, wat betekent dat het water zuurder wordt. Dit proces wordt oceaanzuuring genoemd. Er wordt pas sinds kort (ca. 10 jaar) onderzoek naar oceaanzuuring gedaan, waaruit blijkt dat oceaanzuuring negatieve effecten kan hebben op zoutwater (mariene) organismen en ecosystemen. Een ander langdurig milieuprobleem is eutrofiëring (overbemesting) van oppervlaktewateren door de continue toevoer van voedingsstoffen (nutriënten), met verslechterde waterkwaliteit en verarmde ecosystemen met minder soorten tot gevolg. Vooral zoetwatersystemen zijn aangetast door eutrofiëring en veel meren zijn van heldere, met waterplanten begroeide wateren veranderd in een troebele, groene soep, vaak gedomineerd door blauwalgen.

Deze milieuproblemen beïnvloeden de basis van aquatische voedselwebben die gevormd wordt door planktongemeenschappen. Algen (fytoplankton) zijn de primaire producenten en zetten CO₂ en nutriënten om in organisch materiaal. In een klassiek voedselweb worden de algen gegeten door zooplankton, dat op zijn beurt weer gegeten wordt door grotere organismen, zoals vissen. Een belangrijk onderdeel van planktonvoedselwebben zijn bacteriën, die organisch materiaal verwerken en nutriënten recyclen. De schatting is dat ongeveer de helft van de primaire productie door bacteriën wordt verwerkt. Bacteriën vormen de basis van het microbiële voedselweb en kunnen weer worden gegeten door zooplankton en worden zo onderdeel van het klassieke voedselweb. De balans tussen primaire productie door algen en respiratie (afbraak van organisch materiaal) doorconsumenten (gedomineerd door bacteriën), bepaalt in grote mate of watersystemen netto CO₂ opnemen of afgeven aan de atmosfeer. Daardoor kunnen veranderingen in de structuur van planktonvoedselwebben grote gevolgen hebben voor de globale koolstofkringloop. De menselijke invloed op de structuur van planktonvoedselwebben en de koolstofstromen hierin zijn de belangrijkste thema's van dit proefschrift. Zowel zoetwater als mariene systemen werden bestudeerd, maar in mariene planktongemeenschappen werd vooral gekeken naar de effecten van oceaanzuuring (chapter 1 en 2), terwijl de focus in zoetwaterplankton op eutrofiëring lag (chapter 4, 5 en 6).

Methodes

De onderzoekstechniek in dit proefschrift om koolstofstromen te bestuderen en kwantificeren was analyse van koolstof isotopen, die twee stabiele (niet radioactieve) vormen kent: ¹²C en ¹³C. Er bestaat een natuurlijke variatie in de ratio van deze isotopen ($\delta^{13}\text{C}$) in verschillende primaire voedselbronnen, zoals algen, terrestrisch materiaal en waterplanten. Dat komt doordat planten tijdens fotosynthese bij voorkeur de lichte isotoop (¹²C) inbouwen, oftewel fractioneren tegen ¹³C.

De mate van fractionatie hangt af van biologische processen en omgevingsfactoren, zoals temperatuur en CO₂ beschikbaarheid. De ratio in consumenten reflecteert de ratio van de voedselbronnen en kan dus gebruikt worden om te bepalen wat het dieet van consumenten is. In chapter 6 bijvoorbeeld werd het verschil in isotopen ratio tussen fytoplankton en waterplanten gebruikt om te kwantificeren hoeveel koolstof in bacteriën en zooplankton afkomstig was van beide bronnen. Ook in chapter 4 zijn natuurlijke koolstofverhoudingen gebruikt om voedselweb-interacties te bestuderen. Wanneer de isotopensamenstellingen van verschillende voedselbronnen te veel op elkaar lijken of wanneer voedselweb-interacties op korte tijdschaal bekeken worden, kan de zware stabiele isotoop (¹³C) gericht worden toegevoegd. Door de opname en overdracht van ¹³C in het voedselweb in de tijd te volgen, kunnen ecologische processen gemeten worden, zeker als het gecombineerd wordt met ecologische modellen. In chapter 2 en 3 bijvoorbeeld werd de CO₂ verrijkt met ¹³C en de opname daarvan door fytoplankton en doorgifte aan bacteriën en zooplankton werd gevolgd in de tijd. De koolstofstromen werden gekwantificeerd met een voedselwebmodel.

De koolstofisotopenratio van fytoplankton en bacteriën werden bepaald door het meten van de δ¹³C biomarkers (moleculen specifiek voor bepaalde organismen), omdat het erg lastig is deze organismen handmatig te isoleren. De gebruikte biomarkers waren vetzuren van polaire lipiden (PLFA) die onderdeel zijn van de membranen van de meeste organismen en die verschillend zijn in diverse taxonomische groepen, zoals soorten fytoplankton en bacteriën. Door de isotopenratio van deze vetzuurmoleculen te meten, konden de isotopenratio van fytoplankton en bacteriën worden ingeschat.

Oceaanverzuring

De effecten van toenemende CO₂ concentraties op natuurlijke planktongemeenschappen werden bestudeerd in mesocosms. Dit zijn grote experimentele opstellingen waarin de condities zo natuurlijk mogelijk gehouden worden. Hieraan werd CO₂ toegevoegd in verschillende concentraties om zo de toekomst te simuleren. ¹³C werd toegevoegd aan de CO₂ and de doorgifte van ¹³C in de plankton voedselwebben werd gevolgd door de tijd. Op de bodems van de mesocosms waren sedimentvallen geplaatst om dood organisch materiaal op te vangen.

Het mesocosm experiment, beschreven in chapter 2, vond plaats in Bergen (Noorwegen) in Noord-Atlantisch zeewater en richtte zich op CO₂ effecten op een algenbloei die werd gestart door nutriënten toe te voegen. We vonden dat bacteriën sterk afhankelijk waren van fytoplankton, de ¹³C opname en veranderingen in bacteriële biomassa volgden die van fytoplankton op korte afstand. Na twee weken hadden bacteriën 90 % van hun koolstof van fytoplankton verkregen. We vonden geen CO₂ effecten op de opname van CO₂ door fytoplankton en de overdracht van fytoplankton naar bacteriën. CO₂ effecten ontstonden toen de nutriënten op raakten en de algenbloei instortte. In deze nabloeiperiode was de biomassa van fytoplankton hoger bij hogere CO₂ concentraties, wat kan komen doordat hoger CO₂ fotosynthese kan vergemakkelijken. Fytoplankton hebben mechanismen om CO₂ in hun cellen te concentreren, maar deze mechanismen kosten energie en nutriënten, dus onder nutriëntentekort kan hoog CO₂ voordelig zijn. Ook bacteriële biomassa was hoger in de nabloei bij hogere CO₂ concentraties, waarschijnlijk als gevolg van de hogere fytoplankton biomassa.

Chapter 3 bevat de resultaten van een mesocosm experiment dat werd uitgevoerd op Spitsbergen, in de Arctische oceaan.

De reden om het onderzoek op de Noordpool uit te voeren was dat de pooloceanen zeer kwetsbaar zijn voor oceaanzuring, omdat CO₂ beter oplost in water bij lagere temperatuur. Hier gebruikten we een voedselwebmodel waarin naast ¹³C incorporatie ook biomassa's en concentraties van de componenten meegenomen waren. De componenten waren fytoplankton, bacteriën, zooplankton en dood materiaal dat uitzonk naar de bodem van de mesocosms. De plankton voedselweb structuur was kenmerkend voor een nabloeiperiode, met efficiënte recycling van nutriënten en een dominerende rol van het microbiële voedselweb. Deze structuur werd bevestigd door onze resultaten die hoge bacteriële productie (een derde van de primaire productie) en lage zooplankton begrazing en export van dood materiaal (beide minder dan 10 % van de primaire productie) lieten zien. Maar ook in deze nabloeisituatie ontwikkelde zich een kleine fytoplanktonbloei en CO₂ effecten werden zichtbaar toen deze bloei weer instortte. Alhoewel de export van dood materiaal laag was, was het ca. tien keer hoger bij hoge dan bij lage CO₂ concentraties. We speculeerden dat het organisch materiaal dat vrij kwam bij hoog CO₂ tijdens de bloeiafname plakkeriger was (bijvoorbeeld doordat het meer suikers bevatte) en daardoor sneller aaneen plakte en uitzonk. Zooplankton begrazing was juist lager bij hogere CO₂ concentraties, maar we konden niet de precieze oorzaken achterhalen. Er was geen effect van CO₂ op fytoplankton en bacteriële productie en ook niet op de koppeling tussen fytoplankton en bacteriën. Opmerkelijk was dat de toevoeging van nutriënten, halverwege het experiment, niet leidde tot een sterke toename in de productie van organisch materiaal, maar dat export van dood materiaal sterk toenam. Tegenovergesteld aan het eerste deel van het experiment, nam de export af met toenemende CO₂ concentraties en ook de productie van organisch materiaal nam af met toenemende CO₂, wat waarschijnlijk veroorzaakt werd door een verandering in de soortensamenstelling van fytoplankton.

Beide mesocosm experimenten lieten zien dat CO₂ effecten op planktongemeenschappen erg subtiel zijn en vaak maar net significant. Daarnaast hangt de respons op CO₂ sterk af van de structuur van het voedselweb, waaronder de soortensamenstelling en de nutriëntenstatus. Alhoewel deze experimenten bijdragen om mogelijke CO₂ effecten op planktongemeenschappen te begrijpen, is het moeilijk om een globale toekomstrespons van plankton te voorspellen. Daarnaast wordt verwacht dat ook de temperatuur van zeewater zal stijgen (mondiale opwarming), wat het effect van CO₂ kan versterken of juist tegengaan. Toekomstig onderzoek zou daarom ook naar de gecombineerde effecten van temperatuur en CO₂ moeten kijken.

Eutrofiëring

Voedselwebinteracties en CO₂ balans in meren met verschillende trofische staat (nutriëntenstatus), van oligotroof naar hypereutroof, werden bestudeerd in een cross-systeemanalyse van 22 gematigde meren in de Verenigde Staten (VS). Als bevestiging van algemene kennis vonden we dat zowel fytoplankton als bacteriënbioom toenamen met toenemende nutriëntenconcentraties (trofy), maar de ratio bacteriën: fytoplankton nam af. De CO₂ balans in de meren werd vooral bepaald door productiviteit, gemeten als fytoplankton biomassa, en minder door opgeloste organische koolstof (DOC) concentraties, die dienen als indicatie voor de input van allochtoon materiaal (materiaal dat geproduceerd wordt buiten een meer). De isotopenratio's ($\delta^{13}\text{C}$) van de verschillende componenten van het voedselweb waren meer variabel in eutrofe dan in meso-oligotrofe meren. Dit kwam doordat er meer variabiliteit in de $\delta^{13}\text{C}$ van fytoplankton en allochtoon materiaal was in de eutrofe meren.

De isotoop fractionatiefactoren tussen CO₂ en fytoplankton waren laag (gemiddeld 17 ‰) en lieten een grote variatie zien (8-25 ‰). De meest verrijkte fytoplankton (dus met de laagste fractionatie) bevonden zich in de hypereutrofe meren, met veel blauwalgen. Koolstof isotopen compositie van bacteriën kwam overeen met die van organisch koolstof in partikels (POC), maar niet met die van opgelost organisch koolstof (DOC), alhoewel DOC de voornaamste koolstofbron is voor bacteriën. Bacteriën in de meso-oligotrofe meren gebruikten een mengsel van koolstof uit verschillende bronnen en meer fytoplankton in de eutrofe meren. Zooplankton $\delta^{13}\text{C}$ toonde een sterke correlatie met de $\delta^{13}\text{C}$ van fytoplankton. Dat toonde aan dat fytoplankton de belangrijkste koolstofbron voor zooplankton was, onafhankelijk van de nutriëntenstatus. Over het algemeen toonde bacteriën een sterkere respons op veranderingen in trofische staat dan zooplankton in hun koolstofopnamepatronen. Daarnaast berekenden we ook de bijdragen van autochtoon (door fytoplankton geproduceerd) en allochtoon koolstof aan bacteriën en zooplankton met behulp van een koolstof mengmodel. We vonden hogere autochtone bijdragen aan zooplankton dan aan bacteriën. Een interessante bevinding was dat de $\delta^{13}\text{C}$ van zooplankton niet overeenkwam met de $\delta^{13}\text{C}$ van vetzuren die rijk zijn in blauwalgen in de eutrofe meren, wat er op duidde dat zooplankton de blauwalgen vermeed.

Blauwalgen worden gezien als slecht voedsel voor zooplankton, omdat ze het filtersysteem van zooplankton blokkeren doordat ze kolonies vormen en omdat ze lage voedingswaarde hebben en giftig kunnen zijn. Maar nog steeds komt zooplankton voor in meren, waarbij de fytoplanktonpopulatie bijna geheel uit blauwalgen bestaat (98 % van alle fytoplankton), zoals in het eutrofe Taihu meer in China. In chapter 5 werd de hypothese getest dat blauwalgen een koolstofbron voor zooplankton kunnen zijn, maar dat de meeste koolstof wordt doorgegeven via bacteriële routes, in plaats van via directe begrazing. Hiervoor werden blauwalgen verrijkt met ¹³C en in verschillende vormen aan emmers met natuurlijk water uit het Taihu meer toegevoegd. De verschillende verrijkte substraten waren levende blauwalgen, dode blauwalgen (detritus) en opgelost koolstof (DOC). Na drie dagen kon er ¹³C van alle toevoegingen in zooplankton teruggevonden worden, maar de meeste blauwalg ¹³C werd opgenomen als DOC, gevolgd door detritus en als laatste in levende vorm. Bacteriën in het water, zowel als bacteriën die waren opgegeten door zooplankton bevatten veel van de ¹³C label, wat aantoonde dat bacteriën een belangrijke schakel waren tussen blauwalgen en zooplankton. De hypothese werd bevestigd dat zooplankton niet graag blauwalgen eten, maar dat er wel energie kan worden doorgegeven via bacteriën.

De effecten van eutrofiëring kunnen worden tegengegaan met behulp van biologische manipulatie (biomanipulatie). Dit is een veel gebruikte techniek om meren te restaureren. Een eutroof meer in Zuid-China werd gedeeltelijk gerestaureerd door de vissen te verwijderen en macrofyten (waterplanten) te planten. De plankton gemeenschappen in het gerestaureerde en ongerestaureerde deel van het meer werden gevolgd gedurende een jaar. De concentraties van nutriënten, fytoplankton (vooral blauwalgen) en bacteriën waren significant lager in het gerestaureerde deel, wat een gewenst effect is van restauratie van meren. De natuurlijke $\delta^{13}\text{C}$ van macrofyten waren hoger (meer verrijkt) dan die van fytoplankton. De aanwezigheid van de macrofyten leidde er toe dat de $\delta^{13}\text{C}$ van zooplankton en bacteriën ook significant verrijkt waren in $\delta^{13}\text{C}$, wat er op duidde dat macrofyten koolstof bijdroegen aan het voedselweb. De bijdrages van koolstof afkomstig van macrofyten werden getest met een isotopen mengmodel met twee bronnen, waarbij we fytoplankton als de andere koolstofbron beschouwden. De bijdrages van macrofyten waren gemiddeld over het jaar 55 % naar bacteriën en 47 % naar zooplankton.

Gelijke bijdragen naar bacteriën en zooplankton in iedere maand suggereerden dat de bacteriën een intermediair vormden tussen macrofyten en zooplankton.

Samenvattend vonden we dat fytoplankton (inclusief blauwalgen), allochtoon (terrestrisch) materiaal en macrofyten allemaal koolstofbronnen waren voor bacteriële consumenten en dus (gedeeltelijk) het microbiële voedselweb subsidiëren. Ook zooplankton werd ondersteund door de verschillende koolstofbronnen, alhoewel eukaryote algen (fytoplankton zonder blauwalgen) altijd de voornaamste voedselbron waren. Dit bevestigt de bestaande kennis, omdat eukaryote algen gezien worden als voedsel van hoge kwaliteit en zelfs als cruciaal voor zooplankton. Maar in alle studiesystemen verschaffen andere bronnen een substantieel deel van de koolstofbehoefte van zooplankton, met bacteriën als belangrijke trofische intermediair. In dit proefschrift richtten we ons op maximaal twee of drie mogelijke koolstofbronnen per keer. Het is daarom nog nodig om alle contributies van meer koolstofbronnen voor planktongemeenschappen te integreren, om het functioneren van planktonvoedselwebben in het Anthropoceen te begrijpen. Omdat natuurlijke isotopen samenstellingen van basale koolstofbronnen vaak overlappen, zouden isotoopverrijking en analyses van andere isotopen (zoals waterstof en stikstof) meegenomen moeten worden in het onderzoek. Een andere missende link is de rol van protozoa in voedselwebstudies, omdat ze te klein zijn om met de hand gepikt te worden en in het algemeen geen specifieke biomarkers bevatten. Nieuwe moleculaire technieken en microscopie gecombineerd met isotopenanalyse kunnen worden gebruikt om hun rol in de koolstofstromen in planktonvoedselwebben te bepalen.

Publications from this thesis

- de Kluijver, A.**, K. Soetaert, J. Czerny, K.G. Schulz, U. Riebesell, and J.J. Middelburg (2012). “A ^{13}C labeling study of carbon fluxes in Arctic plankton communities under elevated CO_2 levels”. *Biogeosciences discussions* **9**: 8571-8610
- de Kluijver, A.**, Y. Ju, M. Houtekamer, J.J. Middelburg, and Z. Liu (2012). “Cyanobacteria as a carbon source for zooplankton in eutrophic Lake Taihu, China, measured by ^{13}C labeling and fatty acid biomarkers.” *Limnology and Oceanography* **75**(4): 1245-1254
- de Kluijver, A.**, K. Soetaert, K.G. Schulz, U. Riebesell, R.G.J. Bellerby, and J.J. Middelburg (2010). “Phytoplankton-bacteria coupling under elevated CO_2 levels: a stable isotope labeling study.” *Biogeosciences* **7**: 3783-3797.

Publications outside this thesis

- Van Engeland, T., **A. de Kluijver**, K. Soetaert, F. Meysman, and J.J. Middelburg (2012). “Isotopic information improves predictive capabilities of a biogeochemical model.” *Biogeosciences discussions* **9**: 9453-9486.
- T. Tanaka, S. Alliouane, R. G. B. Bellerby, J. Czerny, **A. de Kluijver**, U. Riebesell, K. G. Schulz, A. Silyakova, and J.-P. Gattuso (2012). “Metabolic balance of a plankton community in a pelagic water of a northern high latitude fjord in response to increased $p\text{CO}_2$.” *Biogeosciences discussions* **9**: 11013-11039.
- Maier, C., **A. de Kluijver**, M. Agis, C.P.D. Brussaard, F.C van Duyl, and M.G. Weinbauer (2011). “Dynamics of nutrients, total organic carbon, prokaryotes and viruses in onboard incubations of cold-water corals.” *Biogeosciences* **8**: 2609-2620.
- De Goeij, J.M., **A. de Kluijver**, F.C. van Duyl, J. Vacelet, R.H. Wijffels, A.F. de Goeij, J.P. Cleutjens, and B. Schutte (2009). “Cell kinetics of the marine sponge *Halisarca caerulea* reveal rapid cell turnover and shedding.” *The Journal Of Experimental Biology* **212**: 3892-3900.
- Verheesen, P., **A. de Kluijver**, S. van Koningsbruggen, M. de Brij, H.J. de Haard, G.J. van Ommen, S.M. van der Marel, C.T. Verrips (2006). “Prevention of oculopharyngeal muscular dystrophy-associated aggregation of nuclear poly(A)-binding protein with a single-domain intracellular antibody.” *Human Molecular Genetics* **15**:105-111.
- Schoon, P.L., **A. de Kluijver**, J.J. Middelburg, J.A. Downing, J.S. Sinninghe Damsté, S.Schouten. “The influence of lake water pH and alkalinity on the distribution of core and intact polar branched glycerol dialkyl glycerol tetraethers in lakes.” To be submitted to Organic geochemistry
- Hopmans E.C, P.L. Schoon, **A. de Kluijver**, J.A. Downing, J.J. Middelburg, J.S. Sinninghe Damsté, S. Schouten. “Environmental controls on the distribution of intact polar lipids in oligotrophic and eutrophic lakes.” To be submitted to Limnology and Oceanography.

Wetenschapscommunicatie over het experiment op Spitsbergen (chapter 3)

- Nederlandse blog schrijver voor de EPOCA Arctic campaign in mei-juli 2010
<http://epocaarctic2010.wordpress.com/category/dutch-blogs/>
- Artikel “Plankton vangen op Spitsbergen” in Bionieuws juli 2010 door G. van Maanen.
- Nederlandse blog “Van poolonderzoekster naar meesterafwasser?” op Zeeinzicht september 2010 door F. Fey.
<http://www.zeeinzicht.nl/php/?target=nieuwsblogs&link=20100913>.
- Artikel als onderdeel van “Viva 400: de succesfactor” in Viva oktober 2010 door S. Bakker.

Een promotie doe je niet alleen. Er zijn veel mensen die een bijdrage hebben geleverd aan het tot stand komen van dit proefschrift. Hen wil ik hierbij graag bedanken. Daarnaast heb ik tijdens de vier jaar die ik aan deze promotie heb gewerkt veel leuke, vriendelijke en interessante mensen ontmoet, die er mede voor hebben gezorgd dat mijn promotieonderzoek vooral een fijne bezigheid was. Ik zal er altijd met veel plezier op terugkijken.

Allereerst wil ik mijn promotor en dagelijks begeleider Jack bedanken. Ik kan geen betere promotor en begeleider bedenken. Door je optimisme zorgde je er altijd voor dat ik na een gesprek met jou positiever was, vooral omdat je vaak zei dat de data toch echt heel mooi en uniek waren. Door de mogelijkheden en vrijheid die je me gaf, heb ik prachtige plaatsen kunnen bezoeken. Ik heb grote waardering voor je visie op de wetenschap en de maatschappij in het algemeen. Verder waren je betrokkenheid en snelheid onmisbaar voor het (tijdig) afronden van dit proefschrift. Mijn copromotor Karline wil ik ook graag bedanken voor haar geduld en inzet voor dit proefschrift. Je kennis van modellen is wonderbaarlijk, maar ook hoe je die weet over te dragen en daarmee mensen enthousiast weet te maken (onder wie mijzelf). En dat doe je altijd met een vrolijke lach! Ook jij was snel met feedback en hulp, wat erg plezierig was.

Daarnaast wil ik alle collega's van het CEME in Yerseke bedanken en een aantal mensen in het bijzonder. Dick, dank je wel voor al je hulp en leuke gesprekken. Het is fijn dat je zo betrokken was bij mijn onderzoek en altijd klaar stond om te helpen. Ik ben erg blij dat jij een aanstelling bij ES hebt gekregen. Nu werk je samen met Jasper, die ik hierbij ook nog graag wil bedanken voor het leggen van de wetenschappelijke basis en de betrokkenheid. Eric, bedankt voor al je hulp, je kennis over PLFA en isotopen hebben me erg geholpen. Hetzelfde geldt voor Jacco, bedankt dat je altijd klaar stond voor vragen over algen. Frederik (mijn eerste kamergenoot), Karel, Tom en Andreas: bedankt voor jullie hulp met modelleren, R en allerlei andere technische vaardigheden, die ik nog niet altijd snap, maar die jullie feilloos beheersen. Adri, bedankt voor je al je hulp met technische zaken. Peter (Herman) en Francesc, bedankt voor jullie hulp met statistiek. Carlo, bedankt voor je interesse. Filip, Bart en Leon, bedankt voor jullie hulp. Frédéric, thanks for learning me about the CO₂ system.

Pieter, jij was onmisbaar voor dit proefschrift en verdient nog veel meer drop dan je al hebt gekregen! Bedankt voor al je hulp, kennis en gezelligheid, variërend van PLFA extracties, dozen pakken, zooplankton vangen, tot kletsen over alles en nog wat. Ook de mensen van het analytische lab wil ik ontzettend bedanken voor hun hulp, daar kunnen geen appeltaarten tegenop. Op het analytische lab voelde ik me erg thuis, want naast de kennis en het werk, hing er ook een heel gezellige sfeer. Marco, bedankt voor al je hulp, gezelligheid en nuchtere kijk. Peter, bedankt voor je hulp, gezelligheid en filosofische levenslessen. Jur, bedankt voor de gezelligheid, ooit hoop ik nog je roofvogels te zien. Ook Yvonne, Coby, Jan en Jan, bedankt! Tanja, bedankt voor je hulp met de suikers en succes met het afronden van je eigen proefschrift. Ook de medewerkers van de ondersteunende dienst van het CEME, die ervoor zorgen dat het een plek is waar goed onderzoek gedaan kan worden, verdienen een bedankje. Jan, Laura, Anneke, Christine, Elly, Joke en Jan Thijs, bedankt!

I want to thank my office mates Eva-Maria and Alessia for the nice time. Even though, I wasn't in Yerseke often, I enjoyed sharing an office with you and our talks together. Lara, thanks for sharing four years of PhD together, it is nice that we started and finish together. Monique, dank je wel voor je rol als chauffeur, dat was erg fijn. Francesc, Ellen en Paul, bedankt voor jullie hulp met wegwijs worden in de promotiewereld en voor de gezelligheid. I also want to thank my fellow PhDs Sarah, Ina, Juliette, Diana, Christian for the nice time at CEME and also in the Keete. The Keete was a warm welcome for a newcomer, I have good memories of my stay there and want to thank the people I shared the Keete with, which are many. Sarah, we see each other too little now, but I am happy we became friends. The same for Saskia, thanks for friendship and the good times at the Keete. Johan, bedankt voor de leuke tijd. Michel bedankt voor de gezelligheid en Zeeuwse duik.

Halverwege de promotie verhuisde ik terug naar Utrecht en werd ik gastmedewerker op de universiteit Utrecht. Ook hier wil ik een aantal mensen bedanken voor de goede tijd daar. Allereerst m'n kamergenoten Marie Louise en Rick: bedankt voor alle gezelligheid! Jullie zijn naast collega's goede vrienden geworden en ik ga jullie ontzettend missen. Hopelijk blijven we nog spelletjes, concerten, biertjes of een ritje in de "Mexicaanse hoedjes" doen. Veel succes met het afronden van jullie proefschriften! Marie Louise, bedankt ook dat je paranimf bent, naast de gezelligheid was je ook erg betrokken bij mijn onderzoek. Ook wil ik Els, Emmy, Julia, Jos, Appy, Gert Jan, Gert, Mathilde, en Sander, Marieke bedanken voor de fijne tijd op de universiteit en daarbuiten. Hamid, Claudia, José and Karoliina, thanks for the nice time at the University and after work. Angela, thanks for being such a nice colleague in Utrecht as well in China, good luck with your thesis. Pien, bedankt voor de ondersteuning.

Als onderdeel van het Darwin project, wil ik mijn projectpartners bedanken: Petra, Astrid, Stefan en Klaas. Petra, bedankt voor de fijne samenwerking. Hierdoor hebben we succesvol veldwerk kunnen doen in de VS, waaruit gezamenlijke manuscripten zijn gekomen. Daarnaast was het ook heel gezellig, onderweg in de auto en tijdens onze minivakantie in Chicago. Stefan, dank voor je hulp en je deelname aan de leescommissie.

Een deel van mijn promotie heb ik op het NIOO-CL in Nieuwersluis doorgebracht. Helaas is het werk niet meer in het proefschrift terechtgekomen, maar ik wil een aantal collega's van daar bedanken. Velen van jullie ben ik nog regelmatig tegengekomen op congressen en bij andere gelegenheden, waar het altijd gezellig was elkaar weer te zien. Anthony, bedankt voor de fijne samenwerking. Nico, bedankt voor je hulp met de experimenten en gezelligheid. Ramesh, bedankt voor je gastvrijheid, betrokkenheid en hulp, zeker met hoofdstuk 5. Lisette, Liesbeth, Martijn, Bas, Anne, Susanne, Alena, Suzanne, Wolf, bedankt voor de fijne tijd op het CL en op het congres in China. Anne, bedankt voor de goede tijd op Puerto Rico. Naast het congres heb ik me uitstekend vermaakt met samen toeren over het eiland. Ellen, dank je voor je gastvrijheid en je deelname aan de leescommissie.

Some of the highlights of my PhD were the visits to China (one of two months!). Beside training my karaoke skills and eating with chop sticks, I learned a lot on freshwater ecology and Chinese culture. Zhengwen, thank you very much for your hospitality, kindness, support, scientific knowledge and overall nice collaboration. Thanks for being part of my reading committee.

Thanks to Yu Jinlei and Ning Jiajia for the nice time and succesful collaboration, I wish you all the best. Also thanks to Han Long, Zhong Lianghu, Mao Jie, Chen Liang, Wang Fengwen, Zhang Leiyan, Liu Yang, Zhong Ping, Li Kuanyi and Chen Feizhou (and I might have forgotten some names!) for support in the lab and field and for giving me such a good time in China. Thanks to Mary and Alfred for their interest and the nice time in Shanghai.

Another highlight was the field campaign in Svalbard in the Arctic, where we spend 6 weeks together in the scientific village Ny Ålesund for the mesocosm experiments. Special thanks for the people from Geomar in Kiel: Ulf, Kai, Jan, Jan, Andrea, Sebastian, Tim, Michael, Matthias and Signe. You were very nice people to work with, but also for having an after-work beer and parties. Matthias and Jan, thanks for your hospitality in Kiel as well. Maarten, dank je wel voor het verblijf in het Nederlandse station (zonder water, maar met internet!). Het verblijf hier met Anna, Corina en later Harry en Merel was gezellig, dank jullie wel hiervoor. Thanks to the British colleagues Susan, Frances and John for providing me with missing equipment, and John for being my best sampling mate! Thanks to Dag en Barbara for their zooplankton expertise. Also thanks to the other participants of this joined experiment, the nice collaboration and spirit made the experiment a success. I generally enjoyed being part of the EPOCA group, because of the nice meetings, people and atmosphere. Thanks to the main organizers: Jean-Pierre, Lina, and Anne-Marin. Jean-Pierre, thanks for being part of the reading committee.

The field campaign in the USA was also pleasant and successful, due to the support and hospitality of the people there. John, thank you very much for your hospitality, kindness, knowledge, support and overall good collaboration. Also thanks for being part of my reading committee. Thanks to Amber, Dan, Kelly and Josh for their help during the campaign. Thanks to David and Susan, who kindly let Petra and me stay at their home in Minnesota and provided us with nice food and boat trips, including waterskiing.

Naast werk is er natuurlijk ook een privéleven, waarin ik ook een aantal mensen wil bedanken. Lieve papa en mama, bedankt voor al jullie liefde, steun en betrokkenheid, zonder jullie was ik nooit zover gekomen. Bedankt ook voor jullie interesse en dat jullie me zelfs zijn komen opzoeken op Spitsbergen. Papa, ook bedankt voor het verzorgen van de opmaak van mijn proefschrift. Paul, Martin en Daphne, bedankt voor de gezellige, nodige afleiding en betrokkenheid. Oma, bedankt voor je liefde en interesse voor wat ik doe. Ook wil ik mijn familie, Mario, Jeanne, Maartje, Magda, Suzanne, Saskia, Aaltje, en schoonfamilie, Frank, Mieke, Maartje en Joost, bedanken voor hun betrokkenheid, steun en gezelligheid. Thanks to my British family, Tony, Nick, Phil, for their support and for the nice times together, including skiing holidays and visits in London.

Mijn vrienden en vriendinnen wil ik graag bedanken voor de gezellige tijden, maar ook voor hun interesse. Tom, bedankt dat je mijn paranimf bent. Als goede vriend heb je me vaak geholpen, kon ik altijd bij je logeren en was je erg begaan met mijn onderzoek, bedankt hiervoor. Sandra, bedankt voor je vriendschap. Door eerst samen biologie te studeren en daarna beiden te promoveren, kon ik, naast over andere dingen, altijd fijn met je praten over het promovendusleven.

Ook m'n andere (via) biologenvrienden, Ischa, Marjolein, Thijs en Alwin, wil ik graag bedanken voor onze uitjes en gezelligheid. Pauli, bedankt voor onze lange vriendschap en steun, ook al zien we elkaar minder vaak, het is altijd vertrouwd. De festivals, wintersportvakantie, huisweekenden, feestjes met onze (uitgebreide) IBB oud huisgenoten groep: Rick, Erik, Tom, Paul, Annemiek, Barbara, Krista, Marijke, Julie, Malou, Ruurd, zijn onvergetelijke herinneringen, dank jullie wel! Jan Willem, Dieuwertje en Renske, bedankt voor de gezelligheid. Dank aan de 'paardrijmeisjes': Famke, Jeannette, Marion, Annemarie, Evelien, Jessica, Xera, voor de gezellige ritten, avonden en weekendjes.

Lieve Abe, bedankt voor alles, maar vooral om wie je bent en dat je er bent. Je betrokkenheid bij mijn proefschrift, je vertrouwen, rust, liefde en wijze raad hebben ervoor gezorgd dat de laatste maanden naast hard werken, ook heel fijn waren.

